EQUILIBRIUM AND KINETIC STUDIES OF ATRAZINE AND LINDANE UPTAKE BY SOILS AND SOIL COMPONENTS

Jinhe Li

A Thesis

in

The Department

of

Chemistry and Biochemistry

Presented in Partial Fulfillment of the Requirements
for the Degree of Doctor of Philosophy at
Concordia University
Montreal, Quebec, Canada

December, 1993

National Library
of Canada

Acquisitions and
Bibliographic Services Branch

395 Wellington Street
Ottawa, Ontario
K1A 0N4

Bibliothèque nationale
du Canada

Direction des acquisitions et
des services bibliographiques

395, rue Wellington
Ottawa (Ontario)
K1A 0N4

Your file Votre référence

Our file Notre référence

ISBN 0-315-90864-5

Canada

ABSTRACT

EQUILIBRIUM AND KINETIC STUDIES OF ATRAZINE AND LINDANE UPTAKE BY SOILS AND SOIL COMPONENTS

JINHE LI, Ph.D.
CONCORDIA UNIVERSITY, 1993

The work presented in this thesis is a systematic study of the uptake of the polar herbicide atrazine (AT) by a mineral soil, GB 843, including the development of a mechanistic model, determination of equilibrium and kinetic parameters, examination of the effects of temperature and soil size fractions, interpretation of sorption mechanisms, and application of the mathematical model and laboratory results in a hydrology model. A stirred batch setup combined with an on-line microfiltration-HPLC technique is introduced for both short- and long-term studies. In addition, this thesis includes an investigation of the complex interaction between the nonpolar insecticide lindane and Laurentian fulvic acid (FA) to demonstrate the generality of the site binding model.

The uptake of atrazine has been commonly observed to follow a relatively fast labile surface sorption and a subsequent slower retarded intraparticle diffusion. A two stage surface-adsorption/intraparticle-diffusion model has been proposed to interpret the

observations. The labile sorption is demonstrated to have a definite capacity (θ_e), with an experimentally measured value of ~0.4 μmoles g^{-1} of soil. Both processes exhibit rapid early uptakes within the first few minutes to hours, and approach steady states over a certain reaction period. With an initial rate approximation, the pseudo first-order sorption rate constant (k_{s1}) is about 8 times higher than the intraparticle diffusion rate constant (k_{d1}). With respect to the much longer equilibrating time scale, intraparticle diffusion can be considered the rate-limiting process in comparison with labile surface sorption.

This work has investigated the effects of soil size fractions and temperature (5 to 35 °C). The results suggest that the labile surface uptake may only involve weak physisorption ($\Delta H^\circ \approx 0$ kJ mol^{-1} and $E_a = 22$ kJ mol^{-1}), while the intraparticle diffusion is dominated by a chemical transformation process ($E_a = 89$ kJ mol^{-1}).

Introduction of the two stage mechanism into a newly-developed hydrology model PESTFADE for simulating atrazine movement in controlled soil columns has shown a much closer agreement with the observed values than the conventional approach.

The interaction between lindane and Laurentian fulvic acid provides confirmation of the binding site complexation model. A small (~ 1 μmole g^{-1} of FA) and limited binding capacity is observed, and it varies as a function of solution pH, ionic strength, and FA concentration.

ACKNOWLEDGEMENTS

First and foremost, I would like to express my sincerest thanks to my supervisor, Dr. C.H. Langford, for both his continued guidance and the generous contribution of his time throughout this entire research project.

I would also like to extend my heartfelt thanks to my co-supervisor, Dr. D.S. Gamble, for the valuable discussion with him and for his enthusiastic care and kind help in the interpretation of the results of this work.

I am also deeply grateful to the member of my dissertation committee, Dr. S.R. Mikkelsen, for her critical review and constructive comments on my research proposal and thesis.

I also wish to convey my great thanks to Dr. S.O. Prasher, the Dept. of Agricultural Engineering, Macdonald Campus of McGill University, for his expert suggestion and assistance in computer program and modeling, to Dr. S. Kumarapeli, the Geology Department of Concordia University, for his invaluable technical assistance, to the Dept. of Chemistry and Biochemistry of Concordia University, for employing me as a Teaching Assistant, and to CLBRR, Research Branch of Agriculture Canada, for providing me state-of-the art instrumental facilities to complete this research.

Finally, a special acknowledgement is given to the Graduate Awards Committee of Concordia University for the Concordia University Graduate Fellowship, to the Natural Sciences and Engineering Research Council of Canada (NSERC), and to the Great Lakes Water Quality Program (GLWQ) of Agriculture Canada, for financial supports.

TO MY MOTHER, MY WIFE AND MY CHILDREN

AND THE MEMORY OF MY FATHER

TABLE OF CONTENTS

	PAGE
LIST OF TABLES	xiii
LIST OF FIGURES	xvii
NOMENCLATURE	xxii
CHAPTER 1	
INTRODUCTION	1
1-1. EQUILIBRIUM AND KINETICS OF PESTICIDE UPTAKE BY SOILS: A REVIEW	1
1-1.1. Sorption Phenomena	2
1-1.2. Sorption Equilibria and Isotherms	7
(1). Langmuir model	7
(2). Freundlich equation	8
(3). Nonsingularity of sorption isotherms	8
1-1.3. Mechanistic Considerations of Sorption	9
(1). Two schools of thought	10
(2). Partition uptake	16
(3). Site binding model	17
1-1.4. Modeling of Sorption Equilibria and Kinetics in the Soil-Water System	20
(1). Rate-limiting processes	20
(2). Reaction rate expression	24
(3). Modeling of mass transfer	26
(4). Nonequilibrium sorption	29
(5). Typical sorption kinetic models	30

1-1.5. Methodologies for Sorption Study 38
(1). Batch techniques 39
(2). Flow methods 41
(3). Rapid kinetic methods 42

1-2. RESEARCH PROSPECTIVES 43

CHAPTER 2
FURTHER TESTING OF THE SITE BINDING MODEL: INTERACTION OF LINDANE WITH LAURENTIAN FULVIC ACID 45

2-1. INTRODUCTION 45

2-2. EXPERIMENTAL 48
(1). Materials 48
(2). Apparatus 50
(3). Procedure 50
(4). Ultrafiltration technique 53

2-3. RESULTS 57
(1). Results of previous studies 57
(2). Lindane-FA interaction 58

2-4. DISCUSSION 70

2-5. SUMMARY 72

CHAPTER 3
ATRAZINE UPTAKE BY MINERAL SOIL GB 843 73

3-1. INTRODUCTION 73

3-2. MECHANISTIC MODEL: A TWO STAGE ADSORPTION/DIFFUSION MECHANISM 76
(1). Equilibria and kinetics of labile surface adsorption/desorption 77

(2). Bound residue formation by retarded intraparticle diffusion 79
(3). Total differential rate law 81
(4). Spreadsheet calculations 82

3-3. EXPERIMENTAL 87
(1). Equipment 87
(2). Reagents and materials 87
(3). General kinetic procedure 88
(4). Mass balance experiments 89

3-4. SOIL CHARACTERIZATION 91
(1). Soil mineral analyses 91
(2). Soil pH 92
(3). Cation exchange capacity (CEC) 92
(4). Model analyses 93
(5). Element identification (SEM/EDS studies) 95
(6). Labile sorption capacity 97
(7). Specific surface area/Organic carbon content 100

3-5. RESULTS AND DISCUSSION 100
(1). Rapid initial uptake 100
(2). Labile sorption steady state 103
(3). Labile sorption kinetics 112
(4). Intraparticle diffusion 117
(5). Long-term sorption kinetic experiments 125

3-6. SUMMARY 130

CHAPTER 4
ATRAZINE UPTAKE BY SOIL SIZE FRACTIONS 132

4-1. INTRODUCTION 132

4-2. EXPERIMENTAL 134
(1). Equipment 134
(2). Reagents and materials 134
(3). General kinetic procedure 134

4-3. CHARACTERIZATION OF SOIL FRACTIONS 136
(1). Soil fractionation 136

(2). Element identification (SEM/EDS studies) 138
(3). Specific surface area 138
(4). Organic carbon analyses 140
(5). Labile sorption capacity 141

4-4. RESULTS AND DISCUSSION 141
(1). Labile sorption 141
(2). Intraparticle diffusion 157

4-5. SUMMARY 168

CHAPTER 5
THE EFFECT OF TEMPERATURE ON ATRAZINE UPTAKE 170

5-1. INTRODUCTION 170

5-2. EXPERIMENTAL 173

5-3. RESULTS AND DISCUSSION 174
(1). Labile sorption 174
(2). Intraparticle diffusion 181
(3). Arrhenius and van't Hoff treatments 189

5-4. SUMMARY 196

CHAPTER 6
APPLICATION OF THE TWO STAGE MECHANISM IN A HYDROLOGY MODEL: PESTFADE 198

6-1. INTRODUCTION 198

6-2. EQUIPMENT AND SOIL COLUMN EXPERIMENTS 200

6-3. MODIFIED PESTFADE MODEL 202
(1). Mathematical model 202
(2). Model components/execution 207

(3). Input data and code specification 209
(4). Model verification 210

6-4. RESULTS AND DISCUSSION 213
(1). Output data 213
(2). Sensitivity analyses 228
(3). Comparison with conventional adsorption approach 231

6-5. SUMMARY 233

CHAPTER 7
CONCLUSION AND SUGGESTION FOR FUTURE RESEARCH 237

7-1. CONCLUSION 237

7-2. SUGGESTION FOR FUTURE RESEARCH 241

REFERENCES 244

APPENDICES 262

CHAPTER 3 262

(1). Appendix A Spreadsheet Showing Raw Data Input (Exp. #14, part) 262
(2). Appendix B Spreadsheet Showing Interpolated Data for Filtrate and Slurry at Rounded Times by Curve Fitting (Exp. #14) 263
(3). Appendix C Spreadsheet Showing Data for Sorption/Desorption Kinetic Calculations (Exp. #14, part) 264
(4). Appendix D Calculation of k_{b1} by Three Methods Outlined in 3-2.(4) 265

CHAPTER 6 268

(1). Appendix A Main Input Data Files for the Modified PESTFADE (Column 1) 268
(2). Appendix A Main Input Data Files for the Modified PESTFADE (Column 2) 269
(3). Appendix B Main Data Files for Model Verification 270
(4). Appendix C Main Output Data for the Modified PESTFADE (Column 1) 271
(5). Appendix C Main Output Data for the Modified PESTFADE (Column 2) 272

LIST OF TABLES

CHAPTER 2 PAGE

Table 2-3.1 Linear Regression Results for Data in Figs. 2-3.1 to 2-3.3 63

Table 2-3.2 Bound Lindane, $L_b = B_o + B_1V_s$ (μmoles/g of FA): Linear Regression for Data in Fig. 2-3.4 65

Table 2-3.3 Correlation of the Binding Capacity (μmoles g^{-1} of FA) with Solution pH 66

Table 2-4.1 Comparison of the Measured Maximum Binding Capacities of Various Natural Organic Matter(NOM) Samples 71

CHAPTER 3 73

Table 3-2.1 Constants for the Spreadsheet Calculations (Exp. #7) 83

Table 3-3.1 Basic Experimental Parameters for Bulk Soil Kinetics 90

Table 3-3.2 HPLC Operating Parameters (Varian Star 9010 or Waters) 91

Table 3-4.1 Results of Mineral Analyses for GB 843 Bulk Soil 92

Table 3-4.2 EDS Peak Listing for Soil GB 843 (Collected over 60x5 seconds) 98

Table 3-4.3 Results for Measurement of the Labile Sorption Capacity (Bulk soil GB 843 at 25 °C) 99

Table 3-5.1 Fitted Data for the Rapid Initial Uptake of Atrazine (Exp. #7, initial atrazine = 1.00 x 10^{-6} M) 104

Table 3-5.2 Fitted Data for Atrazine Species Distribution with Time Shown in Fig. 3-5.4 106

Table 3-5.3 Characteristic Times of the Plateau Region Shown in Labile Sorption Curves 110

Table 3-5.4 Results of Labile Sorption Equilibrium for Bulk Soil at 25 °C 111

Table 3-5.5 Results of Labile Sorption Kinetics by Initial Rate Approximation Method for Bulk Soil at 25 °C 114

Table 3-5.6 Diagnostic Test for Intraparticle Thermal Diffusion (or Any Other Process Describable by an Effective Diffusion Coefficient) Mechanisms (Based on linearized solutions for Fick's law presented by Crank (66)) 119

Table 3-5.7 Diagnostic Tests for Bulk Soil Intraparticle Diffusion at 25 °C 119

Table 3-5.8 Results of Intraparticle Diffusion Kinetics for Bulk Soil at 25 °C (by eqs. 3-2.12 and 3-2.16) 121

Table 3-5.9 Correlation of Diffusion Time Rate ($d\theta_L/dt$) to Labile Site Coverage (θ_L) for Bulk Soil at 25 °C (by eqs. 3-2.15 and 3-2.16) 122

Table 3-5.10 Least Squares Fitting Results for Some Experimental Data of Nonlabile Sorption (Bulk soil at 10 °C) 128

CHAPTER 4 132

Table 4-2.1 Basic Experimental Parameters of Soil Fraction Kinetics 135

Table 4-3.1 Particle Size Limits According to Several Current Classification Schemes (100) 137

Table 4-3.2 Particle Size Distribution of Soil GB 843 138

Table 4-3.3 EDS Peak Listing for Fraction #5 (Collected over 60x5 seconds) 139

Table 4-3.4 Semi-Quantitative Results of EDS for Carbon Contents in Soil Fractions (Collected over 60x5 seconds) 139

Table 4-3.5 Measurements of Specific Surface Area for Soil Fractions 140

Table 4-3.6 Organic Carbon Analyses for Soil Fractions 141

Table 4-3.7 Measurements of Labile Sorption Capacities for Soil Fractions 143

Table 4-4.1 Atrazine Concentration Profile at Selected Times 144

Table 4-4.2 Results of Labile Sorption for Soil Fraction Kinetics 149

Table 4-4.3 Results of Intraparticle Diffusion for Soil Fraction Kinetics 159

Table 4-4.4 Correlation of Diffusion Time Rate with Labile Surface Coverage for Soil Fractions 160

Table 4-4.5 Diagnostic Tests for Soil Fraction Intraparticle Diffusion 160

CHAPTER 5 170

Table 5-2.1 Experimental Conditions for Temperature Effect Kinetics 175

Table 5-3.1 Labile Sorbed Atrazine at the Maximum of Sorption Curves 180

Table 5-3.2 Results of Labile Surface Sorption for Temperature Effect Kinetics 182

Table 5-3.3 Nonlabile Sorbed Atrazine at the Maximum of Sorption Curves 185

Table 5-3.4 Results of Intraparticle Diffusion for Temperature Effect Kinetics 187

Table 5-3.5 Temperature Dependence of $\bar{K}_l$, k_{sl}, and k_{dl} (van't Hoff and Arrhenius treatments) 191

CHAPTER 6 198

Table 6-2.1 Main Operating Conditions for the Soil Columns 202

Table 6-2.2 Basic Properties of the Soil Cores Used in This Study 203

Table 6-4.1 Atrazine Concentration Distribution (by two stage) 222

Table 6-4.2 Atrazine Amount Distribution (by two stage) 224

Table 6-4.3 K_d Profile with Nodal Points for Column 2 227

Table 6-4.4 X_1 Profile with Nodal Points for Column 2 227

Table 6-4.5 Atrazine Concentration Distribution (for Column 1 by conventional approach) 232

LIST OF FIGURES

CHAPTER 1 PAGE

Fig. 1-1.1 Effect of the Clay and Organic Matter on Sorption of Atrazine (124) 14

Fig. 1-1.2 Effect of Organic Matter to Clay Ratio on Sorption and K_{oc} of α-naphthol (120) 14

Fig. 1-1.3 A Schematical Representation for Microfiltration-HPLC Technique 41

CHAPTER 2 45

Fig. 2-1.1 Lindane (γ-1,2,3,4,5,6-hexachlorocyclohexane) 48

Fig. 2-2.1 Stability of Aqueous Lindane Solutions (KCl=0) 51

Fig. 2-2.2 Recovery of Lindane as a Function of Filtrate Volume (A. Static; B. Dynamic) 54

Fig. 2-2.3 Parallel Experiments Showing the Effect of Membrane Background 56

Fig. 2-3.1 Equilibrium Lindane as a Function of Lindane Added (FA=300 ppm, pH=1.17, KCl=0) 59

Fig. 2-3.2 Equilibrium Lindane as a Function of Lindane Added (FA=1,000 ppm, pH=2.04, KCl=0) 60

Fig. 2-3.3 Equilibrium Lindane as a Function of Lindane Added (FA = 1,000 ppm, pH=4.98, KCl=0.100 M) 61

Fig. 2-3.4 Lindane Bound as a Function of Lindane Added (FA=1,000 ppm, KCl: A=0, B=0.100 M) 62

Fig. 2-3.5 Lindane Binding Capacity as a Function of Carboxyl Group Molarity (FA=1,000 ppm) 68

Fig. 2-3.6 Dependence of Lindane Binding on FA Concentration 69

CHAPTER 3 73

Fig. 3-1.1 Atrazine (2-chloro-4-(ethylamino)-6-(isopropylamino)-s-triazine) 75

Fig. 3-2.1 A Schematical Representation of Atrazine Mass Transfer 76

Fig. 3-4.1 Selected Microscopic Pictures for Bulk Soil (a) and Soil Fractions #1-#5 (b-f) 94

Fig. 3-4.2 Selected Microscopic Pictures for Bulk Soil Slurry at 1 (a), 5 (b), 10 (c) and 20 (d) Days 96

Fig. 3-4.3 Spectrum of EDS for Bulk Soil (Collected over 60x5 seconds) 98

Fig. 3-4.4 Measurement of the Labile Sorption Capacity for Bulk Soil GB 843 at 25 °C 99

Fig. 3-5.1 Atrazine Species Distribution with Time (Exp. #7, bulk soil at 25 °C) 101

Fig. 3-5.2 Atrazine Species Distribution with Time (Exp. #7, bulk soil at 25 °C) 102

Fig. 3-5.3 Atrazine Species Distribution with Time (Exp. #7, bulk soil at 25 °C) 105

Fig. 3-5.4 Atrazine Species Distribution with Time (Exp. #20, bulk soil at 25 °C) 108

Fig. 3-5.5 Atrazine Species Distribution with Time (Exp. #20, bulk soil at 25 °C) 109

Fig. 3-5.6 A Plot of $(dC_l/dt)_{t=0}$ vs. M_{AT} Showing the Initial Rate Approximation Calculation of Pseudo First-Order Rate Constant (k_{sl}) 116

Fig. 3-5.7 Diagnostic Test for Bulk Soil Intraparticle Diffusion at 25 °C (Exp. #14) 120

Fig. 3-5.8 Correlation of Diffusion Time Rate ($d\theta_D/dt$) to Labile Site Coverage (θ_L) for Bulk Soil at 25 °C 124

Fig. 3-5.9 Atrazine Species Distribution with Time (Exp. #29, bulk soil at 10 °C) 126

Fig. 3-5.10 Atrazine Species Distribution with Time (Exp. #29, bulk soil at 10 °C) 127

CHAPTER 4 132

Fig. 4-3.1 Measurement of Labile Sorption Capacity for Fraction #1 142

Fig. 4-4.1 Atrazine Concentration Profile with Time for Fraction #4 146

Fig. 4-4.2 Atrazine Species Distribution with Time for Fraction #2 147

Fig. 4-4.3 Rate Constant k_{sl} as a Function of Specific Surface Area 152

Fig. 4-4.4 Rate Constant k_{sl} as a Function of Organic Carbon Contents 153

Fig. 4-4.5 Sorption Capacity θ_c as a Function of Specific Surface Area 154

Fig. 4-4.6 Sorption Capacity θ_c as a Function of Organic Carbon Contents 155

Fig. 4-4.7 Relationship Overview among θ_c, X_1, $\bar{K}_1$, K_d and k_{sl} 156

Fig. 4-4.8 Diagnostic Tests for Soil Fraction Intraparticle Diffusion 161

Fig. 4-4.9 Correlation of D and k_{dl} with Specific Surface Area 165

Fig. 4-4.10 Correlation of D and k_{d1} with Organic Carbon Contents 166

CHAPTER 5 170

Fig. 5-3.1 Atrazine Species Distribution with Time (Fitted data at 5 °C) 177

Fig. 5-3.2 Atrazine Species Distribution with Time (Fitted data at 15 °C) 178

Fig. 5-3.3 Atrazine Species Distribution with Time (Fitted data at 35 °C) 179

Fig. 5-3.4 k_{s1} as a Function of Temperature (Line graph) 183

Fig. 5-3.5 Sorbed Atrazine as a Function of Temperature (Symbols=Exp., Lines=Fit.) 186

Fig. 5-3.6 D and k_{d1} as a Function of Temperature (Line graph) 188

Fig. 5-3.7 $\bar{K}_1$ Temperature Dependence (van't Hoff plot) 192

Fig. 5-3.8 k_{s1} Temperature Dependence (Arrhenius plot) 193

Fig. 5-3.9 k_{d1} Temperature Dependence (Arrhenius plot) 194

CHAPTER 6 198

Fig. 6-3.1 Information Transfer Diagram for the Model Components 208

Fig. 6-3.2 Concentration Profile with Depth (For advection only, t=5 h, K_d=0) 211

Fig. 6-3.3 Concentration Profile with Time (For 1-site, x=100 cm, K_d=0.62 $cm^3\ g^{-1}$) 212

Fig. 6-4.1 Atrazine Conc. Profile with Time: 30 cm (Column 1) 214

Fig. 6-4.2 Atrazine Conc. Profile with Time: 50 cm (Column 1) 215

Fig. 6-4.3 Atrazine Conc. Profile with Depth: 10 days (Column 1) 216

Fig. 6-4.4 Atrazine Conc. Profile with Time: 10 cm (Column 2) 217

Fig. 6-4.5 Atrazine Conc. Profile with Time: 60 cm (Column 2) 218

Fig. 6-4.6 Atrazine Conc. Profile with Depth: 15 days (Column 2) 219

Fig. 6-4.7 Atrazine Conc. Profile with Depth: 0.6 days (Short column) 220

Fig. 6-4.8 Atrazine Amount Distribution (Column 1 by two stage) 225

Fig. 6-4.9 Atrazine Amount Distribution (Column 2 by two stage) 226

Fig. 6-4.10 Sensitivity Analysis: 10 cm (τ^{-1} for Column 2) 230

Fig. 6-4.11 Statistical Analysis: 30 cm (Column 1) 234

Fig. 6-4.12 Statistical Analysis: 10 cm (Column 2) 235

NOMENCLATURE

a	cross sectional area related to particle sizes and shapes (defined by eq. 3-2.16)
b	Langmuir intensity coefficient (defined by eq. 1-1.1)
C (or C_e)	solute concentration in the solution phase, i.e., the mass of the solute retained per unit of aqueous phase (moles L^{-1}, subscript e = equilibrium)
C(k,t)	total concentration of all the unreacted components (moles L^{-1}, defined by eq. 1-1.10, t = time, and k = rate constant)
$C_{o,i}$	initial concentration of i^{th} component (moles L^{-1}, defined by eq. 1-1.10)
C_o	solute aqueous concentration at the upgradient boundary (moles L^{-1}, $\Delta x = 0$, defined by eq. 1-1.25)
C_T	total applied sorbate concentration (moles L^{-1})
C_δ	solute aqueous concentration at the downgradient boundary (moles L^{-1}, $\Delta x = \delta$, defined by eq. 1-1.25)
C_1	steady-state surface coverage (g cm^{-2}, defined by eq. 3-2.11)
C'(r)	sorbate concentration free in pore fluid (moles cm^{-3}, defined by eq. 1-1.32. r = radial distance)
D	diffusion coefficient ($cm^2\ s^{-1}$, defined by Crank's solution, eq. 3-2.11)
D_a	apparent diffusion coefficient ($cm^2\ s^{-1}$)
D_b	bulk aqueous diffusivity ($cm^2\ s^{-1}$)

D_{eff} (or D_e)	effective diffusion coefficient ($cm^2\ s^{-1}$)
D_m	pore fluid diffusivity of the sorbate ($cm^2\ s^{-1}$, defined by eq. 1-1.11)
D_p (or D_s)	effective pore (p) or surface (s) diffusion coefficient ($cm^2\ s^{-1}$)
D_l	diffusion coefficient ($cm^2\ s^{-1}$, defined by eq. 1-1.21)
E_a	activation energy ($kJ\ mol^{-1}$)
F	fraction of sorbent for which sorption is fast (defined by eq. 1-1.42)
$F_{l,x}^{o}$	flux of diffusing substance through unit cross section (defined by Fick's first law, eq. 1-1.21. x = space coordinate measured normal to the section)
f	fraction of micropore (defined by eq. 6-3.2)
$f(\epsilon,\tau)$	pore geometry factor (ϵ = porosity, and τ = tortuosity)
H(k,t)	second-order numerical approximation of the Laplace transform of C(k,t) defined by eq. 1-1.10 ($L\ mol^{-1}\ s^{-1}$)
ΔH^o	standard enthalpy change ($kJ\ mol^{-1}$)
K (or K_{om})	solute partition coefficient, i.e., the ratio of the solute concentration in organic phase to that in water ($L\ g^{-1}$, defined by eq. 1-1.5), or weighted average equilibrium function (M^{-1}, defined by eq. 1-1.9)
K_d (or K_p)	sorption equilibrium distribution (partition) coefficient, i.e., the ratio of solute concentration in solid phase to that in aqueous phase ($L\ g^{-1}$)
K_{di}	internal distribution coefficient ($L\ g^{-1}$, defined by eq. 1-1.40)
K_{eq}	sorption equilibrium constant (M^{-1})
K_F	Freundlich capacity coefficient (defined by eq. 1-1.3)
$\bar{K}_M$	mean law of mass action concentration quotient (M^{-1}, defined by eq. 1-1.7)
K_{oc}	organic carbon-normalized linear isotherm coefficient ($L\ g^{-1}$)

K_{ow}	octanol-water partition coefficient (dimensionless)
K_r	constrictivity factor (≤ 1)
$\bar{K}_1$	weighted average sorption equilibrium function (M^{-1})
k_a	pseudo first-order solute degradation rate for solute loss in the solution phase (h^{-1}, defined by eq. 1-1.34)
k_{b1}	second-order rate constant for adsorption ($L\ mol^{-1}\ d^{-1}$)
k_{d1}	first-order rate constant for inward intraparticle diffusion (d^{-1})
k_f	second-order rate constant for the forward sorption ($L\ mol^{-1}\ d^{-1}$, defined by eq. 1-1.14)
k_f'	pseudo first-order rate constant (d^{-1}, defined by eq. 1-1.19)
k_h	Henry's law constant
k_r	desorption rate constant (d^{-1}, defined by eq. 1-1.15)
k_s	pseudo first-order solute decay coefficient in the solid phase (h^{-1}, defined by eq. 1-1.35)
k_{s1}	pseudo first-order rate constant for adsorption (d^{-1})
k_{s2}	first-order rate constant for desorption (d^{-1})
k_1	adsorption rate constant for type 2 sites (n^{th} order defined by eq. 1-1.28), or forward first-order rate constant (h^{-1}, defined by eq. 1-1.43)
k_{-1}	desorption rate constant for type 2 sites (defined by eq. 1-1.28)
k_2	reverse first-order rate constant (h^{-1}, defined by eq. 1-1.43), or first-order rate constant for net movement into S_2 (d^{-1}, defined by eq. 1-1.29)
L_f (or L_c)	solute concentration in the filtrate (f) and in the cell (c) (μmoles L^{-1})
l	mean particle radius (cm) used as a crude approximation for the dimension of a particle (l^2)

lhs	left-hand side of the partial differential equation
M_A	sorbate concentration in the solution phase (moles L^{-1}, defined by eq. 1-1.14)
M_{AT}	atrazine concentration in the solution phase (moles L^{-1})
M_{L_i}	molarities of free ligands in aqueous phase (defined by eq. 1-1.9)
M_t	total amount of material taken up by diffusion at time t (defined by eq. 3-2.11)
m_c	molarities of ion exchange sites occupied by metal ion M^{n+} (defined by eq. 1-1.7)
m_H	molarities of protons in the external solution (defined by eq. 1-1.7)
m_M	molarities of metal ions in the external solution (defined by eq. 1-1.7)
m_{SH2}	molarities of ion exchange sites occupied by pairs of protons (defined by eq. 1-1.7)
n	Freundlich exponent (defined by eq. 1-1.3)
$p\theta_t$	sorption capacity for the bulk soil (moles g^{-1}, defined by eq. 6-4.7)
Q	conversion factor for time units (86,400 s d^{-1})
Q^o	sorbed solute concentration on the sorbent corresponding to complete monolayer coverage (defined by Langmuir isotherm, eq. 1-1.1)
q (or q_e, q_r)	solid-phase concentration of the solute, i.e., the mass of the solute sorbed per unit of sorbing phase or interface (moles g^{-1} of solids, subscripts e = equilibrium, and r = radial position), or water flux (cm d^{-1}, defined by eq. 6-3.1)
R	gas constant (8.314 J mol^{-1} K^{-1})
R_{d2}	outward intraparticle diffusion term (defined by eq. 1-1.49)
R_{int}	internal retardation factor (defined by eq. 4-4.6)

S	sorbent phase sorbate concentration (moles g^{-1} of solids)
$S(r)$	local total volumetric concentration in porous sorbent (moles cm^{-3}, defined by eq. 1-1.30. r = radial distance)
S_w	molar water solubility of the solute as a liquid or supercooled liquid at the system temperature (defined by eq. 1-1.5)
S_1 (or S_2)	sorbed phase concentration (moles g^{-1} of solids) in labile state or fast domain (1), and nonlabile state or rate-limited domain (2)
$S'(r)$	concentration of the immobile bound state (moles g^{-1}, defined by eq. 1-1.32. r = radial distance)
T	absolute temperature (°K)
t	time (seconds or days)
V	molar volume of the solute (defined by eq. 1-1.5)
V_o	initial volume of the solute in the ultrafiltration cell (mL, defined by eq. 2-2.1)
V_s	volume of standard stock solution having a concentration C_s (mL, defined by eq. 2-2.1)
v (or v_o)	hydraulic conductivity or Darcy flux (cm d^{-1}, subscript o = constant velocity)
v_f	forward rate or velocity of sorption (moles L^{-1} d^{-1}, defined by eq. 1-1.14)
v_r	desorption rate (moles L^{-1} d^{-1}, defined by eq. 1-1.15)
X_1	mole fraction of sorbed solutes in the S_1 state (defined by eq. 1-1.29), or of occupied labile sorption sites (defined by eq. 3-2.8)
x_l (or x_{nl})	mass fraction (defined by eq. 1-1.37. subscripts l = linear sorptions, and nl = nonlinear sorptions)
α	mass transfer constant (defined by eq. 1-1.46)
ϵ	porosity of the sorbent (cm^3 of fluid cm^{-3} total, defined by eq. 1-1.11)

ϵ_i	internal porosity of the sorbing grains (pore volume/volume of grain, defined by eq. 1-1.38)
$\theta_{A\text{-}S}$	concentration of site-binding complex (moles g^{-1}, defined by eq. 1-1.15)
θ_c (or C_c)	labile sorption capacity (θ in moles g^{-1}, and C in moles L^{-1})
θ_D (or C_D)	nonlabile sorbed or intraparticle diffused sorbate concentration, i.e., the portion nonextracted rapidly by the HPLC mobile phase (θ in moles g^{-1}, and C in moles L^{-1})
θ_L (or C_L)	labile sorbed sorbate concentration (θ in moles g^{-1}, and C in moles L^{-1})
θ_o (or C_o)	concentration of vacant sorption sites (θ in moles g^{-1}, and C in moles L^{-1})
θ_w (or θ_{w_s})	volumetric moisture content (cm^3 of soil solution cm^{-3} of bulk soil, subscript s = saturation)
ϕ	sink terms such as volatilization, chemical degradation and microbial degradation (defined by eq. 6-3.1)
ρ (or ρ_s)	solid-phase bulk density, i.e., the mass per unit volume of bulk solids (g cm^{-3})
ρ_r	apparent grain density, i.e., the mass per unit volume of grain (g cm^{-3}, defined by eq. 1-1.38)
γ_w	solute activity coefficient in water
γ_w^*	solute activity coefficient in solvent-saturated water
τ	tortuosity factor (≥ 1)
λ	dispersivity factor
χ	Flory-Huggins interaction parameter
∇^2	Laplacian operator

CHAPTER 1

INTRODUCTION

1-1. EQUILIBRIUM AND KINETICS OF PESTICIDE UPTAKE BY SOILS: A REVIEW

With increasing concern over environmental pollution, research on contaminant transport and fate, contaminant transport modeling, and groundwater/soil remediation technology has grown rapidly. Knowledge of the various physical, chemical, and biological processes that affect the properties and behavior of contaminants is essential for such research. Of the various processes, sorption is one of the most important which can have profound effects on contaminant persistence, movement and removal, and has therefore become an area of active research during the last two decades.

In comparison to well-defined adsorbents, the soil can be regarded as a mixed adsorbent. The main constituents representing the solid phase (making up about 50% of the soil volume) are clay minerals, organic matter, oxides and hydroxides of aluminum and silicon. Both clay and organic matter are considered to be of significance to sorption. The soil organic matter contains compounds that may conventionally be grouped into nonhumic and humic substances. On the other hand, one of the main characteristics of pesticides is that most of them are low molecular weight organic compounds with low

water solubility. Information about soil nature, pesticide structure and some physicochemical properties is important for the understanding of sorption processes.

This chapter will present a review on studies of equilibrium and kinetics of pesticide uptake by soils and soil constituents, including mechanistic concepts, mathematical approaches to sorption phenomena, and experimental methodologies. Particular emphasis is given to the current levels of understanding and typical kinetic models associated with the sorption processes.

1-1.1. SORPTION PHENOMENA

The term *sorption* describes the uptake of a solute by soil or soil constituent without reference to a specific mechanism. Sorption interactions generally operate among all phases present in any subsurface systems and at the interfaces between these phases. Solutes which undergo sorption are commonly termed *sorbates*, the sorbing phase the *sorbent*, and the primary phase from which sorption occurs the *solution* or *solvent*. Thermodynamically, sorption occurs when the free energy of the sorption reaction is negative: $\Delta G = \Delta H - T\Delta S$. The free energy of a sorption reaction can be negative because of the enthalpy term or because of the entropy term or due to contributions of both. The enthalpy term is primarily a function of the difference in interaction between the adsorbing surface and the sorbate (solute) and interaction between the solvent (water) and the solute. The entropy term is related to the increase or decrease in the order of the system upon sorption. For a chemical reaction at equilibrium, the standard free energy

(ΔG°) can be calculated from the equilibrium constant (K), the standard enthalpy change (ΔH°) can be calculated from the variation of K with temperature, and ΔS° calculated as the difference: $\Delta S^\circ = (\Delta H^\circ - \Delta G^\circ)/T$.

Two broad categories of sorption phenomena, adsorption and absorption, can be differentiated by the degree to which the sorbate molecule interacts with and is free to migrate within the sorbent phase. In adsorption, solute accumulation is generally restricted to a surface or interface between the solution and adsorbent. In contrast absorption is a process in which solute transferred from one phase to another penetrates the sorbent phase by at least several nanometers.

Sorption processes can be driven by a variety of forces and/or mechanisms that can affect the relative bonding (ΔH) of the sorbate and sorbent vs. the solvent and solute and by factors that affect the overall randomness (ΔS) or order of the system (113,124,136). Although there is not universal agreement on the best description of these forces or mechanisms, physisorption and chemisorption are operationally defined by interaction energy. In a complex matrix such as soil, a number of types of forces and interactions are possible. The most frequently mentioned are enthalpy and entropy related adsorption forces.

(1). *Enthalpy related adsorption forces*

London-van der Waals/Dipole-Induced Dipole/Dipole-Dipole. The former includes the forces that arise from momentary dipoles about atoms or molecules caused by small perturbations of electronic motions. These dipoles induce small dipoles in neighboring

atoms of opposite sign. The dipole-dipole or induced dipole forces result from the attracion of permanent dipoles or the attraction of an induced dipole brought about by either a permanent dipole or a charged site or species. Dipole-dipole (and ion-dipole) forces can be much larger, except for van der Waals forces which are short range and weak (<8 kJ mol^{-1}), but their additive nature may result in considerable attraction for large molecules (204). Haque and Coshow (116) attributed adsorption of isocil on both montmorillonite and kaolinite to van der Waals interactions.

Coulombic-Electrostatic. An electrostatic force results from charged surfaces due to isomorphous substitution in the mineral lattice or protonation or dissociation of surface H_2O and OH groups. This force results in the Coulombic attraction of oppositely charged species (ion-ion, ion-dipole). Ion exchange adsorption takes place for those pesticides that either exist as cations or anions, or that become charged through protonation or deprotonation. There is little doubt that organocations (e.g., paraquat and diquat) bind by a cation exchange mechanism in soils (128). This binding is driven by electrostatic forces at specific sites of negative charge on clay surfaces, clay interlayers, and in humic matrix, where the anions most often are dissociated carboxyl groups.

Charge Transfer. Formation of a donor-acceptor complex between an electron-donor molecule and an electron-acceptor molecule. It involves the partial overlap of their respective molecular orbitals and a partial exchange of electron densities between high energy HOMOs (high occupied molecular orbitals) and low energy LUMOs (low unoccupied molecular orbitals). For example, π orbital interactions are perpendicular to the aromatic rings. These bonds have been hypothesized to explain, partially, the bonding

of alkenes, alkylenes, and aromatic compounds to soil organic matter (124).

Hydrogen Bonding. This is a special type of dipole-dipole interaction between the hydrogen atom in a polar bond such as O-H or N-H, and an electronegative atom O, N, or F. The average energy of a hydrogen bond is quite variable (ranging from 8 to 42, up to 167 kJ mol^{-1}). Thus, hydrogen bonds play a very important role in determining the structures and properties of many systems (43). Hydrogen bonding appears to be the most important mechanism for adsorption of hydroxylated or amine nonionic organic molecules on clay minerals (152). Participation of a hydrogen bonding mechanism in s-triazines and organic matter interactions has been reported by a number of investigators (126,281-283). Evidence for this type of bonding was obtained from infrared studies by Sullivan and Felbeck (268).

Ligand Exchange. Adsorption by this mechanism involves replacement of one or more ligands of matrix-bound metal complexes by the adsorbate molecule. The necessary condition is that the molecule is a sufficiently strong ligand.

(2). ***Entropy related adsorption forces***

Hydrophobic Bonding. This type of interaction denotes the binding or partitioning of nonpolar organics out of the polar aqueous phase onto hydrophobic surface sites in soil. The hydrophobic sites are most often assigned to soil organic matter, but may also include -Si-O-Si- bonds at the mineral surfaces (124). The major feature of hydrophobic sorption is a weak interaction. The primary force appears to be the large entropy change resulting from the removal of the solute from solution. The entropy change is large due

to the destruction of the cavity occupied by the solute in the solvent and the disruption of the structured water shell surrounding the solvated organic. Nonpolar pesticides or compounds whose molecules often have nonpolar regions of significant size in proportion to polar regions are likely to adsorb onto soil organic matter by this type of bonding. Pierce et al. (224) indicated that the association of nonpolar (chlorinated hydrocarbons) pesticides with lipid fraction of soil organic matter and humus can be described by hydrophobic bonding.

Of the above, the sorption forces outlined in section (1), and to some extent in section (2), are site-directed; that is, they involve interactions that occur with particular functional groups at discrete sites on soil surfaces or within the soil organic phase. Carboxyl and phenolic hydroxyl groups are the primary surface functional groups involved in surface complexation reactions on soil organic matter, whereas the most abundant surface group on oxide surfaces and clay minerals is the hydroxyl group (262). In addition, several forces may operate simultaneously for sorption of a given compound, but one type is usually more significant than the others. Speaking kinetically, it is widely held that physisorption of small molecules on exposed surfaces occurs with zero or negligible activation energies (6,129). This applies to the vast majority of contaminants of interest in soils. In contrast, bonding in the category called chemisorption usually involves covalent or other strong bond making between solute molecules and sorbent specific surface sites, and is characterized by relatively large heats of sorption (>29 kJ mol^{-1}). The kinetics may exhibit substantial activation energies (226,288).

1-1.2. SORPTION EQUILIBRIA AND ISOTHERMS

The eventual equilibrium distribution of a solute between the solution phase and sorbent (absorption) or interface (adsorption) is determined by a corresponding energy balance, and thus may be discussed thermodynamically. The mathematical approach for describing the equilibrium distribution typically relates the amount of solute sorbed per unit of sorbing phase or interface, q_e, to the amount of solute retained in the solution phase, C_e. An expression of this type evaluated at a fixed system temperature constitutes what is termed a sorption "isotherm". A number of conceptual and empirical models have been developed to describe these adsorption patterns. The most widely used are the Langmuir model and Freundlich equation.

(1). *Langmuir model*

The Langmuir model is conceptually the most straightforward isotherm. It was initially derived from the adsorption of gases by solids using the assumptions that the energy of sorption for each molecule is the same and independent of surface coverage, and that sorption occurs only on localized sites and involves no interactions between sorbent molecules. The Langmuir adsorption equation may be expressed as:

$$q_e = Q^o bC_e/(1 + bC_e) \qquad (1\text{-}1.1)$$

The parameter Q^o represents the sorbed solute concentration on the sorbent corresponding to complete monolayer coverage, i.e., a limiting capacity, and b is a sorption coefficient related to the free energy of adsorption. Where $bC_e << 1$, the Langmuir isotherm

reduces to a linear relationship, similar to the behavior described by a diffusion coefficient. The reciprocal of eq. 1-1.1 gives:

$$1/q_e = 1/Q^o + (1/bQ^o)1/C_e \qquad (1\text{-}1.2)$$

If the Langmuir isotherm is a quantitative description, it suggests sorption at well defined specific sites separated from each other and similar in chemistry.

(2). ***Freundlich equation***

Another nonlinear sorption model is the Freundlich equation which describes the accumulation of solute by the sorbent as exponentially proportional to the solution phase concentration:

$$q_e = K_F C_e^n \qquad (1\text{-}1.3)$$

where parameter K_F relates to sorption capacity, and n to sorption intensity. The linear portion of the isotherm represents the case where the exponential term (n) of eq. 1-1.3 is equal to unity. For determination of these empirical derived parameters, data are usually fit to the logarithmic form of eq. 1-1.3:

$$\mathrm{Log}q_e = \mathrm{Log}K_F + n\mathrm{Log}C_e \qquad (1\text{-}1.4)$$

The Freundlich parameters have no specific thermodynamic or stoichiometric significance.

(3). ***Nonsingularity of sorption isotherms***

The reversibility of sorption reactions between dissolved organic chemicals and naturally occurring soils, sediments, and suspended particles is of fundamental

importance in the understanding of the fate of these chemicals in the environment. This becomes critical if the adsorption-desorption behavior of a chemical is to be expressed quantitatively within the framework of mass balance equations, which are frequently used in mathematical models of chemical leaching and transport. Ideal or reversible behavior means that the same isotherm applies for adsorption and desorption at equilibrium. Many laboratory adsorption/desorption experiments, however, appear to demonstrate hysteresis or nonsingularity; that is, the measured desorption does not coincide with the adsorption isotherm (68,74,113,135,157,226,232).

The potential causes for the nonsingularity could be as follows: 1) artifacts due to the method; 2) chemical or biological transformations of sorbed compounds; 3) competitive adsorption from natural (implicit) adsorbates; 4) irreversible or resistant fractions of sorbed chemicals; and 5) failure to establish adsorption and/or desorption equilibrium. A number of studies have shown a fraction of sorbed compounds as being unrecoverable, even after extensive extraction procedures. It has been labeled the irreversible or resistant fraction (74,109,135,137,271), or bound residues (151,232,264).

1-1.3. MECHANISTIC CONSIDERATIONS ABOUT SORPTION

A surface complexation model accounting for aqueous metal ion adsorption onto oxide surfaces has been well understood and appreciated for several decades (6,16,17,22,71,125,130,269). In recent years, investigations of the factors controlling the uptake of organic compounds by soils have become much more prominent because of the

widespread use of pesticides, and the public concern over the likelihood of environmental contamination. As a result of this continuing effort, this area of research has been focused on the mechanism involved in sorption interactions between organic compounds and soils.

(1). *Two schools of thought*

For nonionic organic compounds in soils, which covers the most common situations for pesticide-soil interactions in the soil subsurface environment, there are generally two schools of thought on the nature of the sorptive interactions. One holds that sorption occurs by hydrophobic partitioning between soil solution and a hydrophobic phase found in soil organic matter (49,53). Another is a surface adsorption or site binding model based on specific interactions between a solute and specific soil surface sites and analogous to the complexation model for metal ions (17,97,124,177,203,281-283).

The partition model with a characteristic distribution coefficient, K_d, has been favored for organic compounds with low water solubility. It is based on three postulates. The first is that the soil organic matter or a humic material simply acts as organic solvent that is present as a separate physical phase. The second is that this second physical phase has only non-specific, nonlocalized solute-solvent interactions. The third postulate is that the solute is distributed between the aqueous and organic solvent phases according to the entropy of mixing as modified by activity coefficients in the two phases. This model has successfully correlated structure-binding tendency relationships over a wide range of compounds (53,124). In contrast, the site binding model considers the sorption processes

as arising from specific interactions between functional groups, resulting from most of the driving forces addressed earlier. These may be direct interactions with the sorbent or interactions with the sorbent which creates hydrophobic sites. The site binding model involves a wide range of reaction types, such as charge transfer, hydrogen bonding, a variety of London-van der Waals, dipole or induced dipole interactions, and even the bonding with hydrophobic sites (113,124,169,281-283).

The problem with the partition model is that the dominant soil organic component, humics, are more than 40% oxygen and rich in polar functional groups (-OH, -COOH) which are hydrophilic and bind water strongly (247,265,266,281). Moreover, the polyelectrolyte molecules of a low MW humic, fulvic acid do not possess a separate, macroscopic phase volume into which a monomeric solute can be partitioned in a nonlocalized fashion. This is highlighted by the polydisperse nature of typical fulvic acids. Their molecular weights range from a few thousand daltons down to values not much greater than that of DDT (42). At the lower end of this range in solution, there is an awkward question about which of the molecules is solute and is being partitioned into the other. As well, the specific interaction model has been supported by more recent experimental results. In particular, for the case of atrazine interacting with soil organic matter, theoretical prediction and experimental demonstration of specific, localized binding sites have been in the literature for about a decade. Borggaard and Streibid, in studying atrazine adsorption by soils, observed that hydrogen bonding was closely related to undissociated carboxyl and phenol groups (22). The Bronsted acid catalysis of atrazine hydrolysis that was demonstrated by Perdue and Wolfe, as has been verified by more

recent work (89,93,221,222), depends on a limited set of specific sites. The mechanism for the catalysis requires that the atrazine be sorbed onto specific, localized, catalytically active binding sites. Kinetic rate constants correlated with numbers of protonated carboxylic groups, but 1% or less of the total carboxylic groups served as catalytic binding sites. In addition, the titration of both fulvic and humic acids with atrazine revealed a plateau caused by the saturation of sorption sites (281,282). The pH dependence of the binding capacities observed in this way for both fulvic and humic acids was consistent with pH and ionic strength effects on aggregation that were investigated by Rayleigh light scattering (275). Hydrolysis rate constants and binding capacities independently indicated that protonated carboxylic groups were essential to atrazine binding, and 1% or less of these protonated carboxylic groups participated in the interaction with atrazine. The partition model is not consistent with this 10-year accumulation of experimental results. Chapter 2 will take up a demonstration of the same problems for a nonpolar pesticide, challenging the use of the K_d model in its most favorable domain (169).

As will be seen in the next section, four categories of experimental phenomena have been observed to be the characteristics of the partition model (53). In fact, it is possible to interpret these with the site binding model.

The sorption of many if not most nonpolar organics on soils and sediments produces linear isotherms up to 60 to 80% of the aqueous concentrations of the sorbing species water solubility (47,123,141,184). At aqueous concentrations above that range, however, the isotherms usually appear to turn down sharply. This phenomenon has also been

observed in the reactions of polar herbicide atrazine with aqueous or soil humics (281-283), and has been explained with a specific site binding mechanism. The nonlinearity at higher concentrations is the result of site saturation. It is generally accepted that isotherm linearity is associated with the low aqueous concentration of sorbing species as shown in the Langmuir equation (eq. 1-1.1) where $bC_e << 1$, and in the Freundlich equation (eq. 1-1.3) where $n = 1$, regardless of mechanism.

The sorption of nonionic organic compounds by soils has been shown to be highly correlated with soil organic matter content (47,123,141,184), which has been viewed as an important supporting characteristic for the partition uptake model (53). Although this observation can be readily correlated to the water solubility of individual compounds, it is equally readily correlated to the polyfunctional group property of soil organics. As indicated by Hassett and Banwart in studying the correlation of compound properties with sorption behavior (122,124), the sorption of compounds where a specific interaction between functional groups is involved could also show a strong positive linear correlation with soil organic matter. Furthermore, they pointed out that one major limitation to the use of K_{oc} (organic carbon sorption coefficient) - K_{ow} (octanol-water partition coefficient) or K_{oc} - S_w (water solubility) relationships is that these relationships do not include the potential contribution of soil minerals to sorption, particularly in low organic matter, high clay soils (120,124,149). Fig. 1-1.1 illustrates the effect of clay and organic matter on the sorption of atrazine by soils with a wide range of organic matter contents (267). When the organic matter content was below 6 to 8%, the magnitude of the estimated sorption "constant" K_d was significantly correlated with both clay and organic matter. K_d

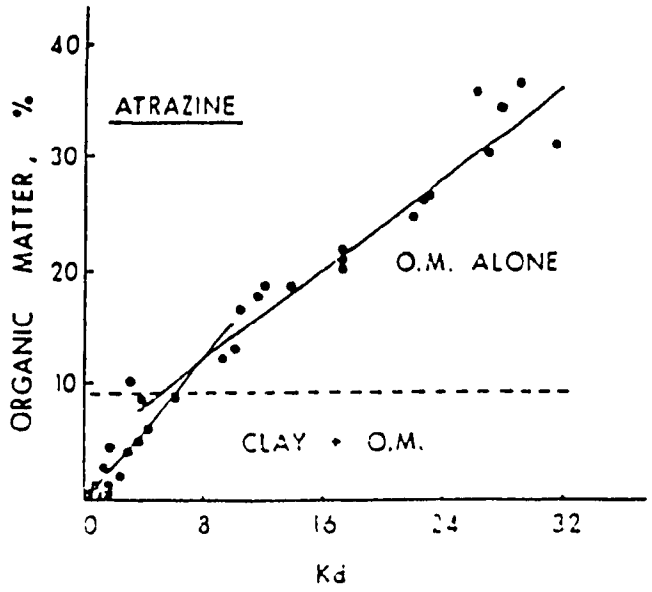

Fig. 1-1.1, Effect of the Clay and Organic Matter on Sorption of Atrazine (124)

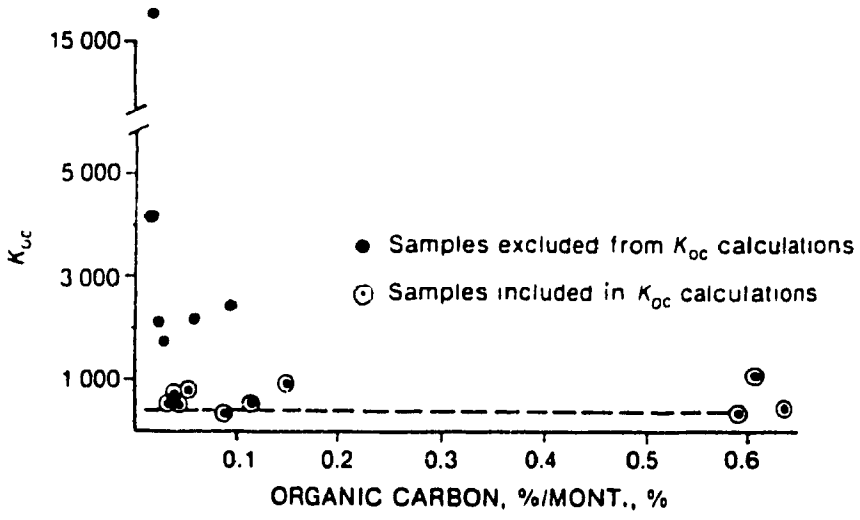

Fig. 1-1.2, Effect of Organic Matter to Clay Ratio on Sorption and K_{oc} of α-naphthol (120)

was a single valued function of soil organic matter for soil with more than 6 to 8% organic matter. A similar effect of clay on sorption was found for the sorption of α-naphthol by soils and sediments with different % organic C to montmorillonite ratios. K_{ss} values calculated from apparent sorption constants were in good agreement with the predicted K_{oc} value (dashed line) when there was sufficient organic matter present to mask the effect of the clay. But when the ratio of % organic C to % montmorillonite was < 0.1 there were greater amounts of sorption than predicted from the water solubility or K_{ow} of α-naphthol and hence, the measured K_{ss} values were from three to six times greater than the predicted values (Fig. 1-1.2) (120).

Perusal of the literature reveals that the temperature dependence of sorption shows a more complex picture. A relatively small thermal effect is commonly observed with the film diffusion and surface adsorption processes, but a quite significant activation energy (E_a) with the intrasorbent diffusion (47,123,226). In addition to the nonpolar organics (47,123), slightly polar compounds such as atrazine have demonstrated a near zero of enthalpy change (ΔH^o) in the surface adsorption equilibrium, as will be seen in Chapter 5. The small enthalpy change could be explained as being due to the lack of strong bond formation between the sorbing species and the sorbent (e.g., physisorption) (122,124).

The last characteristic for the partition model to be defended is the absence of sorptive competition among solutes (53). In fact, this has been noted not only by Chiou (47,48,51,52) with nonpolar compounds, but also by Wang et al. (281,282) with the more polar atrazine. The latter study indicated that the binding of atrazine by FA (fulvic acid) or HA (humic acid) was not competitive with the binding of hydroxyatrazine. The

reason for this is that the similar molecules AT (atrazine) and ATOH (hydroxyatrazine) have their own specific binding sites. An important practical implication is there is no catalyst poisoning by the reaction product hydroxyatrazine (281,282) in the catalyzed hydrolysis.

(2). *Partition uptake*

Chiou et al. (47,48,51,52) considered the sorption data in aqueous systems and presented evidence for the presumed partitioning (solubilization) of nonionic organic compounds into soil organic matter as the major process of soil uptake. The basis for such partition uptake is evidenced by characteristics similar to those found in solvent-water partition. These characteristics include: 1) the linearity of the uptake isotherm; 2) the inverse linear relationship between sorption (partition) coefficient (K_{oc} or K_{ow}) and solute water solubility (S_w); 3) the generally low exothermic reaction enthalpy for solutes in solvent-water and soil-water equilibria; and 4) the absence of sorptive competition between solutes. By applying the Flory-Huggins theory to account for solute solubility in (amorphous) soil organic phase, Chiou et al. (51) established a partition equation to evaluate the magnitudes of the observed sorption coefficients (K_{oc}). The modified partition equation is of the form:

$$\text{Log}K = -\text{Log}S_wV - \text{Log}\rho - (1+\chi)/2.303 - \text{Log}(\gamma_w/\gamma_w^*) \qquad (1\text{-}1.5)$$

where K is the solute partition coefficient (i.e., the ratio of the solute concentration in organic phase to that in water), S_w is the molar water solubility of the solute as a liquid or supercooled liquid at the system temperature, V is the molar volume of the solute, ρ

is the density of the organic phase introduced to express the concentration of the solute in the organic phase on a mass-to-mass basis, χ is the Flory-Huggins interaction parameter, γ_w is the solute activity coefficient in water, and γ_w^* in solvent-saturated water.

This analysis led to the conclusion that the primary factor affecting the sorption coefficients of slightly water-soluble organic compounds is the solubility of the compounds in water. The frequently observed empirical correlation between sorption coefficient (K_{oc}) and octanol-water partition coefficient (K_{ow}) was recognized to be merely a consequence of the fact that water solubility is the major determinant of both K_{oc} and K_{ow} values (51,54). The activity correction is needed to account for about 20% and cannot be obtained independently.

(3). ***Site binding model***

Numerous experimental observations leading to a site binding model have been reported since the 1970s (17,97,124,169,177,203,281-283). A typical theoretical description was developed by Gamble and Langford, and was first presented in the related studies of complexation equilibria and kinetics of multiple metal ion-humic acid interactions (92,96,159). The supporting experimental results have been accumulated over the last two decades in extensive research on the pesticide uptake behavior by soils or soil constituents (86-91,93,95,97,103,159,169,170,275,281-283).

In the case of cation binding, they pointed out that the equilibrium complexing of multiple ions or molecules by a mixture of binding sites is a general type of chemical

system that has widespread geological and biological importance. Humic materials are one type of natural cation exchangers in soils and surface waters. The central characteristic of this general type of equilibrium system is that a given reagent is complexed by a mixture of chemically nonidentical ligand sites. In one paper (92), the authors introduced a law of mass action formalism and mole fraction relationships to account for two-phase simultaneous ion exchange equilibria between twelve cations and undissolved humic acid. The following equation was used to describe the ion exchange equilibrium of a particular ion M^{n+} with the whole collection of ion exchange sites:

$$\overline{SH_2} + M^{n+} = \overline{SM^{(n-2)+}} + 2H^+ \qquad (1\text{-}1.6)$$

$$\bar{K}_M = m_c m_H^2 / m_{SH2} m_M \qquad (1\text{-}1.7)$$

where the solid lines indicate ion exchange sites within the humic acid gel phase. The cations without these are in the external solution. $\bar{K}_M$ is the mean law of mass action concentration quotient. It is the equilibrium function for the overall reaction of metal ion M^{n+} with the whole mixture of ion exchange sites. m_c and m_{SH2} are the molarities of ion exchange sites occupied respectively by M^{n+} and pairs of protons, defined for the interior gel solutions of the humic ion exchanger phase. The molarities of the metal ions and the protons in the external solution are m_M and m_H. The $\bar{K}_M$ is related to the behavior of the components of the ion exchanger site mixture by:

$$\bar{K}_M = \Sigma_{i=1\text{-}j} K_{iM} m_{SiH2} / \Sigma_{i=1\text{-}j} m_{SiH2} \qquad (1\text{-}1.8)$$

where K_{iM}, m_{SiH2} have similar meanings with $\bar{K}_M$ and m_{SH2}, but account for the i^{th} small portion of the whole system of sites. Eq. 1-1.8 gives a fundamental insight into the physical chemical implication of the experimental equilibrium function $\bar{K}_M$, which is now

recognizable as a weighted average of the equilibrium functions K_{iM} of the components of the mixture. The weighting factor is m_{SiH2}, the molarity of the protonated part of the i^{th} component. It is obvious that $\bar{K}_M$ is a variable, depending on the chemical composition of the system. Both the pH of the external solution and the metal ion loadings of the sites directly affect the weighting factor m_{SiH2}, and thus the $\bar{K}_M$.

The above theoretical description was further developed in a subsequent study of the complexation equilibria in a mixed four-ligand system (96). The expression of the weighted average equilibrium function is:

$$\bar{K} = \Sigma_{i=1-4} K_i M_{Li} / \Sigma_{i=1-4} M_{Li} \qquad (1\text{-}1.9)$$

If complexiметric titration of the mixture with a given reagent is performed, each free ligand will decrease in its turn to zero, with the strongest complex always forming first. As a result, it can be predicted that $\bar{K}$ will decrease as the mole fraction of complexation sites occupied increases. In addition, due to a buffering effect, usually two or more of the component ligands will react at the same time as the titration proceeds. This model has been extended to a hypothetical system with 100 ligands (96).

The use of kinetics of metal ion transfer from naturally occurring colloidal ligand systems to complexes with spectrophotometrically favorable ligands as a means of speciation of metal ions in natural systems has been systematically studied by Langford and coworkers since the 1970's (5,110,160-165,179,180,228,250). More recently, the authors (159) presented the results of applying this kinetic speciation method to multi-site complexants present in natural polymeric ligand systems (e.g., FA), in which Laplace transform calculations have been used to extract rate constant spectra from macroscopic

kinetic measurements on the whole mixtures. The macroscopically measured total kinetic effect was described by the sum:

$$C(k,t) = \Sigma_i C_{o,i} EXP(-k_i t) \qquad (1\text{-}1.10)$$

where C(k,t) is the total concentration of all the unreacted components at a subsequent time t. $C_{o,i}$ is the initial concentration of i^{th} component. The k_i is the component rate constant. The rate constants and concentrations can be obtained from graphical plots of H(k,t) vs. Ln(k). The calculated H(k,t) is a second-order numerical approximation of the Laplace transform of C(k,t). In addition, an experimental method based on laser thermal lensing (LTL) has been proposed, which offers sufficient analytical resolution for many environmentally important trace metals. Application of this approach has been made to complexes of metal ions with humic colloids and hydrous ferric oxides, and extended to natural waters (159).

1-1.4. MODELING OF SORPTION EQUILIBRIA AND KINETICS IN THE SOIL-WATER SYSTEM

The goal of any model is to provide an accurate mechanistic picture, ultimately at the molecular level, and to be able to predict events based on the known properties of sorbate, sorbent, and extrinsic factors. This section will discuss relevant mathematical approaches to outline the equilibrium and rate or kinetic aspects of sorption processes.

(1). *Rate-limiting processes*

Equilibrium relationships comprise a set of final outcomes of sorption processes.

Pignatello (226) suggested the following processes can contribute to the time it takes for sorption equilibrium to arise in a soil-water system: 1) diffusion through bulk aqueous solution to the surfaces of sorbing materials that are accessible to bulk solution; 2) diffusion in solution through small pores in the sorbent matrix to surfaces of sorbing materials that are less accessible to bulk solution; 3) diffusion through soil solids (i.e., organic matter gels) to sites that are not accessible to solution; and 4) reaction steps including phase transfer (i.e., aqueous to organic gel), sorption at surface sites, reaction with discrete sites in an organic matter or mineral component. Brusseau and Rao (33) depicted the solute transfer process as: 1) advective-dispersive transport from bulk solution to the boundary layer (i.e., adsorbed water surrounding the sorbent); 2) diffusive transport across the adsorbed water (i.e., film diffusion); and 3) pore and/or surface diffusion within the immobile region (i.e., intra-aggregate diffusion). The last of these includes the chemisorption steps which can occur at some sites.

In general, rate-limiting processes regarding mass transport and transfer operative in subsurface environments may be categorized as either macroscopic (transport related) or microscopic (sorption related). Macroscopic transport refers to movement of solute controlled by the motion of flowing water, i.e., advection or dispersion, which is influenced by macroscopic heterogeneities (e.g., aggregates, macropores, stratified media). In what follows we will have little to say about macroscopic factors. The studies reported are "well stirred" laboratory conditions. However, an effort to bridge the field issues in the last chapter will remind us to remember these factors.

Microscopic mass transfer refers to movement of solute under the influence of its own

molecular or mass distribution, which may result from rate-limited chemical interactions or from rate-limited diffusive mass transfer. Reaction rate control will be discussed later, although it is noted that the effective rates of sorption in subsurface systems are frequently controlled by rates of solute transport or transfer other than by sorption reactions. Under fluid flow conditions typical of subsurface systems, molecular diffusion generally dominates the microscopic mass transfer (288).

Brusseau et al. (30) proposed that three different processes can involve molecular diffusive mass transfer: film diffusion, retarded intraparticle diffusion, and intrasorbent diffusion.

Many researchers have shown that film diffusion is generally fast in comparison to other steps (33). Retarded intraparticle diffusion involves aqueous-phase diffusion of solute within pores of microporous particles mediated by retardation resulting from instantaneous sorption to pore walls. Such a mechanism has been proposed for the rate-limited uptake/release of some hydrophobic organic chemicals by sediments (296) and by aquifer materials (9). By using a representative value of < 1 nm for the molecular diameter of solutes, the same authors indicated that the pore hindrance may not be important for many solutes of interest to a sandy aquifer material with pore diameters 10 to 25 nm. The porosity of soil is a consequence, in part, of its aggregate nature. Pore sizes within aggregates span a tremendous range, including an appreciable proportion of total porosity below 500 nm effective diameter (106). Advection of water through pores of this size is slow or nonexistent, and thus solute transport must take place primarily by molecular diffusion. Diffusion through micropores may contribute substantially to

sorption times. The diffusion coefficient for typical organic contaminants in pure aqueous solution generally fall in the range 0.5 to 1.5 x 10^{-5} cm^2 s^{-1} (285). It should be noted, however, that the diffusivity of organic compounds in small pores can be much slower owing to pore surface sorption effects. For pore wall sorption that is reversible and rapid with respect to diffusion through the pore fluid, it can be shown mathematically that the *effective* diffusion coefficient (D_{eff}) will be inversely related to the sorption equilibrium distribution coefficient K_d:

$$D_{eff} = D_m\epsilon \,/\, [\epsilon + (1-\epsilon)\rho_s K_d] \qquad (1\text{-}1.11)$$

where D_m is the pore fluid diffusivity of the sorbate, ϵ is the porosity, and ρ_s the density of the sorbent (18,296). At sufficiently large K_d:

$$D_{eff} = D_m\epsilon \,/\, (1-\epsilon)\rho_s K_d \qquad (1\text{-}1.12)$$

Thus, the greater the sorptive uptake, the slower the diffusion through a small pore, even without chemisorption.

Intrasorbent diffusion involves the diffusive mass transfer of sorbate within the matrix of the sorbent. This is usually considered as intraorganic matter diffusion when organic matter is the predominant sorbent for hydrophobic organic compounds. Intraorganic diffusion has been proposed as a rate-limiting process by Hamaker (112), for example, as well as several others (29,33). Diffusion of an organic solute through soil organic gels will in general be slower than through aqueous solution. For this model, a primary assumption is that sorbent organic matter is a polymer-type substance within which sorbate can diffuse. The migration of a solute can be envisioned to occur by steps or jumps over a series of potential barriers, following a path of least resistance. The

apparent activation energy (E_D) for small organic molecule diffusion in mobile liquids that are not highly viscous are generally around 21 to 42 kJ mol^{-1}, but in polymers they may be much higher. Values approaching 170 kJ mol^{-1} are not uncommon in some systems (226). In this case, we must regard binding of the molecule as a type of chemisorption, even though the chemical changes may occur in the polymer rather than the pesticide. As noted earlier, the organic matter associated with natural sorbents has been reported to be a flexible, cross-linked, branched, amorphous, hydrophilic, polyelectrolytic polymeric substance (57,127,248,265,292). It is a water swollen gel. Direct confirmation of the porous nature of organic matter has been reported (73,248).

(2). *Reaction rate expression*

Sorption reaction rates depend on the nature of specific interactions that occur between the solute and sorbent in the sorption processes. The larger activation energies associated with chemisorption lead to slower rates. In contrast, physical sorption processes are generally rapid. The fundamental basis for molecular characterization of reaction kinetics is the law of mass action, which states that the rate of an elementary homogeneous chemical reaction is directly proportional to the product of the masses (more rigorously, activities) of the reacting species. While sorption reactions are clearly not homogeneous and rarely elementary, it is possible to draw a stoichiometric analogy involving a sorbate molecule, A, and a sorbent site, S, may be characterized schematically as:

$$A + S \underset{k_r}{\overset{k_f}{\rightleftharpoons}} A\text{-}S \qquad (1\text{-}1.13)$$

The term A-S represents the sorbed complex. For the simple case in which only one reacting species and only one type of site are involved in a one-step chemical reaction, the law of mass action analogy suggests that the forward rate or velocity of sorption, v_f, will be second order and of the form:

$$v_f = -dM_A/dt = k_f M_A (W/V)\theta_o \qquad (1\text{-}1.14)$$

where the parameter k_f is the second-order sorption rate constant (in L mol^{-1} d^{-1}), and M_A (in moles L^{-1}) and θ_o (in moles g^{-1}) represent the concentrations of the sorbate in solution phase, and of unoccupied sorption sites, respectively. The term W/V is a unit conversion factor (g L^{-1}). In a well stirred system, the bulk concentrations will have a constant relationship to concentrations in the diffusion layer. Similarly, the rate of desorption, v_r, is defined in terms of a desorption rate constant, k_r, (in d^{-1}) and the concentration, $\theta_{A\text{-}S}$, of site-binding complex, A-S, (in moles g^{-1}):

$$v_r = dM_A/dt = k_r (W/V)\theta_{A\text{-}S} \qquad (1\text{-}1.15)$$

The net rate of sorption, and thus the time rate of pesticide uptake in a completely mixed batch system, is then given by the difference between the rates of the forward and reverse reactions:

$$v_{net} = (W/V)d\theta_{A\text{-}S}/dt = v_f - v_r = k_f M_A (W/V)\theta_o - k_r (W/V)\theta_{A\text{-}S} \qquad (1\text{-}1.16)$$

At equilibrium, the net rate of sorption is zero and the following relationship is given:

$$k_f M_A (W/V)\theta_o = k_r (W/V)\theta_{A\text{-}S} \qquad (1\text{-}1.17)$$

Upon rearrangement an effective equilibrium constant, K_{eq}, (in L mol^{-1}) for this sorption

reaction yields:

$$K_{eq} = k_f/k_r = \theta_{A,S}/M_A\theta_o \qquad (1\text{-}1.18)$$

A first-order approximation to the forward rate law can be employed in cases where the number of surface sites is sufficiently greater than the number of solute molecules that θ_o in eq. 1-1.14 can be considered constant; that is, a low coverage approximation for the forward reaction rate is:

$$-dM_A/dt = k_f(W/V)\theta_o M_A = k_f' M_A \qquad (1\text{-}1.19)$$

where k_f' is the pseudo first-order rate constant (in d^{-1}). The resulting expression for the overall rate is then:

$$(W/V)d\theta_{A\text{-}S}/dt = k_f' M_A - k_r(W/V)\theta_{A\text{-}S} \qquad (1\text{-}1.20)$$

The fact that natural sorbents frequently exhibit a functionally nonuniform surface means that the empirical application of the simplified rate expressions usually involves determination of sample-averaged coefficients, which may not be applicable beyond the conditions of experimental measurement. To counter this potential deficiency, a number of heterogeneous reactive site rate models have beeen suggested (288).

(3). *Modeling of mass transfer*

Microscopic mass transfer in the liquid phase is generally described by Fick's laws of diffusion, i.e., the velocity at which solute migrates along a linear path within a particular coordinate system is directly proportional to the gradient in its chemical potential, μ_i, along the path; that is, to the thermodynamic driving force. The chemical potential of a substance is directly related to its activity and, in dilute aqueous solutions,

to its concentration, C_i. It was derived then that the time rate of solute mass flow by diffusion in a one-dimensional isotropic medium is governed by Fick's first law (66):

$$F^{o}_{i,x} = D_i \partial C/\partial x \qquad (1\text{-}1.21)$$

where $F^{o}_{i,x}$ is the flux of diffusing substance through unit cross section, C is the concentration of the substance, x is the space coordinate measured normal to the section, and D_i is the diffusion coefficient.

In a recent review (288) Weber et al. outlined the following models which depict the microscopic molecular transfer of solutes, and basically involve applications of the one-dimensional Fick's law (eq. 1-1.21) in different domains. The transport of conservative substances (those which do not undergo chemical transformations) in homogeneous or single-phase domains is referred to as Type I models. If the domain is homogeneous but also involves a reaction of the species being transported, the transport is described by Type II models. Transport in heterogeneous domains (multi-phase) by either Type III or Type IV models, depending upon whether solute reactions are involved.

For example, in Type I models, the mass continuity relationship states that the time rate of change in mass is given by the difference between the mass fluxes into and out of that domain. Thus, for a domain of volume V, length Δx, and unit cross-sectional area:

$$V(\Delta C/\Delta t)_v = F^{o}_{i,x}\big|_{x} - F^{o}_{i,x}\big|_{x+\Delta x} \qquad (1\text{-}1.22)$$

In the limit ($\Delta x \to 0$, $\Delta t \to 0$), eq. 1-1.22 takes the form:

$$(\partial C/\partial t)_v = \partial/\partial x\ (-F^{o}_{i,x}) \qquad (1\text{-}1.23)$$

In this case the flux associated with the microscopic mass transfer process is defined by

Fick's first law (eq. 1-1.21), and eq. 1-1.23 can be written:

$$(\partial C/\partial t)_v = \partial/\partial x\ (D_1 \partial C/\partial x) \qquad (1\text{-}1.24)$$

For a steady-state diffusion, a solute velocity or mass transfer coefficient, k_f, is as follows:

$$F^o_{1,x}\Big|_{x=0} = -D_1(C_\delta - C_o)/\delta$$

$$= k_f(C_o - C_\delta) \qquad (1\text{-}1.25)$$

where δ represents a fixed distance ($\Delta x = \delta$), C_o and C_δ are the upgradient and downgradient boundary concentrations, respectively. Eq. 1-1.25 is similar in form to a first-order reaction rate equation, and its solution can be approached in similar fashion.

The Type IV models involve the mass transfer in heterogeneous domains in which there may be reactions such as sorption and catalyzed transformation with the surfaces. For the case of transport through a Type IV domain with only sorption reaction by a solid phase of density ρ_s, the steady-state continuity equation can be expressed:

$$(\partial C/\partial t)_v = (1/\epsilon)\partial/\partial x\ (\epsilon D_e \partial C/\partial x) - (\partial C/\partial t)_r \qquad (1\text{-}1.26)$$

The reaction term $(\partial C/\partial t)_r$ is related to the rate of change of the solid phase concentration, q, as follows:

$$(\partial C/\partial t)_r = (1-\epsilon)\rho_s/\epsilon\ \partial q/\partial t \qquad (1\text{-}1.27)$$

where D_e is the effective diffusion coefficient which incorporates the effects of both tortuosity and pore constriction, and ϵ is the porosity which is equal to the volumetric water content, θ_w, if the void space is saturated with water. It is apparent from eq. 1-1.27 that relative rates of solute sorption and diffusion dictate the extent to which the concentration profile, and therefore flux, decreases with distance through the domain. It

is also apparent that more strongly sorbed solutes will exhibit a greater retardation in overall rates of migration through such domains.

Subsurface systems are often comprised by multiple diffusion domains of different types and degrees of impedance. As a consequence, application of the above models should consider their combination, and in particular, the rate-limiting step (288).

(4). ***Nonequilibrium sorption***

The local equilibrium assumption (LEA) is a major component of conventional solute transport equations used in modeling process in soils on the larger scale. In order for the LEA to be valid, the rate of the sorption process must be fast relative to the other processes affecting solute concentration so that equilibrium may be established between the sorbent and the pore fluid. Initially, it was thought that, because of the generally slow movement of water in the subsurface, equilibrium conditions should prevail and, therefore, the LEA would be valid. Detailed laboratory and field investigations, however, have revealed that, in many cases, this assumption is invalid. Sorption data from batch experiments, such as the ones to be described below, have been found to exhibit at least a two-step approach to equilibrium: one or more short initial phases of uptake, followed by an extended period of much slower uptake. This pattern is followed by most if not all sorption reactions. The typical shape of solute uptake curves shows that roughly 50% of the sorption occurs within the first few minutes to hours, with the remainder occurring over periods of days or months (10,67,138,143,185,215,296). Corresponding to this, the breakthrough curves (BTCs) exhibit asymmetry (102).

Rate-limited, or nonequilibrium, sorption of organic chemicals by natural sorbents has been a topic of interest for quite some time (28,32,33). Several different processes have been proposed as causing nonequilibrium sorption. As addressed previously, these include transport-related and sorption-related factors (27,33). Brusseau et al. show that nonequilibrium sorption of hydrophobic organic chemicals (HOCs) was caused mainly by a sorption-related mechanism, i.e., intraorganic diffusion, compared to retarded intraparticle diffusion (30).

To model nonequilibrium sorption kinetics, a bicontinuum model of some type is presently most often used. In these models, the sorbent is hypothesized as having two classes of sorption sites where sorption is fast for one class and rate-limited for the other (30,37,249), or two soil pore-water regions: mobile and immobile (77,105,147).

(5). ***Typical sorption kinetic models***

Many of early approaches (78,115,133,150,167,173,211,276) have treated sorption as an activated surface adsorption process and ignored diffusion, which has been shown to be unrealistic for soils by a number of laboratory and field observations over recent years.

(i). Leenheer and Ahlrichs (167) studied the sorption of carbaryl and parathion by particles of soil organic matter that remained after dissolution of the mineral fraction, and found that sorption was rapid initially but then became linear with the square root of time after the first few minutes. Since a dependence on $t^{1/2}$ is typical of diffusion processes, they proposed that the rapid phase occurred by surface adsorption while the slower phase

occurred by diffusion into the sorbent particle. These results first presented evidence that diffusion was important to soil components in stirred batch systems.

(ii). Selim et al. (249) and Cameron and Klute (37) proposed a two-site model to describe saturated flow of pesticide solutions in soil columns, in which one group of sites achieves instantaneous equilibrium (type 1) while the other group does not (type 2):

$$\delta S/\delta t = [nK_dC^{n-1}]\delta C/\delta t + [k_1C^n - k_{-1}S] \qquad (1\text{-}1.28)$$

In this equation, the first term on the right applies to type 1 sites and is simply the first derivative of a non-mechanistic Freundlich equation; while the second term on the right applies to type 2 sites. Rao et al. (231) found that this equation did not adequately describe breakthrough curves of 2,4-D dimethylammonium salt and atrazine in soil columns.

(iii). Karickhoff (143) and Karickhoff and Morris (144) used an approach similar to Selim et al. (249), but termed it a two-compartment model for analyzing the sorption kinetics of neutral hydrophobic compounds in sediments. They found that these compounds existed in labile (S_1) and nonlabile (S_2) sorbed states in the sediment:

$$C \overset{X_1,K_d}{\rightleftharpoons} S_1 \overset{k_2}{\rightleftharpoons} S_2 \qquad (1\text{-}1.29)$$

where X_1 is the fraction of sorbed compound in the S_1 state, K_d is an equilibrium distribution coefficient, and k_2 is the first order rate constant for net movement into S_2. The model could not distinguish between entry to S_2 from S_1 or from water. Using a similar model, McCall and Agin (185) found that S_2 contains a majority of bound picloram after a month of incubation. Note that this model should be viewed as a middle form between nondiffusion and diffusion models, in which the rate constant (k_2) was

conceptually blurred.

(iv). Direct use of diffusion kinetics to describe organic sorption in soil systems was not heavily used until the work of Wu and Gschwend (296) on the sorption of chlorinated benzenes in soils and sediments. Their kinetic model was based on the assumption of the sediment and soil particles of most concern for hydrophobic organic compound sorption as porous aggregates of fine mineral grains and natural organic matter. As sorbate molecules diffused into the interior of a spherical homogeneous porous particle, they were retarded by instantaneous local or microscale partitioning between the pore fluid and particle solid, described by a bulk K_p obtained from isotherms. The time rate of change of compound S(r) present within a particle sphere of radius (r) can be expressed mathematically as:

$$\partial S(r)/\partial t = D_{eff}[\partial^2 S(r)/\partial r^2 + (2/r)\partial S(r)/\partial r] \qquad (1\text{-}1.30)$$

This equation is simply a variant of Fick's law (eq. 1-1.21) derived for a sphere in polar coordinates (66), in which D_{eff} is the effective diffusion coefficient. The further derived expressions for D_{eff}, S(r) and K_p are:

$$D_{eff} = D_m \epsilon\, f(\epsilon,\tau)/(1-\epsilon)\rho_s K_p \qquad (1\text{-}1.31)$$

$$S(r) = (1-\epsilon)\rho_s S'(r) + \epsilon C'(r) \qquad (1\text{-}1.32)$$

$$K_p = S'(r)/C'(r) \qquad (1\text{-}1.33)$$

where D_m is the diffusion coefficient in aqueous pore fluid, S(r) is the local total volumetric concentration in porous sorbent, S'(r) is the concentration of the immobile bound state, C'(r) is the sorbate concentration free in pore fluid and varying with radial distance (r), ϵ the porosity of the sorbent, ρ_s the density of the sorbent. The term $f(\epsilon,\tau)$

accounts for the fact that the path length of diffusion inside a particle is in general longer than the radius; this factor is a function of porosity ϵ and tortuosity τ. With this model, they observed an inverse dependence of D_{eff} on K_p.

Similarly, Steinberg et al. (264) examined the desorption kinetics of EDB (1,2-dibromoethane) from contaminated field soils by modeling the release both as a simple first-order process and as a diffusion process. EDB desorption was found to be highly temperature dependent. In addition, the radial diffusion model was applied to describe gas/particle sorption kinetics by Rounds and Pankow (242).

In recent years, a number of sorption kinetic approaches have been reported, showing an in-depth analysis or advance in this area concerning the mechanisms of sorption of organic chemicals in the natural subsurface environment.

(v). Miller, Weber, and co-workers (196,198-200,289) presented a dual-resistance surface-diffusion model in which sorption rates are represented as the result of the resistance due to diffusion through a boundary layer and diffusion radially along the solid surface within a spherical particle. Surface-diffusion models usually assume equilibrium between the sorbent and solution at the exterior portion of a particle. For the case of a pseudo first-order degradation reaction in the solution phase and no solute source other than the initial condition, a material balance expression in a batch reactor may be written as:

$$dC/dt = -(M_s/V)(dq/dt)_{srp} - k_a C \qquad (1\text{-}1.34)$$

where M_s is the mass of the solid phase in the batch reactor, V is the volume of the solution phase, q or q_r is the solid-phase solute concentration as a function of radial

position r, k_s is the pseudo first-order solute degradation rate for solute loss in the solution phase, the subscript srp indicates sorption. The companion solid-phase equation is:

$$\partial q_r/\partial t = D_s[\partial^2 q_r/\partial r^2 + (2/r)\partial q_r/\partial r] - k_s q_r \qquad (1\text{-}1.35)$$

where D_s is a surface-diffusion coefficient, k_s is a pseudo first-order solute decay coefficient for solute in the solid phase. They found that the boundary-layer mass-transfer resistance was an unimportant factor in determining the rate of sorption; that is, the D_s ($\sim 10^{-8}$ magnitudes) was sufficiently small that internal particle diffusion was the rate-determining step. The minimization procedure yielded a best-fit value for k_s that was about 61% as large as k_a.

A latest version for the above model, termed as the distributed reactivity model (DRM), has been reported by Weber et al. (291) to account for the fact that soils appearing homogeneous at a macroscopic level can be implicitly heterogeneous, comprising a variety of matrix components and interfaces exhibiting a variety of reactivities with respect to organic solutes. The basic equation for a linear isotherm assumption is:

$$q_{cr} = \Sigma_{i=1\,m}\, x_i q_{ci} = \Sigma_{i=1\text{-}m}\, x_i K_{di} C_e = K_{dr} C_e \qquad (1\text{-}1.36)$$

If one or more of the component elements of sorption is nonlinear, the composite expression is:

$$q_{ci} = x_1 K_{d1} C_e + \Sigma_{i=1\text{-}m}\, (x_{ni})_i K_{Fi} C_e^{ni} \qquad (1\text{-}1.37)$$

where q_c is the solute mass sorbed per unit mass of bulk solid, x is the mass fraction, K_d is the partition coefficient, C_e is the concentration in solution phase, K_F is the Freundlich

unit-capacity coefficient, x_l is the summed mass fraction of solid phase exhibiting linear sorptions, x_{nl} is the mass fraction with nonlinear sorptions. The subscript i denotes i^{th} region or component, r denotes summed terms.

(vi). In contrast to the above, Ball and Roberts (11,12) presented a model that accounts for the driving forces for diffusion both by pore diffusion and by surface diffusion. For transient conditions of uptake into a sorbent, mass balance considerations over a volume element of the porous sorbent can be combined with Fick's first law of diffusion (eq. 1-1.21) to obtain:

$$\rho_a(\partial q/\partial t) + \epsilon_i(\partial C/\partial t) = \epsilon_i D_p \nabla^2(C) + \rho_a D_s \nabla^2(q) \qquad (1\text{-}1.38)$$

where D_p and D_s are effective pore and surface diffusion coefficients, respectively, q is the sorbed-phase concentration, ∇^2 is the Laplacian operator, ρ_a is the grain density, and ϵ_i is the internal porosity. For the case of linear partitioning, reversible equilibrium within the pores, and spherical geometry, eq. 1-1.38 can be rewritten as:

$$\partial C/\partial t = (D_a/r^2)\, \partial/\partial r[r_2(\partial C/\partial r)] \qquad (1\text{-}1.39)$$

where the apparent diffusion coefficient is defined as:

$$D_a = \epsilon_i D_p/(\epsilon_i + \rho_a K_{di}) + \rho_a K_{di} D_a/(\epsilon_i + \rho_a K_{di}) \qquad (1\text{-}1.40)$$

where K_{di} is an internal distribution coefficient, considering only the diffusively limited sorbed phase. For a pore diffusion interpretation:

$$D_a = D_p/[1 + (\rho_a/\epsilon_i)K_{di}] \qquad (1\text{-}1.41)$$

On the other hand, for a surface diffusion, D_a will be mathematically equivalent to D_s. By using this model to study the sorption of halogenated organic chemicals (PCE, tetrachloroethene and TeCB, 1,2,4,5-tetrachlorobenzene) by aquifer materials, they found

that the rates of uptake (D_e/a^2) were quite slow in comparison with previously reported results, that pulverization of a given size fraction greatly expedited the uptake.

(vii). A recent application of a bicontinuum model for modeling nonequilibrium sorption kinetics has been reported by Brusseau et al. (30). On the basis of first-order mass transfer, sorption is conceptualized to occur in two domains:

$$S_1 = FK_pC \qquad (1\text{-}1.42)$$

$$dS_2/dt = k_1S_1 - k_2S_2 \qquad (1\text{-}1.43)$$

where C is the solution phase solute concentration, S_1 is the sorbed phase concentration in the fast domain, S_2 is the sorbed phase concentration in the rate-limited domain, K_p is an equilibrium sorption constant for the fast process, F is the fraction of sorbent for which sorption is fast, t is time, and k_1 and k_2 are forward and reverse first-order rate constants, respectively.

The two sorptive domains assumed by the bicontinuum model are further represented by volume fractions V_1 and V_2, which are the volumes of the respective domains per total sorbent mass. The microscopic sorbed phase concentrations, S_1 and S_2, may be defined in terms of microscopic concentrations:

$$S_1 = s_1V_1 \quad S_2 = s_2V_2 \qquad (1\text{-}1.44)$$

where s_i is the sorbate mass in region i per volume of region i. The change in the sorbed phase concentration of domain 2 is described by:

$$V_2ds_2/dt = k_tA(s_1 - s_2) \qquad (1\text{-}1.45)$$

where k_t is a mass transfer coefficient and A is the cross-sectional area through which mass transfer occurs. In cases where it is difficult to explicitly define A and V, a mass

transfer constant (α) may be used:

$$\alpha = k_t A/(V_1 + V_2) \qquad (1\text{-}1.46)$$

Equation 1-1.45 may be rewritten in terms of the macroscopic sorbed phase concentrations and rate constants:

$$dS_2/dt = \alpha[S_1/F - S_2/(1-F)]$$

$$= k_1 S_1 - k_2 S_2 \qquad (1\text{-}1.47)$$

where

$$k_1 = \alpha/F = (k_t A/V_1)$$

$$k_2 = \alpha/(1-F) = (k_t A/V_2) \qquad (1\text{-}1.48)$$

This model has been used to evaluate the results of experiments designed to identify the process responsible for nonequilibrium sorption of hydrophobic organic chemicals by natural sorbents (30).

(viii). Gamble, Langford, and coworkers (97,103) have developed a two stage surface-adsorption/intraparticle-diffusion model to account for the sorption behavior of atrazine by soils, which is a refined form of previous work (93,94). The solute mass transfer involves: 1) diffusive transport across the adsorbed water film driven by the concentration gradient from the bulk solution; 2) labile adsorption driven by interactions at the solid-water interface; and 3) intraparticle or nonlabile diffusive transfer driven by the surface accumulation and/or specific interactions within the particle. As we will see in the subsequent chapters, some of main features are: 1) the two stage model employs a second-order rate law (with exception, a pseudo first-order approximation to low surface coverage) to describe the adsorption kinetics; 2) this model postulates the surface

accumulated or labile sorbed amount to be the driving force for the intraparticle diffusion, and treats it as a first-order kinetic process, which can be characterized by either of two parameters: the rate constant (k_{d1}) and the diffusion coefficient (D); and 3) this model is constructed on the basis of an uptake mechanism of site binding or specific interactions. Therefore, there exists a definite labile sorption capacity whch is measurable experimentally. The two stage model has the general form:

$$(d\theta_L/dt)_T = d\theta_t/dt - d\theta_D/dt$$

$$= k_{b1}(V/W)M_{AT}\theta_o - k_{s2}\theta_L - k_{d1}\theta_L + (V/W)R_{d2} \qquad (1\text{-}1.49)$$

where $d\theta_L/dt$ and $d\theta_D/dt$ represent the contributions from the first stage and the second stage; θ_L and θ_D, (in moles g^{-1}) the labile surface sorbed and intraparticle diffused atrazine; M_{AT} (in moles L^{-1}) the atrazine in solution phase; k_{b1}, k_{s2} and k_{d1} the rate constants for adsorption (second order, in L mol^{-1} d^{-1}), desorption (in d^{-1}) and forward intraparticle diffusion (in d^{-1}), respectively. R_{d2} is the outward diffusion term, and the factor V/W in (L g^{-1}) is for converting units. A detailed discussion about this mechanism will be presented in Chapter 3.

Except for the local or microscopic scale models presented above, a number of field-scale or macroscopic models, incorporating advection and dispersion processes, for solute transport in subsurface systems have been developed (59,287,288).

1-1.5. METHODOLOGIES FOR SORPTION STUDY

One of the most important aspects of a kinetic study on soil constituents is the method

being used to independently measure rate coefficients and other equilibrium/kinetic parameters. A number of methods have been suggested for this purpose (259). It is obvious that none of them is a panacea for kinetic studies of heterogeneous systems such as soils, and each has strengths and weaknesses.

Additionally, the time scales of reactions that are studied, and the objective of experiments that are carried out are important considerations in choosing a kinetic method. For example, reactions that are exceedingly rapid and occur on microsecond, millisecond, and second time scales cannot be measured using traditional batch or flow techniques. However, for most pesticide reactions in soils such methods would be quite satisfactory.

(1). ***Batch techniques***

Many kinetic studies investigating reactions on soil constituents have used batch techniques. The traditional batch method involves placing an adsorbent and adsorbate in a reaction vessel such as a centrifuge tube. The suspension is stirred or agitated using a shaker. Then the suspension is centrifuged or filtered to separate a clear supernatant solution for subsequent analysis. Some disadvantages have been revealed with this technique such as: 1) centrifugation could create electrokinetic effects close to soil constituent surfaces that would alter the ion distribution; 2) centrifugation may require up to 5 min to separate the solid from the liquid phase; 3) most batch studies involve large solution:soil ratios that would alter the kinetic behavior from that in soils with much smaller ratios; and 4) another problem is the mixing technique which is important

to maintain the sample uniformly suspended. If mixing is inadequate, it would affect the reaction rate, and may cause abrasion of the soil constituent particles (15,213,214).

Many of the disadvantages of batch techniques given above can be eliminated to some extent by using modified or improved methods developed in recent years, such as the batch methods used by Zasoski and Burau (300) to study the metal sorption rate on colloids, by Harter and Lehmann (119) to study metal reaction kinetics on soils, by Phelan and Mattigod (223) to study calcium phosphate precipitation, etc. (259).

A Batch Method Coupled with a MF-HPLC Technique. Under this heading, a novel batch method combined with a microfiltration (MF)-HPLC technique will be outlined (90,93,94). This experimental method can monitor the chemical species including free and labile sorbed forms of both reactants and products, and any material balance loss throughout the course of a kinetic experiment. The batch setup includes a Pyrex cylinder reaction vessel having a screw cap with sample constituents. During use it was equipped with a Teflon-coated stirring bar, and placed in a fitted double-walled Pyrex container, and connected to a circulating bath maintained at constant temperature. The assembly can be mounted on a stirrer. Fig. 1-1.3 shows the on-line microfiltration system involving two replaceable stainless steel microfilters (0.5 and 2.0 μm) and a cartridge-type guard column to trap solids and protect the main HPLC analytical column. Two types of HPLC analyses, a preinjection filtration by 0.22 μm filters and a postinjection filtration by combining the 2.0 μm with 0.5 μm on-line filters, were done alternately during measured times. With flow rates of 1.0 mL min^{-1} and retention times of 6-18 min, the relative amount of extractant was about 200-450 L g^{-1} of organic soil.

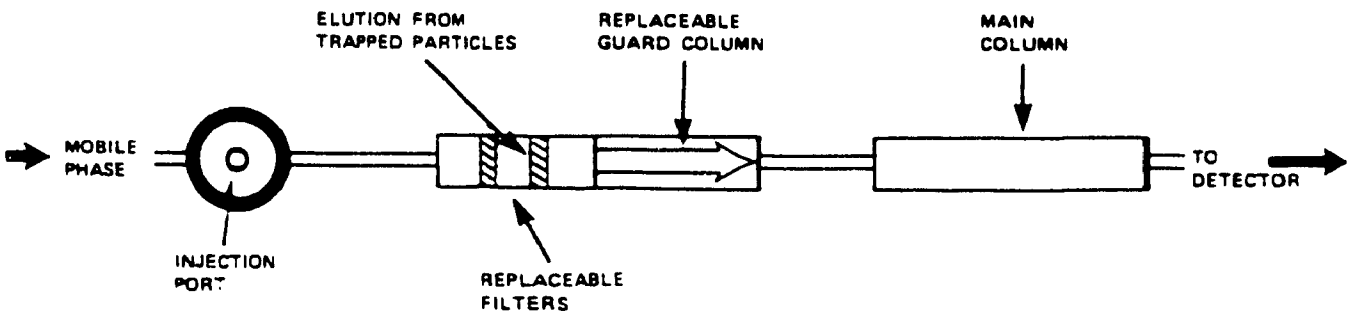

Fig. 1-1.3, A Schematical Representation for Microfiltration-HPLC Technique

This was about 4-5 orders of magnitude greater than the conventional volumes of extractant per gram. This method is suitable for studying the kinetics of heterogeneous systems. The required chemical analyses are simple and fast, and do not deplete the sample by using large aliquots. Preliminary trials indicate that it should be possible to extend the method to other potential uses (93).

(2). *Flow methods*

Flow methods have recently been used in a number of kinetic studies of soils and soil constituents. These techniques usually involve a sample holder which is attached to a fraction collector and a peristaltic pump to maintain a constant flow rate. Samples are leached with sorptive solutions, and effluents are collected at various time intervals.

Using a continuous flow technique, one can measure reactions at frequent intervals ($\sim$ 1 min), and employ small solution:solid ratios (usually $\leq$ 1). The main problems are: 1) often the colloidal particles are not dispersed, and consequently the reaction kinetics may be more significantly subject to mass transfer; 2) with a continuous flow method, flowing is the sole way the sample is mixed, and as a result, there may be imperfect mixing, leading to pronounced diffusion; and 3) use of liquid to load the sorbent into the sample holder will result in the dilution of incoming sorptive solution (212,213).

The above disadvantages with continuous flow techniques can be eliminated by using a stirred-flow method (41). In addition, fluidized bed reactors have been widely used (56,131,132,294).

(3). *Rapid kinetic methods*

Rapid reactions, such as those involving some soil constituents and adsorbates with $t_{1/2}$ < 10-20 seconds, can only be measured by using rapid kinetic methods. These methods include the stopped-flow method and various relaxation kinetic methods. With the relaxation methods, the equilibrium of a reaction mixture is perturbed by a rapid alteration of some external factor such as pressure (p-jump), temperature (t-jump), or electric field strength. One then obtains kinetic information by measuring the relaxation time of the approach to a new equilibrium. The theory behind each of these methods and their application to soil constituent reactions have been presented in a recent review by Sparks (259). According to Sparks (259), the application of these methods to the study of reactions on soil constituents remains limited to date.

1-2. RESEARCH PROSPECTIVES

Three or more decades ago it was assumed that it would never be fully possible to do rigorously quantitative chemistry with such complicated natural mixtures as agricultural soils, aquatic sediments, natural waters, or even their components. One of the practical implications of that assumption was the physicochemical interactions of metal ions and organic chemicals with natural geochemical mixtures could never be fully understood or described quantitatively in terms of molecular level mechanisms. However, the frontier work, as reviewed above even from the point of sorption phenomena only, has indicated substantial progress and success. With this, a research strategy for pesticide-soil interactions has been evolved in our research group during the course of last few years. The purpose of this strategy is to accumulate empirical results by scanning experimentally a series of particular sample combinations, and to interpret the physicochemical data by exploiting quantitative stoichiometry and molecular level mechanisms, and then in turn to contribute to the further understanding and solution of practical environmental problems by predictive computer modeling. The research of this thesis was initiated with the strategy outlined above, and will mainly focus on the uptake of the herbicide atrazine by a mineral soil, GB 843, emphasizing the equilibria and kinetics related to such processes as adsorption/desorption, and intraparticle diffusion. The research includes:

(1). Presentation of an equilibrium/kinetic laboratory batch setup combined with the on-line microfiltration-HPLC technique which was previously developed by Gamble et al. (90,93,94).

(2). Examination of the equilibria and kinetics of the uptake processes in terms of surface or labile adsorption and intraparticle diffusion or nonlabile sorption, identification of the rate-determining steps, experimental measurement of the labile sorption capacity, and investigation of the factors such as soil particles (inherently, soil organic matter and specific surface area) and temperature which have been proven to substantially affect the uptake behavior.

(3). Application of a two stage surface adsorption/intraparticle diffusion model to describe atrazine-soil interactions, and to interpret the uptake mechanisms. As noted above, a frequently expressed view of the sorption of organic chemicals by soils and soil constituents now is a fast adsorption equilibrium followed by a slow diffusive uptake, which has been treated with an isotherm equation or first-order rate approximation for the first type of sites, and a radial solution of Fick's law for the second type. In contrast, the two stage model will employ a second-order rate law (with exception, a pseudo first-order limit) to describe the labile sorption and introduce a first-order kinetics for the nonlabile diffusive uptake.

(4). Introduction of the theoretical basis for, and mathematical approach to, a hydrology solute transport model PESTFADE to simulate atrazine transport on soil columns for evaluating the use of the mechanisms described in quantitative prediction of field processes (59-61,171).

(5). This thesis also includes an investigation of the complex interaction between a nonpolar insecticide lindane and Laurentian fulvic acid, carried out to demonstrate the generality of the discrete binding site model which is the basis of this work.

CHAPTER 2

FURTHER TESTING OF THE SITE BINDING MODEL: INTERACTION OF LINDANE WITH LAURENTIAN FULVIC ACID

2-1. INTRODUCTION

The ubiquitous contamination of natural waters with chlorinated hydrocarbons has long been documented (289). A number of investigations have demonstrated that these hydrophobic pollutants can bind to dissolved humic materials, which could significantly affect their environmental behavior including aqueous persistence, chemical degradation, transfer to sediments, and biological uptake (121). A significant literature on the behavior of lindane in the natural environment has been developed over the past four decades (196), with much of this literature summarized in a thorough recent review (134). Lindane has been shown to sorb to natural solids, degrade abiotically, biodegrade aerobically, and biodegrade anaerobically. Factors affecting the sorption and desorption of lindane in solution-solid systems have been widely investigated (1,24,147,175,201,270), and results show that the organic carbon content of a solid phase is an important factor affecting both the extent and the rates of lindane uptake (1,147,175,198,289). Lindane sorption has been found to require more than 100 hours (24,198).

It has been established that the interaction between relatively insoluble organic compounds and dissolved humic substances is closely related to their hydrophobicity. In general, as reviewed in Chapter 1, two binding models have been developed: a "complexation" or adsorption model and a partition model (295). A majority of studies have used DDT as a representive halogenated hydrocarbon, or a PCB as a representive of polynuclear aromatic hydrocarbons (55,121). The partition model with a characteristic distribution coefficient, K_d, has been favoured for compounds with low water solubility. The partition model is based on three postulates. The first is that a humic material simply acts as an organic solvent that is present as a separate physical phase. The second is that this second physical phase has only nonspecific, nonlocalized solute-solvent interactions. The third postulate is that the solute is distributed between the volumes of the aqueous and humic solvent phase according to the entropy of mixing as modified by activity coefficients in the two phases. The partition model does not account for the fact that while undissolved humic acids are a separate physical phase, fulvic acids in true solution are just another type of solute within a single aqueous phase. The polyelectrolyte molecules of a fulvic acid do not possess a separate, macroscopic phase volume into which a monomeric solute can be partitioned in a nonlocalized fashion. This is highlighted by the polydisperse nature of typical fulvic acids. Their molecular weights range from a few thousand daltons down to values not much greater than that of DDT (42). At the lower end of this range in solution, there is the awkward question about which of the solute molecules is being "partitioned" into the other. Even if they do bind together, the concept of nonlocalized partitioning into a second physical phase is not

applicable. According to the law of mass action, there would not however be any significant amount of such binding in dilute aqueous solutions of fulvic acid and pesticide, unless there were specific fulvic-pesticide interactions that were relatively stronger than the interactions of each solute with the solvent common to both. Specific interactions could include the types of hydrophobic effects that produce micelles.

For the particular case of atrazine interacting with humic materials, theoretical description and experimental proof for specific, localized binding sites have both been in the literature for about a decade. There are several types of experimental proof. The Bronsted acid catalysis of atrazine hydrolysis that was demonstrated by Perdue and Wolfe has been verified by more recent work (89,93,221,222). The mechanism for the catalysis requires that the atrazine be adsorbed onto specific, localized, catalytically active binding sites. Kinetic rate constants correlated with numbers of protonated carboxylic groups, but 1% or less of the total carboxylic groups served as catalytic binding sites. In addition, the titration of both fulvic and humic acids with atrazine revealed plateaus that were caused by the saturation of sorption sites (282,283). The pH dependence of the binding capacities observed in this way for both fulvic and humic acids was consistent with pH and ionic strength effects on aggregation that were investigated by Rayleigh light scattering (275). Hydrolysis rate constants and binding capacities independently gave the same two clues: 1) protonated carboxylic groups were essential to atrazine binding; and 2) 1% or less of these protonated carboxylic groups participated in the interaction with atrazine. The partition model is not consistent with this 10-year accumulation of experimental results.

In our earlier work (281), a discrete binding site model was suggested to account for the limited binding capacity of Laurentian fulvic acid for the more polar herbicide atrazine. Not only is this consistent with the available experimental evidence, but it is also equally applicable to both solution phase fulvic acid and undissolved humic acid present as a second physical phase. Unlike the partition model, it does not require a distribution throughout the volume of a second macroscopic physical phase. In order to evaluate the generality of the atrazine results, this chapter considers a nonpolar insecticide lindane (γ-1,2,3,4,5,6-hexachlorocyclohexane, Fig. 2-1.1) and presents quantitative measurements of the extent of lindane-Laurentian FA binding under various experimental conditions, using a gas chromatographic ultrafiltration method.

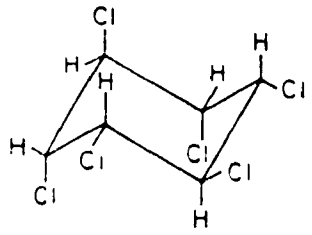

Fig. 2-1.1, Lindane (γ-1,2,3,4,5,6-hexachlorocyclohexane)

2-2. EXPERIMENTAL

(1). *Materials*

Laurentian fulvic acid was prepared following established procedures (108,217) from a sample of a podzol collected in the Laurentian forest preserve of Laval University,

Quebec, Canada. This soil is a part of the reference collection of Agriculture Canada (188). The spectroscopic and structural characterization of the whole sample and of its molecular weight fractions have been reported (281). Elemental analyses were done, and the stoichiometry of the acidic properties were exactly determined by acid-base titration (281). The number of carboxyl groups and their distribution as a weighted average acid dissociation equilibrium function were both measured in this way. A stock solution was made by dissolving 2.500 g of the fulvic acid in 100 mL of distilled water.

Lindane (~99% purity) was purchased from Sigma Chemical Company (St. Louis, Mo, U.S.A.). A 21.08 μM lindane solution was prepared by dissolving 0.01226 g of lindane in the minimum amount of methanol (Anachemia Accusolv Grade), and the solution was quantitatively transferred to an Erlenmeyer flask and diluted with 2 liters of distilled water. It was heated gently overnight with stirring, and then stored at room temperature. This stock solution was used for the investigation of lindane binding by fulvic acid.

Standard lindane solutions for gas chromatographic calibration purpose were prepared by dissolving an appropriate amount of lindane in hexane (Caledon ACS Spectro Grade) in a 100 mL volumetric flask to give a 348.0 μM standard stock solution. This solution was refrigerated until required. Working GC standards were obtained by dilution of this stock solution to the desired concentrations with hexane.

Aqueous solutions of 2.50 M potassium chloride, 1.00 M hydrochloric acid, and 1.00 M sodium hydroxide were prepared using certified reagents and distilled water.

(2). *Apparatus*

The pH values were measured with a Metrohm Model E300B instrument equipped with a Fisher EA-1210-UX glass combination electrode.

An Amicon Model 8050 stirred ultrafiltration cell (50 mL) was used with an Amicon YM2 (nominal 1,000 M.W. cut off) ultrafiltration membrane for separation of free lindane in solution from fulvic acid having bound lindane. The membrane was prepared by soaking in 70% ethanol for 3 to 4 hours followed by distilled water for at least 6 hours. When not in use the membrane was stored in distilled water. During filtration, the solution in the cell was stirred with a magnetic stirrer. Lindane was determined using a Perkin-Elmer Sigma 4B Gas Chromatograph equipped with an electron capture detector, and a 6 ft x 4 mm i.d. glass column packed with 2% OV-1 plus 3% QF-1 on 100-120 mesh Chromosorb W-HP maintained at 205 °C. The 95% argon/5% methane carrier gas was used with a flow rate 60 mL min^{-1}. The injector/detector temperature was 240 °C.

(3). *Procedure*

A preliminary study was conducted to estimate the stability (recovery of lindane over time) of aqueous lindane solutions at different pH values. The results are shown in Fig. 2-2.1. Lindane solutions are relatively stable in the pH range of natural waters (pH 4 to 9) in agreement with Lichtenstein et al (172). Loss of lindane response at lower or higher pH was attributed to both the adsorption and the degradation of lindane itself (196). These factors made the use of the paired control and test solutions obligatory in the subsequent study of binding of lindane to fulvic acid. The assumption was made that loss

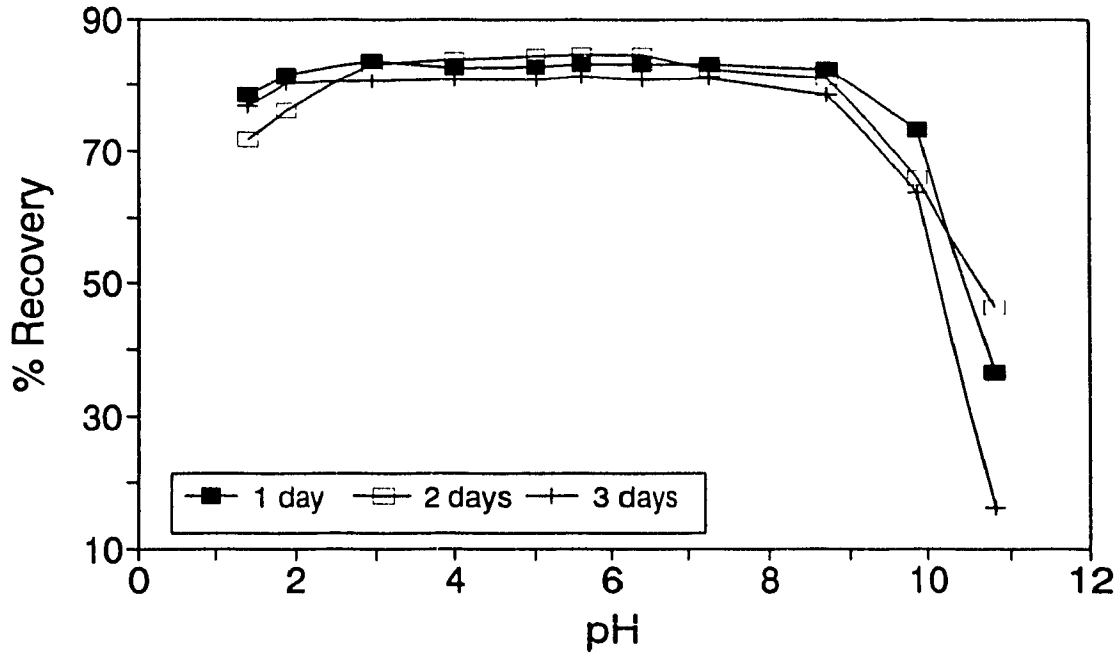

Fig. 2-2.1, Stability of Aqueous Lindane Solutions (KCl=0)

of lindane was the same in test solutions and in control solutions, and unaffected by fulvic acid. Since this may not be entirely correct, experiments were limited to pH values within which lindane solution stability was at a maximum. In addition, diagnostic tests based on the slopes and intercepts of plotted ultrafiltration data can be used for detecting interferences from the ultrafiltration membranes and correcting for them (98,99).

To determine the amount of lindane bound to fulvic acid under various conditions, lindane and fulvic acid stock solutions in required amount were mixed together, adjusted to the required pH values with hydrochloric acid or sodium hydroxide and diluted to a final volume of 50.00 mL with distilled water. Paired control (one additional control solution was needed for equilibrating the membrane) and test solutions were shaken simultaneously for 2 days at room temperature (22 ± 1 °C) in the dark. Each solution was then transferred to an ultrafiltration cell and filtered at 50 psi. The first 4 mL of filtrate were discarded and then another 2 mL of filtrate were collected. This has been shown to cause no observable disturbance of the complexing equilibrium. It was noted that if the lindane and water have the same ratio in the filtrate as in the cell solution above the ultrafilter, then the complexing equilibrium will not be shifted (99). Wang et al. confirmed this experimentally by measuring concentrations in the filtrate as a function of filtrate volume (281). For extracting the free lindane, an aliquot of 1.00 mL of the filtrate was mixed with desired volumes of hexane, gently shaken for 20 minutes and then kept in the refrigerator overnight. Under the above operational conditions the extraction efficiency is not lower than 97%. The hexane extracts were analyzed for lindane content by GC. The difference between the responses obtained for control and

test filtrates was taken as a measure of lindane bound to fulvic acid.

(4). *Ultrafiltration technique*

The ultrafiltration technique has been previously used to fractionate humic substances and determine metal ion binding (20,34,98). Unfortunately, there was a loss of lindane due to adsorption on the cell wall and, especially, on the membrane. The loss to the membrane was found to be ten times higher than that to the cell wall. Therefore, use of a pre-ultrafiltration equilibration procedure to condition the filtration devices (including the membrane) was necessary. That is, prior to a set of measurements, 50 mL of control solution was added to the cell under N_2 pressure and with stirring. Tests were run in either standing mode (static) or flowing mode through the membrane (dynamic) for various times. Fig. 2-2.2 shows the corresponding results in which the L_f and L_c refer to lindane concentrations in the filtrate and in the cell, respectively. These led to the choice of a dynamic conditioning time of 45 minutes in experiments reported here, with a lindane recovery of up to 80%.

The analytical chemical method and the binding experiments consisted of closely linked ultrafiltration procedures, but should be recognized as being distinct from each other. One was the "probe" and the other was the experiment being monitored with it. The control curve was an analytical chemical calibration in the absence of complexing agent, that checked the effects, if any, of the filter membrane on the dilution curve. The slope and intercept of the postcomplexing part of the test curve were checked directly against it. The net result of the separate analytical chemical calibration curve and the test

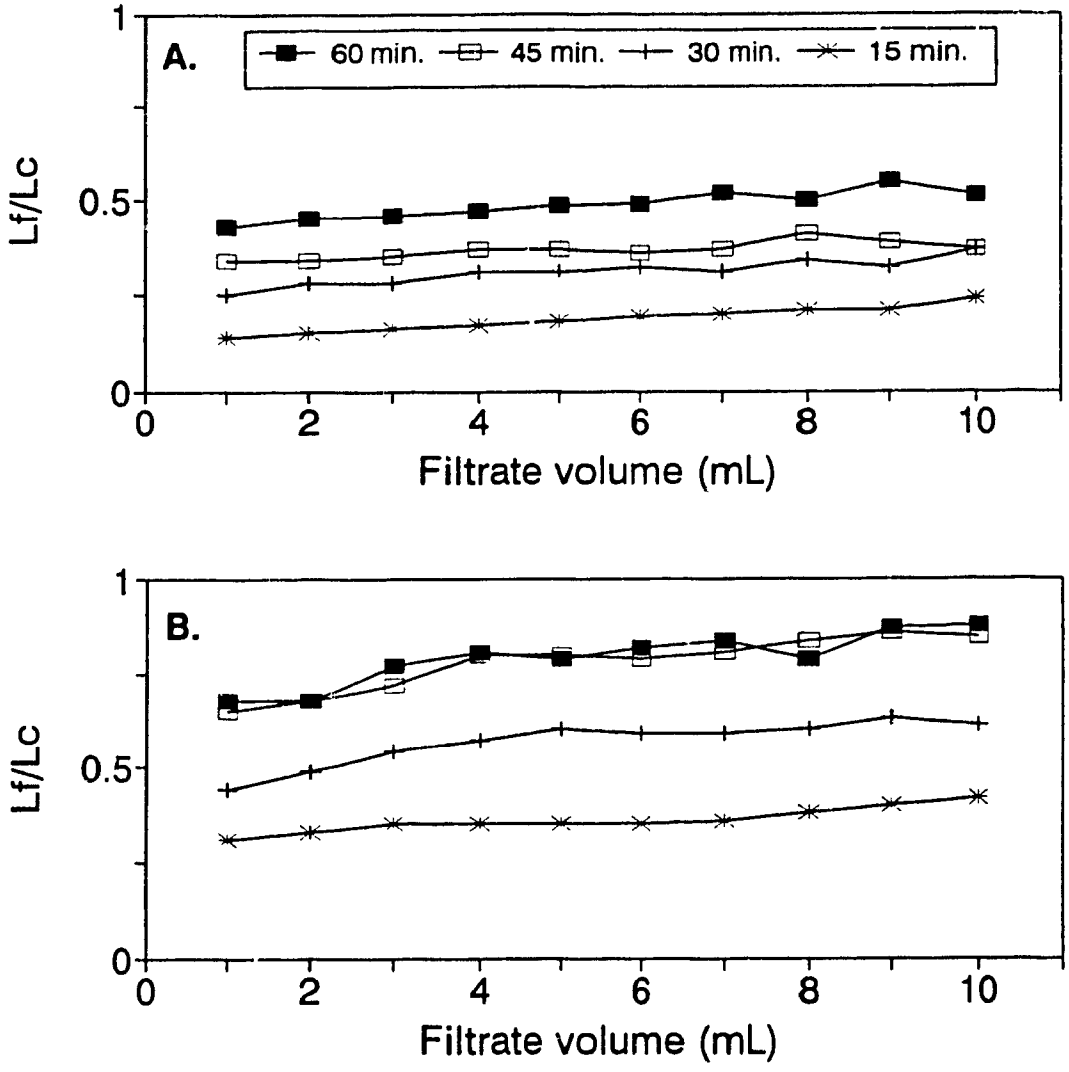

Fig. 2-2.2, Recovery of Lindane as a Function of Filtrate Volume (A. Static; B. Dynamic)

curve was lindane complexed that was determined by difference. These measurements used were made on the same side of the ultrafilter both with and without fulvic acid, after allowance for possible membrane effects. If GC measurements were made on both sides of the filter membrane, then bound lindane would still have to be calculated by difference.

Simple experimental tests with atrazine have been demonstrated for detecting possible membrane effects on the control curves in the absence of fulvic acid (99). The atrazine concentration L_f in the filtrate was predicted by:

$$L_f = B_o + B_1 V_s \qquad (2\text{-}2.1)$$

in which V_s was the volume of standard stock solution having a concentration of C_s. For ideal behaviour, $B_o = 0$ and $B_1 = C_s/V_o$, where V_o was the initial volume in the ultrafiltration stirred cell. The experimental values of B_o and B_1 provided tests as described (99), for such membrane interferences as rejection, sorption and desorption of atrazine. There were similar tests for deviation from nonideal behaviour in the presence of fulvic acid. It is anticipated that the test methods are general, so that they may be adapted to the lindane experiments. In the experiments with the lowest initial lindane concentration, 1.049 μM, the GC analysis usually gave equilibrium concentrations that were higher than the ideal ones. Control experiments indicated that this was caused by desorption of pre-equilibrated lindane from the membrane (Fig. 2-2.3). This background effect has been encounted before, together with the correction method for it (99). Low lindane concentration points were reported but given low weighting during data analysis. In addition to pesticide-membrane interactions, it is necessary to account for fulvic acid-

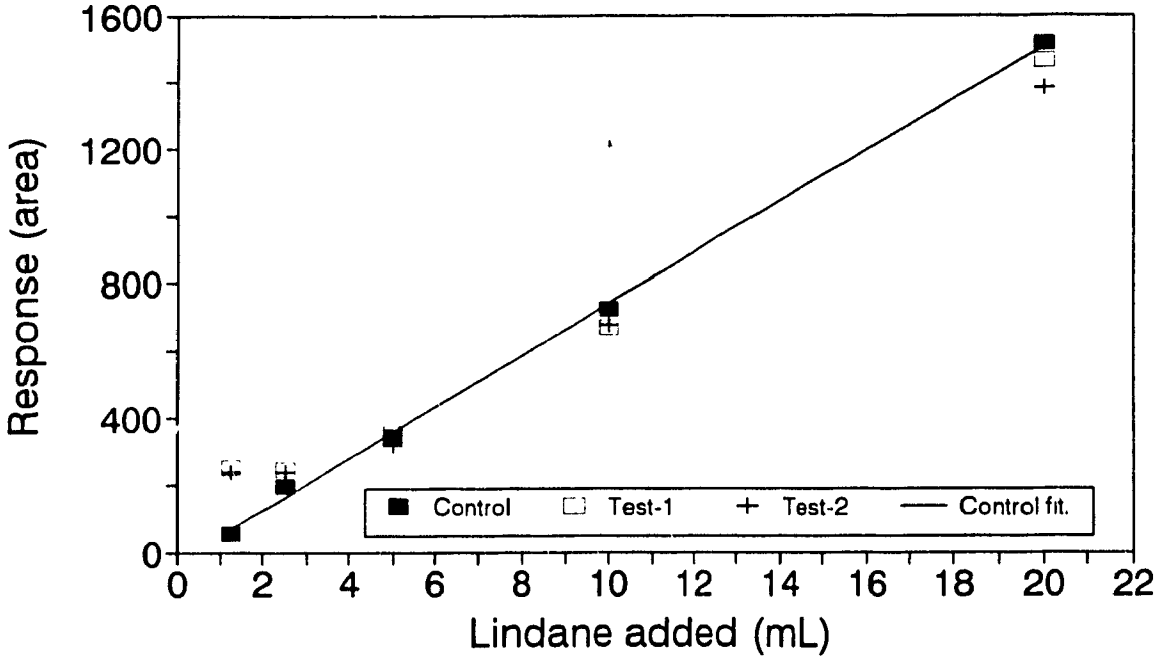

Fig. 2-2.3, Parallel Experiments Showing the Effect of Membrane Background
(Control = without filtration, Test = with filtration)

membrane effects. Wang et al. determined by the spectroscopic examination of filtrates that fulvic acid leakage through the ultrafilter was less than 1%, and would not cause significant experimental errors (281).

2-3. RESULTS

(1). *Results of previous studies*

Wang et al. (281-283) have systematically studied the interactions of polar herbicide atrazine with Laurentian fulvic acid, humic acid, and Laurentian soil, using an ultrafiltration-HPLC method. Some of the main points are:

(i). Laurentian FA contains 5.11 mmole Type A (highly and moderately acidic) and 3.49 mmole Type B (very weakly acidic) carboxyl groups per gram FA, and 3.03 mmole phenolic groups per gram FA. Laurentian HA contains 2.50 mmole carboxyl groups and 5.10 mmole phenolic groups per gram HA. Structurally, they are polymer mixtures.

(ii). The studies indicate that unionized carboxyl groups are involved in atrazine binding sites, and only a very small fraction of total carboxylate (less than 1%) act in atrazine binding. These special sites are created by conformational and configurational changes of the polymer molecules. The maximal binding of atrazine by FA, HA and soil are 8.8 μmoles g^{-1} FA (at pH 1.4-1.9), 15.3 μmoles g^{-1} HA (at pH 3.05), and 7.4 μmoles/20.00 g soil (at pH 2.50), respectively.

(iii). Two main factors which largely affect FA and HA aggregation are hydrogen ion and electrolyte concentration. In the presence of 0.100 M KCl and at high H^+

concentration the aggregation becomes significant and important.

(iv). The predominant mechanism for atrazine-FA and atrazine-HA interactions is probably the formation of hydrogen bonding between the protonated carboxyl groups and ring or chain nitrogen of atrazine. The nitrogen atom is electron-donor and the hydrogen atom of protonated carboxyl groups is electron-acceptor. The calculated free energies of atrazine binding are of the order of hydrogen bond energies, and correspond to the formation of one or two hydrogen bonds.

(2). ***Lindane-FA interaction***

Several parallel experiments with an initial lindane concentration of 4.181 μM and FA concentration of 1,000 ppm at pH 5.40 gave the time dependence of lindane binding equilibration. After shaking for 12, 24, 36, and 48 hours, the bound lindane was 0.23, 0.32, 0.38, and 0.37 μmoles g^{-1} of FA, respectively. Hence at least 36 hours were required to establish the binding equilibrium, which was slower than the rate of lindane adsorption by sediments (182).

A series of experiments at constant FA concentration but variable lindane concentration (from 1.03 to 11.7 μM) were used for investigating the effects of solution parameters such as pH, and ionic strength on lindane binding. The pH range was 1.17 to 8.38 in 13 steps. As an example, the titration of 300 ppm FA with lindane stock solution at pH 1.17 is presented in Fig. 2-3.1. Similar results with FA = 1,000 ppm and pH 2.04 and 4.98 are shown in Figs. 2-3.2 and 2-3.3. Lindane bound vs. total lindane at pH 2.04, 4.98 and 5.83 is given in Figs. 2-3.4A (KCl = 0) and 2-3.4B (KCl

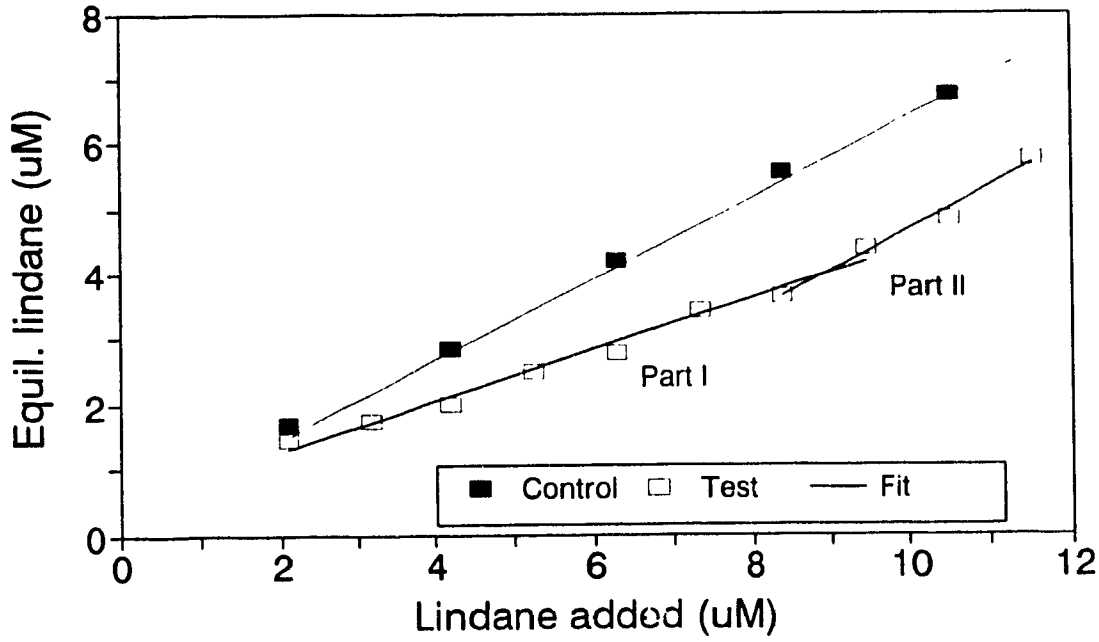

Fig. 2-3.1, Equilibrium Lindane as a Function of Lindane Added (FA=300 ppm, pH=1.17, KCl=0)

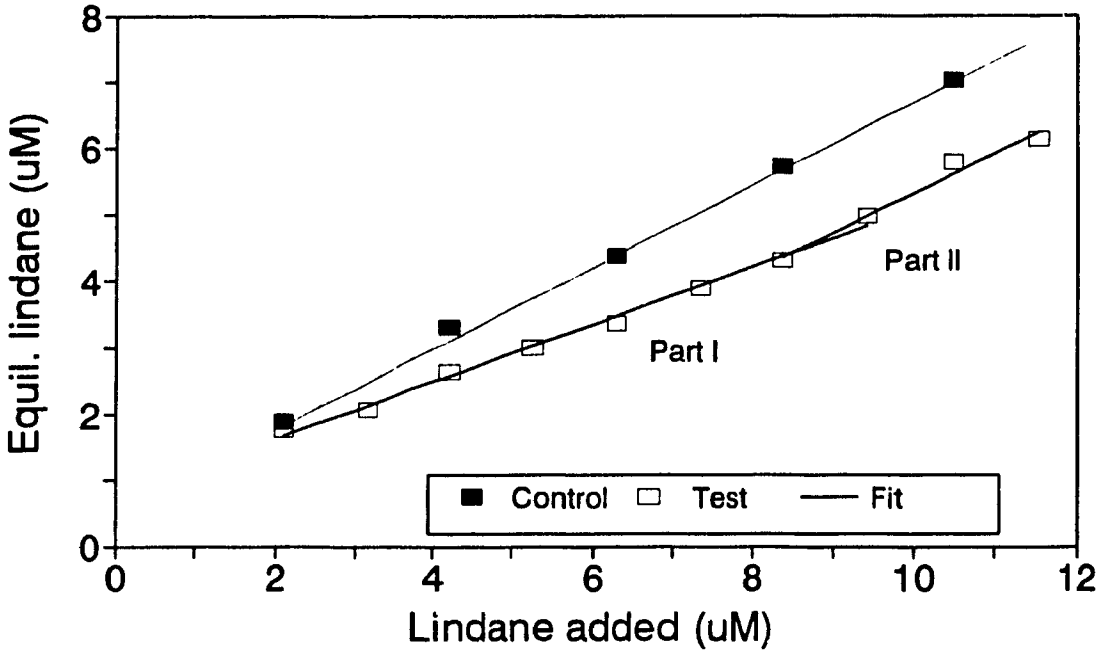

Fig. 2-3.2, Equilibrium Lindane as a Function of Lindane Added (FA=1,000 ppm, pH=2.04, KCl=0)

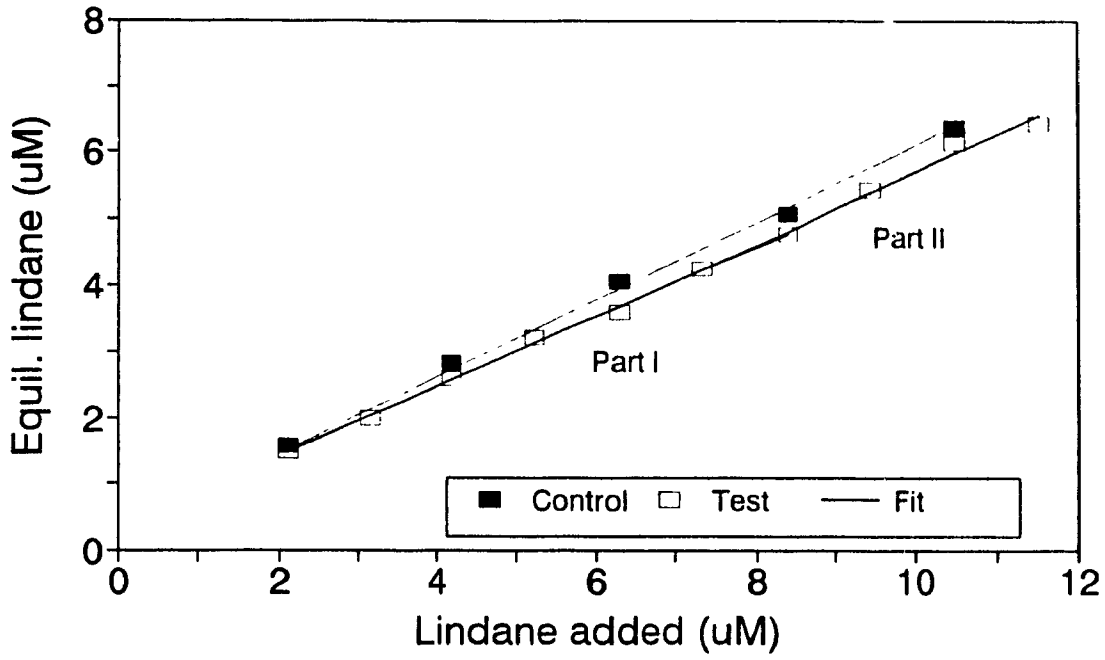

Fig. 2-3.3, Equilibrium Lindane as a Function of Lindane Added (FA = 1,000 ppm, pH=4.98, KCl=0.100 M)

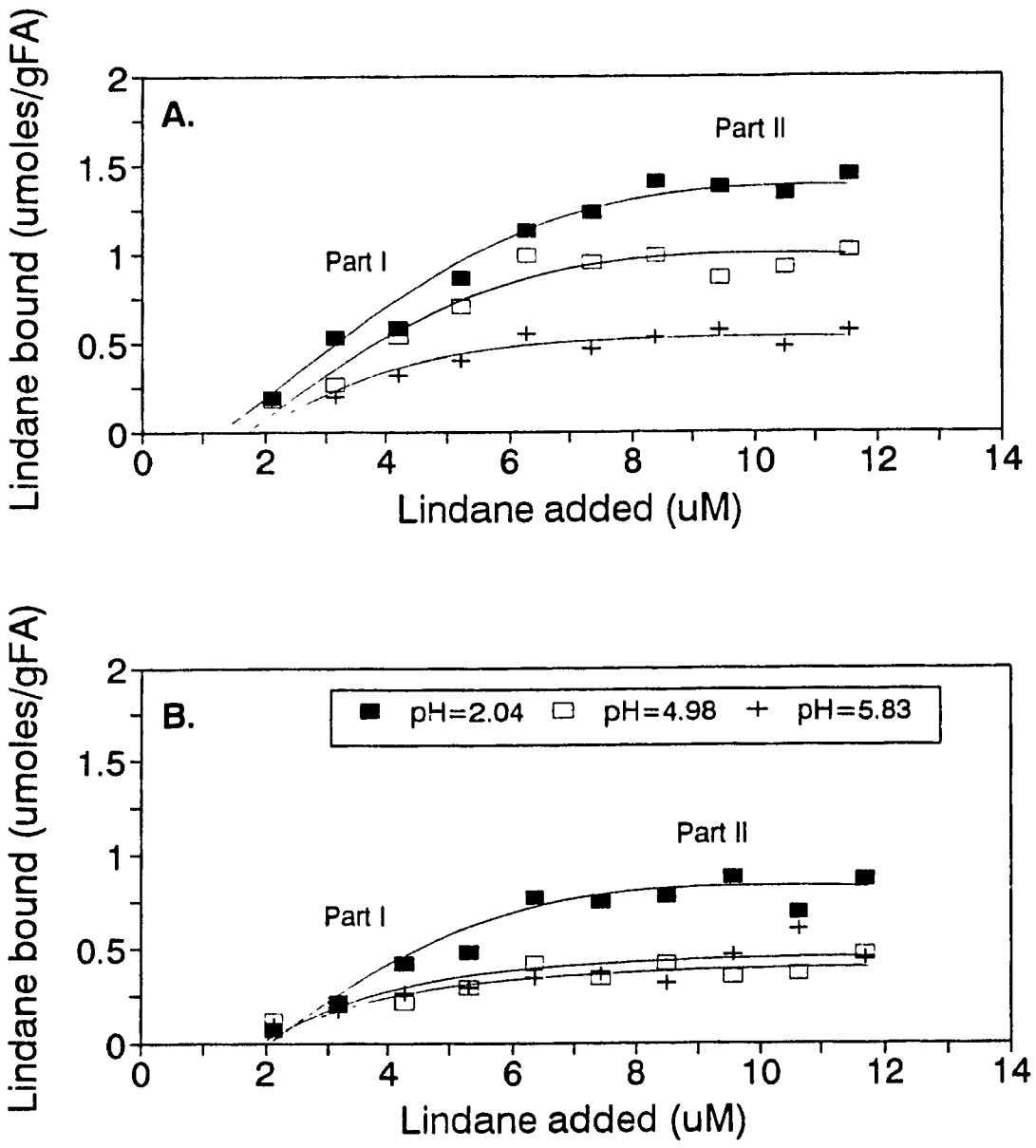

Fig. 2-3.4, Lindane Bound as a Function of Lindane Added (FA=1,000 ppm, KCl: A=0, B=0.100 M)

Table 2-3.1, Linear Regression Results for Data in Figs. 2-3.1 to 2-3.3

$$L_f = B_o + B_1 V, \qquad (2\text{-}2.1)$$

Data	Intercept B_o	σ	Slope B_1	σ	R^2
Fig. 2-3.1:					
Control	0.359	0.081	0.603	0.011	0.999
Test(Part I)	0.475	0.140	0.386	0.022	0.990
Test(Part II)	-1.83	0.555	0.642	0.055	0.993
Test(Total)	0.236	0.186	0.436	0.025	0.987
Fig. 2-3.2:					
Control	0.640	0.079	0.606	0.012	0.999
Test(Part I)	0.758	0.093	0.430	0.014	0.994
Test(Part II)	-0.670	0.152	0.598	0.065	0.988
Test(Total)	0.568	0.170	0.471	0.018	0.977
Fig. 2-3.3:					
Control	0.444	0.077	0.561	0.012	0.999
Test(Part I)	0.397	0.067	0.521	0.015	0.997
Test(Part II)	0.129	0.109	0.557	0.025	0.992
Test(Total)	0.339	0.089	0.535	0.009	0.995

= 0.100 M), respectively.

Lindane possesses a moderate hydrophobicity. The reported aqueous solubility is from 6.6 to 10 ppm (23 to 34 μM) and the octanol-water partition coefficient, $\log K_{ow}$, is 5.50 at room temperature (54,85,284). The primary result which emerges clearly from Figs. 2-3.1 to 2-3.4 is the resolution of choice of models for treatment of the data. In a partition model characterized by a distribution coefficient, K_d, a single straight line with a slope different from the control slope should fit the test points in Figs. 2-3.1 to 2-3.3. In a binding site model with a well defined binding capacity, the expectation for these figures is the test points which lie below the control curve but appear as a straight line

parallel to the control curve at a large excess of lindane. In both cases, the intercept of test and control curves must coincide. Table 2-3.1 shows the linear regression results for the data in Figs. 2-3.1 to 2-3.3. Clearly, the second interpretation is the better fit.

In Fig. 2-3.4 the saturation of lindane binding at high lindane concentration is clearly indicated. This holds at each of the pH and ionic strength conditions examined. The regression results for the data in Fig. 2-3.4 were incorporated into Table 2-3.2. Both of the B_1 slope values were zero to within the standard deviations, and the very small R^2 values for the plateaus in Part II of the curves are consistent with this. The intercepts (B_o) correspond to the binding capacities at each pH. As a consequence, the remainder of this paper exploits the binding constant, definite binding site model. In the introduction it was noted that the hydrophilicity and smaller molecular weight of FA argue against a distribution coefficient model. The distribution coefficient model fails empirically as expected.

Over the region where FA carboxyl group deprotonation occurs, lindane binding by fulvic acid is seen to be inversely related to pH (Table 2-3.3). With decrease in pH the degree of protonation of FA carboxylic groups increases. The atrazine binding capacities of humic materials have been found to correlate with the number of protonated carboxyl groups, but with a carboxylic group participation rate of 1% or less (281). This is consistent with the postulate that the formation of the structure-specific binding sites has a labile equilibrium in which the protonated carboxyl groups participate. The number of protonated carboxyl groups depends on pH, ionic strength, and the total carboxyl-carboxylate concentration. Inorganic electrolyte screens the electrostatic charge of the

Table 2-3.2, Bound Lindane, $L_b = B_o + B_1V_s$ (μmoles g^{-1} of FA): Linear Regression for Data in Fig. 2-3.4

Data	pH	KCl (M)	Intercept B_o	σ	Slope B_1	σ	R^2
Part I:							
	2.04	0	-0.248	0.118	0.205	0.021	0.975
		0.100	-0.139	0.087	0.120	0.015	0.962
	4.98	0	-0.188	0.099	0.168	0.020	0.974
		0.100	0.037	0.047	0.047	0.008	0.931
	5.83	0	0.003	0.111	0.073	0.020	0.901
		0.100	0.017	0.028	0.049	0.005	0.976
Part II:							
	2.04	0	1.32	0.238	0.008	0.024	0.222
		0.100	0.729	0.462	0.008	0.046	0.116
	4.98	0	0.972	0.135	-0.002	0.015	-0.064
		0.100	0.335	0.115	0.006	0.012	0.250
	5.83	0	0.487	0.100	0.005	0.011	0.206
		0.100	0.221	0.145	0.021	0.015	0.817

(cont'd)						
Total:						
	0	0.082	0.147	0.135	0.020	0.925
2.04						
	0.100	0.051	0.107	0.078	0.014	0.890
	0	0.169	0.133	0.084	0.018	0.858
4.98						
	0.100	0.110	0.047	0.030	0.006	0.866
	0	0.188	0.074	0.036	0.009	0.822
5.83						
	0.100	0.049	0.049	0.041	0.007	0.913

Table 2-3.3, Correlation of the Binding Capacity (μmoles g^{-1} of FA) with Solution pH

pH	1.17	1.53	2.04	2.57	3.25	3.79	4.57	4.98	5.40	5.83	6.87	7.73	8.38
KCl=0:													
	1.42	1.36	1.40	1.35	1.36	1.16	0.94	0.92	0.64	0.51	0.35	0.31	0.33
KCl=0.100 M:													
	0.85	0.84	0.79	0.75	0.66	0.49	0.41	0.36	0.31	0.34	0.32		

humic polyelectrolyte and increases aggregation (275). Competition from intrahumic complexing then reduces pesticide-humic complexing. In Fig. 2-3.5, lindane exhibits these effects to a lesser extent. It is worth noting that the curves in Fig. 2-3.5 reflect the shapes of acid-base titration curves. For example, the upper curve has an inflection point between carboxyl group molarities (3.98 to 3.25) x 10^{-4} M (pH 5 to 6). This is the approximate location of the titration end point for the carboxylic groups. If there is a linear dependence of binding capacity on the number of protonated carboxylic groups as was found for atrazine, then a plot of binding capacity vs. carboxyl group molarity would be expected to reflect the titration curve for the carboxylic groups. In addition, the extent of binding observed at all pH was diminished at high ionic strength (0.100 M). Higher ionic strength is connected to increased dissociation of FA type A acid group (85). Such ionic strength effects agree with those obtained for DDT (42).

Lindane binding also varies with the total FA concentration. This effect was investigated quantitatively at pH 1.17 in the absence of KCl and pH 2.10 in the presence of 0.100 M KCl. These pH values were chosen to be near the maximum binding capacity. FA concentrations were varied from 100 to 1,000 ppm in 4 intervals. Fig. 2-3.6 shows the capacity for lindane binding expressed intensively, per g of fulvic acid. The results are similar to those reported for atrazine binding (281). The increase of FA concentration, which favours aggregation (274,275), reduces the lindane binding capacity. Components, presumably lower molecular weight ones as in the atrazine case, of the FA compete to block the sites for binding of lindane. This is in striking contrast to the expectation for a phase distribution model.

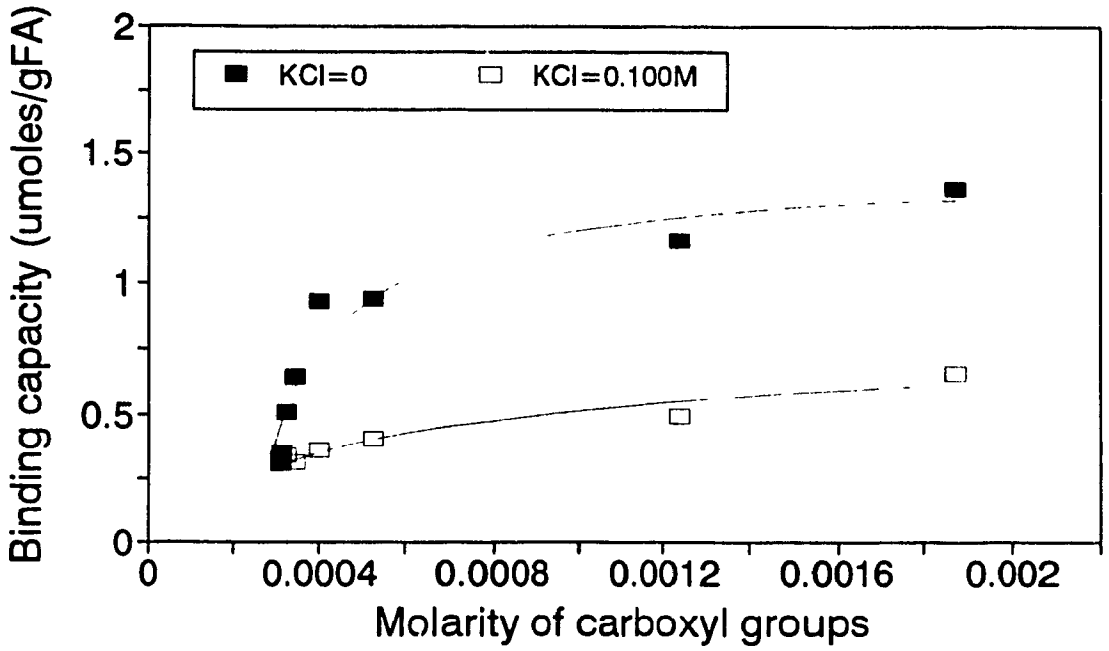

Fig. 2-3.5, Lindane Binding Capacity as a Function of Carboxyl Group Molarity (FA = 1,000 ppm)

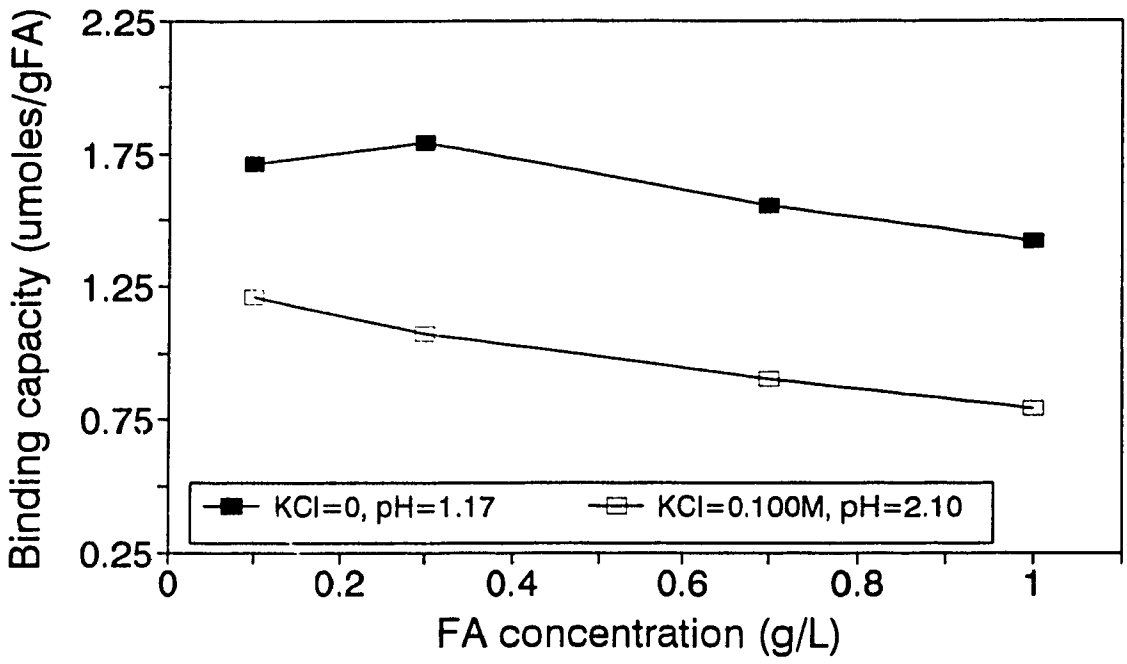

Fig. 2-3.6, Dependence of Lindane Binding on FA Concentration

2-4. DISCUSSION

There is a close relation between the protonation of FA carboxylate groups and lindane binding, as well the capacity of Laurentian FA to bind lindane has been demonstrated to be small. For example, the binding capacity near 1.42 μmoles g^{-1} of FA is less than 1% of the carboxylic group density of several millimoles g^{-1} of FA. This is similar to the result for atrazine. In that case (281), it was suggested that hydrophobic sites on the FA are closely linked to carboxylate protonation because it is conformational equilibria of the polymer which create the relatively rare hydrophobic sites which bind pesticides of low water solubility.

The rarity of specific sites is consistent with the largely hydrophilic character of humic substances. In this context, it is to be expected that changes in the polymer conformation would affect the availability of such sites. The dependence of capacity on ionic strength and FA concentration (aggregation) is entirely consistent. A consistent picture of the "hydrophobic binding" behavior of humic substances emerges from the study of both atrazine and lindane. In this picture a small number of hydrophobic sites are assumed to be produced in the large polymer components of the humic materials by dynamic conformational equilibria. These sites may be destroyed by the conformational changes associated with carboxylate deprotonation or blocked by aggregation of smaller molecular weight fractions of the humic substances.

The question which remains is how closely this model of pesticide binding is appropriate to other samples of natural organic matter. In the case of atrazine, it was

demonstrated that the model appropriate to the FA was generalizable to the humic acid and to the pH dependent part of the behavior of the whole soil (282,283). A suggestion is contained in Table 2-4.1 where various maximum pesticide binding capacities which have been quoted in the literature are collected. We see that normalized to the units of μmoles g^{-1} of organic carbon the capacities are suggestively similar, although the available cases where an explicit stoichiometric binding capacity is known remain few.

Table 2-4.1, Comparison of the Measured Maximum Binding Capacities of Various Natural Organic Matter(NOM) Samples

Pesticide	Amount*	pH	Adsorbent	Ref.
Lindane	1.52	5.4	Organic soils	14
Lindane	1.60	1.20	Armadale Bh FA	274
Lindane	5.85	5.3	Sediment (#3)	175
Lindane	3.48	5.5	Sediment (#6)	175
Lindane	6.56	5.5	Sediment (#8)	175
Lindane	3.16	1.17	Laurentian FA	This work
Atrazine	19.8	1.40	Laurentian FA	281

* μmoles g^{-1} of OC.

In addition, it is still possible that some possible models other than discussed above, e.g. an association as an electron acceptor with suitable electron-rich sites (193,194) or trapping within voids in the polymer (153,225) may also play a role.

2-5. SUMMARY

As a preliminary chapter to this thesis, an investigation of the binding site complexation model was carried out with the interaction between slightly polar insecticide lindane and Laurentian fulvic acid. It was shown that:

(1). The GC-ultrafiltration method is an important technique in studying the binding behavior of pesticides with both undissolved and soluble humic substances. In particular, the dynamic pre-ultrafiltration equilibration procedure has been shown to be effective for diminishing material loss due to the membrane sorption.

(2). The small (~ 1 μmole g^{-1} of FA) and limited binding capacity for this system was observed and varied as a function of solution pH, ionic strength, and FA concentration. This result favors a definite binding site model which is related to the protonation of carboxylate groups, and suggests that these hydrophobic sites are created by conformational equilibria of the FA polyelectrolyte.

Consequently, more investigations with a broad range of natural organic matter are substantially needed in order to evaluate the generality of this binding site model.

CHAPTER 3

ATRAZINE UPTAKE BY MINERAL SOIL GB 843

3-1. INTRODUCTION

Pesticide-soil interactions involve several processes such as sorption/desorption, intraparticle diffusion, chemical and microbiological degradations. It has been well documented in recent years that sorption is one of the most important processes in determining the persistence and transport of pesticides in the soil subsurface environment. As previously stated in Chapter 1, considerable advancements have been made in the studies of pesticide uptake by soils over the last decade (33,196,197,287,288).

The general consensus for sorption processes in the literature is mostly based on the two-domain models (33,226,287,288), which usually specifies a labile contribution and a nonlabile contribution to the uptake kinetics occurring in batch experimental systems. The labile uptake has been often treated as an instantaneous process, and described mathematically with an isotherm equation (K_d) or first-order rate expression (32,63,78,142-144,150,185,222,264,293). For the nonlabile uptake, in fact, there have been relatively few batch soil sorption studies in which experimental data have been directly interpreted by diffusion rate models, except for the recently reported work

(11,12,296) that described diffusive rates with the radial solution of Fick's first law (66).

In contrast, a two stage adsorption/diffusion model has been developed by Gamble, Langford, and coworkers (93-95,97,103,170), to account for pesticide-soil interactions by assuming at least two kinetically linked processes: a relatively fast labile surface adsorption followed by a highly retarded intraparticle diffusion. It differs from the existing models: 1) on the basis of a site binding or specific interaction mechanism (281-283,169; see Chapter 2), the uptake by sorption is stoichiometrically limited by the labile sorption capacity; 2) a second-order differential rate law is generally used to account for the labile surface adsorption, and also a first-order initial rate approximation is employed for the case of low coverage; and 3) the intraparticle diffusion process is treated with a particular solution of Crank's model set (66), i.e., labile sorbate coverage serves as the driving force, and is described by a first-order rate law.

A fundamental requirement for effective assessment of sorption mechanisms is the analytical chemical methodology for measuring the distribution of pesticide species between solution and suspended soil phases. As stated in Chapter 1, conventional batch experimental methods are unable to distinguish between labile surface sorbed species, and bound residues formed by intraparticle diffusion, but referred to totally as the "sorbed phase". This prevents the correct use of chemical stoichiometry. The microfiltration (MF)-HPLC technique combined with a batch method (93,94,97), however, has been found to meet the requirements for the kinetic speciation studies of pesticide uptake.

In addition, long-term sorption/desorption is just beginning to receive attention (11,12,33,63,144,154,185,215). These investigations have shown that time scales of

weeks to months, or even years, were required to achieve sorption equilibrium. For a pertinent mechanism study, the information regarding the relationship between surface adsorption/desorption and intraparticle diffusion over a sufficiently long period is obviously needed.

In view of the foregoing, some sorption phenomena have not yet been fully identified and explained. In particular, although the two stage mechanism has been checked by the ongoing experimental results, and also has undergone some field or soil column testing by being introduced into a newly established solute transport model PESTFADE (59-61,171), it needs further modifications or improvements as a potential mechanistic model.

The objective of this chapter is to present a derivation for the two stage adsorption/diffusion mechanistic model, to experimentally identify the labile sorption and bound residue formation processes which occur between a widely used herbicide atrazine (2-chloro-4-(ethylamino)-6-(isopropylamino)-s-triazine, Fig. 3-1.1) and a mineral soil Green Belt (GB 843) over independent short-term or long-term periods, and to determine the relevant equilibrium/kinetic parameters. An attempt can be made to better understand the sorption mechanisms, by using a batch experimental method combined with MF-HPLC technique (93,94,97).

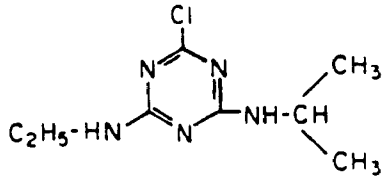

Fig. 3-1.1, Atrazine (2-chloro-4-(ethylamino)-6-(isopropylamino)-s-triazine)

3-2. MECHANISTIC MODEL: A TWO STAGE ADSORPTION/DIFFUSION MECHANISM

As stated in Chapter 1, a two stage surface-adsorption/intraparticle-diffusion mechanism has been proposed to describe the equilibrium and kinetic behavior of atrazine uptake by soil (93-95,97,103,170,171). The two mass transfer processes can be schematically expressed as Fig. 3-2.1 and eq. 3-2.1:

$$SS \underset{k_{s2}}{\overset{k_{b1}}{\rightleftharpoons}} SL \underset{k_{d2}}{\overset{k_{d1}}{\rightleftharpoons}} SD \qquad (3\text{-}2.1)$$

where SS, SL, and SD represent the dissolved species in soil solution, labile surface sorbed species, and intraparticle diffusion trapped species, respectively. This latter species is one type of bound residue. SL is defined by the amount of sorbed species

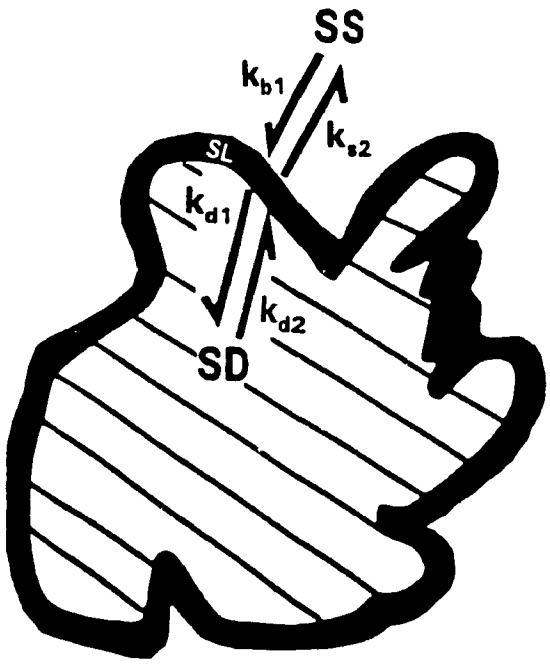

Fig. 3-2.1, A Schematical Representation of Atrazine Mass Transfer

which are "desorbed" in the MF-HPLC experiment by extracting the soil with mobile phase.

(1). *Equilibria and kinetics of labile surface adsorption/desorption*

As shown in Chapter 1, the two stage model uses the following equations to account for the rate behavior of surface adsorption/desorption (the first stage):

$$-dM_{AT}/dt = (W/V)d\theta_L/dt$$

$$= k_{b1}M_{AT}(W/V)\theta_o - k_{s2}(W/V)\theta_L \qquad (3\text{-}2.2)$$

$$-dM_{AT}/dt = (W/V)d\theta_L/dt$$

$$= k_{s1}M_{AT} - k_{s2}(W/V)\theta_L \qquad (3\text{-}2.3)$$

where M_{AT} (in moles L^{-1}), θ_L and θ_o (in moles g^{-1}) represent atrazine concentrations in solution phase, occupied (or labile sorbed), and unoccupied sorption sites, respectively, k_{b1} and k_{s2} are the rate constants for adsorption (second-order, in L mol^{-1} d^{-1}) and desorption (in d^{-1}), k_{s1} is the pseudo first-order rate constant for adsorption, $k_{s1} = k_{b1}(W/V)\theta_o$ (in d^{-1}), which is an approximation to the low site coverage (i.e., θ_L being small, thus $\theta_o \approx$ constant), and t is time (in days). The term W/V is a unit converting factor (in g L^{-1}).

Analogous to the treatment for a mixed ligand system (96), the sorption of atrazine to a heterogeneous mixture of n types of sorption sites can be expressed as:

$$\bar{K}_1 = (K_{eq1}C_{o1} + K_{eq2}C_{o2} + \ldots + K_{eqn}C_{on})$$

$$/(C_{o1} + C_{o2} + \ldots + C_{on}) \qquad (3\text{-}2.4)$$

or

$$\bar{K}_l = \Sigma_{i=1\text{-}n} K_{eqi} C_{oi} / \Sigma_{i=1\text{-}n} C_{oi} \qquad (3\text{-}2.5)$$

where $\bar{K}_l$ (in L mol^{-1}) is the weighted average equilibrium function, K_{eq} (in L mol^{-1}) is the equilibrium binding constant, C_o (in moles L^{-1}) is the concentration of vacant sorption sites, and i (1 to n) indicates the types of sorption sites.

Stoichiometric, kinetic, and equilibrium analysis of pesticide sorption by soils (93-95,97,103,170) has indicated that the labile sorption has a definite capacity or saturation limit which is termed labile sorption capacity, C_c or θ_c, as shown in a mass balance expression:

$$C_c = C_L + C_o \qquad (3\text{-}2.6)$$

or

$$\theta_c = \theta_L + \theta_o \qquad (3\text{-}2.7)$$

where C terms represent concentrations in moles L^{-1} of slurry, and θ in moles g^{-1} of soil. The measurement of this parameter will be given in section 3-4.(6).

Consequently, the mole fraction of covered surface sites, X_l, can be obtained:

$$X_l = \theta_L / \theta_c \qquad (3\text{-}2.8)$$

In hydrology models, a parameter K_d, the distribution coefficient (in L g^{-1}), is usually used:

$$K_d = \theta_L / M_{AT} \qquad (3\text{-}2.9)$$

The relationship between K_d and $\bar{K}_l$ can be given by combining eq. 1-1.18 with eq. 3-2.8:

$$K_d = \bar{K}_l (1\text{-}X_l) \theta_c \qquad (3\text{-}2.10)$$

K_d is a partition-based parameter, and thus its practical limitation in describing the uptake

of polar or ionic pesticides by soils with low organic matter contents should be noted.

(2). *Bound residue formation by retarded intraparticle diffusion*

A number of authors have reported that an initially fast sorption of organic chemicals by soils is followed by a second stage that is much slower and apparently irreversible, and have suggested that the organic chemicals slowly diffuse into the interior of the soil particles (2,46,70,74,83,112,142-144,150,176,218,254,272). Gamble, Langford, and coworkers have observed this nonlabile sorption phenomenon using the microfiltration-HPLC technique and have concluded that the diffusion of atrazine into the interior* of soil particles is the most likely explanation for the material balance loss (93-95,97,103,170).

Since the initial sorption is fast and labile, the particle surfaces can be generally viewed as having a steady state concentration layer fed by the solution phase atrazine and consumed by the diffusion process. Crank (66) has presented a set of solutions for the application of Fick's law differential equations to similar diffusion models. A solution for the particular case of diffusion into semi-infinite media from a steady state surface coverage, C_1, is given by:

$$M_t = 2C_1(Dt/\pi)^{1/2} \qquad (3\text{-}2.11)$$

where M_t is the total amount (in g cm^{-1}) of material taken up by diffusion at time t, D is the diffusion coefficient (cm^2 s^{-1}), and t is the time (seconds). The "constant"

---

* "interior" here means that region from which sorbate cannot be extracted rapidly by the HPLC mobile phase. Since the labile sorption can take hours, much of it must be to the "interior" in a physical rather than chemical sense.

concentration (C_1) which is expressed as the amount of diffusing species per unit area of surfaces (in g cm^{-2}), is related to the labile surface coverage (θ_L) by $\theta_l = C_1/l$, where l is a particle dimension related to diffusion (in cm). Letting $M_t/l^2 = \theta_D$, in which θ_D has the same meaning as M_t (but in moles g^{-1}), and l^2 is introduced for converting the mass distribution from one-dimensional to three-dimensional, then the eq. 3-2.11 can be rewritten as:

$$\theta_D = [2(\theta_L/l)(D/\pi)^{1/2}]t^{1/2} \qquad (3\text{-}2.12)$$

thus

$$Ln(\theta_D) = Ln(A) + 1/2Ln(t) \qquad (3\text{-}2.13)$$

where $A = 2(\theta_L/l)(D/\pi)^{1/2}$. A plot of $Ln(\theta_D)$ versus Ln(t) will be a straight line with a slope equal to 0.5, and θ_D will be proportional to θ_L.

The differential rate law for the second stage of the mass transfer between labile sorption sites and diffusion trapped state can be described as inward and outward diffusion processes:

$$d\theta_D/dt = k_{d1}\theta_L - (V/W)R_{d2} \qquad (3\text{-}2.14)$$

where k_{d1} is the rate constant (in d^{-1}) for the forward process, and R_{d2} represents the reverse diffusion term. When the diffusive uptake of atrazine is sufficiently small, i.e., $R_{d2} << k_{d1}\theta_L$, this reduces to eq. 3-2.15:

$$d\theta_D/dt = k_{d1}\theta_l \qquad (3\text{-}2.15)$$

Although the existing literature (144,148,150,296) generally assumes that uptake by the forward diffusion ($k_{d1}\theta_L$) can be approximated by first-order kinetics, no simple theoretical support has been found for this. Some of more recently published works

(12,296) use a second-order partial differential equation derived from the one-dimensional solution of Fick's law to describe the diffusive uptake, in which two parameters, total sorbed amount (q or S) and solution phase concentration (C), are main measurable data. In contrast to this, the MF-HPLC/batch technique can track the distinction between labile sorbed species and material balance loss, which makes independent use of eq. 3-2.14 or eq. 3-2.15 possible. To date, not much information has been obtained for the reverse diffusion term, R_{d2}, because its rate has not readily been detected during the first two or three weeks of the reaction (97).

The two stage model postulates eq. 3-2.16 as a simple relationship between the rate of nonlabile uptake and the diffusion coefficient:

$$k_{d1} = Q(D/a) \qquad (3\text{-}2.16)$$

where a is a cross sectional area related to particle sizes and shapes. Due to the lack of detailed information about the particle shapes and sizes, the value of a is not known. The dimension of a particle, l^2, therefore, is usually used as a crude approximation. Q is introduced here for the conversion of time units. With steady state site coverage, the diffusion coefficient, D, can be determined by the term Ln(A) in eq. 3-2.13.

(3). ***Total differential rate law***

In the absence of chemical reaction and microbiological degradation, the total differential rate law for atrazine accumulation on the surfaces can be described by combining the two mass transfer stages (eqs. 3-2.2 and 3-2.14) as follows:

$$(d\theta_l/dt)_T = d\theta_l/dt - d\theta_D/dt$$

$$= k_{b1}(V/W)M_{AT}\theta_o - k_{s2}\theta_L - k_{d1}\theta_1 + (V/W)R_{d2} \qquad (3\text{-}2.17)$$

or approximately (eqs. 3-2.3 and 3-2.15):

$$(d\theta_L/dt)_T = d\theta_L/dt - d\theta_D/dt$$

$$\approx k_{s1}(V/W)M_{AT} - k_{s2}\theta_L - k_{d1}\theta_L \qquad (3\text{-}2.18)$$

The kinetic rate parameters for the labile surface adsorption, such as k_{s1} and k_{b1}, will be generally evaluated either by an initial rate approximation, or by an iterative calculation. In particular, the pseudo first-order rate constant, k_{s1}, being frequently used and available for comparison in the existing literature, will be given more attention in the subsequent sections.

In addition, as indicated above, the outward diffusion term, R_{d2}, has not usually been identified with short-term experiments. Therefore, the following calculations will be confined to the early parts of the experiments during which diffusion out of particle interiors can be negligible so that $R_{d2} << k_{d1}\theta_L$. This would lead to an approximation $R_{d2} \approx 0$. The approximation is not valid late in the experiments. We will also see that θ_L is close enough to steady state in most measurements that $k_{d1}\theta_L$ is approximately constant.

(4). *Spreadsheet calculations*

The MF-HPLC technique is the only available method that identifies species in solution, recoverable from the surfaces, and bound residue formed by intraparticle diffusion. This offers opportunities for a choice of rate laws and calculation methods. A microcomputer spreadsheet was set up with the equilibrium/kinetic equations discussed

above, and used for processing the resulting experimental data, and calculating chemical species and physicochemical parameters. Table 3-2.1 is an example of the lists of constants entered into the spreadsheet. In addition, a raw data entry, interpolated data at rounded times, and data for kinetic calculations in the spreadsheet are shown in Appendices A to C, respectively.

Table 3-2.1, Constants for the Spreadsheet Calculations (Exp. #7)

Item	Value
Year	91
Init month	4
Init day	8
Init hour	10
Init min	37
Std AT, M	1.00E-06
Soln, mL	24.95
Soil dry wt, g	0.5040
Days at t=0	33336.44
Init AT, M	9.99E-07

(i). Calculations of k_{s1} and k_{b1} by an initial rate approximation:

At the early beginning of an experiment, θ_L (the labile sorption coverage) $<< \theta_c$ (the labile sorption capacity), and both $k_{s2}\theta_L$ (the desorption term) and $k_{d1}\theta_L$ (the inward diffusion term) in eq. 3-2.18 can be approximated to be zero. Therefore, the above relationship can be reduced to:

$$(d\theta_L/dt)_I = k_{s1}(V/W)M_{AT} \qquad (3\text{-}2.19)$$

The actual calculation of k_{s1} and k_{b1} in the subsequent sections will be generally carried out with a polynomial regression to fit experimental θ_L data (the initial labile

uptake) against t, and then take the value at t = 0 (206):

$$\theta_L = B_o + B_1 t + B_2 t^2 + \ldots\ldots \quad (3\text{-}2.20)$$

$$d\theta_L/dt = B_1 + 2B_2 t + \ldots\ldots \quad (3\text{-}2.21)$$

$$(d\theta_L/dt)_{t=0} = B_1 \quad (3\text{-}2.22)$$

By doing so, a set of B_1 data (i.e., the initial time rates) corresponding to different solution phase concentrations (M_{AT}) will be produced. Then, the k_{s1} value can be determined from the slope of plotting $(d\theta_L/dt)_{t=0}$ versus initial concentrations (M_{AT} at t = 0). Also, the second-order rate constant k_{b1} can be evaluated by (see section 3-5.(3)):

$$k_{b1} = k_{s1}/(W/V)\theta_o \quad (3\text{-}2.23)$$

(ii). Iterative calculation of k_{b1} from labile sorption term (C_L or θ_L):

From eq. 3-2.17:

$$(dC_L/dt)_T = k_{b1}M_{AT}C_o - k_{s2}C_L - k_{d1}C_L \quad (3\text{-}2.24)$$

k_{s2} is substituted with $k_{b1}/\bar{K}_1$ (ref. eq. 1-1.18):

$$(dC_L/dt)_T = k_{b1}M_{AT}C_o - (k_{b1}/\bar{K}_1)C_L - k_{d1}C_L \quad (3\text{-}2.25)$$

In the absence of losses from chemical reaction, microbiological degradation, evaporation, or sorption onto the apparatus, the total atrazine C_T is a constant, and let

$$X_{A2} = C_L/C_T \text{ and } X_{A3} = C_D/C_T \quad (3\text{-}2.26)$$

Rewriting eq. 3-2.25 gives:

$$(dX_{A2}/dt)_T = k_{b1}C_o(1-X_{A2}) - (k_{b1}/\bar{K}_1)X_{A2} - k_{d1}X_{A2} - k_{b1}C_oX_{A3} \quad (3\text{-}2.27)$$

Rearranging eq. 3-2.27:

$$dX_{A2}/(1-X_{A2}) = k_{b1}C_o dt - F(t)dt \qquad (3\text{-}2.28)$$

where

$$F(t) = [(k_{b1}/\bar{K}_1)X_{A2} + k_{d1}X_{A2} + k_{b1}C_oX_{A3}]/(1-X_{A2}) \qquad (3\text{-}2.29)$$

Integrating with integration limits for X_{A2} of x_a and x_b, the final equation is obtained:

$$-Ln[(1-x_b)/(1-x_a)] = k_{b1}C_o(t_2-t_1) - \int_{t1\text{-}t2} F(t)dt \qquad (3\text{-}2.30)$$

At the beginning of the reaction, the initial k_{b1} value can be estimated from eq. 3-2.30 by assuming $F(t) \approx 0$. An iterative calculation may then be carried out with eqs. 3-2.29 and 3-2.30, until the change in resulting k_{b1} values is small enough compared to the experimental errors. Except for k_{b1}, all the parameters are available from the experimental data.

An alternative method for estimating the initial k_{b1} value may use the initial rate approximation method, as described in section (i) (eq. 3-2.23).

(iii). Iterative calculation of k_{b1} from solution concentration (M_{AT}):

From eq. 3-2.17:

$$-(dM_{AT}/dt)_T = k_{b1}C_oM_{AT} - (k_{b1}/\bar{K}_1)C_L + k_{d1}C_L \qquad (3\text{-}2.31)$$

Rearranging gives:

$$-dLn(M_{AT})/dt = k_{b1}C_o - F(t) \qquad (3\text{-}2.32)$$

where

$$F(t) = (k_{b1}/\bar{K}_1 - k_{d1})(C_L/M_{AT}) \qquad (3\text{-}2.33)$$

Integrating with M_a and M_b as the integration limits of M_{AT}:

$$-Ln(M_b/M_a) = k_{b1}C_o(t_2-t_1) - \int_{t1\text{-}t2} F(t)dt \qquad (3\text{-}2.34)$$

A similar iterative calculation can be performed with eqs. 3-2.33 and 3-2.34 to evaluate k_{b1}.

Of the three calculation methods, the method (i) is a first-order approximation to the kinetics of early period of sorption experiments. By taking the k_{s1} value at $t = 0$, the influences of other kinetically simultaneous processes such as desorption, and intraparticle diffusion can be avoided (206). This method is simple, and would be expected to produce more accurate, if less precise, k_{s1} and k_{b1} values than those derived from the methods (ii) and (iii). In contrast, the methods (ii) and (iii) can provide numerical values for k_{b1}. Both have similar mathematical expressions (eqs. 3-2.30 and 34), except that the key data are C_L or θ_1 for method (ii) while M_{AT} for method (iii). Also, both involve the parameter $\bar{K}_1$ in calculations. This parameter has a relatively steady value only at the plateau region. Consequently, any uncertainties arising in kinetic experiments will affect the independent measurements of these key parameters. Some examples showing more detailed application of methods (i) to (iii) are incorporated in Appendix D.

It is important to note that, unlike calculations of diffusivity parameters (k_{d1} and D), the early measurable data (e.g., within the first few minutes to hours) appear to be critically essential for calculations of adsorption rate parameters (k_{b1} and k_{s1}). In this regard, the MF-HPLC method might exhibit its weakness.

3-3. EXPERIMENTAL

(1). *Equipment*

The batch setup included a reaction vessel which was a Pyrex cylinder 7.3 cm high by 3.0 cm diameter, with a screw cap. A Teflon coated stir bar and magnetic stirring base were used to keep the soil samples suspended. A thermostatted circulating bath connected to double-walled Pyrex jackets were used to maintain the slurry temperature at 25.0 or 10.0 ($\pm$0.2) °C. HPLC analyses were performed with a Varian Star 9010 solvent delivery system, a Varian Star 9050 UV-VIS variable wavelength detector set to 220 nm, and a Model 4400 integrator. A Waters Associates LC system with a Model 441 detector and a Rheodyne Model 7125 injector was also used. The column was a Beckman C-18 Ultrasphere ODS or CSC-Chromosorb LC-7, 25 x 0.46 cm i.d. A C-18 Adsorbosphere Alltech guard column cartridge with replaceable 2.0 μm and 0.5 μm stainless steel microfilters was used to trap solids and protect the main HPLC analytical column. Microfiltration of the slurry prior to injection was done with disposable B-D 1 cc 26G 3/8 Turberculin syringes and MSI Cameo Nylon 66 0.22 μm disposable microfilters. For direct injections of standards, filtrates and whole slurries, 100 μL Hamilton 710 syringes with fixed needles were used. Further details about the equipment have been published previously (93,94).

(2). *Reagents and materials*

The mineral soil GB 843 was collected from the Field no. 8, in the Green Belt area

of the Central Experimental Farm, Ottawa-Carleton Regional Municipality. This is a cultivated field that has been in use for several years for agricultural field experiments. The soil is described as a "rock flour", deposited by glaciers that had ground up Precambrian shield rocks. Soil fractions with different particle sizes were obtained by sieving (see Chapter 4).

Standard stock solution of 1 x 10^{-4} M atrazine was freshly prepared from the crystalline solid (Supelco, Inc., Bellefonte, PA, USA) using distilled deionized water. Analytical standards were prepared by serial dilution of the stock solution. Methanol and acetonitrile (HPLC grade, Caledon Lab. Ltd., Georgetown, Ont., Canada) were used for HPLC work. The use of these solvents as mobile-phase modifiers for extracting atrazine has been previously documented by a number of investigators (65,229,255,281).

(3). *General kinetic procedure*

A 0.5 g portion of the mineral soil was suspended with stirring in approximately 15 mL of distilled deionized water for about 2 days. This wetted all the surfaces and sorbed water into the soil particles. The kinetics reaction was started by the addition of a calculated aliquot of atrazine standard stock solution, with the total slurry volume being adjusted to 25 mL. Stirring maintained a uniform suspension of soil particles throughout the whole solution. Two types of HPLC analyses, a preinjection filtration by the 0.22 μm filters and a postinjection filtration by combining the 2.0 μm with 0.5 μm on-line filters, were done alternately as previously described (93,94). Methanol/H_2O (62.5/37.5 with 1.58 x 10^{-3} M HCl) or acetonitrile/H_2O (50/50 with 3.18 x 10^{-3} M HCl) were used as

mobile phases with a flow rate of 1.0 mL min^{-1}.

Each experiment was run for 3 weeks (short-term kinetics) or 12 weeks (long-term kinetics). The basic experimental parameters for the equilibrium/kinetics of bulk soil-atrazine interactions and for HPLC operation are shown in Tables 3-3.1 and 3-3.2, respectively.

(4). ***Mass balance experiments***

In order to experimentally determine the amount of recoverable intraparticle atrazine, a supercritical fluid extraction (SFE) was conducted, in which a 0.5 g of GB 843 soil was slurried in 25.0 mL of solution having an initial atrazine concentration of 3.94×10^{-5} M. The slurry was mixed in a thermostatted reaction vessel at 25.0 ($\pm$0.2) °C using a magnetic stir bar for a period of 5 weeks. At the end of this time, 1.0 mL aliquot of the slurry was placed in a laboratory made soil trap. The soil trap was an 85 mm length of 1/8 inch (outside diameter) stainless steel tube fitted with a 0.5 mm tube type stainless steel frit and two 0.22 μm membrane filters. The soil trap was fitted in place on the HPLC column and the labile atrazine was removed by washing with mobile phase. The soil trap was placed directly into a Suprex SFE/50 supercritical fluid extractor (Pittsburg, PA, USA). Some of the nonlabile atrazine was extracted using a mixture of supercritical CO_2 (1.0 mL min^{-1}) and CH_3OH (0.4 mL min^{-1}) heated to 125 °C and pressurized to 350 atm.

For the purpose of comparison, the soil slurry was dispersed in an ultrasonic bath (Sonic 300 Dismembrator, Fisher Scientific, Artek Systems Corp., Farmingdale, N.Y.).

Table 3-3.1, Basic Experimental Parameters for Bulk Soil Kinetics

Init.AT (10^{-6} molesL^{-1})	Temp. (°C)	Soil wt. (g)	Slurry vol. (mL)	Exp.duration (day)	Data points	Exp't no.
1.00	25	0.5040	24.95	18.76	176	7
3.32	25	0.4870	25.01	19.23	45	4
5.70	25	0.5041	24.95	19.10	47	3
7.93	25	0.5086	24.94	19.90	46	2
7.93	25	0.5084	24.94	19.90	46	14
8.00	25	0.5054	25.01	18.58	55	19
8.00	25	0.5053	25.02	18.77	56	20
20.0	25	0.5076	24.99	19.10	45	5
29.8	25	0.5335	25.16	18.72	51	6
4.08	10	0.5079	24.97	69.91	20	G5
8.00	10	0.5038	24.97	80.07	107	GT
16.0	10	0.4996	24.81	69.91	22	G6
79.9	10	0.5000	24.95	80.98	44	31
79.9	10	0.4999	24.96	81.01	44	32
100	10	0.5016	24.92	80.96	44	29
100	10	0.5008	24.92	80.98	44	30

Table 3-3.2, HPLC Operating Parameters (Varian Star 9010 or Waters)

Temp. (°C)	22(±1)
Flow rate (mL min^{-1})	1.0
Pressure (psi)	150-500 for new column
Injection loop (μL)	20.0
Standard (μL)	50.0
Filtrate (μL)	50.0
Slurry (μL)	50.0
Anal. column	Beckman C-18 Ultrasphere ODS or CSC-Chromosorb LC-7
Mobile phase	CH_3OH/H_2O (62.5/37.5, pH=2.80) or CH_3CN/H_2O (50/50, pH=2.50)
Retention time (min)	~9.2
Detector	UV at 220 nm or 254 nm
Recorder	Model 4400 integrator or Watanabe Servocorder SR 6254, range 10 mv
Chart speed (cm min^{-1})	0.5

Then an aliquot (5.0 mL) of the slurry was centrifuged (Dynac Centrifuge, Caly Adams Comp., Parsippany, N.J.). The resulting residue was extracted for 2 days by acetonitrile and analyzed by the HPLC method.

3-4. SOIL CHARACTERIZATION

(1). *Soil mineral analyses*

Mineral analysis and clay analysis were done by X-ray diffraction (Scintag PAD V X-ray diffractometer, Scintag, Sunnyvale, CA) at CLBRR, Research Branch of Agricultural Canada, Ottawa. The results are shown in Table 3-4.1.

(2). *Soil pH*

Soil pH was measured by inserting a pH electrode (Corning M220, Corning Science Products, Corning, N.Y.) into the soil slurry with a soil to distilled water ratio of 1 : 1 (W/W) (190). The average reading for the bulk soil was 5.63 ± 0.02. At this pH, there is no significant hydrolysis of atrazine by proton catalysis (281).

Table 3-4.1, Results of Mineral Analyses for GB 843 Bulk Soil

Mineral analysis		Clay analysis	
Material	% of soil	Material	% of clay
Plagiolase	45	Mica/vermiculite - long spacing	1-10
Microcline	8	- intermediate spacing	1-10
Quartz	15	chlorite	1-10
Amphibole	3	Mica	1-10
Dolomite	2	Amphiboles	1-10
Clay	27	Quartz	10-35
		Feldspar	
		- microcline	1-10
		- plagioclase	1-10

(3). *Cation exchange capacity (CEC)*

Cation exchange capacity (CEC), usually expressed in milliequivalents per 100 g of

soil, is a measure of the quantity of readily exchangeable cations neutralizing negative charges in the soil. The CEC for soil GB 843 was determined by saturating the cation exchange sites of 4.5 g of the soil with three successive portions of 30 mL each of 0.9 N $Ca(OAc)_2$ + 0.1 N $CaCl_2$ solution at pH 7.0, rinsing with distilled water and eluting the Ca^{2+} twice with 40 mL each of 2 N NaCl solution, and measuring Ca^{2+} in the eluate by a AA-975 atomic absorption spectrophotometer (Varian Techtron, Ottawa, Canada) (236). The result of three measurements was 8.8 ± 0.2 meq/100 g of soil.

(4). *Modal analyses*

In order to obtain more geological and geochemical knowledge of the soil, modal analyses were performed in the Geology Department of Concordia University, Montreal and CLBRR, Research Branch of Agriculture Canada, Ottawa. A stereomicroscope (Wild Photomakroskop M400, Wild Leitz Canada Ltd.) under plane polarized light (PPL) or crossed polarized light (XPL) was used. The sample slides (thin sections) were prepared by normal procedures (251). Briefly, thin sections are made by impregnating soil sample powder with plastic, mounting on a glass slide, and grinding the soil layer down to 25 to 30 μm. Examination of soil thin sections can provide the information about the size, shape and arrangement of solid particles and voids, and determine the nature of soil mineral and organics. Fig. 3-4.1 shows the pictures taken from the whole soil and fractions (zoom 32 x 2). In addition, a series of samples were collected at different time steps from the reaction vessel during the kinetic experiment, so as to check whether or not soil particles were affected. The pictures at 1, 5, 10, and 20 days for the whole soil

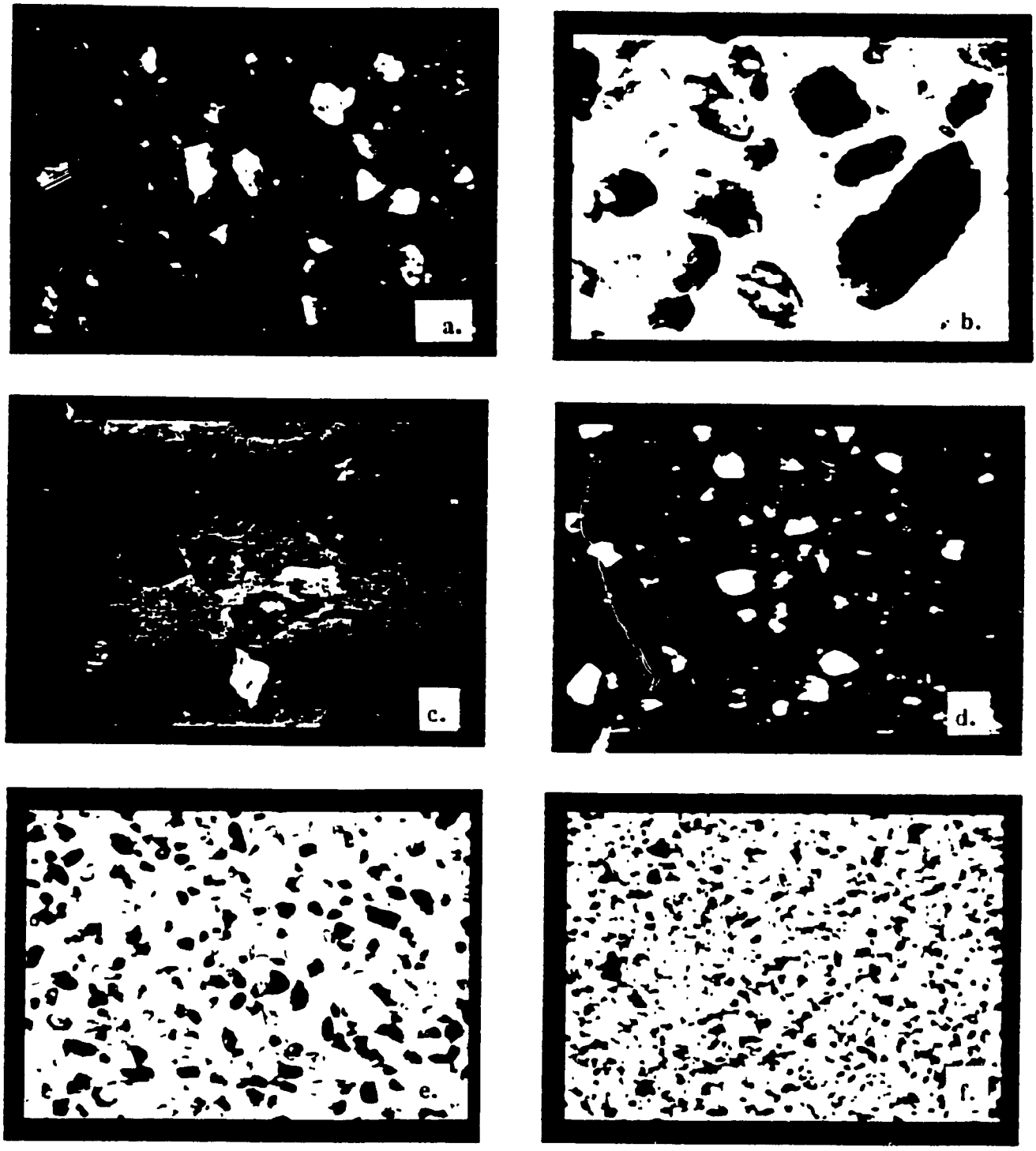

Fig. 3-4.1, Selected Microscopic Pictures for Bulk Soil (a) and Soil Fractions #1-#5 (b-f)

are shown in Fig. 3-4.2, which indicated that there was no important change within the first 3 weeks under the present conditions. Similar observations have been reported by Ball and Roberts (12), Wu and Gschwend (296), etc. However, the considerable scatter revealed in the long-term experiments (after about 60 days, see section 3-5.(6)) indicated the disaggregation of loosely bound fine particles to some extent under the long-term stirring conditions (12). In addition, gentle stirring techniques appear to be important for maintaining the distribution of soil particles. Ogwada and Sparks (213) found that the specific surface area for a soil was relatively constant under stirring conditions for mixing rates of 0 to 478 rpm, but increased abruptly at higher mixing rates (> 2,318 rpm).

(5). *Element identification (SEM/EDS studies)*

For the purpose of element identifications of the soil fractions, scanning electron microscopy (SEM) and energy dispersive spectrometry (EDS) studies were conducted at the Electron Microscopy Centre of Research Branch, Agriculture Canada, Ottawa. Samples were analyzed by a specimen mounting method, using a digital scanning microscope (DSM 940A, ZEISS, Germany) equipped with a X-ray fluorescence analysis system (Tracor Northern-5500, USA). All samples were mounted on 1/2" spectrographically pure carbon planchets. Coarser fractions (#1-#3) were glued to the planchet with Sellotape glue, while all other fractions were glued with Formvar (plastic) dissolved in chloroform. X-ray emission data from five areas (each area approx. 1.8 x 1.8 mm) of each sample were collected over 60 seconds. Escape peaks were stripped

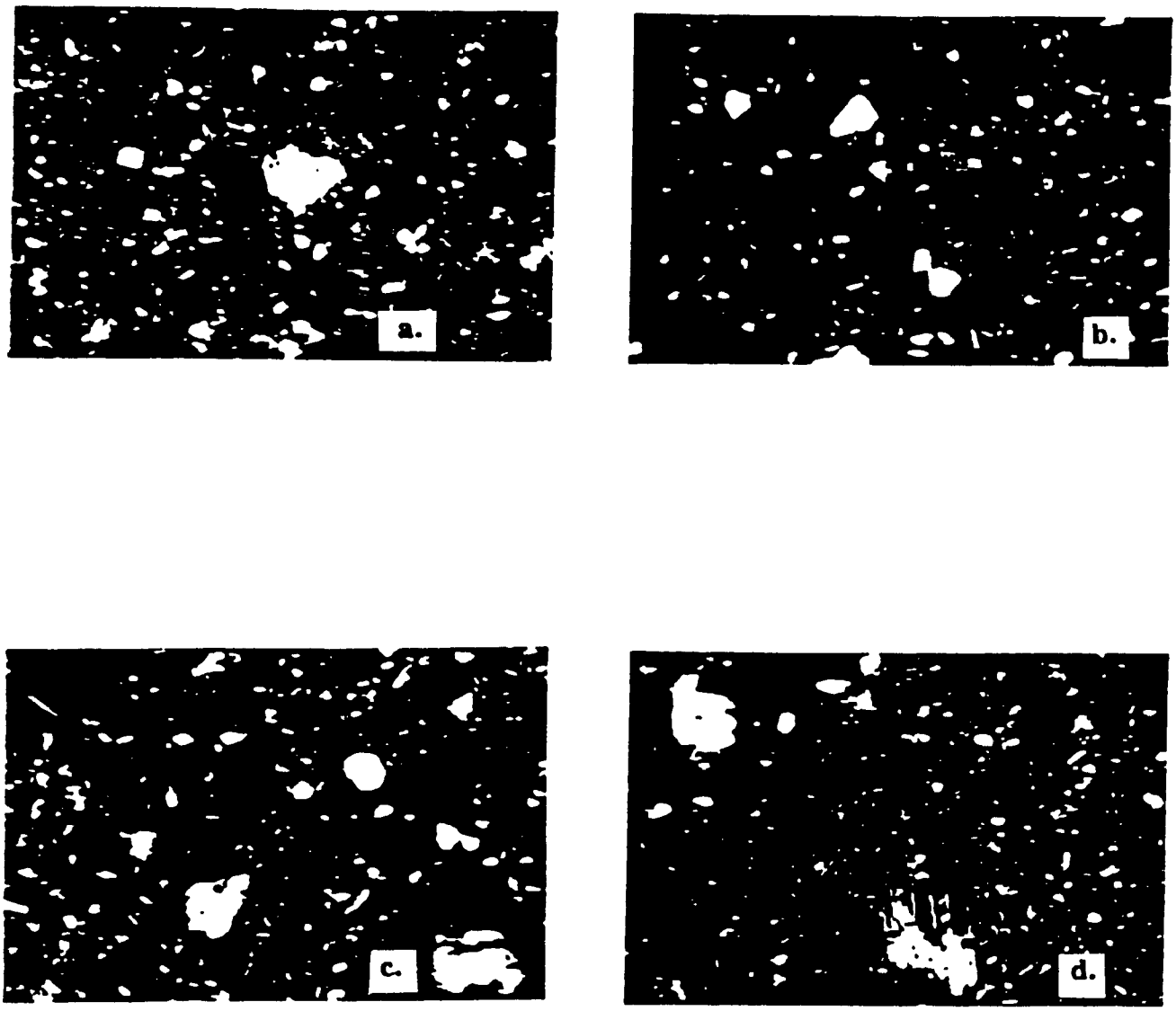

Fig. 3-4.2, Selected Microscopic Pictures for Bulk Soil Slurry at 1 (a), 5 (b), 10 (c) and 20 (d) days

from the spectra. Diagnostic peaks were identified at maximum sensitivity and peak areas were calculated. The application of SEM/EDS to soil analysis has been described (19,189).

A result of semi-quantitative element identifications for the bulk soil is shown in Table 3-4.2 and Fig. 3-4.3, in which the peak area (X-ray intensity collected over 5 scans of 60 s duration) was plotted against the energy (keV).

(6). *Labile sorption capacity*

The labile sorption capacity for the bulk soil was determined by saturating the surface sorption sites with solutions having higher atrazine concentrations (at the magnitude of $\sim 10^{-4}$ M). The higher concentration led to a faster approach (usually 2 to 4 days) to sorption equilibrium, which can be tracked with the MF-HPLC technique. The equilibrium sorbed atrazine was calculated as the difference between slurry analyses and filtrate analyses. By doing so, a set of equilibrium sorbed concentrations can be obtained by taking the plateau values of each of the curves with labile sorbed atrazine vs. time. Eventually, a type of adsorption isotherm comprising each of the above equilibrium concentrations at constant temperature was then constructed, with equilibrium sorbed atrazine plotted against solution concentration. Table 3-4.3 and Fig. 3-4.4 show the results in which the plateau indicates a saturation limit of the surface sorption, with an average value of $0.397 \pm 0.036 \times 10^{-6}$ moles g^{-1} of soil (or $7.94 \pm 0.72 \times 10^{-6}$ moles L^{-1} of slurry).

Table 3-4.2, EDS Peak Listing for Soil GB 843 (Collected over 60 x 5 seconds)

No.	Energy (keV)	Area	Element	Line
1	0.250	5,622	C	Kα
2	0.511	90,018	O	Kα
3	1.021	4,388	O	Sum or Na Kα?
4	1.232	913	As	Lα
5	1.471	29,778	Al	Kα or Br Lα?
6	1.740	131,000	Si	Kα or Rb Lα?
7	2.267	421	S	Kα or Mo Lα?
8	2.620	771	Cl	Kα
9	3.315	6,142	K	Kα or In Lα?
10	3.687	4,589	Ca	Kα
11	4.029	398	Ca	Kβ
12	4.507	1,254	Ti	Kα
13	6.405	5,759	Fe	Kα
14	7.053	952	Fe	Kβ

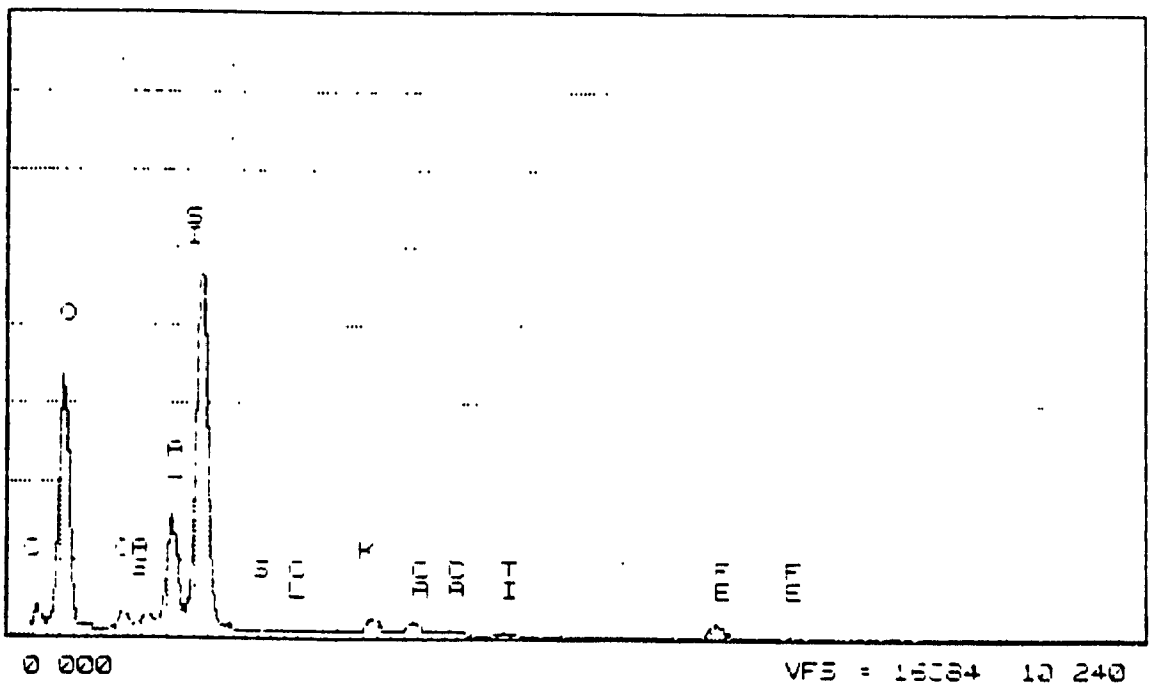

Fig. 3-4.3, Spectrum of EDS for Bulk Soil (Collected over 60 x 5 seconds)

Table 3-4.3, Results for Measurement of the Labile Sorption Capacity (Bulk soil GB 843 at 25 °C)

No.	Sol'n conc. (moles L^{-1})	Labile sorbed (moles g^{-1}) Exp't	Fit.
1	1.00E-6	7.52E-9	1.29E-8
2	3.20E-6	2.74E-8	2.57E-8
3	5.70E-6	3.62E-8	4.03E-8
4	7.93E-6	4.96E-8	5.33E-8
5	7.93E-6	4.16E-8	5.33E-8
6	7.99E-6	5.70E-8	5.36E-8
7	8.00E-6	6.40E-8	5.37E-8
8	2.00E-5	1.32E-7	1.23E-7
9	2.98E-5	1.86E-7	1.81E-7
10	6.40E-5	3.75E-7	3.91E-7
11	7.99E-5	3.90E-7	3.95E-7
12	8.80E-5	4.33E-7	3.97E-7
13	9.59E-5	4.09E-7	3.99E-7
14	1.08E-4	3.77E-7	4.02E-7

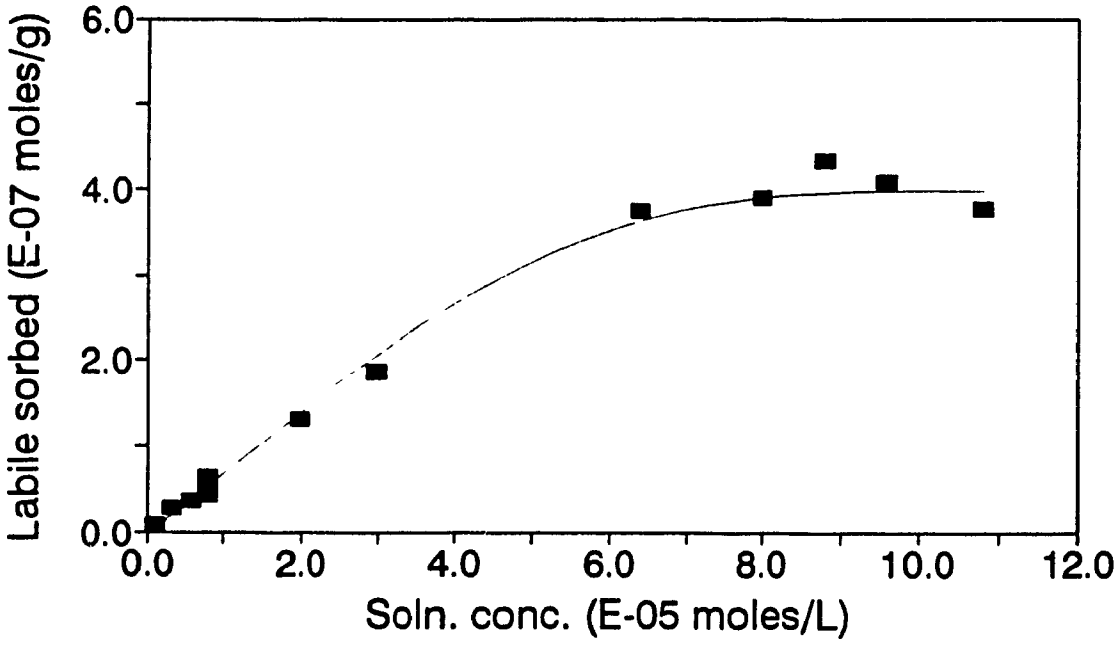

Fig. 3-4.4, Measurement of the Labile Sorption Capacity for Bulk Soil GB 843 at 25 °C (The line indicates the fit of the experimental data)

(7). *Specific surface area/Organic carbon content*

The characterization of soil GB 843 for specific surface area and organic carbon content will be presented in Chapter 4.

3-5. RESULTS AND DISCUSSION

The objective of the sorption equilibrium/kinetic experiments was to determine the distribution of atrazine between the aqueous and sorbed phases. The MF-HPLC technique can produce direct, time resolved data for the atrazine free in solution and the total recoverable atrazine (solution phase plus labile sorbed) by performing filtrate analysis and slurry analysis, respectively. By difference, in addition, the slurry analysis can further provide the nonlabile sorbed atrazine. By carrying out the subsequent short-term and long-term kinetic experiments, two mass transfer processes, a relatively fast reversible process and a subsequent slower reversible process, have been generally identified.

(1). *Rapid initial uptake*

Figs. 3-5.1 and 3-5.2 show the results of an experiment having an atrazine concentration of 1.00×10^{-6} M at the beginning of the reaction (within 1.25 days). Fig. 3-5.1 is the results of the filtrate and slurry analyses, and Fig. 3-5.2 shows the distribution of atrazine species. It can be seen that within the first 1.5 hours ($\sim$0.06 days) there are two relatively fast uptake processes: One is the rapid initial surface adsorption which is driven by the concentration gradient between the surfaces and the

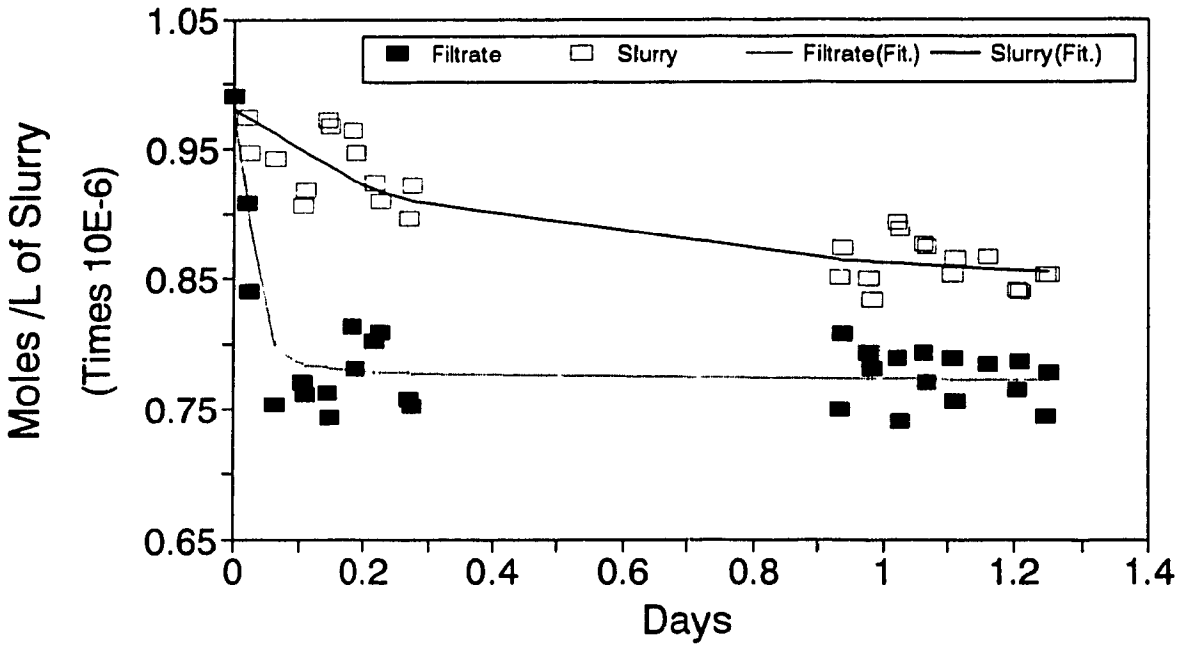

Fig. 3-5.1, Atrazine Species Distribution with Time (Exp. #7, bulk soil at 25 °C)

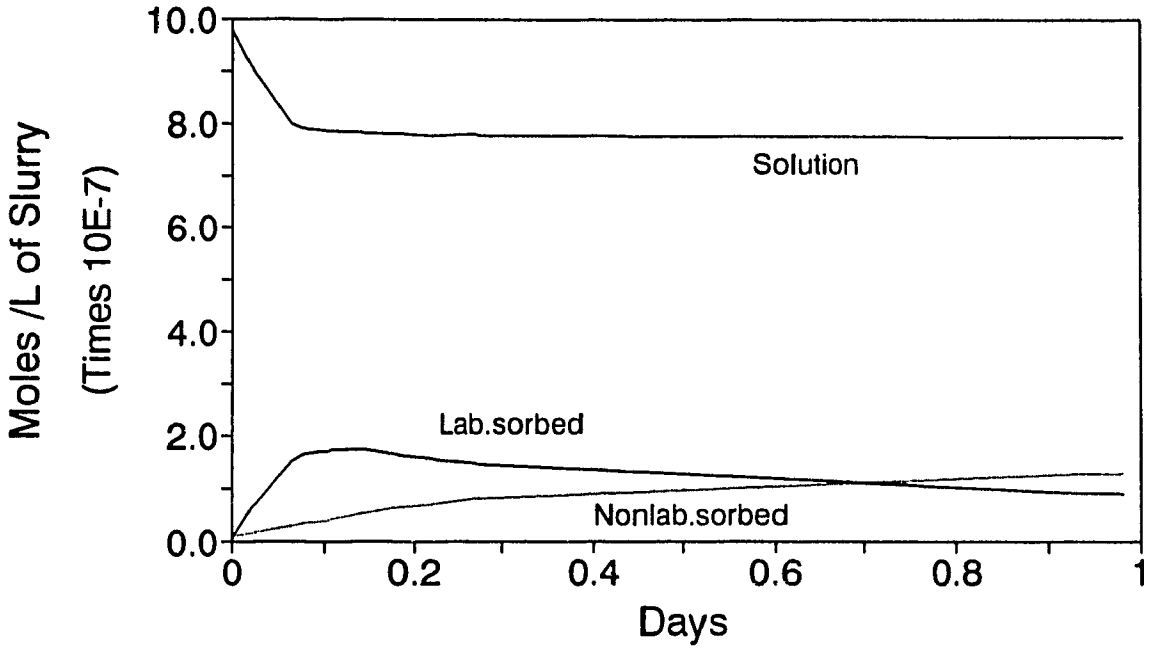

Fig. 3-5.2, Atrazine Species Distribution with Time (Exp. #7, bulk soil at 25 °C)

solution, and causes the filtrate curve to drop down sharply. The other is the both labile and nonlabile intraparticle diffusion which has begun an initial relatively fast rise, but has not yet had a measurable effect on the labile sorption curve. After 1.5 hours, the labile sorption curve begins to drop caused by the increasing intraparticle diffusion.

The phenomenon of the rapid initial uptake of pesticides has been commonly observed in the literature (2,46,70,74,83,112,142-144,150,176,218,254,272). But batch techniques using centrifugation and sampling of the supernatant liquid are incapable of distinguishing between labile sorbed and nonlabile sorbed pesticides, and hence will be confound by the general term "sorbed phase". With the MF-HPLC methodology, calculated curve fitting results for the early uptake of atrazine at selected times are shown in Table 3-5.1. Given an initial concentration of 1.00×10^{-6} moles L^{-1}, the first early rise in the labile sorption accounts for as much as 16% (1.56×10^{-7} moles L^{-1}) while the intraparticle sorption is less than 3% (2.84×10^{-8} moles L^{-1}) and the solution atrazine drops to 80% (8.00×10^{-7} moles L^{-1}). But the labile sorption portion, even combined with the irreversible sorption, covers only about 2% of the labile sorption sites on the basis of a labile sorption capacity of 8.00×10^{-6} moles L^{-1} of slurry.

(2). *Labile sorption steady state*

As noted above, following the rapid early uptake, an approximate dynamic steady state will be reached with respect to the labile surface sorption/desorption. Fig. 3-5.3 shows the results of the above sorption experiment with an extended period of reaction time (16 days). The corresponding data are shown in Table 3-5.2. It is apparent that

Table 3-5.1, Fitted Data for the Rapid Initial Uptake of Atrazine (Exp. #7, initial atrazine = 1.00 x 10^{-6} M)

No.	Time (day)	Soln. ($molesL^{-1}$)	%*	Lab.sorbed ($molesL^{-1}$)	%	Nonlab.sorbed ($molesL^{-1}$)	%
1	0.00	9.76E-7	97.6	4.59E-9	0.46	9.31E-9	0.93
2	0.02	9.12E-7	91.2	6.22E-8	6.22	1.57E-8	1.57
3	0.03	8.92E-7	89.2	7.11E-8	7.11	1.68E-8	1.68
4	0.06	8.00E-7	80.0	1.56E-7	15.6	2.84E-8	2.84
5	0.10	7.87E-7	78.7	1.69E-7	16.9	3.75E-8	3.75
6	0.11	7.84E-7	78.4	1.71E-7	17.1	4.15E-8	4.15
7	0.14	7.82E-7	78.2	1.71E-7	17.1	5.20E-8	5.20
8	0.15	7.81E-7	78.1	1.71E-7	17.1	5.32E-8	6.32
9	0.18	7.80E-7	78.0	1.65E-7	16.5	6.25E-8	6.25
10	0.19	7.79E-7	78.0	1.62E-7	16.2	6.30E-8	6.30
11	0.22	7.78E-7	77.8	1.55E-7	15.5	6.99E-8	6.99
12	0.23	7.78E-7	77.8	1.52E-7	15.2	7.19E-8	7.19
13	0.28	7.77E-7	77.7	1.45E-7	14.5	7.84E-8	7.84
14	0.93	7.74E-7	77.4	9.10E-8	9.10	1.25E-7	12.5
15	0.98	7.74E-7	77.4	8.89E-8	8.89	1.27E-7	12.7
16	1.02	7.74E-7	77.4	8.80E-8	8.80	1.28E-7	12.8
17	1.06	7.73E-7	77.3	8.69E-8	8.69	1.30E-7	13.0
18	1.11	7.73E-7	77.3	8.57E-8	8.57	1.31E-7	13.1
19	1.16	7.73E-7	77.3	8.45E-8	8.45	1.33E-7	13.3
20	1.20	7.73E-7	77.3	8.33E-8	8.33	1.34E-7	13.4
21	1.25	7.72E-7	77.2	8.21E-8	8.21	1.35E-7	13.5

* % shows the concentration as the percentage of total atrazine.

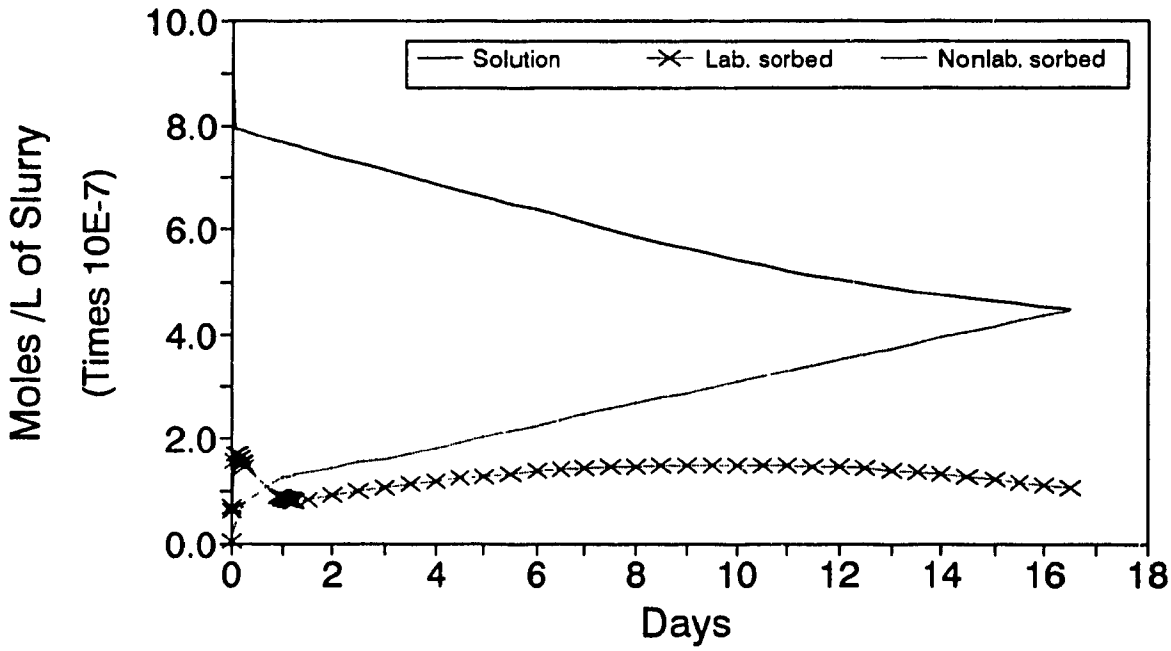

Fig. 3-5.3, Atrazine Species Distribution with Time (Exp. #7, bulk soil at 25 °C)

Table 3-5.2, Fitted Data for Atrazine Species Distribution with Time Shown in Fig. 3-5.4 (Exp. #7, part)

No.	Time (day)	Soln. ($moles L^{-1}$)	% *	Lab.sorbed ($moles L^{-1}$)	%	Nonlab.sorbed ($moles L^{-1}$)	%
1	0.00	9.76E-7	97.6	4.59E-9	0.46	9.31E-9	0.93
2	0.03	8.92E-7	89.2	7.11E-8	7.11	1.68E-8	1.68
3	0.06	8.00E-7	80.0	1.56E-7	15.0	2.84E-8	2.84
4	0.11	7.84E-7	78.4	1.71E-7	17.1	4.15E-8	4.15
5	0.15	7.81E-7	78.1	1.71E-7	17.1	5.32E-8	5.32
6	0.22	7.78E-7	77.8	1.55E-7	15.5	6.99E-8	6.99
7	0.28	7.77E-7	77.7	1.45E-7	14.5	7.84E-8	7.84
8	0.93	7.74E-7	77.4	9.10E-8	9.10	1.25E-7	12.5
9	1.06	7.73E-7	77.3	8.69E-8	8.69	1.30E-7	13.0
10	1.20	7.73E-7	77.3	8.33E-8	8.33	1.34E-7	13.4
11	1.25	7.72E-7	77.2	8.21E-8	8.21	1.35E-7	13.5
12	1.50	7.55E-7	75.5	8.50E-8	8.50	1.35E-7	13.5
13	2.50	7.27E-7	72.7	1.00E-7	10.0	1.55E-7	15.5
14	3.50	7.00E-7	70.0	1.13E-7	11.3	1.71E-7	17.1
15	4.50	6.75E-7	67.5	1.24E-7	12.4	1.92E-7	19.2
16	5.50	6.50E-7	65.0	1.33E-7	13.3	2.14E-7	21.4
17	6.50	6.25E-7	62.5	1.41E-7	14.1	2.35E-7	23.5
18	7.50	5.98E-7	59.8	1.46E-7	14.6	2.56E-7	25.6
19	8.50	5.74E-7	57.4	1.49E-7	14.9	2.77E-7	27.7
20	9.50	5.51E-7	55.1	1.50E-7	15.0	2.98E-7	29.8
21	10.5	5.31E-7	53.1	1.50E-7	15.0	3.19E-7	31.9
22	11.5	5.12E-7	51.2	1.47E-7	14.7	3.41E-7	34.1
23	12.5	4.96E-7	49.6	1.43E-7	14.3	3.62E-7	36.2
24	13.5	4.81E-7	48.1	1.36E-7	13.6	3.83E-7	38.3
25	14.5	4.68E-7	46.8	1.28E-7	12.8	4.04E-7	40.4
26	15.5	4.58E-7	45.8	1.17E-7	11.7	4.25E-7	42.5
27	16.5	4.49E-7	44.9	1.05E-7	10.5	4.46E-7	44.6

* % shows the concentration as the percentage of total atrazine.

there is a plateau region on the labile surface sorption curve which maximizes at about 9.9 days, accounting for 15% of the total atrazine and 1.9% of the labile sorption sites. At this point, the curve has a singularity, $d\theta_L/dt = 0$.

In contrast, the atrazine species free in solution phase and trapped by intraparticle diffusion respectively show a gradual decrease or increase with time. The intraparticle diffusion curve should be inherently nonlinear (eq. 3-2.12). But departure from linearity is usually not observable outside the ordinary error limits during the first 2 or 3 weeks of the reaction. This reflects the small departure of $d\theta_L/dt$ from zero in this time zone. At the end of the experiment, a significant portion ($\sim$45%) of atrazine appears to be trapped by intraparticle diffusion.

It is note-worthy that the labile sorption curve exhibits a slight decline beyond the plateau region. This can be attributed to the depletion of the labile sorbed atrazine layer as the solution phase atrazine is getting lower. The figure closely resembles standard kinetics for the system: $A \rightarrow B \rightarrow C$.

Similarly, Figs. 3-5.4 and 3-5.5 show atrazine species distribution with time for an experiment having a higher initial concentration (8.00×10^{-6} moles L^{-1}). The plateau ($d\theta_I/dt = 0$) occurs at about 9.7 days. If we define the zero slope point of a plateau region as characteristic time, it usually takes 9 to 11 days (Table 3-5.3) in most of the sorption experiments with bulk soil at 25 °C. In addition, as will be seen in the subsequent chapters, the characteristic time varies as a function of temperature or soil particle size.

Table 3-5.4 shows the relevant parameters of labile sorption equilibrium in terms of

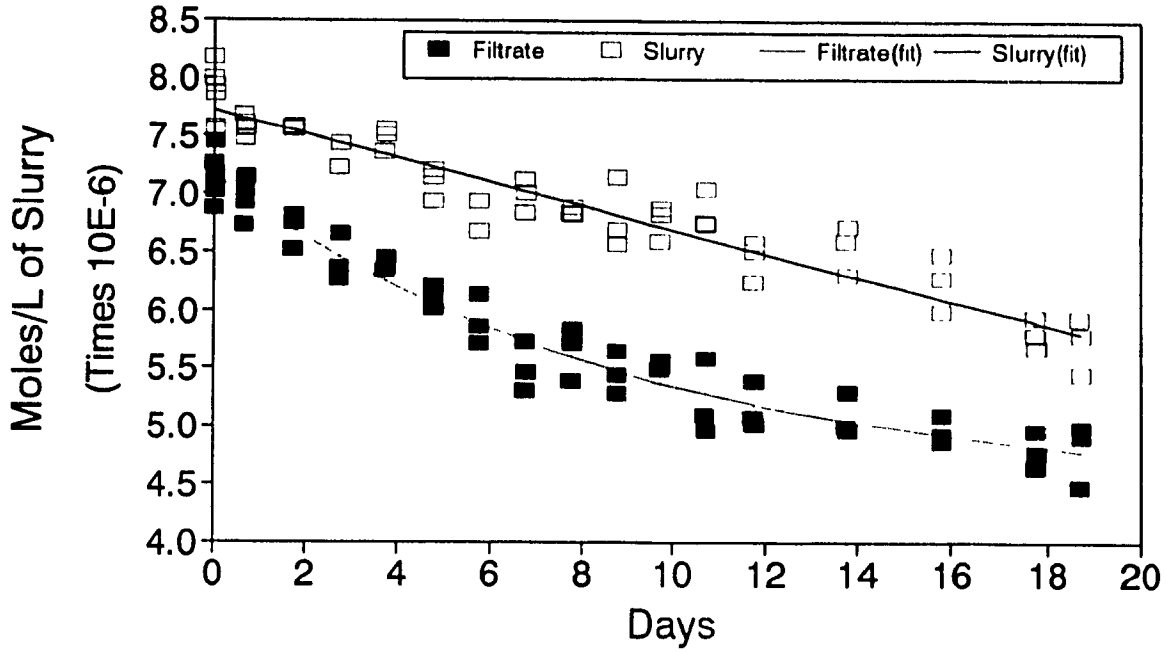

Fig. 3-5.4, Atrazine Species Distribution with Time (Exp. #20, bulk soil at 25 °C)

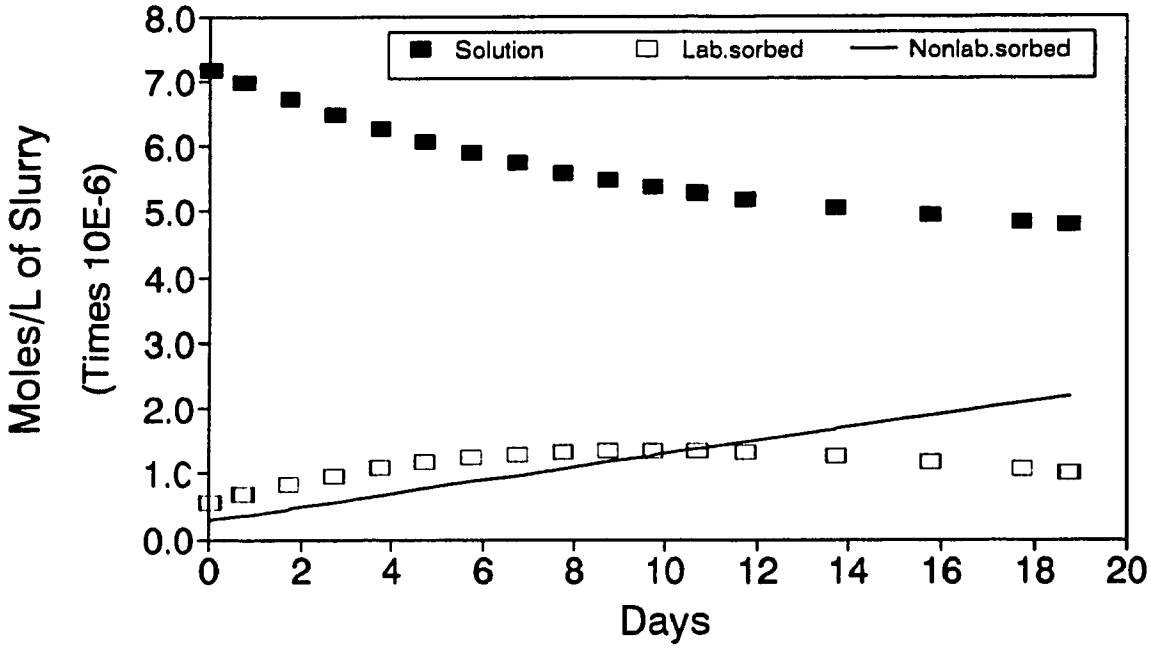

Fig. 3-5.5, Atrazine Species Distribution with Time (Exp. #20, bulk soil at 25 °C)

Table 3-5.3, Characteristic Times of the Plateau Region Shown in Labile Sorption Curves (for bulk soil at 25 °C)

No.	Temp. (°C)	Init. (10^{-6} molesL^{-1})	Equil. sorbed (10^{-6} molesL^{-1})	(%)	Charac. time* (Day)
7	25	1.00	0.15	15.1	9.9
4	25	3.20	0.55	17.1	10.9
3	25	5.70	0.72	12.7	11.1
2	25	7.93	0.99	12.5	11.7
14	25	7.93	0.83	10.5	10.9
20	25	7.99	1.14	14.2	9.7
19	25	8.00	1.28	16.0	8.6
5	25	20.0	2.63	13.2	8.9
6	25	29.8	3.73	12.5	8.2

* i.e., the time when $d\theta_L/dt = 0$.

θ_c, $\bar{K}_l$, K_d, and X_l, in which the weighted average equilibrium function, $\bar{K}_l$, was calculated according to eq. 1-1.18. The labile sorption capacity, θ_c, conceptually defines a saturation limit of sorbed atrazine on labile sorption sites, but also, is experimentally measurable with a properly designed batch setup as described earlier. For this, an average value of $0.397 \pm 0.036 \times 10^{-6}$ moles g^{-1} of soil has been determined. As a key equilibrium parameter, it will participate essentially in the chemical stoichiometry of the sorption reaction. Unfortunately, there are few reference values available for comparison. Perusal of the literature reveals that this term has been often confused with "sorbed phase", if it is recognized that sorbed amount should comprise the labile surface sorbed plus the intraparticle diffused. Wang et al. (281-283) have studied the interactions of atrazine with Laurentian humic substances, and reported binding capacity values of 8.8 μmoles g^{-1} of FA, 15.3 μmoles g^{-1} of HA, and 0.37 μmoles g^{-1} of soil, respectively. The

Table 3-5.4, Results of Labile Sorption Equilibrium for Bulk Soil at 25 °C

No.	Init.conc. (10^{-6} molesL^{-1})	Equil.sorbed (10^{-7} molesL^{-1})	$\bar{K}_l$ (10^{4} M^{-1})	K_d (10^{-2} Lg^{-1})	θ_c (10^{-6} molesg^{-1})	X_l
7	1.00	1.50	3.50	1.36	0.397	0.0188
4	3.20	5.49	3.28	1.21	0.397	0.0693
3	5.70	7.24	2.17	0.783	0.397	0.0912
2	7.93	9.92	2.90	1.01	0.397	0.125
14	7.93	8.32	2.06	0.732	0.397	0.105
20	7.99	11.4	3.05	1.04	0.397	0.142
19	8.00	12.8	3.47	1.16	0.397	0.161
5	20.0	26.3	3.39	0.960	0.397	0.287
6	29.8	37.3	3.46	0.783	0.397	0.430
Average			3.03±0.97	1.01±0.35	0.397±0.036	

last number is very close to the value measured here. But considering the organic matter contents (a few percent for Laurentian soil), the difference between these values is apparently quite significant.

As indicated earlier, the partition-based distribution coefficient, K_d, is directly proportional to $\bar{K}_1$ (eq. 3-2.10). Given an appreciation of its fundamental theoretical weakness and limitation, K_d is a useful parameter in most solute transport hydrology models, and therefore has been frequently reported in the existing literature (59,60). It can be seen that the K_d data are not very sensitive to the sorption site coverage (X_1), being equal to an average value of 10.1 ± 3.5 mL g^{-1}. Comparable results can be found in a study of the sorption of halogenated organics (PCE and TeCB) onto Borden aquifer materials by Ball and Roberts (11). Note that the K_d data shown in Table 3-5.4 are slightly higher (about 5 to 10 times) than those in the above paper, which can be explained by the fact that soil GB 843 has a higher organic carbon content (~ 40 times) and BET surface area (~ 10 times) compared to Borden aquifers. In addition, the K_d value seems to be more sensitive to the hydrophobicity of a sorbate. In this regard, Wu and Gschwend (296), in studying the sorption kinetics of hydrophobic chlorobenzene congeners by sediments and soils, presented much higher K_d results (a few orders of magnitude) than those in Table 3-5.4. Apparently, this is caused not only by the higher organic carbon content (~ 5 to 10 times) of their soils, but also by the greater hydrophobicities of the benzene derivatives.

(3). ***Labile sorption kinetics***

On a time scale of three weeks, the kinetic behavior of atrazine labile sorption can be described qualitatively as an early fast uptake (within the first few hours, e.g., 0.06 days in the case of Exp. #7), a relaxation period (between 0.06 to 9 days) until a plateau is reached (around 9 or 11 days), and a decline (beyond the plateau region). Corresponding to the three regions, the labile sorption curve shows a steep positive, a slightly positive to near zero, and a slightly negative slope, respectively (see Figs. 3-5.2 and 3-5.3). As indicated above, the initial rate approximation method (section 3-2.(4)) can be reasonably used to account for the adsorption kinetics of the first region where C_o is much greater than C_L, and can be considered constant. Also, C_D is still quite small (usually less than 3% of the total), and can be neglected. The pseudo first-order rate constant, k_{s1}, can therefore be evaluated with eq. 3-2.19. Note that the actual approximate calculation was usually carried out using the value of labile sorption time rate dC_l/dt at $t = 0$ (i.e., the intercept) in order to avoid the influence of other kinetic processes such as desorption and intraparticle diffusion. On the other hand, in the second region a dynamic surface adsorption/desorption equilibrium is approximately maintained, that is:

$$k_{b1}(V/W)M_{AT}\theta_o - k_{s2}\theta_L = 0 \qquad (3\text{-}5.1)$$

and

$$k_{d1}\theta_l > 0 \qquad (3\text{-}5.2)$$

By the third region, the intraparticle diffusive uptake has become significant enough to deplete the surface sorbed atrazine, leading to the decline curve.

Table 3-5.5 shows the regression results, including the labile sorption time rate

Table 3-5.5, Results of Labile Sorption Kinetics by Initial Rate Approximation Method for Bulk Soil at 25 °C

No.	Init.conc. (10^{-6} molesL^{-1})	B_o Const.	Std.err.	B_1 (molesL^{-1}d^{-1}) Coeffi.	Std.err.
7	1.00	5.20E-9	6.55E-9	2.48E-6	1.87E-7
4	3.32	7.21E-9	1.51E-8	2.20E-6	2.70E-7
3	5.70	1.53E-9	3.35E-9	3.15E-6	1.38E-8
2	7.93	7.11E-10	1.01E-9	5.97E-6	3.07E-7
14	7.93	1.93E-9	2.05E-8	6.93E-6	4.25E-7
20	7.99	4.64E-9	7.50E-9	8.12E-6	2.36E-7
19	8.00	4.82E-10	1.84E-8	7.52E-6	4.79E-7
5	20.0	8.20E-8	1.43E-7	2.27E-5	2.06E-6
6	29.8	3.80E-8	1.23E-7	2.19E-5	1.13E-6

k_{s1} = 0.831±0.093 (d^{-1}) with R^2 = 0.909
k_{b1} by eq. 3-2.23: 1.05±0.12 x 10^5 (Lmol^{-1}d^{-1})

(dC_L/dt) and the resulting pseudo first-order rate constant (k_{s1}). It can be seen that, apparently, the labile sorption time rate (dC_L/dt) is directly proportional to the initial atrazine concentration (M_{AT} at t = 0). Fig. 3-5.6 is a plot of $(dC_L/dt)_{t=0}$ against solution phase atrazine (i.e., the initial concentration), which shows that the uptake rate varies linearly with initial concentration. This is expected behavior for first-order kinetics. The straight line has a slope (k_{s1}) = 0.831 ± 0.093 (d^{-1}) and $R^2 = 0.909$. At this kinetic stage, the second-order rate constant, k_{b1}, is calculated by eq. 3-2.23, giving a value of $1.05 \pm 0.12 \times 10^5$ L mol^{-1} d^{-1}.

Relatively few and very scattered reference k_{s1} data have been reported in existing literature, in part because the surface adsorption process has been treated as an instantaneous equilibrium and described with an isotherm equation (K_d), as stated earlier. In an early study Lindstrom et al. (173) reported rate constant (k_1') results for the adsorption of 2,4-D, isocil, and bromacil from aqueous solution onto illite clay and silica gel surfaces. The magnitudes were in range 10^{-1} to 10^{-5} s^{-1} (~9,000 to 0.9 d^{-1}). The present result (Table 3-5.5) approaches their lower boundary value. A lower result was reported by Leenheer and Ahlrichs (167) in a study of the adsorption of carbaryl and parathion upon soil organic matter surfaces. The values, at the order of 10^{-4} s^{-1} (~9 d^{-1}), are 10 times higher than reported here. These authors all treated the uptake as a surface adsorption/desorption process (nondiffusion kinetics). There is little reason to believe these different systems would give similar values. Gamble and Khan (93) presented a k_{s1} value of 0.0502 d^{-1} for atrazine sorption by an organic soil (Typic Mesisol peat, 37.7% organic matter), which is 15 times lower than that observed here. Gilchrist et al. (103)

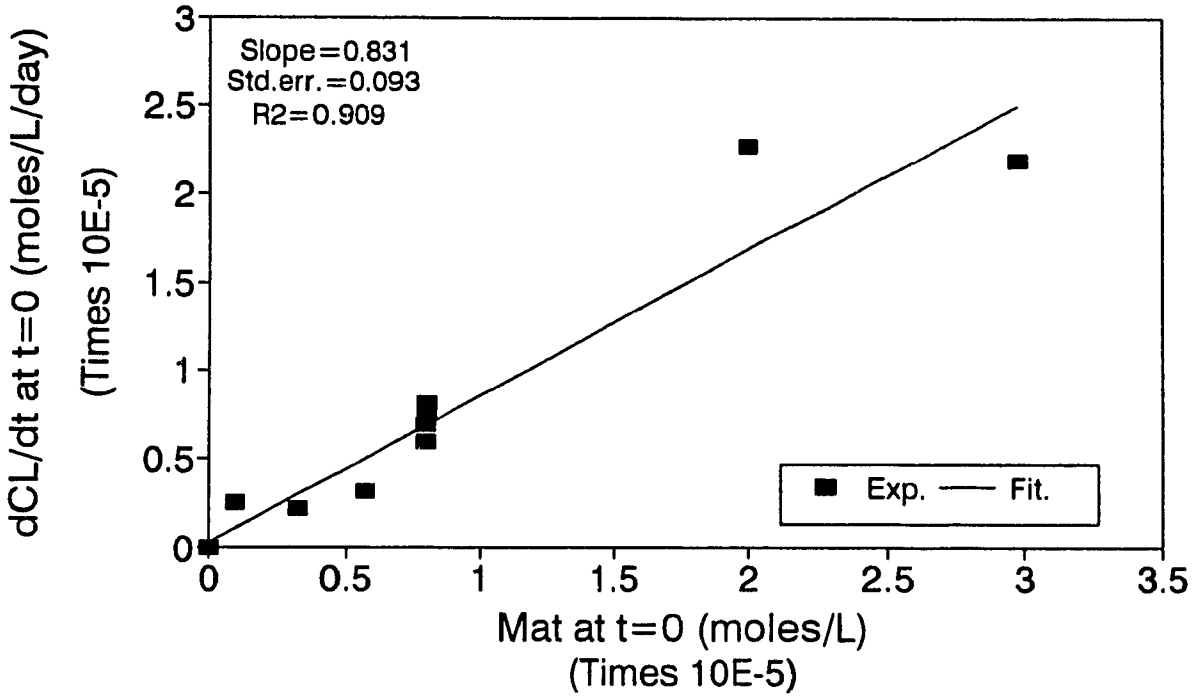

Fig. 3-5.6, A Plot of $(dC_L/dt)_{t=0}$ vs. M_{AT} Showing the Initial Rate Approximation Calculation of Pseudo First-Order Rate Constant (k_{s1})

have studied atrazine interactions with clay minerals and reported a greater k_{s1} value of about 8 x 10^{-4} s^{-1} ($\sim$70 d^{-1}), in which no intraparticle diffusion was observed. This difference might be accounted for by considering the specific surface area (a few hundred m^2 g^{-1} in EGME) and organic matter (zero percent) for the clay minerals. A recently reported rate constant (k_a) by Miller and Pedit (196), in studying lindane sorption/desorption hysteresis in a subsurface sand material with a reactive surface-diffusion model, has a value of 1.23 x 10^{-4} h^{-1} (2.95 x 10^{-3} d^{-1}), which is about 250 times lower than the k_{s1} obtained in this study. All these results underline that observed kinetics are controlled by factors other than diffusion across the surface film layer. "Surface" adsorption must involve the structure of the particle which is, in many cases, highly penetrable.

(4). ***Intraparticle diffusion***

In the absence of chemical reactions (e.g., hydrolysis) and microbiological degradations, for a well mixed and closed batch system, the mass difference between the initial atrazine and the slurry analyses should be attributed to the loss trapped by intraparticle diffusion, as shown in Figs. 3-5.3 and 3-5.5. The mass balance experiments (3-3.(4)) show an 18.5$\pm$1.5% recovery of the nonlabile sorbed atrazine (i.e., nonextractable atrazine by the MF-HPLC mobile phase). The low recovery may imply the heterogeneity and spatial difference of the interior sorption. The unrecovered atrazine is responsible for the trapped portion which can eventually account for as much as 30 to 50% of the total atrazine as irreversible or nonextractable bound residues (36,151,241).

This material balance loss has been commonly observed both under field conditions and in laboratory studies (2,46,70,74,83,112,142-144,150,176,218,254,272).

As indicated earlier, the diagnostic test for Crank's (66) intraparticle diffusion model (eq. 3-2.13 and Table 3-5.6) has been applied to all the MF-HPLC experiments with the bulk soil at 25 °C by plotting $Ln(\theta_b)$ against Ln(t). Table 3-5.7 and Fig. 3-5.7 show the results. It can be seen that, except for #2, all of the experiments gave a slope value (Z) of ~ 0.5 to within the experimental errors, which is consistent with the case (I) of steady state sorption site coverage (C_1) in Table 3-5.6, a condition we know to be inexact but apparently a satisfactory approximation within experimental errors.

Within a reaction period of about three weeks, the intraparticle diffusion clearly does not reach equilibrium. As shown in Figs. 3-5.3 and 3-5.5, the nonlabile atrazine exhibits a continuous increase. In order to account for the kinetics, two closely related parameters, the diffusion coefficient (D) and the first-order rate constant (k_{dl}), have been evaluated from the experimental results with the bulk soil at 25 °C. Tables 3-5.8 and 3-5.9 show the results, in which both D and k_{dl} were calculated by two methods based on eqs. 3-2.15 and 3-2.16 (Table 3-5.9), or eqs. 3-2.12 and 3-2.16 (Table 3-5.8), respectively. It can be seen that the diffusion coefficient (D) shows a magnitude of $\sim 1 \times 10^{-10}$ cm^2 s^{-1}, and the first-order rate constant (k_{dl}) has an average value of 0.0914 ± 0.0085 d^{-1}. The observed D values are in close agreement with the results reported by Wu and Gschwend (296), which is probably an accident given the difference in these systems. Considering the effect of soil organic matter on diffusivity (11,12,144,226,296), the D values observed here may be slightly lower than would be

Table 3-5.6, Diagnostic Test for Intraparticle Thermal Diffusion (or Any Other Process Describable by an Effective Diffusion Coefficient) Mechanisms
(Based on linearized solutions for Fick's law presented by Crank (66))

$$Ln(\theta_D) = Ln(A) + Z\ Ln(t)$$

Mechanism no.	$C_{x=0}$	A	Z
I	C_l	$[2C_l(D/\pi)^{1/2}]$	1/2
II	kt	$[(4/3)k(D/\pi)^{1/2}]$	3/2
III	$kt^{1/2}$	$[(1/2)k(\pi D)^{1/2}]$	1

Table 3-5.7, Diagnostic Tests for Bulk Soil Intraparticle Diffusion at 25 °C

No.	θ_l (10^{-8} molesg^{-1})	Ln(A)	Z
7	0.750	-25.18±0.27	0.488±0.103
4	2.75	-24.29±0.11	0.465±0.106
3	3.62	-23.91±0.01	0.471±0.030
14	4.16	-23.59±0.05	0.506±0.027
2	4.96	-25.46±0.04	0.719±0.013
20	5.68	-23.69±0.08	0.516±0.016
19	6.41	-23.36±0.19	0.488±0.027
5	13.2	-22.52±0.07	0.556±0.031
6	18.7	-22.57±0.15	0.519±0.025
Average			0.525±0.042

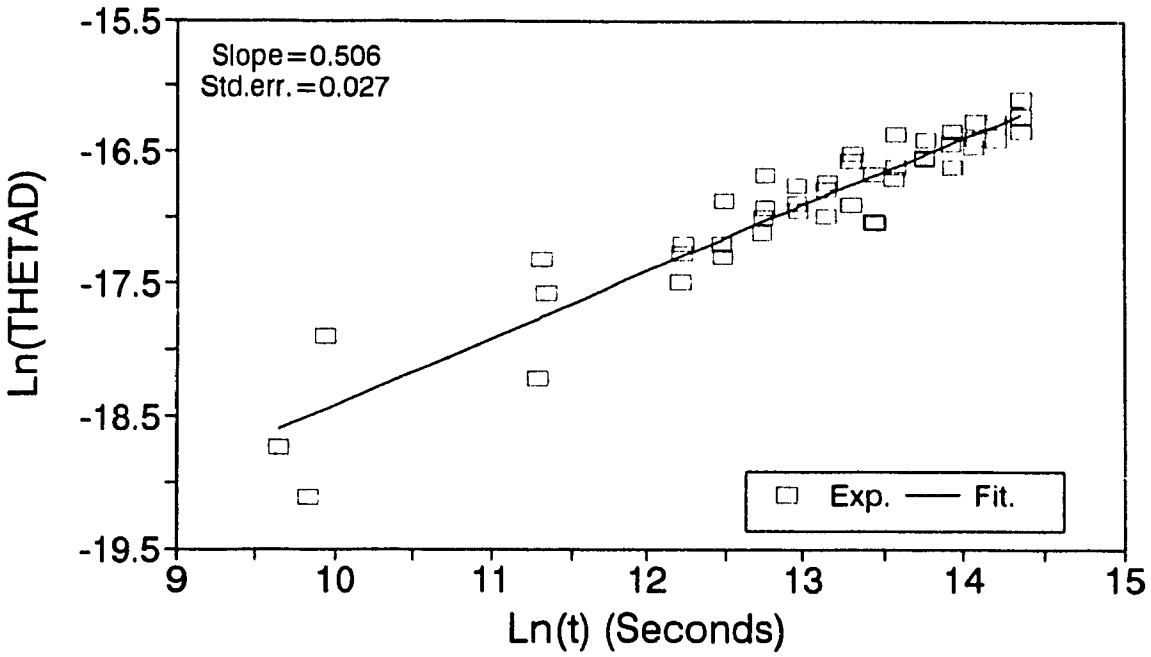

Fig. 3-5.7, Diagnostic Test for Bulk Soil Intraparticle Diffusion at 25 °C (Exp. #14)

expected. In addition, the k_{dl} values compare well to those of Ball and Roberts (12). This paper used alternative but related models to evaluate the diffusion rate constant. Note that the k_{dl} values here are slightly higher than those from the one- or two-parameter model (D_a/a^2), but slightly lower than the pore diffusion model (D_p/a^2). The earlier reported data for both D and k_{dl} can be found in Karickhoff and Morris' study (144) of the sorption of hydrophobic pollutants in sediment suspensions by viewing their k_2 as a first-order diffusive rate constant. Their results (on the order of 10^{-11} to 10^{-13} cm^2 s^{-1} for D, an average of a few tenths d^{-1} for k_2) are comparable to those reported here.

Table 3-5.8, Results of Intraparticle Diffusion Kinetics for Bulk Soil at 25 °C (by eqs. 3-2.12 and 3-2.16)

No.	θ_L ($molesg^{-1}$)	D (cm^2s^{-1})	k_{dl} (d^{-1})
7	7.50E-9	1.71E-10	1.62E-1
4	2.75E-8	7.53E-11	7.13E-2
3	3.62E-8	9.32E-11	8.83E-2
14	4.16E-8	1.34E-10	1.27E-1
2	4.96E-8	2.24E-12	2.12E-3
20	5.68E-8	5.88E-11	5.57E-2
19	6.41E-8	8.93E-11	8.46E-2
5	1.32E-7	1.13E-10	1.07E-1
6	1.87E-7	5.11E-11	4.84E-2
Average		8.75(±8.44)E-11	8.29(±8.00)E-2

As addressed above, the two methods (Tables 3-5.8 and 3-5.9) for evaluating both D and k_{dl} give similar results within experimental errors, and this suggests an important implication. In principle, the first method (eqs. 3-2.12 and 3-2.16) is directly based on

Table 3-5.9, Correlation of Diffusion Time Rate ($d\theta_D/dt$) with Labile Site Coverage (θ_L) for Bulk Soil at 25 °C (by eqs. 3-2.15 and 3-2.16)

No.	θ_L (molesg^{-1})	Intercept Const.	Std.err.	$d\theta_D/dt$ (molesg^{-1}d^{-1}) Coeffi.	Std.err.
7	7.50E-09	4.41E-09	5.31E-10	1.10E-09	1.73E-11
4	2.75E-08	-3.40E-10	1.24E-08	2.75E-09	3.21E-10
3	3.62E-08	1.15E-10	1.10E-08	3.17E-09	2.99E-10
14	4.16E-08	1.92E-08	8.72E-09	4.72E-09	2.23E-10
2	4.96E-08	-1.70E-08	3.46E-09	4.60E-09	9.03E-11
20	5.68E-08	1.38E-08	1.21E-08	5.12E-09	2.75E-10
19	6.41E-08	1.01E-08	9.33E-09	5.56E-09	2.25E-10
5	1.32E-07	5.83E-08	1.33E-09	1.53E-08	3.51E-09
6	1.87E-07	2.08E-08	1.33E-09	1.76E-08	3.24E-10
k_{dl} regression result*:		-2.90E-11	1.03E-9	9.99E-02	6.42E-03
D value with eq. 3-2.16:		1.05E-10	(cm^2 s^{-1})		

* R^2 = 0.972.

the solution for a particular model among Crank's set of diffusion models (66), whereas the second method (eqs. 3-2.15 and 3-2.16) is derived from an assumption of first-order nonlabile sorption kinetics. Although the existing literature (144,148,150,296) generally assumes that uptake by diffusion can be approximated by first-order kinetics, no simple theoretical support has been given for this. Here, the theoretical connection between the two approaches is specified. In the same way, the simple relationship between the rate (k_{dl}) of nonlabile uptake and the diffusion coefficient (D) has not been previously tested. A check is therefore required. Accordingly, the resulting consistency of the two approaches shows the self-consistency of the theories. In this regard, a typical differential plot, showing the correlation between the diffusion time rate ($d\theta_D/dt$) and the labile site coverage (θ_L), is presented in Fig. 3-5.8 and Table 3-5.9. The fitted straight line (R^2 = 0.972) has a slope (k_{dl}) of 0.0999 ± 0.0064 (d^{-1}), which is in very good agreement with the calculated average value by eqs. 3-2.12 and 3-2.16 (0.0829 d^{-1} in Table 3-5.8).

Of the two methods, the use of a polynomial regression to fit the experimental data of nonlabile sorption (θ_D) versus time (t), i.e., the latter method, can provide single k_{dl} and D values, and was shown to be more intuitive and simple. At least two factors, the intercept (Ln(A)) scatter caused by ordinary experimental errors, and the bias in the labile site coverage (θ_L) estimated by taking the mean value of the plateau region, could contribute to the uncertainties in the former method.

In addition, it should be recognized that none of experimental methods used in this research can be guaranteed to give the value of cross sectional area, a, in eq. 3-2.16. As is commonly done, the mean particle radius (l = 0.955×10^{-2} cm for the bulk soil) has

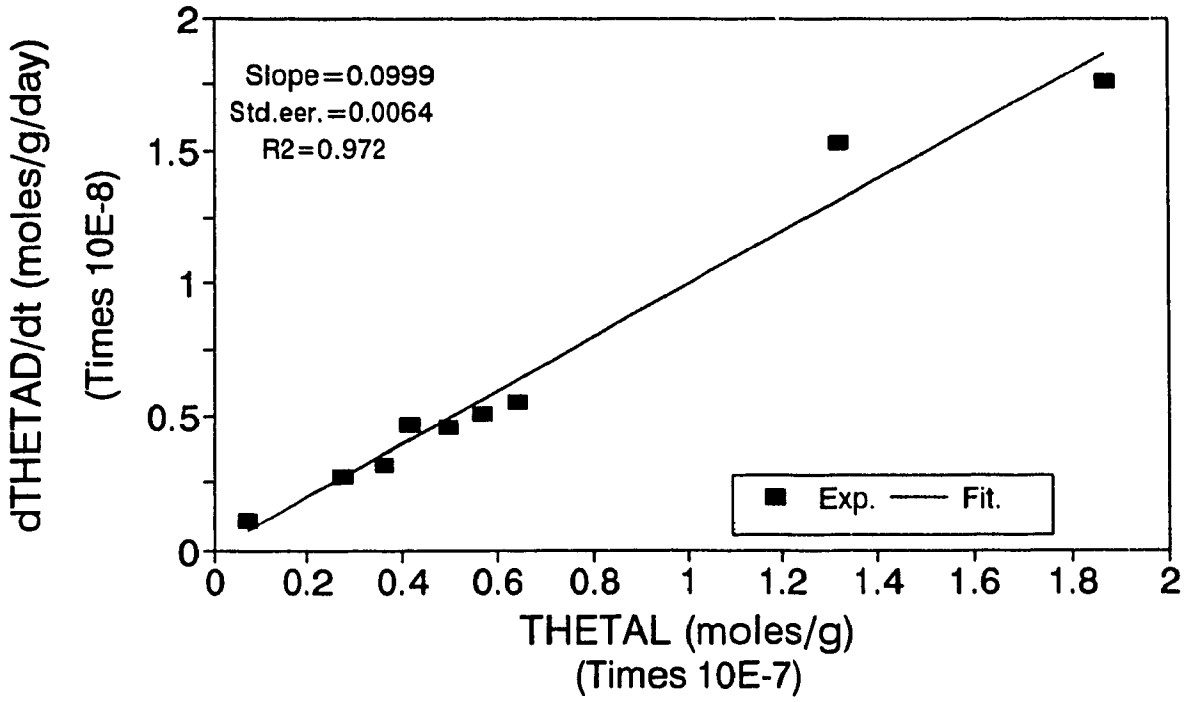

Fig. 3-5.8, Correlation of Diffusion Time Rate ($d\theta_D/dt$) to Labile Site Coverage (θ_l) for Bulk Soil at 25 °C

been used in the calculations.

(5). ***Long-term sorption kinetic experiments***

To date there has been relatively little work investigating the kinetics of intraparticle diffusion processes over a sufficiently long time scale, and especially no report dealing in depth with such a process in a separate way from surface adsorption (11,12,33,63,144,154,185,215), although the intraparticle diffusion does contribute to the so-called bound residue problems in the natural environment. This may be mainly due to experimental limitations. Fortunately, the MF-HPLC technique makes it possible to conduct either short-term or long-term sorption studies. As a result, a set of sorption batch experiments with various initial concentrations of atrazine for the bulk soil at 10 °C over a period of about 80 days have been carried out (Table 3-3.1).

Figs. 3-5.9 and 3-5.10 show the results of one experiment at a higher atrazine concentration (1.00×10^{-4} moles L^{-1}). It can be seen that the nonlabile sorption curve normally appears linear with time within the first 20 days, then becomes curved indicating that the net rate decreases, and apparently approaches a plateau region, after about 50 days until the end of the experiment. The fitted results for the experimental data of nonlabile sorption (Table 3-5.10), showing the slopes near zero within the standard errors, are further indications of the plateau regions. At this stage of the reaction, there are two linked equilibria in the system:

$$k_{b1}(V/W)M_{A1}\theta_o - k_{s2}\theta_1 = 0 \qquad (3\text{-}5.1)$$

$$k_{d1}\theta_1 - (V/W)R_{d2} = 0 \qquad (3\text{-}5.3)$$

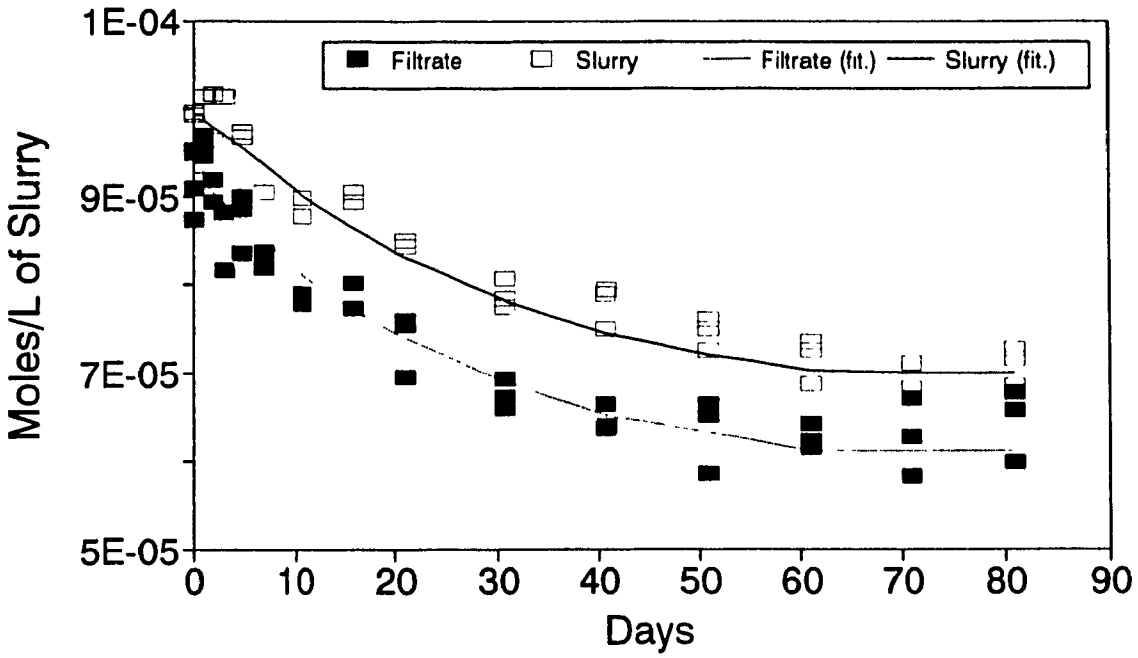

Fig. 3-5.9, Atrazine Species Distribution with Time (Exp. #29, bulk soil at 10 °C)

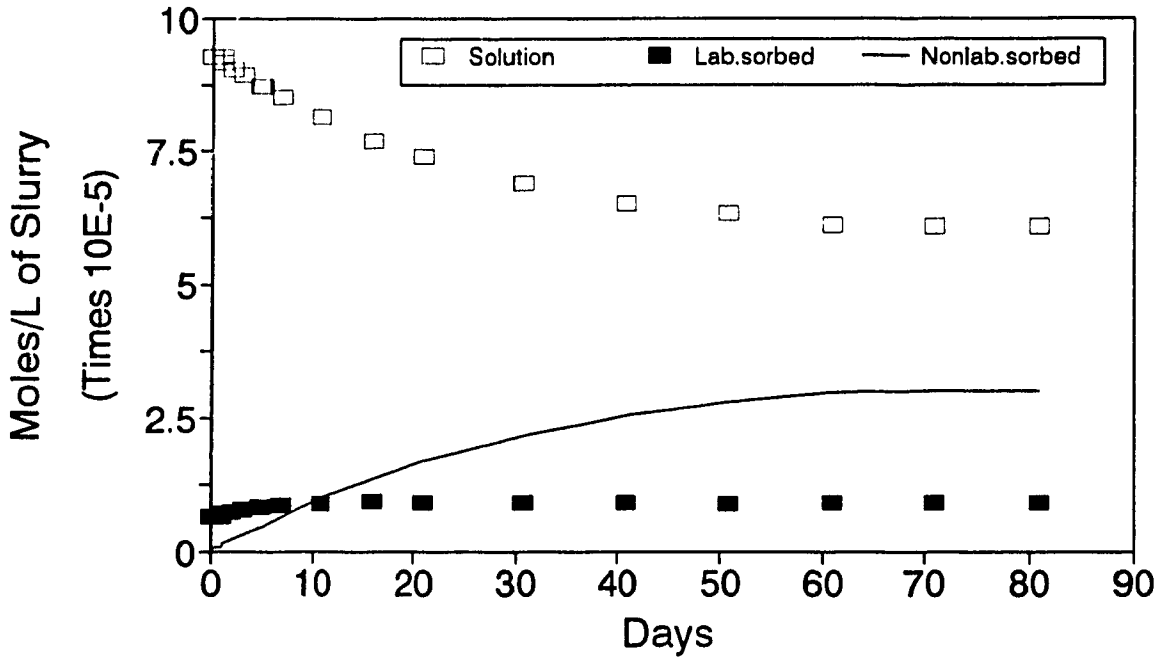

Fig. 3-5.10, Atrazine Species Distribution with Time (Exp. #29, bulk soil at 10 °C)

Table 3-5.10, Least Squares Fitting Results for Some Experimental Data of Nonlabile Sorption (Bulk soil at 10 °C)

No.	Duration (day)	Intercept ($molesL^{-1}$) Const.	Std.err.	Slope ($molesL^{-1}d^{-1}$) Coeffi.	Std.err.	R^2
29	0-20	-1.59E-6	3.85E-6	1.60E-6	1.08E-7	0.90
	20-50	2.42E-5	4.75E-6	3.43E-7	1.23E-7	0.44
	50-80	4.14E-5	1.86E-6	4.77E-8	5.05E-8	0.01
30	0-20	-1.83E-6	2.48E-6	1.60E-6	6.94E-8	0.96
	20-50	2.09E-5	3.14E-6	4.30E-7	8.14E-8	0.74
	50-80	4.03E-5	2.74E-6	6.45E-8	7.05E-8	0.077
31	0-20	-1.31E-6	2.48E-6	1.69E-6	6.93E-8	0.96
	20-50	2.42E-5	4.01E-6	3.04E-7	1.04E-7	0.46
	50-80	4.21E-5	1.49E-6	4.90E-9	3.84E-8	0.0016
32	0-20	-1.29E-7	1.24E-6	6.96E-7	3.46E-8	0.94
	20-50	9.33E-6	1.91E-6	2.40E-7	4.96E-8	0.70
	50-80	2.53E-5	1.96E-6	-4.67E-8	5.04E-8	0.079

$$(dM_{AT}/dt)_I = 0,\ (d\theta_I/dt)_I = 0 \text{ and } (d\theta_D/dt)_T = 0 \qquad (3\text{-}5.4)$$

The observed phenomena suggest an equilibrium state of reversible inward and outward intraparticle diffusion processes. The atrazine sorbed by intraparticle diffusion is labile with respect to an 80 day experiment, but will not be extracted by the HPLC mobile phase in a few minutes, and hence has been called nonlabile. If the intraparticle diffusion were irreversible then the final value of θ_D (i.e., the plateau) would equal the initial concentration of atrazine, indicating a complete sorption of atrazine, or would be constant above some initially applied atrazine value, indicating saturation of the intraparticle sorption capacity. In fact, the final value of θ_D appears to depend on the value of the initial concentration (M_{AT} at t = 0), and hence the labile surface sorption (θ_I). For example, θ_D has a value of $\sim 2.5 \times 10^{-5}$ moles g^{-1} for the experiment with atrazine equal to 1.00×10^{-4} moles L^{-1}, a value of $\sim 2.0 \times 10^{-5}$ moles g^{-1} for atrazine 8.00×10^{-5} moles L^{-1}, and $\sim 6.5 \times 10^{-6}$ moles g^{-1} for atrazine 8.00×10^{-6} moles L^{-1}. Note that the water solubility of atrazine is about 33 ppm ($\sim 1.5 \times 10^{-4}$ M) (281-283). Therefore, the resulting value of $\sim 2.5 \times 10^{-5}$ moles g^{-1} in the experiment (1.00×10^{-4} moles L^{-1}) might approach the upper limit of the θ_D value for the sorption in this pair of pesticide-soil system (nonlabile sorption capacity).

It is interesing to note that a parallel between the filtrate curve and the slurry curve (Figs. 3-5.9 and 3-5.10) has been maintained throughout the experiment. This empirical observation simply reflects the difference between the two curves (averaging $8.23 \pm 1.80 \times 10^{-6}$ moles L^{-1} of slurry), which is actually the labile sorption capacity that has already been determined experimentally (7.94×10^{-6} moles L^{-1} of slurry). Due to the higher

concentration in the solution phase, the effect of depletion on labile sorption, observable otherwise, is no longer pronounced.

3-6. SUMMARY

With this chapter, the two stage adsorption/diffusion mechanistic model has been presented and employed to describe the behavior of atrazine uptake by mineral soil GB 843. It can be seen that:

(1). The labile surface sorption has been shown to have a definite capacity (θ_c), with an experimentally determined value of $0.397 \pm 0.036 \times 10^{-6}$ moles g^{-1} of soil for the bulk soil which is further confirmed by the long-term experiment. The related equilibrium parameters, such as $\bar{K}_1$ and K_d, have been also evaluated, and the K_d value is comparable to published results on other systems.

(2). Both labile sorption curves and intraparticle diffusion curves exhibit rapid early uptakes within the first few minutes to hours. Corresponding to this stage, the rate constants (k_{s1}, k_{d1}) determined by an initial rate approximation have shown that the pseudo first-order adsorption rate constant k_{s1} is about 8 times higher than the inward diffusion rate constant k_{d1}.

(3). The two stage model describes the labile sorption process of atrazine uptake generally by a second-order rate law. With an initial rate approximation for the low coverage, instead, the first-order sorption or diffusion kinetics has been demonstrated to be suitable both for the labile sorption and for the intraparticle trapping. For example,

the k_{bl} value obtained by the first-order initial rate approximation (method (i)) is comparable to those obtained by the second-order iterative calculations (methods (ii) and (iii), see Appendix D). Two uptake time rates (dC_L/dt and dC_D/dt) have been shown to vary linearly with solution phase (M_{AT}) or labile sorbed (C_L) atrazine, respectively. The slow process rate parameters (D and k_{dl}) compare well with those reported elsewhere. It is hard to find comparable reference values for k_{sl}, since systems vary with respect to soil and pesticide.

(4). Over a certain reaction period (~2 to 11 days for labile sorption, after ~70 days for intraparticle diffusion) both curves apparently approach plateau regions, indicating the attainments of steady state. With respect to the much longer equilibrating time scale, intraparticle diffusion can be considered the rate-limiting process, in comparison with labile surface sorption.

To gain further understanding of the physical chemical mechanisms on atrazine uptake processes, more detailed investigations accounting for: 1) very early surface adsorption, 2) intraparticle diffusive uptake over a sufficiently long time scale, and 3) factors affecting the equilibrium and kinetics, with critical data analyses, are definitely needed in future research, some of which will be elaborated in subsequent chapters.

CHAPTER 4

ATRAZINE UPTAKE BY SOIL SIZE FRACTIONS

4-1. INTRODUCTION

The effects of particle size distribution have been studied and recognized during the last two decades. Previous studies (141,145) have shown a significant role of particle size or soil component variation in pesticide uptake. Fredeen et al. (83) found that the insecticide DDT was adsorbed by suspended solids, mainly clay and fine silt. Boucher (23) showed that particle size and cation exchange capacity influenced the adsorption of lindane by a natural aquifer substrate. Richardson and Epstein (237), in a study of retention of three insecticides, found that two hydrophobic compounds, DDT and methoxychlor, tended to concentrate in finer particle sizes (clay), whereas the more soluble endosulfan preferred coarser material.

Natural sorbents are commonly mixtures with a broad range of particle sizes, various organic and mineralogical compositions, as well as structural features. However, many transport and degradation models account for sorption by assuming an equilibrium or uniform distribution of pesticides between the sorbed and aqueous phases over the bulk soil body. The key equilibrium/kinetic parameters used, such as the equilibrium

distribution coefficient (K_d or K_p) and rate constants, are often estimated on the basis of bulk soil properties (11,80,297). Increasing evidence suggests that sorption often displays more complex behavior. A quantitative expression and pertinent prediction of the more subtle situation are required if environmental analyses and decision making are to achieve more accurate results. Several predictive modeling approaches (79,139,252) have recognized the need to separate total bulk loads into size fractions to better simulate the transport of pollutants.

These efforts have placed an emphasis on the importance of pesticide distribution as a function of particle size in evaluating sorption behavior. As noted above, however, there have been only a few papers in this area (23,83,141,145,237) which directly dealt with the effects of particle size, and in particular, to date relatively little attention has been paid to developing a model of solute transport that recognizes the heterogeneity of natural geochemical systems, and describes the sorption behavior without including empirical fitting parameters. In some existing modeling studies with batch systems, such as those by Ruthven and Loughlin (244), Rao and Jessup (233), Cooney et al. (64), Wu and Gschwend (296,297), Ball and Roberts (11,12), and Fong and Mulkey (80), etc., the independent measurable parameters are generally limited to only two: solution phase and total sorbed phase. One factor that is crucial is the methodology. Most conventional methods, such as batch technique, do not make it possible to distinguish between surface sorption and intraparticle diffusion. This precludes subsequent analyses.

The objective of this chapter is to further investigate the uptake behavior of atrazine by soil GB 843 as a function of distribution over the soil size fractions, using the batch

method combined with the on-line microfiltration-HPLC technique described in the previous chapters. Observed phenomena will be continuously interpreted by the two stage adsorption/diffusion model presented in Chapter 3. Treatments of the soil sample, such as fractionation and characterization, will be briefly described.

4-2. EXPERIMENTAL

(1). *Equipment*

The batch setup and the microfiltration-HPLC system used for soil fraction equilibrium/kinetic studies were the same as described in Chapter 3.

(2). *Reagents and materials*

The fractions of soil GB 843 with different particle sizes were obtained by sieving (see section 4-3). Other reagents and materials were prepared in the same ways as described in Chapter 3.

(3). *General kinetic procedure*

All the experiments for soil fraction kinetics were carried out at 25.0 ($\pm$0.2) °C. The general kinetic procedure and HPLC operating parameters can refer to Chapter 3. The batch experimental conditions are shown in Table 4-2.1.

Table 4-2.1, Basic Experimental Parameters of Soil Fraction Kinetics

Fraction no.	Parti. size (μm)	Soil wt. (g)	Slurry vol. (mL)	Init. AT (moles L^{-1})	Exp.duration (day)	Data points
1	425-180	0.5312	25.06	4.03E-06	18.79	52
1	425-180	0.5125	24.95	4.01E-06	18.77	49
2	180-150	0.4985	24.97	4.00E-06	18.70	52
2	180-150	0.5027	25.02	4.02E-06	18.79	52
3	150-75	0.4987	24.90	4.01E-06	18.67	52
3	150-75	0.4988	24.90	4.02E-06	18.74	49
4	75-45	0.5030	24.93	4.03E-06	18.74	53
5	≤45	0.5052	24.91	4.02E-06	18.81	53

4-3. CHARACTERIZATION OF SOIL FRACTIONS

(1). *Soil fractionation*

Soil particles cover an extreme size range, varying from stones and rocks (exceeding 0.25 m in size) down to submicron clay (< 1 μm). Various systems of size classification have been used to define arbitrary limits and ranges of soil particle size. Soil particles smaller than 2,000 μm are generally divided into three major groups: sands, silts and clays. These groups are sometimes called soil separates and can be subdivided into smaller size classes. Table 4-3.1 shows the particle size, sieve dimension, and defined size class by commonly-used systems of classification (100).

Particle size analysis is often used in soil science to evaluate soil texture, which is a measurement of the proportions of the various sizes of primary soil particles as determined usually either by their capacities to pass through sieves of various mesh size or by their rates of settling in water. In this work soil fractionation has been done using the American standard sieve system with nylon screens (101). The probability of a particle passing through a sieve in a given shaking time depends on the nature of the particle, the number of particles of that size, and the properties of the sieve. For smaller particles, the fractionation requires prolonged shaking. Table 4-3.2 presents the results. Comparing with Table 4-3.1, the soil GB 843 covers a broad range of particle size spectrum from medium sand ($\sim 50\%$) to silt and clay.

Table 4-3.1, Particle Size Limits According to Several Current Classification Schemes (100)

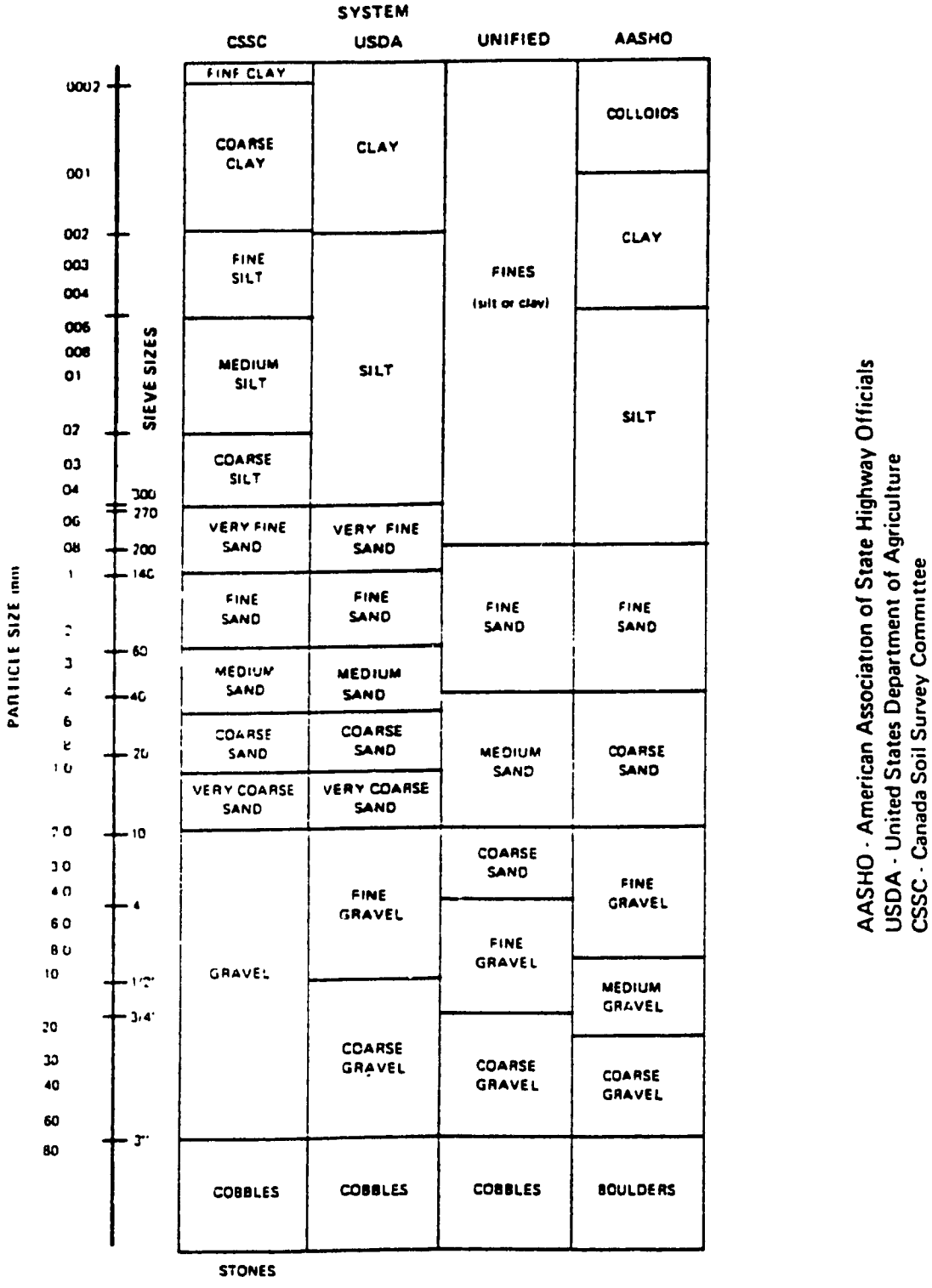

AASHO - American Association of State Highway Officials
USDA - United States Department of Agriculture
CSSC - Canada Soil Survey Committee

Table 4-3.2, Particle Size Distribution of Soil GB 843

Fraction no.	Sieve opening (mesh)	Particle size (μm) Max.	Min.	Mass fraction (%)
1	40	425	180	45.8
2	80	180	150	12.5
3	100	150	75	19.4
4	200	75	45	13.2
5	325	45	ND	9.1
Weighted average		191±234		100.0

(2). *Element identification (SEM/EDS studies)*

In the same way as for the bulk soil (Chapter 3), scanning electron microscopy (SEM) and energy dispersive spectrometry (EDS) studies were conducted with the soil fractions. A semi-quantitative result for element identification for fraction #5 is shown in Table 4-3.3. Table 4-3.4 shows the carbon contents of the fractions. It is worthy of note that the carbon contents, shown as peak areas in Table 4-3.4, should indicate the total carbon (organic carbon plus carbonates), rather than organic carbon only, within a certain thickness of surface layer.

(3). *Specific surface area*

In order to measure the specific surface area for the different soil fractions, a method named EGME (Ethylene glycol monoethyl ether) was used in this work. A soil sample previously dried at 110 °C was totally wetted with EGME. The coated sample was then vacuum dried to constant weight. The quantity of EGME retained by the sample was

Table 4-3.3, EDS Peak Listing for Fraction #5 (Collected over 60 x 5 seconds)

No.	Energy (keV)	Area	Element	Line
1	0.251	6,475	C	Kα
2	0.513	72,346	O	Kα
3	1.021	3,667	Na	Kα
4	1.229	1,129	Mg	Kα or As Lα?
5	1.474	46,805	Al	Kα or Br Lα?
6	1.741	154,465	Si	Kα or Rb Lα?
7	3.317	10,445	K	Kα or In Lα?
8	3.687	7,911	Ca	Kα
9	4.025	1,009	Ca	Kβ
10	4.516	2,250	Ti	Kα
11	6.406	11,199	Fe	Kα
a				
12	7.061	1,586	Fe	Kβ

Table 4-3.4, Semi-Quantitative Results of EDS for Carbon Contents in Soil Fractions (Collected over 60 x 5 seconds)

Fraction no.	Energy (keV)	Area	Line
1	0.260	8,325	Kα
2	0.258	7,234	Kα
3	0.261	4,058	Kα
4	0.253	4,150	Kα
5	0.251	6,475	Kα
Bulk soil	0.250	5,622	Kα

used for calculating the specific surface area (58). The resulting EGME areas are presented in Table 4-3.5.

Table 4-3.5, Measurements of Specific Surface Area for Soil Fractions

Fraction no.	Particle size (Avg., μm)	EGME area (m^2 g^{-1})
1	302.5	27.3±3.2* (24.1,30.5, 28.9,25.8)
2	165.0	30.2±9.4 (39.6,27.2,23.9)
3	112.5	36.9±1.2 (35.7,38.0)
4	60.0	41.4±2.9 (38.5,44.3)
5	22.5	48.6±0.4 (49.0,48.2)
Weighted sum		33.3
Bulk soil	191.0	38.9±2.3 (41.2,36.5)
		3.90±0.20**

* Average values. ** BET area.

(4). *Organic carbon analyses*

This work used a modified Mebius method (192), i.e., a rapid dichromate oxidation technique, to determine the content of organic carbon (OC) in the soil fractions. In brief, an excess of potassium dichromate solution was added to oxidize the soil organic carbon; the remaining dichromate was then back-titrated with ferrous ammonium sulfate solution. *o*-Phenanthroline-ferrous complex (0.025 M) was used as an indicator. The detailed procedure can be found in reference (210). Table 4-3.6 shows the results.

Clearly, the OC contents are not fully consistent with the semi-quantitative EDS results, in particular for fractions #1 and #2. This may be due mainly to nonuniform sampling in the EDS tests.

Table 4-3.6, Organic Carbon Analyses for Soil Fractions

Fraction no.	Particle size (Avg., μm)	Organic carbon (%)
1	302.5	0.60±0.01* (0.61,0.60,0.60)
2	165.0	0.67±0.01 (0.67,0.68)
3	112.5	0.94±0.00 (0.94,0.94)
4	60.0	0.98±0.01 (0.97,0.98,0.98)
5	22.5	1.26±0.16 (1.42,1.21, 1.22,1.20)
Weighted sum		0.79
Bulk soil	191.0	0.83±0.01 (0.84,0.83, 0.83,0.83)

* Average values.

(5). *Labile sorption capacity*

In the same way as for the bulk soil (Chapter 3), labile sorption capacity for each of the soil fractions was measured by saturating the surface sorption sites with solutions having higher atrazine concentrations. Fig. 4-3.1 shows a plot of the labile sorbed atrazine against the solution concentration for fraction #1. The measured values are given in Table 4-3.7.

4-4. RESULTS AND DISCUSSION

(1). *Labile sorption*

As indicated previously, the MF-HPLC technique can monitor atrazine species varying with time throughout the uptake reaction occurring in a stirred batch setup in

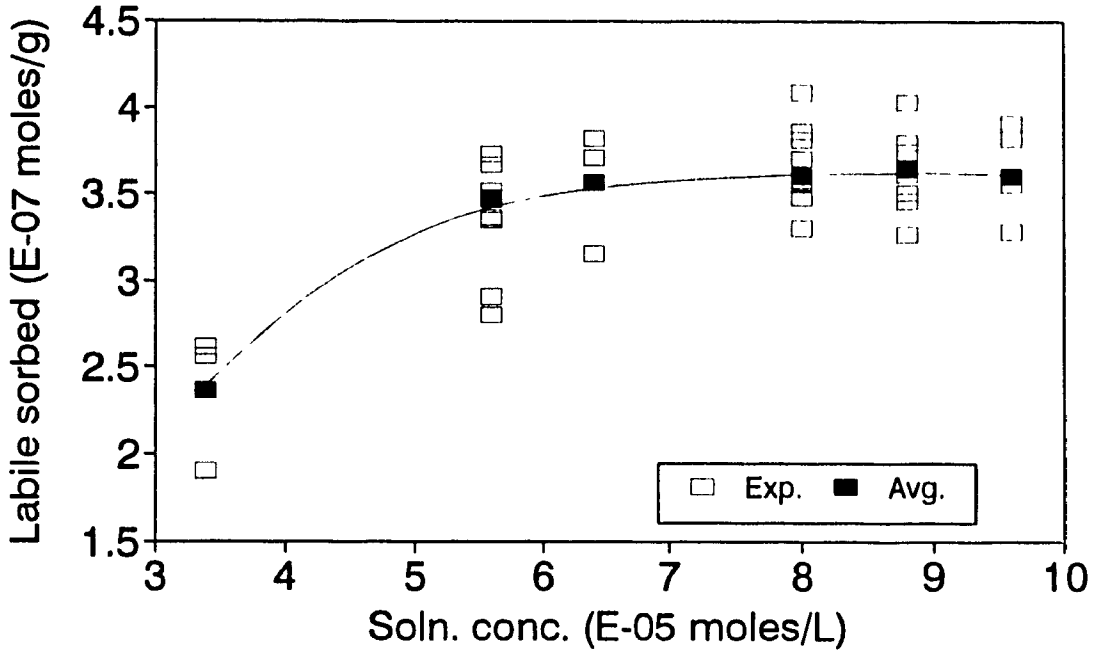

Fig. 4-3.1, Measurement of Labile Sorption Capacity for Fraction #1

Table 4-3.7, Measurements of Labile Sorption Capacities for Soil Fractions

No.	Init. conc. (10^{-6} molesL^{-1})	Equil.labile sorbed (10^{-6} molesg^{-1})	(10^{-6} molesL^{-1})
1	96	0.370±0.013* (0.357,0.376,0.371, 0.374,0.370)	7.40±0.26
2	96	0.467±0.024 (0.449,0.467,0.470, 0.491,0.456)	9.34±0.48
3	96	0.527±0.014 (0.541,0.513)	10.5±0.3
4	96	0.581±0.031 (0.551,0.571,0.602, 0.612,0.569)	11.6±0.6
5	100	0.630±0.010 (0.583,0.619,0.633, 0.640,0.627)	12.6±0.2
Sum**		0.435	8.70
Bulk	96	0.397±0.036 (0.375,0.390,0.433, 0.409,0.378)	7.94±0.72

* Average values. ** Sum=Weighted sum.

which the soil particles are assumed to be well suspended, and the bulk solution phase is completely mixed.

Table 4-4.1 presents atrazine concentration profile as a function of selected times, and Figs. 4-4.1 and 4-4.2 show atrazine species distribution as filtrate and slurry phases, or as solution, labile sorbed, and intraparticle diffused phases, including both raw and fitted data for fractions #4 and #2, respectively. It can be generally seen that atrazine in the solution phase decreased with time until 60 to 70% of the total atrazine remained at about

Table 4-4.1, Atrazine Concentration Profile at Selected Times

Fraction no.	Time (day)	Soln. (10^{-6}molL^{-1})	%	Lab.sorbed (10^{-7}molL^{-1})	%	Nonlab.sorbed (10^{-7}molL^{-1})	%
1	Total = 4.03E-06 moles L^{-1}						
	0.01	3.53	87.6	4.20	10.4	0.814	2.02
	0.05	3.51	87.1	4.30	10.7	0.870	2.16
	3.84	3.03	75.1	4.87	12.1	5.16	12.8
	8.80	2.72	67.5	4.90	12.2	8.17	20.3
	15.9	2.70	67.0	3.49	8.66	9.81	24.3
1	Total = 4.01E-06 moles L^{-1}						
	0.01	3.54	88.1	4.48	11.2	0.297	0.74
	0.05	3.53	88.0	4.49	11.2	0.326	0.81
	3.83	3.15	78.6	5.62	14.0	2.97	7.40
	8.80	2.72	67.7	7.26	18.1	5.69	14.2
	15.8	2.54	63.2	6.66	16.6	8.09	20.2
2	Total = 4.00E-06 moles L^{-1}						
	0.01	3.70	92.5	3.51	8.78	0.476	1.19
	0.06	3.70	92.4	2.55	6.36	0.495	1.24
	3.71	3.35	83.7	4.53	11.3	1.99	4.97
	8.71	3.03	75.7	5.69	14.2	4.03	10.1
	15.7	2.79	69.8	5.19	13.0	6.89	17.2
2	Total = 4.02E-06 moles L^{-1}						
	0.01	3.72	92.6	2.17	5.39	0.812	2.02
	0.05	3.72	92.5	2.19	5.45	0.828	2.06
	3.80	3.40	84.6	3.86	9.60	2.31	5.75
	8.76	3.06	76.2	5.27	13.1	4.30	10.7
	15.8	2.76	68.7	5.18	12.9	7.09	18.4

(cont'd)

3	Total = 4.01E-06 moles L^{-1}						
	0.01	3.55	88.6	3.65	9.09	0.933	2.33
	0.05	3.54	88.4	3.72	9.27	0.949	2.37
	3.76	3.23	80.5	5.36	13.4	2.45	6.11
	8.67	2.96	73.7	6.08	15.2	4.43	11.1
	15.7	2.66	66.3	6.27	15.6	7.27	18.1
3	Total = 4.02E-06 moles L^{-1}						
	0.01	3.64	90.5	1.97	4.89	1.87	4.65
	0.05	3.63	90.2	2.07	5.15	1.88	2.93
	3.77	3.23	80.3	4.99	12.4	2.92	7.25
	8.80	2.96	73.6	6.32	15.7	4.31	10.7
	15.8	2.81	69.9	5.89	14.6	6.25	15.5
4	Total = 4.03E-06 moles L^{-1}						
	0.01	3.57	88.6	2.44	6.05	2.14	5.31
	0.05	3.56	88.4	2.49	6.19	2.16	5.36
	3.70	2.97	73.8	6.31	15.7	4.23	10.5
	8.72	2.51	62.4	8.06	20.0	7.08	17.6
	15.7	2.49	61.8	6.78	16.8	8.61	21.4
5	Total = 4.02E-06 moles L^{-1}						
	0.01	3.49	86.8	4.24	10.6	1.07	2.60
	0.05	3.47	86.4	4.36	10.9	1.08	2.70
	3.70	2.89	72.1	8.73	21.7	2.49	6.19
	8.80	2.70	67.3	8.65	21.5	4.47	11.1
	15.7	2.44	60.8	8.64	21.5	7.11	17.7

* % shows the concentration as the percentage of total atrazine.

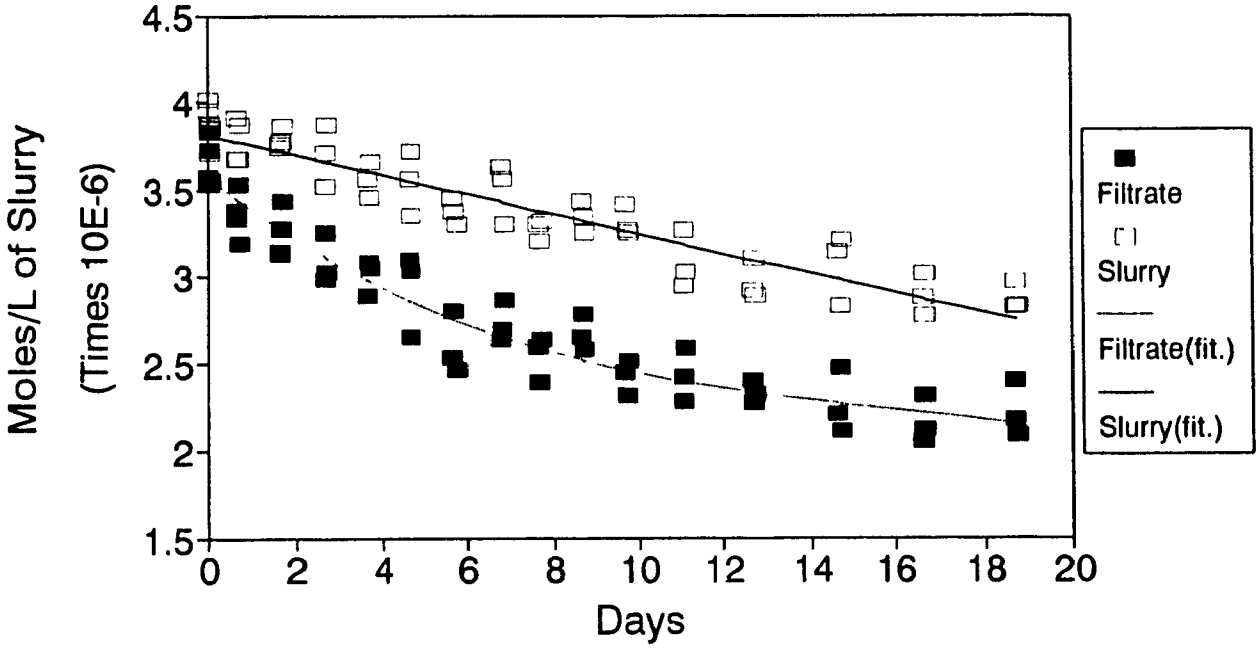

Fig. 4-4.1, Atrazine Concentration Profile with Time for Fraction #4

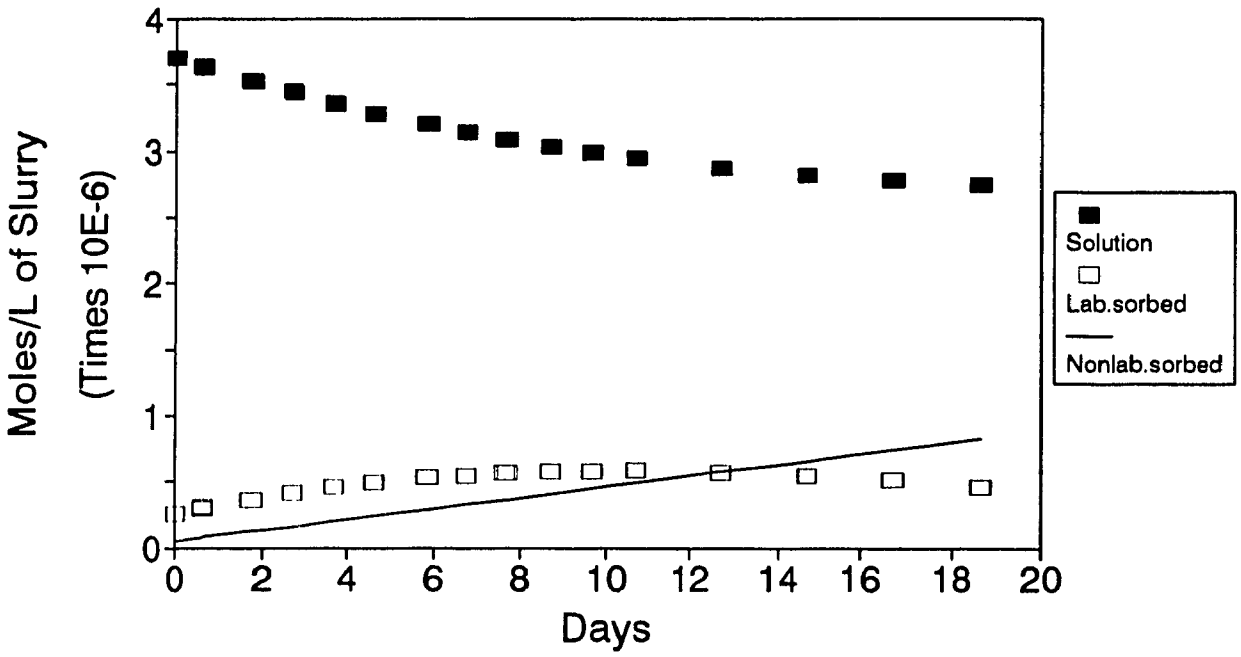

Fig. 4-4.2, Atrazine Species Distribution with Time for Fraction #2

16 days. In contrast, the sorbed portion (the labile plus the nonlabile) increased with time. Within the first 0.05 days (1.2 h) more than 10% of the total atrazine were taken up.

Gamble and Langford (96) have examined the adsorption of pesticides to a heterogeneous collection of sites, and used a weighted average equilibrium function ($\bar{K}_1$) instead of an equilibrium constant for the equilibria in a mixed ligand system. In analogy with this, an assumption can be generally made that the overall behavior of atrazine uptake by bulk soil should be the integral of its fractions. For the sorption capacity (θ_c or C_c), consequently, it is reasonable to consider the total (or bulk) capacity as the sum of contributions of each site type. That is, the sorption capacity of a given fraction i can be expressed in a site loading-weighted sum:

$$\theta^i_c f^i = \theta^i_{c1} f^i_1 + \theta^i_{c2} f^i_2 + \ldots + \theta^i_{cj} f^i_j = \Sigma_j \theta^i_{cj} f^i_j \qquad (4\text{-}4.1)$$

and, furthermore, for the total capacity:

$$\theta_c f = \theta^1_c f^1 + \ldots + \theta^i_c f^i = \Sigma_i \theta^i_c f^i \qquad (4\text{-}4.2)$$

where the superscript i denotes the soil fractions (i=1 to 5 in this case), the subscript j denotes the type of sorption sites, f is the mole fraction of the sites, and θ_c is the sorption capacity in moles g^{-1} of soil. Assuming each fraction contains a similar type of organic matter (sorption sites), on this basis, the mole fraction (f) can be substituted with the mass fraction (using the same symbol as mole fraction f) that is available from Table 4-3.2. Thus, eq. 4-4.2 can be viewed as a mass-weighted sum.

As shown in Table 4-3.7 (also, in Table 4-4.2) the measured values of θ_c for the soil fractions exhibit a clear trend: the finer the size fractions, the higher the sorption

Table 4-4.2, Results of Labile Sorption for Soil Fraction Kinetics

Fraction no.	θ_c (10^{-6} molesg^{-1})	$\overline{K}_l$ (10^4 M^{-1})	K_d (10^{-2} Lg^{-1})	k_{sl} (d^{-1})	X_l (10^{-2})
1	0.370	2.37±0.43* (1.94,2.80)	0.807	0.450±0.038* (0.488,0.412)	7.92±1.22* (6.70,9.14)
2	0.467	2.79±0.08 (2.86,2.71)	1.22	0.574±0.093 (0.670,0.483)	6.00±0.17 (6.17,5.82)
3	0.527	3.03±0.02 (3.01,3.05)	1.50	0.889±0.032 (0.921,0.857)	6.02±0.00 (6.02,6.02)
4	0.581	4.63	2.52	1.20±0.08	6.47
5	0.630	4.21	2.47	2.04±0.16	6.78
Sum	0.435	3.02	1.37	0.792	7.02
Bulk	0.397±0.036	3.03±0.97	1.01±0.35	0.831±0.093	10.2

* Average values.

capacities. By applying eq. 4-4.2, the mass-weighted sum for θ_c is 0.435 x 10^{-6} moles g^{-1} of soil which agrees with the measured value for the bulk soil, 0.397 x 10^{-6} moles g^{-1} of soil.

As discussed previously in Chapter 3, the weighted average equilibrium function ($\bar{K}_l$), the distribution coefficient (K_d), and the mole fraction of occupied sorption sites (X_l) for the labile uptake of atrazine by the soil fractions have been respectively calculated according to:

$$\bar{K}_l = \theta_L/\theta_o M_{AT} \qquad (4\text{-}4.3)$$

$$X_l = \theta_L/\theta_c \qquad (3\text{-}2.8)$$

$$K_d = \bar{K}_l\theta_c(1-X_l) \qquad (3\text{-}2.10)$$

where the definitions for θ_L, θ_o, and M_{AT} are the same as Chapter 3.

The resulting values for $\bar{K}_l$, K_d, and X_l are incorporated in Table 4-4.2. The trends for $\bar{K}_l$ and K_d are consistent with those would be expected on the basis of specific surface area and organic matter content; that is, both $\bar{K}_l$ and K_d increase slightly as the soil fractions vary from coarser to finer. Similar observations have been reported by Karickhoff et al. (23,83,141,145,237). In contrast, the X_l values do not show significant differences among the particle size fractions. This suggests that the same or similar types of organic matter are distributed in the soil fractions as hypothesized above.

The kinetic treatment for the labile uptake process of each fraction will follow an analogous procedure to the bulk soil as discussed in Chapter 3. Briefly, the labile sorption kinetics are inherently second order, and can be expressed as:

$$-dM_{AT}/dt = k_{b1}M_{AT}(W/V)\theta_o - k_{s2}(W/V)\theta_L \qquad (3\text{-}2.2)$$

where k_{b1} is the second-order rate constant for adsorption, and k_{s2} is the first-order rate constant for desorption.

Applying a first-order rate approximation to the early beginning of the reaction (i.e., $\theta_o \approx$ constant, and neglecting the desorption and intraparticle diffusion terms), the initial rate approximate calculation (see section 3-2.(4) in Chapter 3) is operational according to:

$$-dM_{A1}/dt = (W/V)d\theta_1/dt = k_{s1}M_{AT} \qquad (3\text{-}2.19)$$

where

$$k_{s1} = k_{b1}(W/V)\theta_o \qquad (3\text{-}2.23)$$

and k_{s1} is the pseudo first-order rate constant for adsorption. The resulting k_{s1} values for the soil fractions are shown in Table 4-4.2. It can be seen that the k_{s1} values consistently increase as the particle sizes decrease. For fraction #5 and #1, as an example, the values of k_{s1} differ by a factor of ~ 4. Such a trend agrees with frequently reported results (22,104,141,142,145,158,191,207,243,253,273).

Both specific surface area and organic matter content are important contributors to the labile sorption. Figs. 4-4.3 and 4-4.4 show the plots of k_{s1} versus EGME and OC, in which the fitted straight lines have $R^2 = 0.948$ and 0.937, respectively. Similarly, the plots of θ_e against EGME and OC are shown in Figs. 4-4.5 and 4-4.6. In addition, Fig. 4-4.7 is a chart giving an overview of the relationships among the equilibrium/kinetic parameters describing the labile uptake process of atrazine over the size fractions in terms of θ_e, $\bar{K}_1$, X_1, K_d, and k_{s1}.

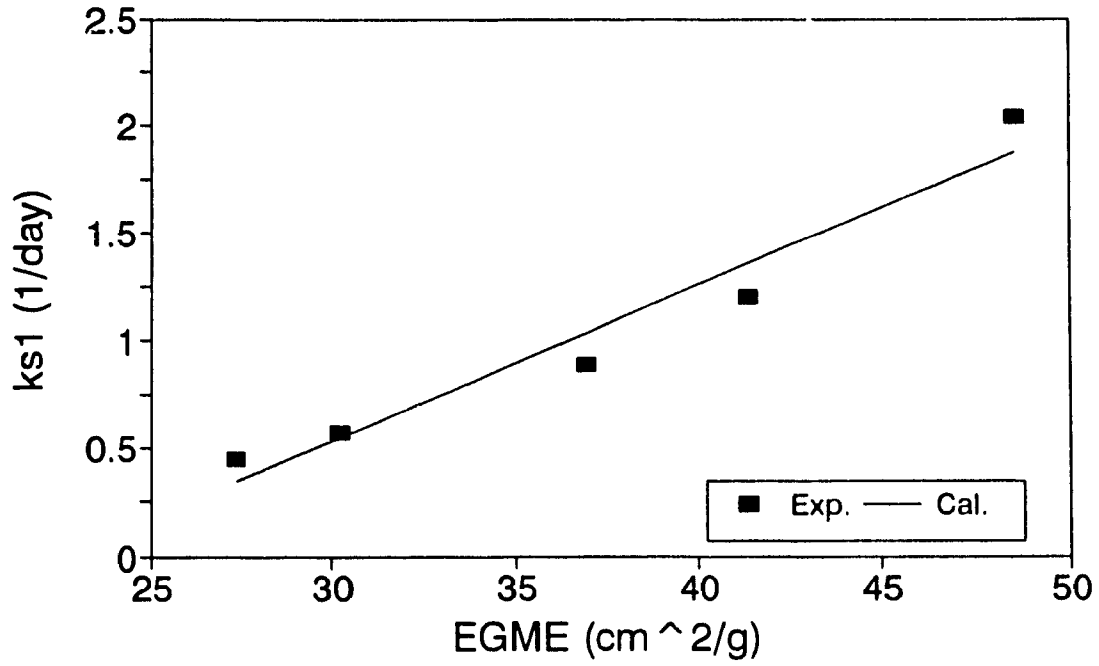

Fig. 4-4.3, Rate Constant k_s as a Function of Specific Surface Area

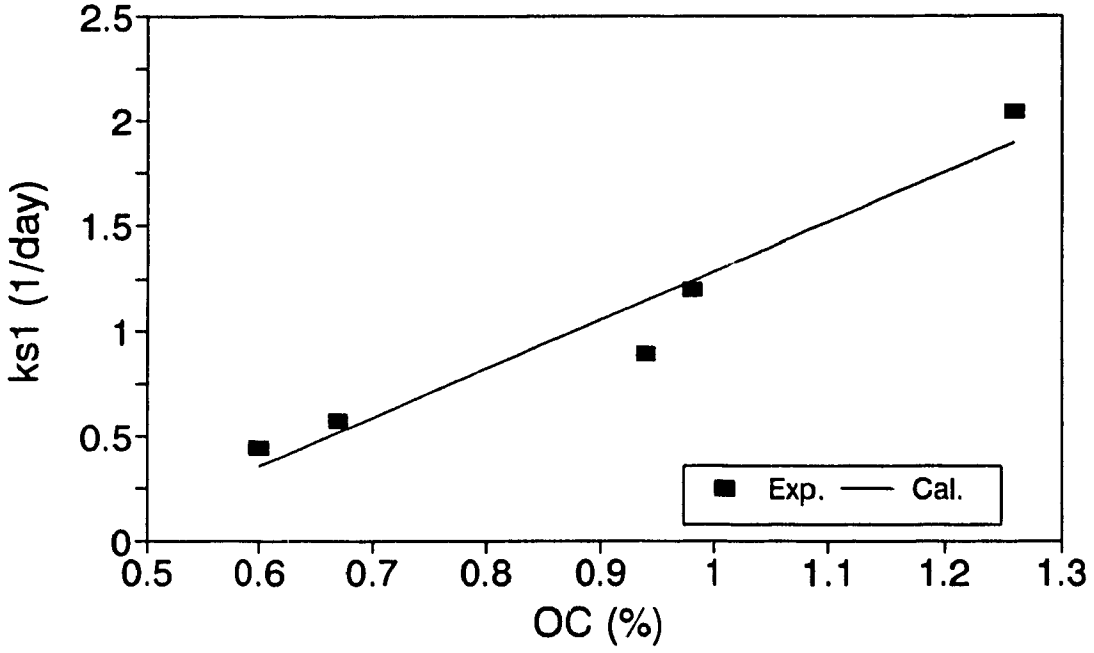

Fig. 4-4.4, Rate Constant k_{s1} as a Function of Organic Carbon Contents

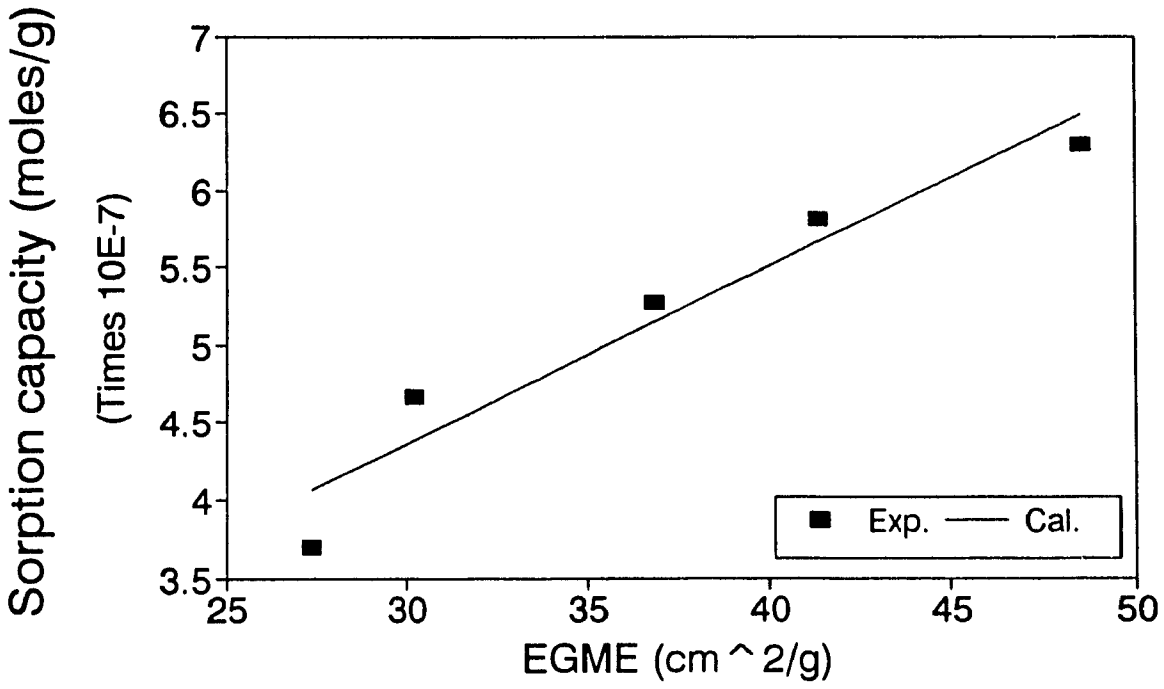

Fig. 4-4.5, Sorption Capacity θ_c as a Function of Specific Surface Area

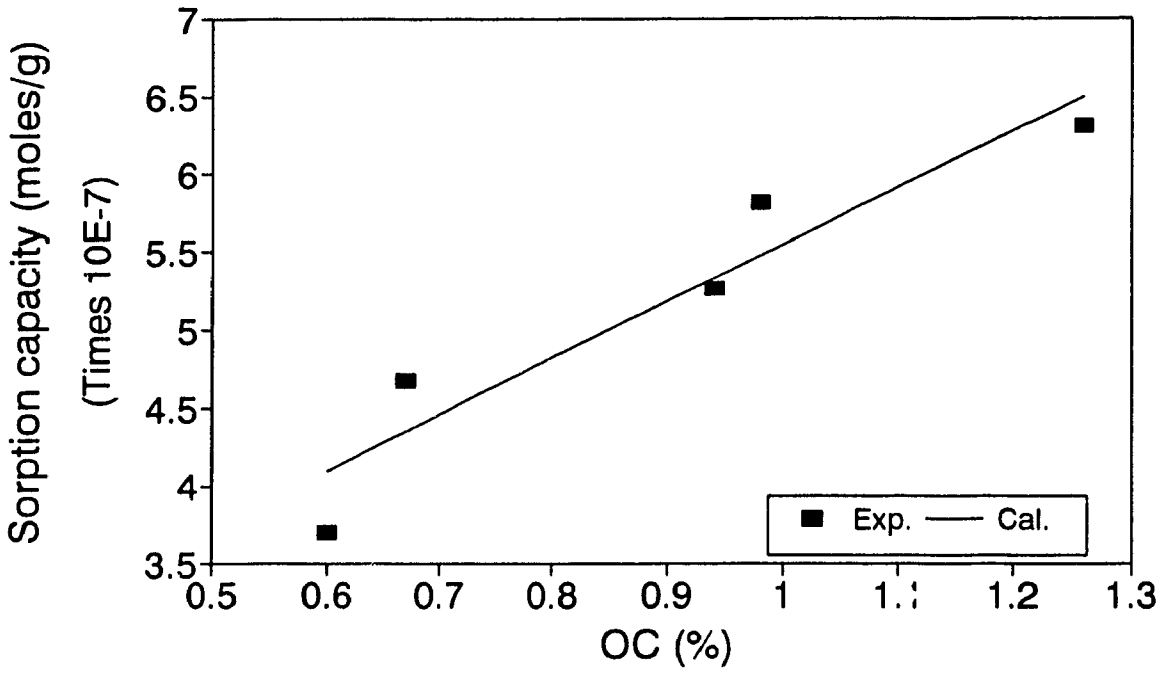

Fig. 4-4.6, Sorption Capacity θ_c as a Function of Organic Carbon Contents

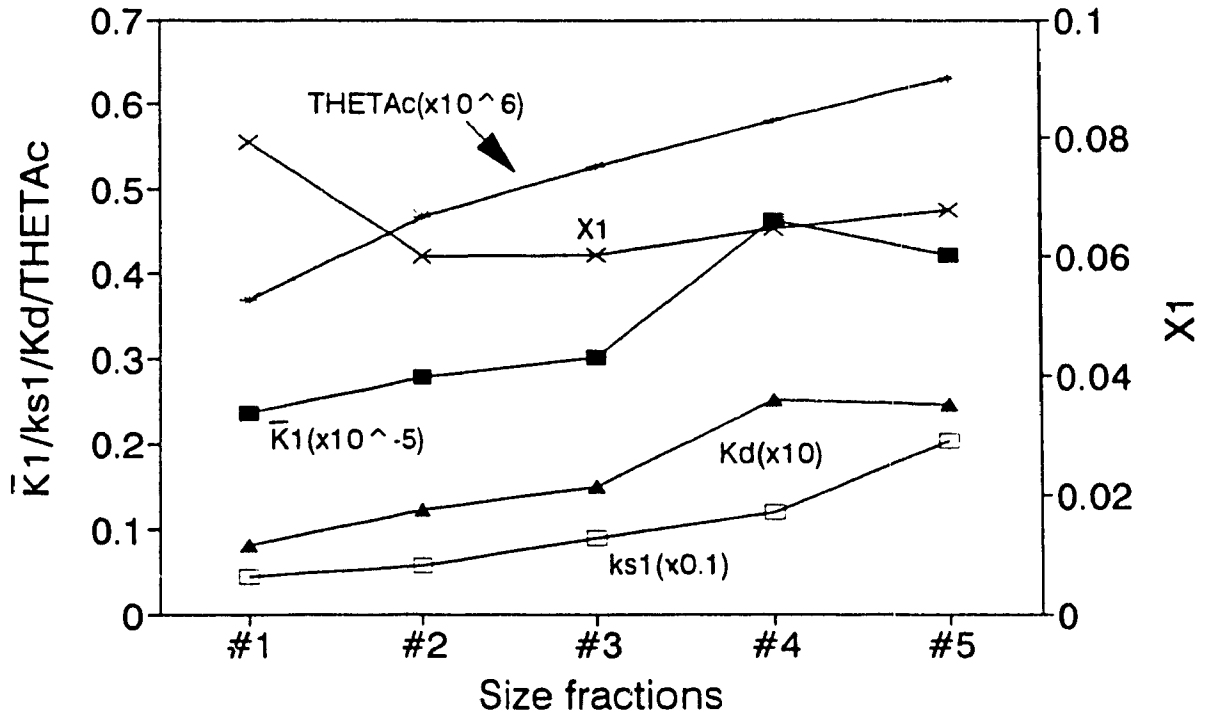

Fig. 4-4.7, Relationship Overview among θ_c, X_1, $\bar{K}_1$, K_d and k_{s1}

(2). *Intraparticle diffusion*

As noted in Fig. 4-4.2, atrazine species trapped by intraparticle diffusion show a steady increase with reaction time, which will eventually account for a significant portion of total atrazine by the end of the experimental period. The phenomenon that an initially fast sorption followed by a much slower uptake has been usually observed (33,63,74,83,111,143,144,150,176,181,183,195,219,226,227,234,245,272,278,299). Existing literature (148,150,296) generally assumes that the uptake by diffusion can be approximated with first-order kinetics, but no simple theoretical support has been found for this. As addressed in Chapter 3, the two stage model applies the law of mass action and Crank's solution to Fick's law (66) to the kinetics of intraparticle diffusive uptake, and leads to the following differential rate law for describing the mass transfer between labile sorption sites and diffusion trapped state:

$$d\theta_D/dt = k_{d1}\theta_1 - (V/W)R_{d2} \qquad (3\text{-}2.14)$$

where θ_D is the amount of diffused material (moles g^{-1} of soil). An approximation to the early period of the diffusive uptake (i.e., the outward diffusion term $R_{d2} \approx 0$) will lead to a reduced expression of eq. 3-2.14:

$$d\theta_D/dt = k_{d1}\theta_1 \qquad (3\text{-}2.15)$$

in which k_{d1} is the first-order rate constant for diffusion in d^{-1}, which is associated with the effective diffusion coefficient (D, in $cm^2\ s^{-1}$), and a particle dimension related to diffusion (a in eq. 3-2.16). It has been generally accepted that the particle radius (l, in cm) is the appropriate length scale. Therefore:

$$k_{d1} = Q(D/l^2) \qquad (4\text{-}4.4)$$

where Q = 86,400 s d^{-1}. D is calculated by:

$$D = B(Al/\theta_L)^2 t^n \qquad (4\text{-}4.5)$$

where B = 0.7854, and n = 0 in this case. Eq. 4-4.5 is derived from a particular solution of Fick's diffusion law (i.e., a steady state surface coverage) presented by Crank (66).

Table 4-4.3 shows the resulting k_{dl} and D values calculated by eqs. 4-4.4 and 4-4.5, respectively. The k_{dl} values shown in Table 4-4.4 were calculated by eq. 3-2.15. In addition, in a similar way with the bulk soil (Chapter 3), the diagnostic test for intraparticle diffusion of the soil fractions can be carried out with eq. 3-2.13:

$$Ln(\theta_D) = Ln(A) + 1/2Ln(t) \qquad (3\text{-}2.13)$$

where $A = 2(\theta_l/l)(D/\pi)^{1/2}$. The results are shown in Table 4-4.5 and Fig. 4-4.8.

In order to evaluate the data for nonlabile intraparticle diffusion, it is necessary to review the parameters k_{dl} and D first.

k_{dl} is a lumped parameter which includes contributions from the apparent intraparticle diffusivity (D) and the particle radius (l) by eq. 4-4.4. Both D values and l values vary in the same direction with particle size. Therefore, the final effect on k_{dl} will be dependent upon their relative results as shown in Table 4-4.3. On the other hand, k_{dl} can be determined by the first-order rate expression (eq. 3-2.15) from the diffusion time rate ($d\theta_D/dt$) and the labile surface coverage (θ_L). The coarser fractions have larger $d\theta_D/dt$ values and smaller θ_L values (resulting in larger k_{dl}), while the opposite is true for the finer fractions, as shown in Table 4-4.4. It is important to note that k_{dl} values calculated by the both ways generally have the same magnitude (the weighted sum being 0.0787 to

Table 4-4.3, Results of Intraparticle Diffusion for Soil Fraction Kinetics

Fraction no.	Avg. l (10^{-2} cm)	D* (10^{-11} cm^2s^{-1})	k_{dl}* (10^{-2} d^{-1})
1	1.513	25.8±14.2** (40.0,11.6)	9.74±5.36
2	0.825	6.12±1.82 (4.30,7.94)	7.77±2.31
3	0.563	2.15±0.36 (1.79,2.51)	5.86±0.98
4	0.30	0.699	6.71
5	0.113	0.0668	4.52
Sum	0.955	13.1	7.87
Bulk	0.955	8.75	8.29

* Calculated by eqs. 4-4.4 and 4-4.5, respectively.
** Average values.

0.100 d^{-1}), and decrease slightly with decreasing particle size. By applying the first-order rate approximation, Karickhoff and Morris (144) reported exchange constants (k_2) between two supposed compartments (S_1 and S_2), having the range of 0.1 to 1.0 d^{-1}. Ball and Roberts (12) employed a rate parameter (D_a/a^2) to describe the rate behavior of diffusive uptake. The k_{dl} values obtained here are slightly higher than their results by the one- or two-parameter model (D_a/a^2), but lower than the pore diffusion model (D_p/a^2).

According to eq. 3-2.16, the effective diffusion coefficient, D, is related to both the rate constant (k_{dl}) and a diffusion-related dimension (a). It has been generally accepted that the particle radius (l in eq. 4-4.4) is the appropriate length scale for diffusive uptake within a spherical particle (12,296). As mentioned above, both k_{dl} and l for the coarser

Table 4-4.4, Correlation of Diffusion Time Rate with Labile Surface Coverage for Soil Fractions

Fraction no.	θ_1 (10^{-8} molesg^{-1})	$d\theta_D/dt$ (10^{-9} molesg^{-1}d^{-1}) (exp.)	(fit.)	k_{d1}** (10^{-2} d^{-1})
1	2.93±0.45* (2.48,3.38)	3.72	3.36	12.7±2.0
2	2.80±0.08 (2.88,2.72)	3.05	3.49	10.9±0.3
3	3.17±0.00 (3.17,3.17)	2.52	3.11	7.94±0.00
4	3.76	2.61	2.52	6.94
5	4.27	1.90	2.01	4.44
Sum	3.19			10.0
Bulk	5.30			9.99±0.64

* Average values.
** Calculated by eq. 3-2.15 and $d\theta_D/dt$ with exp. values.

Table 4-4.5, Diagnostic Tests for Soil Fraction Intraparticle Diffusion

Fraction no.	θ_1 (10^{-8} molesg^{-1})	Ln(A)	Z
1	2.48	-24.02±0.21	0.550±0.024
	3.38	-24.33±0.27	0.500±0.021
2	2.88	-24.38±0.25	0.515±0.029
	2.72	-24.13±0.21	0.506±0.029
3	3.17	-24.34±0.08	0.504±0.017
	3.17	-24.17±0.05	0.505±0.013
4	3.76	-24.01±0.08	0.506±0.017
5	4.27	-24.08±0.05	0.465±0.022

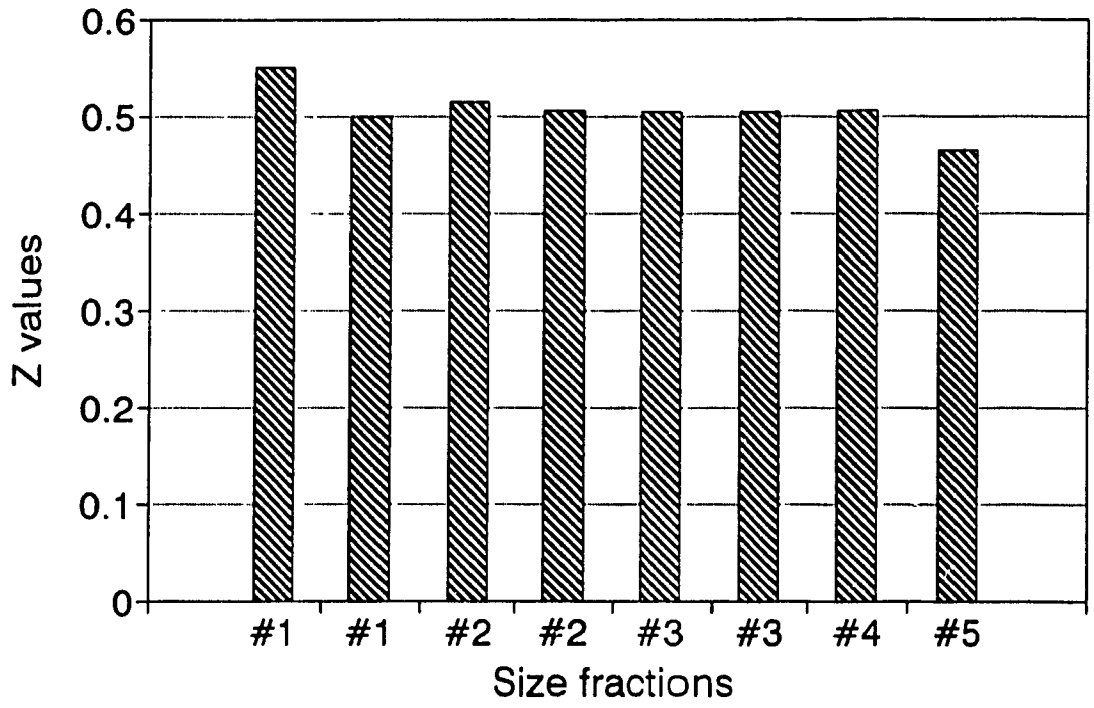

Fig. 4-4.8, Diagnostic Tests for Soil Fraction Intraparticle Diffusion (Z is defined by eq. 3-2.13)

fractions favor larger D values, whereas the finer the reverse. Similar trends in D values varying with particle size can be derived from the parameters I and θ_I by eq. 4-4.5 which is a particular solution of Fick's diffusion law (66). Viewing the D values shown in Table 4-4.3, they usually have the magnitudes of 10^{-10} to 10^{-13} ($cm^2\ s^{-1}$) over the fractions which fall well within the ranges reported by Karickhoff and Morris (144), and Wu and Gschwend (296), are very close to the upper values of Duursma and Bosch (76), and the lower values of Ball and Roberts (12). It is also seen that fraction #1 apparently has a relatively large D value, followed by a gradual decrease as the fractions get smaller.

A general view on the diffusive uptake is given by the pore transport model (12,287,296) that treats the uptake as a surface adsorption plus a pore diffusion. That is, solute molecules are assumed to diffuse into the pore voids and adsorb onto pore surface sites. The migration of adsorbed solutes can occur only by desorption followed by pore transport to a new site. By contrast, the other model for describing diffusive uptake is the surface diffusion model, supposing that diffusion occurs predominantly in the sorbed phase (198 289). In a more specific case where diffusion is envisioned to occur through organic matter, the apparent sorbed-phase diffusivity will be related to an intraorganic matter diffusivity (30,33). With a pore diffusion interpretation, the apparent diffusion coefficient D_a (having the same meaning as the effective diffusion coefficient D in this work) contains contributions from aqueous pore diffusion, pore tortuosity and constrictivity, as well as internal retardation as shown by:

$$D_a = D_p/R_{int} \qquad (4\text{-}4.6)$$

$$D_p = (D_b K_r)/\chi \qquad (4\text{-}4.7)$$

where D_p and D_b refer to the pore diffusivity and bulk aqueous diffusivity, respectively. K_r is a constrictivity factor (≤ 1), χ is the tortuosity factor (≥ 1), and R_{int} is an internal retardation factor, $R_{int} = 1 + (\rho_a/\epsilon_i)K_{di}$ (where ρ_a = apparent grain density, ϵ_i = internal porosity of sorbing grains, and K_{di} = internal distribution coefficient), which is mainly related to internal sorption sites (K_{di}).

Such a relationship between the observed intraparticle diffusivity and particle size can be most likely elucidated by the existence of organic matter and soil porosity. In fact, supposed chemically specific binding between diffusing atrazine and organic moieties on the pore surfaces may become more predominant with fine fractions due to the higher organic contents, which makes the surface diffusion more significant than the pore diffusion, and contributes a slower diffusivity (226). Clay (e.g., fraction #5) was reported to contain internal sites for sorption that are not easily accessible (e.g., vermiculite interlayer sites) (213). A number of investigators have reported the presence of organic matter-clay complexes in most mineral soils (154). Burns (35) pointed out that a humus-clay micro-environment is a site of high biological and nonbiological activity. Moreover, many investigators observed that chemicals with higher hydrophobicities penetrate natural sorbents with slower diffusivities (31,144,226,296). On the other hand, considering both the physical and chemical effects on the apparent diffusivity (eqs. 4-4.6 and 4-4.7), it can be concluded that the finer fractions possess relatively higher micropore proportions which have radii comparable to the size of diffusing species (leading to smaller K_r and larger χ) and more organic matter contents (resulting in greater R_{int}) in comparison with the coarser fractions. Both factors would lead to greater resistance to the diffusion, and

make the pore diffusivity slower (i.e., small D_p and thus small D_a). Chantong and Massoth (44) indicated that pore diameters less than 2 nm could lead to greater than 10 fold reductions in effective diffusivity (D_p). Ball et al. (13) observed that a significant portion of surface area is attributed to such small pores. It is conceivable that an important fraction of the sorption capacity could be located in microporous regions. Therefore, although the contribution of microporosity to total intraparticle pore volume may be small, the possibility of steric hindrance as a factor in pore diffusion cannot be ruled out. In contrast, the lower organic matter contents, which leads to more physical sorption on the pore surfaces or makes the pore diffusion more significant than the surface diffusion, should provide a reasonable explanation for atrazine diffusive uptake by the coarser fractions, especially fraction #1. Some physically-based contributions from soil texture and geometry such as macropores and aggregates (11,12,30-32,166,209,216,287), where there exist easily accessible sites and easily passed pathways (leading to greater D_p), may be expected (refer to the microscopic pictures shown in Chapter 3). In fact, advective transport of a solute is possible through macropores (226).

Figs. 4-4.9 and 4-4.10 show the results of both D and k_{d1} plotted against specific surface area or organic carbon content. It can be seen that, in contrast to k_{s1} that shows direct correlations with specific surface area and organic carbon content (Figs. 4-4.3 and 4-4.4), there exists no simple relationship between them, which may imply a more complex and multiple effect on the both parameters. Note that, to date, there has been no reliable information about the parameter "a", and no reliable way of relating it to particle sizes, shapes, or estimates of surface area. This may constitute some

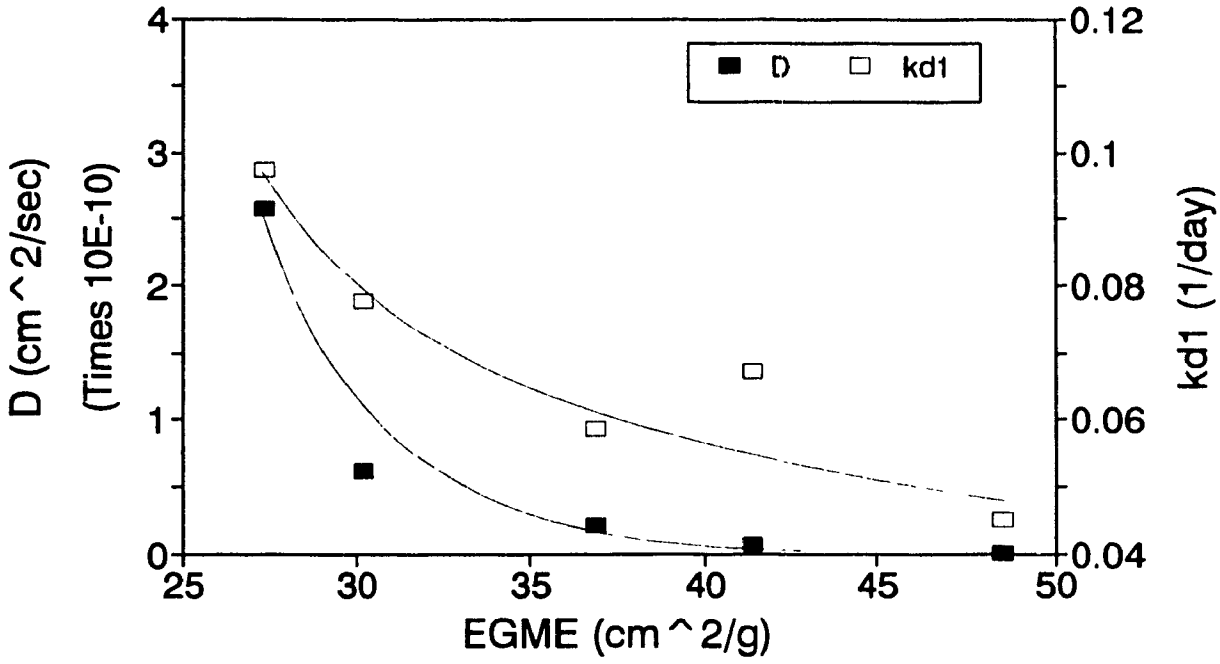

Fig. 4-4.9, Correlation of D and k_{d1} with Specific Surface Area

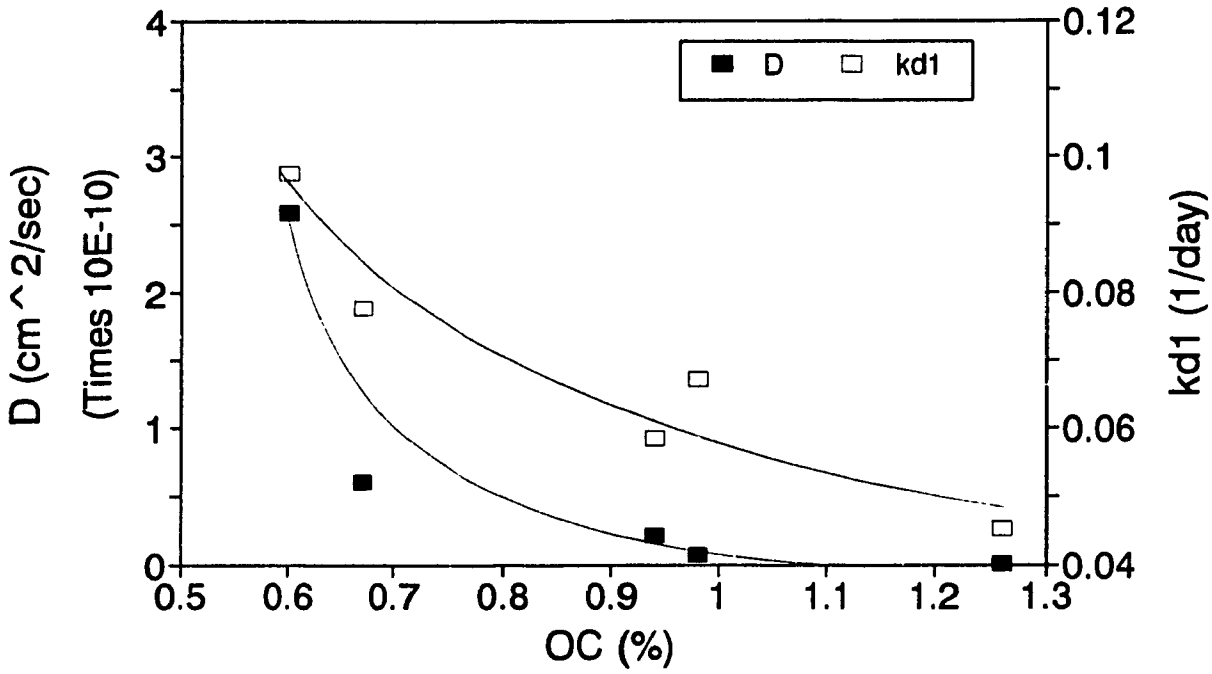

Fig. 4-4.10, Correlation of D and k_{dl} with Organic Carbon Contents

uncertainties in describing the relationship among the above parameters. The most important result of the present work is that surface areas and rates change relatively little with particle size. This shows that much of θ_c is not on the geometrically simple surface of a sphere. Labile atrazine is adsorbed in particle interiors.

It is useful to compare the present results with those published more recently. Wu and Gschwend (296) reported a trend that more rapid rates of uptake for smaller sieve sizes, so long as other properties of the grains are invariant. Ball and Roberts (12) observed significant mineralogical and sorptive differences from one size fraction to the next, and such differences tend to confound particle size effects. Irrespective of this, however, the study still reported dramatic increases in uptake rates as the result of particle pulverization, being 40 to 80 times higher than rate constants obtained with unaltered solids. An explanation for this is that the diffusive length scale (l) has been reduced by the pulverization.

In order to elucidate the non-consistency of the uptake rates for various soil fractions as seen among the above results and those determined here, one must consider the conceptual basis, and the experimental methodology. Both the Wu and Gschwend and the Ball and Roberts studies invoked the spherical solutions of Fick's diffusion law to treat the uptake processes as a single diffusive phenomenon. Their experimental methods were unable to distinguish uptake by surface adsorption from uptake by intraparticle diffusion. In contrast, the two stage model describes the uptake as a relatively fast labile sorption (the first stage) and a slower retarded intraparticle diffusion (the second stage). The on-line microfiltration-HPLC technique can provide the simultaneous speciation analyses for

atrazine as solution, labile sorbed and intraparticle trapped phases. As noted earlier, the pseudo first-order sorption rate constant (k_{s1}) increases with decreasing particle size, as the results of increasing organic matter and exposed surface area with the fine fractions. Although k_{s1} values are unavailable in their work, decreasing equilibration times with pulverization have been observed (12,296). As to the diffusive parameters (k_{d1} and D), their results (D_a/a^2 and D_{eff}) should be viewed as integrative results of the two uptake stages.

4-5. SUMMARY

The experimental results provided in this chapter were intended to account for particle size effects in atrazine uptake by soil GB 843 fractions, in which the main points are:

(1). Measurements of specific surface area, organic carbon content, and labile sorption capacity have shown relatively small changes with the soil size fractions. The parameters all varied inversely with particle size, and shown mass-weighted averages.

(2). The labile sorption process as the first and fast stage of the overall sorption processes has been demonstrated to have a definite capacity (θ_c) for each fraction, being greatest for the smallest grains. The observed rate constant (k_{s1}) for the finest fraction (#5) differed from the coarsest (#1) by a factor of ~ 4. Both θ_c and k_{s1} have been shown to be linearly correlated to surface area and organic carbon content, and these might be the important factors in the labile sorption process. However, a factor of 4 is not a large change. This emphasizes that labile sites are not all on geometrically simple spherical

surfaces which should increase as l^2.

(3). The intraparticle diffusion characterized by the effective diffusion coefficient (D) and rate constant (k_{dl}) exhibited a more complex behavior, as indicated from the fact that both D and k_{dl} decreased with decreasing particle size, but in a nonlinear fashion. This trend is opposite to what might be expected on the basis of surface area, and especially to what had been observed in the labile sorption process. Therefore, the most likely explanation for this might emphasize the variation of organic matter distributions over the soil fractions. In addition, variations of some physically-based contributions such as microporous texture may be important.

(4). Nonetheless, the very slow rates of intraparticle uptake (D values being at $\sim 10^{-11}$ cm^2 s^{-1} magnitude and k_{dl} being 8 to 10 times lower than k_{sl} values) suggested that the kinetics of the overall sorption processes were limited by diffusion to nonlabile sites. This is particularly true for the finer fractions.

(5). The important point is that the measured surface area (Table 4-3.5) is *only* weakly dependent upon particle size (l). If the particles were spheres, surface areas would increase as l^2. Since most parameters vary slowly as l increases, it is evident that surface area is determined as an interior of gel-like phases, and relates more closely to mass than to "size". This means that all particles are very similar internally. Perhaps they are nearly "self-similar" and follow fractal geometry.

In a word, the effort to explore particle size effects in atrazine uptake has received little attention to date. Further investigations with a properly designed experimental setup would be very useful.

CHAPTER 5

THE EFFECT OF TEMPERATURE ON ATRAZINE UPTAKE

5-1. INTRODUCTION

Temperature is one of the important climatic factors in determining soil-pesticide relationships. As well, the study of temperature effects on interactions may lead to an understanding of the nature and mechanism of pesticide sorption, and give information pertinent to predicting pesticide transport and significance in the soil and groundwater environments (298). Temperature dependence studies give activation energies for kinetic processes, which can be used to distinguish physisorption from chemisorption. This information is of particular interest in the modelling of contaminant fate and effect.

The effect of temperature on the adsorption process has been investigated by a number of authors during the last 2 or 3 decades. But apparently, there has been a lack of sufficient attention being given to this topic in recent years. Earlier work provided a broad range of practical examples of soil/pesticide systems. Most of these, unfortunately, dealt only with the total amount of pesticide sorbed or the distribution coefficient (K_d). In particular, little is known about the effect of temperature on the kinetic parameters of sorption processes which usually comprise surface adsorption and intraparticle diffusion,

as described in the earlier chapters. Also, there exist some ambiguous or contradictory results as described below.

With respect to adsorption capacity, Weber et al. (286) found temperature had no effect on the total amount of diquat and paraquat adsorbed by montmorillonite, but it did have a substantial effect on the quantity of prometone adsorbed. Similarly, McGlamery and Slife (187) found the adsorption of atrazine by Drummer clay loam soil was affected only slightly by temperature. In contrast, the temperature effect on the adsorption of atrazine by humic acid was quite marked. Adsorption increased as the temperature increased being nearly twice as great at 40 °C as at 0.5 °C. Harris and Warren (118), in studying the temperature effect on the adsorption of various herbicides, found that an inverse temperature-adsorption relationship did not hold in all cases. Adsorption of herbicides such as simazine, atrazine, monuron, 2,4-D, and amiben by bentonite was much greater at 0 °C than at 50 °C. But the adsorption by a muck soil was approximately the same at the both temperatures. The negligible effect of temperature was explained on the basis of an ion exchange mechanism. These results are similar to those of Stark (263) for the adsorption of chloropicrin by soil. Talbert and Fletchall (272) confirmed the importance of organic matter, temperature and pH in the adsorption process. They indicated that the adsorption of atrazine and simazine by Marshall silty clay loam shown a reversible temperature dependence, and apparently had a linear decrease of distribution coefficient (K_d) with increasing temperature. A similar inverse relationship has been observed by Liu et al. (174) in studying the adsorption of ametryne and diuron by soils, by Peck et al. (220) in studying the adsorption of diuron by sediments, by Yaron and

Saltzman (298), and by Kishk et al. (155) in studying the adsorption of parathion and methyl parathion by soils and clays, etc. Most of these studies relate to the temperature dependence of K_d or the stoichiometry. Little energetic information is extractable.

For each step or stage of the sorption processes described in Chapter 3, the temperature dependence of kinetic rate constants and the temperature dependence of equilibrium constants should not be confused with each other. As stated in Chapter 1, sorption processes can be driven by a variety of forces and/or mechanisms (208) that affect the relative bonding (ΔH°) of the sorbate and solvent. In the case of paraquat and diquat (272), both are divalent cations. The consequence of this is that montmorillonite takes them up from solution by cation exchange on labile sites with little or no activation energy barrier (ΔE_a), so that the temperature dependence of the kinetics is small. And also, the equilibrium in this case would show $\Delta H^\circ \approx 0$, or depend on the partial molal enthalpy of ions exchanged. This is in contrast to the uptake of uncharged molecules, which might have both specific interactions and traps, and where physical sorption or chemical sorption can be specified, depending on the energy levels involved (288). Under such cases, temperature dependence to some extent might be observed. In a recent study, Wu and Gschwend (296) indicated that the temperature could potentially affect the sorption rates of four chlorobenzene congeners by sediments and soils. Steinberg et al. (264) examined the desorption kinetics of EDB from contaminated field soils and found that the release was highly temperature dependent. When modeled as a first-order reaction, the temperature dependence yielded an apparent activation enthalpy ΔH° of 66 kJ mol^{-1}. More recently, Santana-Casiano and Gonzalez-Davila (245), in studying the

sorption and desorption of lindane by chitin in seawater based on a two-component model, found that the reversible component was not affected by temperature while the nonlabile component was affected, and the retarded diffusion velocity of lindane increased at higher temperatures.

The study undertaken in this chapter is designed to determining the effect of temperature on the equilibrium and kinetics of atrazine uptake by the mineral soil GB 843, in terms of labile sorption and nonlabile intraparticle diffusion, using the experimental method as described in Chapter 3. The results derived by this study are critical toward an appropriate modeling of atrazize movement on soil columns with a newly established pesticide transport model, PESTFADE (61,171), but the immediate issue will be the insight into sorption mechanisms.

5-2. EXPERIMENTAL

To study the effect of temperature on adsorption, a series of batch experiments with bulk soil were carried out at 5.0, 10.0, 15.0, 25.0, and 35.0 ($\pm$0.2) °C, controlled by a thermostatted circulating bath (Lauda K-2/R, Brinkmann Instruments). The detailed description of the equipment, reagents and materials, as well as the kinetic procedures can be found in Chapter 3 and references (93,94).

All the atrazine concentrations used in these experiments were 8 to 12 x 10^{-6} M, which was far below its solubility ($\sim 1.5 \times 10^{-4}$ M). Therefore, it was not necessary to consider the solubility correction arising from temperature variation (298).

The experimental parameters for the temperature effect on kinetic runs are shown in Table 5-2.1.

5-3. RESULTS AND DISCUSSION

(1). *Labile sorption*

As discussed in Chapter 3, the main conceptual equations describing the labile surface uptake of atrazine, including both the equilibrium aspect and the kinetic aspect, are as follows:

$$\bar{K}_l = k_{b1}/k_{s2} = \theta_L/\theta_o M_{AT} \qquad (4\text{-}4.3)$$

$$\theta_c = \theta_o + \theta_L \qquad (3\text{-}2.7)$$

$$X_l = \theta_L/\theta_c \qquad (3\text{-}2.8)$$

$$-dM_{AT}/dt = (W/V)d\theta_l/dt$$

$$= k_{b1}(W/V)\theta_o M_{AT} - k_{s2}(W/V)\theta_L \qquad (3\text{-}2.2)$$

$$-dM_{AT}/dt = (W/V)d\theta_L/dt = k_{s1}M_{AT} \qquad (3\text{-}2.19)$$

$$k_{s1} = k_{b1}(W/V)\theta_o \qquad (3\text{-}2.23)$$

where $\bar{K}_l$ is the weighted average equilibrium function, k_{b1} is the second-order rate constant for the adsorption reaction, k_{s2} is the first-order rate constant for the desorption reaction, M_{AT} is the concentration of solution phase atrazine, θ_c, θ_L and θ_o represent the labile sorption capacity, the concentrations of sorption sites occupied and unoccupied by atrazine, respectively, X_l is the mole fraction of occupied sorption sites, and k_{s1} is the pseudo first-order rate constant. Eq. 3-2.19 is an approximate expression of eq. 3-2.2 at

Table 5-2.1, Experimental Conditions for Temperature Effect Kinetics*

Exp. no.	Temp. (°C)	Soil wt. (g)	Slur.vol. (mL)	Init.AT (10^{-6} molesL^{-1})	Exp.duration (day)	Data points
27	5	0.5027	24.86	8.03	18.76	51
28	5	0.5035	25.06	7.95	19.70	51
GT	10	0.5038	24.97	8.00	80.07	107
9	15	0.5030	24.93	8.01	18.72	67
12	15	0.5019	24.94	8.01	18.76	54
15	15	0.5054	24.99	8.01	18.55	55
8	35	0.5036	24.84	8.02	19.81	59
13	35	0.5043	25.01	12.0	18.73	53
16	35	0.5029	24.99	12.0	18.58	55
17	35	0.5008	25.01	7.96	18.70	52
18	35	0.5030	24.95	7.95	18.72	52

* Excluding 25 °C experiments shown in Chapter 3.

the very beginning of a sorption reaction (93,94,97).

Labile Surface Sorption Maximum. Figs. 5-3.1 to 5-3.3 show atrazine species distribution with time in terms of solution, labile sorbed, and intraparticle diffused phases at 5, 15, and 35 °C, respectively. It is evident that the labile sorbed atrazine is first going up, then dropping down slightly with the reaction time in all the cases, as expected. This produces a maximum, $d\theta_L/dt = 0$, in the labile sorption curve, which shifts to shorter times as temperature is increased (Table 5-3.1). A similar observation has been reported by Leenheer and Ahlrichs (167).

In the next sections, the effect of temperature on atrazine uptake will be discussed with respect to both the equilibrium aspect (e.g., the extent) and kinetic aspect (e.g., the rate).

Labile Sorbed Extent. It is commonly observed that adsorption is an exothermic process (155,220,245,296,298). Decreasing temperature might favor atrazine uptake. We can appraise this prediction qualitatively by comparing the values of θ_L at the point when $d\theta_l/dt = 0$ at various temperatures. The earlier occurrence of the point as temperature rises indicates that all rate constants increase with temperature, as they should. The slight increase in θ_l at the maximum at 5 °C compared to 35 °C, as shown in Table 5-3.1, is consistent with the above expectation.

Adsorption Rate. However, it is important to recognize that soil/pesticide systems in batch experiments or in the actual subsurface environment differ from a simplified sorbent/sorbate system. The micro-environment for adsorption in a batch experiment includes at least two phases (260,287): the surrounding solution (even being well stirred)

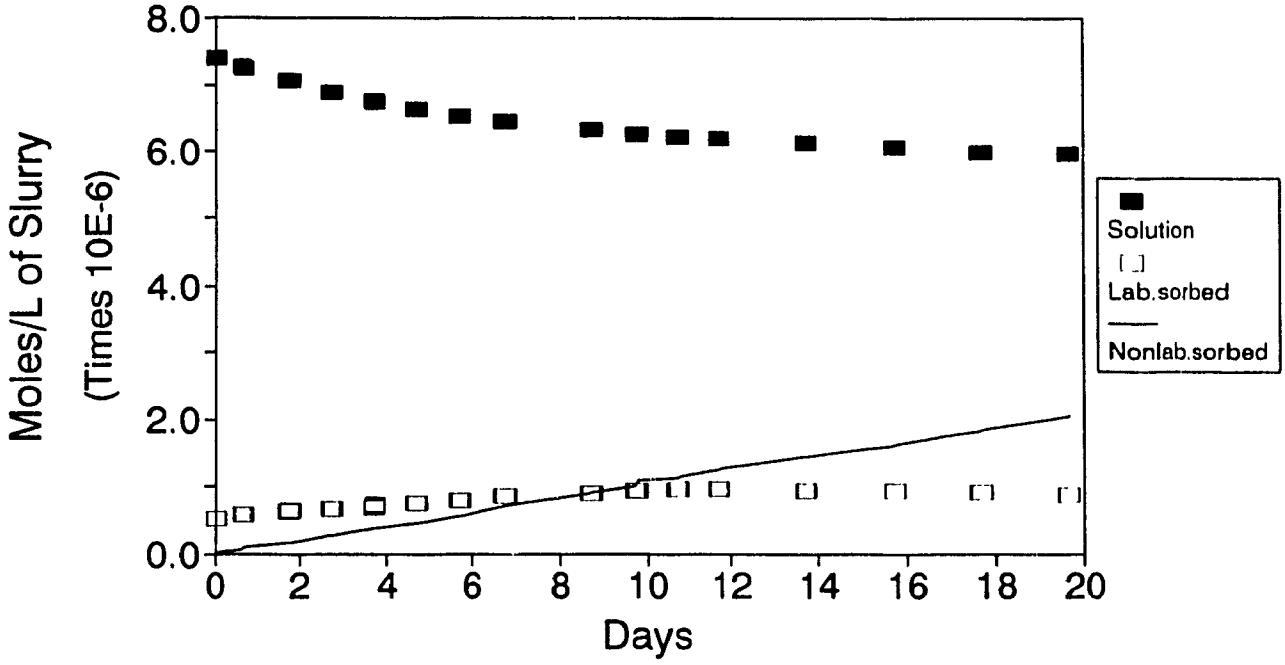

Fig. 5-3.1, Atrazine Species Distribution with Time (Fitted data at 5 °C)

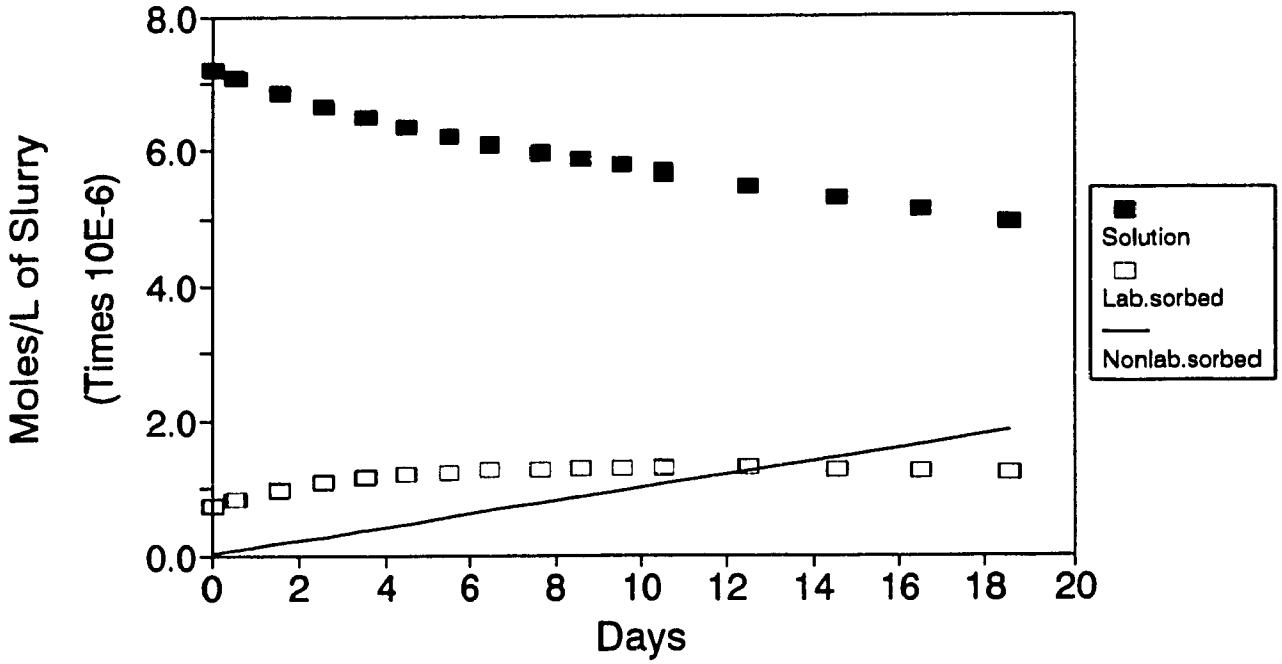

Fig. 5-3.2, Atrazine Species Distribution with Time (Fitted data at 15 °C)

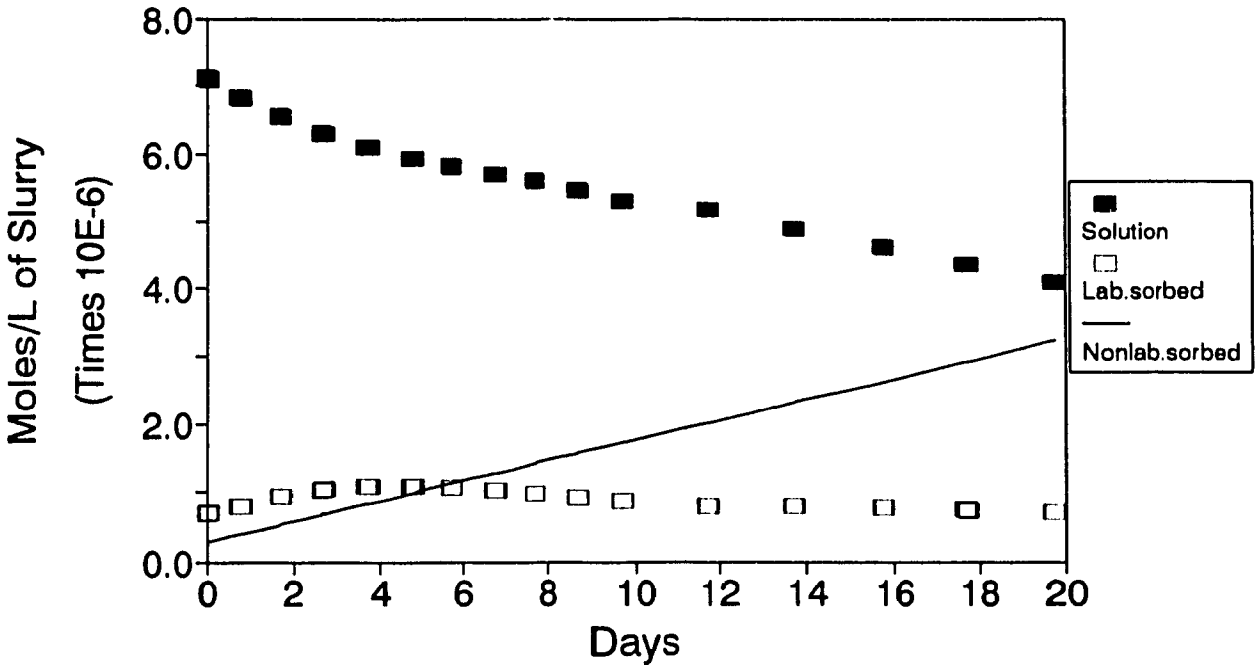

Fig. 5-3.3, Atrazine Species Distribution with Time (Fitted data at 35 °C)

Table 5-3.1, Labile Sorbed Atrazine at the Maximum of Sorption Curves

Exp. no.	Temp. (°C)	Labile sorbed (θ_L) (10^{-8} molesg^{-1})	Labile sorbed (θ_L) %*	Time at max.*** (day)
27	5	6.63	16.6	12.4
28	5	4.65	11.6	11.7
		(5.64)**	(14.1)	(12.1)
GT	10	5.60	14.0	15.0
9	15	4.58	11.5	8.7
12	15	6.32	15.8	12.6
15	15	6.35	15.9	10.5
		(5.75)	(14.4)	(10.6)
2	25	4.96	12.4	11.7
14	25	4.16	10.4	10.9
19	25	6.41	16.0	8.6
20	25	5.68	14.2	9.7
		(5.30)	(13.3)	(10.2)
8	35	4.33	10.8	4.7
13	35	7.64	12.7	10.6
16	35	8.04	13.4	4.6
17	35	5.06	12.6	5.7
18	35	4.58	11.5	7.7
		(4.66)	(11.6)	(5.7)

* % = (θ_L/Initial atrazine)x100.
** Average values.
*** i.e., $d\theta_L/dt = 0$.

and the soil particle surfaces. From a dynamic point of view, the adsorption process consists of mass transfer process (film diffusion and pore diffusion) and reaction process (chemisorption and/or physisorption) in sequence. On this basis, increasing temperature will promote mass transfer by the film diffusion in the overlying solution, and often favor specific binding on surfaces (96,187,245).

According to the kinetic differential equation (eq. 3-2.19) for labile sorption, the pseudo first-order rate constant (k_{s1}) is calculated by using the initial rate approximation method (Chapter 3). The results are shown in Table 5-3.2 and Fig. 5-3.4. It can be seen that k_{s1} increases with increasing temperature, averaged values being: 0.498, 0.549, 0.589, 0.831, and 1.24 (d^{-1}) at 5, 10, 15, 25, and 35 °C, respectively. The equilibrium surface sorbed amount of atrazine varies little, as has been seen earlier (Table 5-3.1). The reverse reaction must increase in rate similarly. A similar phenomenon has been observed by a number of authors in the earlier literature (118,155,167,173,174,187,220,272,286,298).

Detailed calculations of $\bar{K}_1$, K_d and X_1 reveal a similar lack of trends with temperature as they should (Table 5-3.2). Note, this work did not cover the effect of temperature on the sorption capacity (θ_c) which is assumed to be a constant value (0.397×10^{-6} moles g^{-1}) in all cases (93,94,97). But, this parameter could vary slightly as a function of temperature.

(2). *Intraparticle diffusion*

In the same manner as in Chapter 3, the following equations were used for describing atrazine uptake by the nonlabile intraparticle sorption in the temperature effect kinetics:

$$d\theta_D/dt = k_{d1}\theta_L - (V/W)R_{d2} \qquad (3\text{-}2.14)$$

$$d\theta_D/dt = k_{d1}\theta_L \qquad (3\text{-}2.15)$$

$$k_{d1} = Q(D/l^2) \qquad (4\text{-}4.4)$$

$$D = B(Al/\theta_L)^2 t^n \qquad (4\text{-}4.5)$$

Table 5-3.2, Results of Labile Surface Sorption for Temperature Effect Kinetics*

Exp. no.	Temp. (°C)	θ_L (10^{-8} moles g^{-1})	K_d (10^{-2} Lg^{-1})	$\overline{K}_l$ (10^4 M^{-1})	k_{sl} (d^{-1})	X_l
27	5	6.63	1.25	3.77	0.462±0.026	0.167
28	5	4.65	0.747	2.13	0.535±0.018	0.117
			(1.00±0.25)**	(2.95±0.82)	(0.498±0.036)	
GT	10	5.60	1.14	3.35	0.549±0.016	0.141
9	15	4.58	1.16	3.31	0.583±0.005	0.115
12	15	6.32	1.55	4.65	0.565±0.007	0.159
15	15	6.35	1.10	3.30	0.621±0.016	0.160
			(1.27±0.28)	(3.75±0.90)	(0.589±0.032)	
	25	(5.30)	(1.01±0.35)	(3.03±0.97)	(0.831±0.093)	(0.102)
8	35	4.33	0.799	2.26	1.12±0.05	0.109
13	35	7.64	1.51	4.70	1.19±0.01	0.193
16	35	8.04	1.10	3.47	1.40±0.03	0.202
17	35	5.06	1.17	3.38	1.32±0.08	0.128
18	35	4.58	0.977	2.78	1.17±0.08	0.115
			(1.11±0.40)	(3.32±1.38)	(1.24±0.17)	

* The labile sorption capacity (θ_c) = 0.397 x 10^{-6} moles g^{-1}.
** Average values.

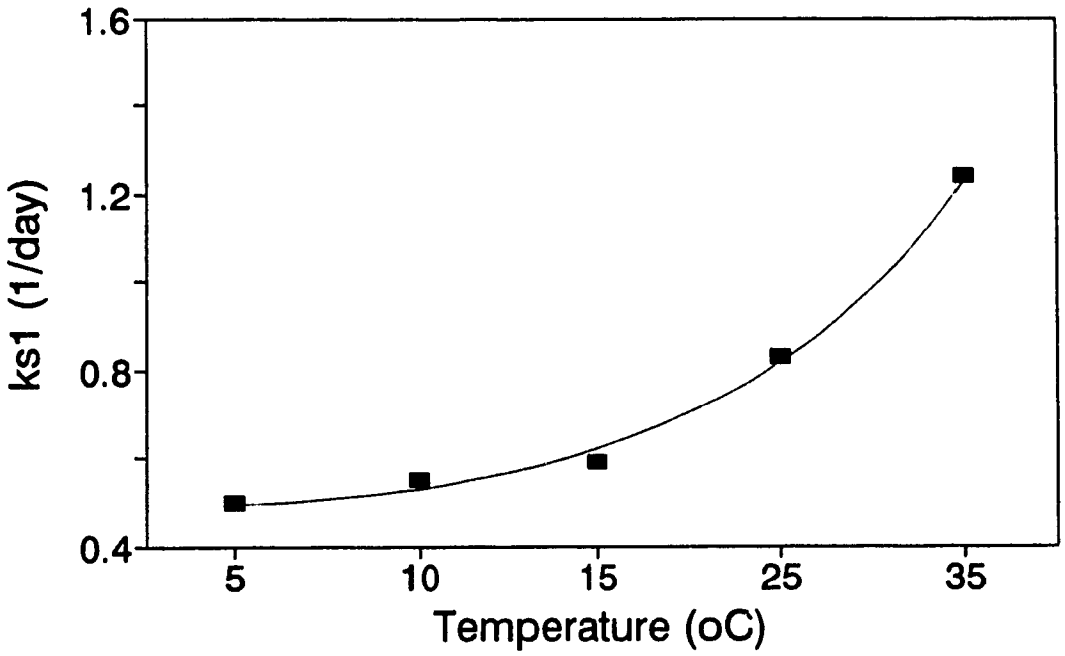

Fig. 5-3.4, k_{s1} as a Function of Temperature (Line graph)

where θ_{ll} is the amount of nonlabile atrazine, t is the time, k_{dl} is the first-order rate constant for diffusion, R_{d2} is the outward diffusion term, D is the effective diffusion coefficient, $A = 2(\theta_L/l)(D/\pi)^{1/2}$, B is a constant (0.7854), $n = 2Z - 1 = 0$ in this case, $Q = 86{,}400$ (s d^{-1}), l is the particle dimension (weighted average 0.955×10^{-2} cm) related to diffusion, and eq. 3-2.15 is an approximate expression of eq. 3-2.14 for early uptake.

Nonlabile Amount. As stated in Chapter 1, the MF-HPLC technique can track the distinction between labile sorbed atrazine and material balance loss throughout a whole kinetic experiment. The latter was calculated as the difference between total applied atrazine and slurry as shown in Figs. 5-3.1 to 5-3.3, which varies nearly linearly within the first 20 days. The nonlabile amount of atrazine calculated at the period corresponding to the maximum ($d\theta_L/dt = 0$) of sorption curves is tabulated in Table 5-3.3. Once again, no trend may be confirmed with confidence. However, an inverse correlation between the nonlabile amount and the temperature is hinted, since averages differ by a factor of ~ 1.8 between 35 °C and 5 °C. That is, the rates change simultaneously with temperature and ΔH^o is probably small. Fig. 5-3.5 shows the sorbed atrazine as a function of temperature, including the labile surface adsorbed (Table 5-3.1), nonlabile sorbed or intraparticle diffused (Table 5-3.3), and their sum. These results are consistent with those in the literature (118,155,167,173,174,187,220,245,272,286,298).

Diffusion Rate. In order to determine the effect of temperature on the kinetics of intraparticle diffusion, both the diffusion coefficient (D) and the first-order diffusion rate constant (k_{dl}) were calculated by using eqs. 4-4.4 and 4-4.5, respectively. The results are

Table 5-3.3, Nonlabile Sorbed Atrazine at the Maximum of Sorption Curves

Exp. no.	Temp. (°C)	Nonlabile AT (θ_D) (10^{-8} molesg^{-1})	Nonlabile AT (θ_D) %*	Time at max.*** (day)
27	5	8.15	20.4	12.4
28	5	6.89	17.2	11.7
		(7.52)**	(18.8)	(12.1)
GT	10	9.39	23.5	15.0
9	15	6.30	15.7	8.7
12	15	10.9	27.2	12.6
15	15	5.22	13.0	10.5
		(7.46)	(18.7)	(10.6)
2	25	5.18	12.9	11.7
14	25	6.07	15.2	10.9
19	25	5.21	13.0	8.6
20	25	5.62	14.1	9.7
		(5.52)	(13.8)	(10.2)
8	35	3.84	9.6	4.7
13	35	16.5	27.6	10.6
16	35	6.66	11.1	4.6
17	35	4.24	10.6	5.7
18	35	6.13	15.3	7.7
		(4.74)	(11.8)	(5.7)

* % = (θ_D/Initial atrazine)x100.
** Average values.
*** i.e., $d\theta_L/dt = 0$.

shown in Table 5-3.4 and Fig. 5-3.6. It can be seen that temperature has a considerable effect. Both the diffusion coefficient D and the rate constant k_{dl} increase as the temperature is increased from 5 °C to 35 °C, differing by a factor of up to 40.

Based on a sorption kinetic study of hydrophobic organic compounds to natural sediments and soils using a radial diffusion model, Wu and Gschwend (296) reported a

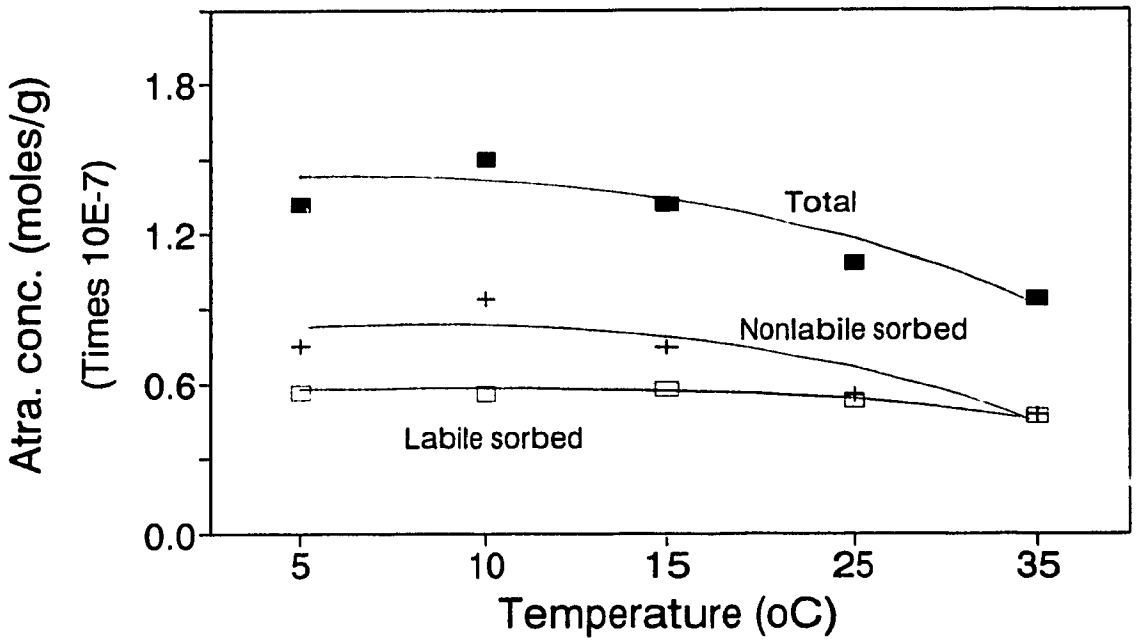

Fig. 5-3.5, Sorbed Atrazine as a function of Temperature (Symbols=Exp., Lines=Fit.)

Table 5-3.4, Results of Intraparticle Diffusion for Temperature Effect Kinetics

Exp. no.	Temp. (°C)	θ_L (10^{-8} molesg^{-1})	D (cm^2s^{-1})	k_{dl} (d^{-1})
27	5	6.63	7.32E-12	6.94E-3
28	5	4.65	1.79E-11	1.69E-2
		(5.64)*	(1.26±0.53E-11)	(1.19±0.50E-2)
GT	10	5.60	1.87E-11	1.77E-2
9	15	4.58	3.18E-11	3.01E-2
12	15	6.32	6.15E-11	5.83E-2
15	15	6.35	7.80E-12	7.39E-3
		(5.75)	(3.37±2.78E-11)	(3.19±2.64E-2)
	25	(5.30)	(1.05E-10)	(9.95E-2)
8	35	4.33	3.40E-10	3.22E-1
13	35	7.64	7.28E-10	6.89E-1
16	35	8.04	5.83E-10	5.52E-1
17	35	5.06	4.55E-10	4.31E-1
18	35	4.58	5.95E-10	5.64E-1
		(4.66)	(5.40±2.00E-10)	(5.12±1.90E-1)

* Average values.

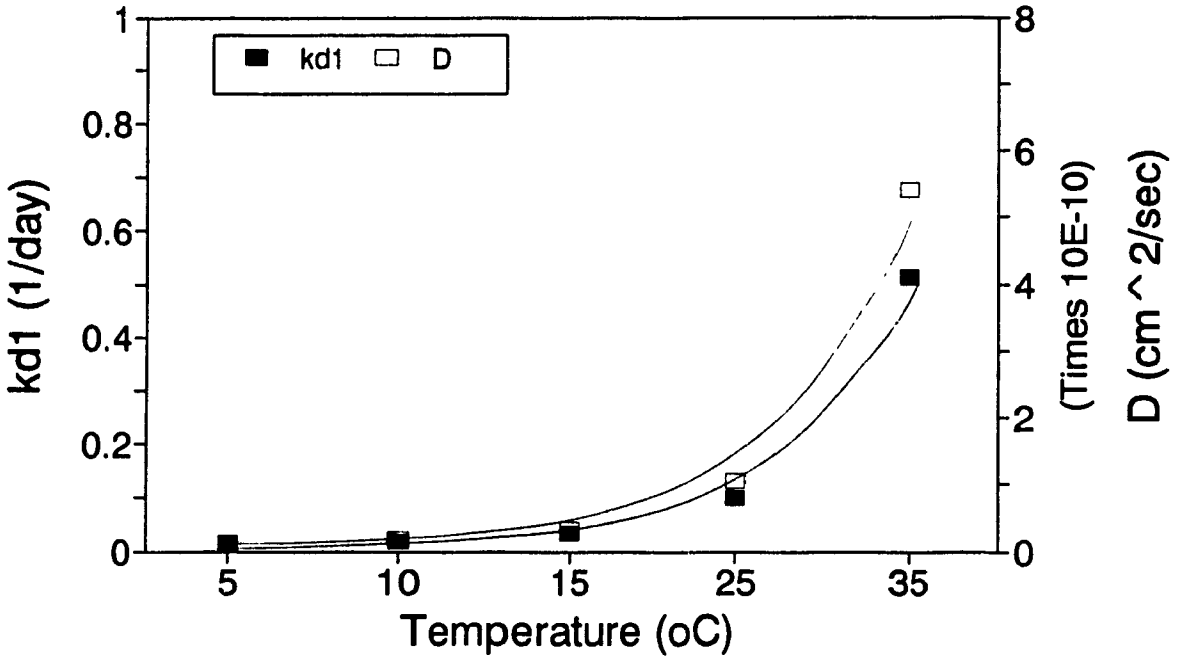

Fig. 5-3.6, D and k_{dl} as a Function of Temperature (Line graph)

similar correlation between the diffusion coefficient (D_{eff}) and temperature. It is worth noting that the apparatus used for their kinetic experiments did not allow individual monitoring of sorbed portions. As indicated by Sparks (259), these parameters are strongly dependent on the kinetic technique employed. In fact, increasing temperature will promote the adsorption on surfaces (k_{s1}) as have been seen earlier, and also favor the inward intraparticle diffusion as the result of both increasing the pore fluid diffusivity and decreasing the attractive forces between sorbing molecules and specific surface sites (245). In particular, the parallel correlation between the diffusion rates (D and k_{d1}) and the temperature may be likely ascribed to the specific binding of atrazine with organic matter, which is usually favorable to higher temperature (187). As will be seen later, in contrast to the surface adsorption, atrazine uptake by the intraparticle diffusion is more dominately associated with chemisorption.

(3). *Arrhenius and van't Hoff treatments*

To gain an insight into the mechanism related to above phenomena, Arrhenius and van't Hoff equations have been used to treat the equilibrium and kinetic data observed in the temperature effect experiments.

The van't Hoff equation (204,259) relates the equilibrium constant $\bar{K}_1$ to absolute temperature T (°K) as:

$$d(Ln\bar{K}_1)/dT = \Delta H^o/RT^2 \qquad (5\text{-}3.1)$$

The integrated form is:

$$Ln\bar{K}_1 = LnC - \Delta H^o/RT \qquad (5\text{-}3.2)$$

where ΔH^o is the standard enthalpy, LnC is a constant, and R is the universal gas constant. A plot of $Ln\bar{K}_1$ versus 1/T would give a straight line with a slope equal to $-\Delta H^o/R$ and an intercept LnC.

A similar treatment by the Arrhenius equation (205,259) for the rate constants (k_{s1}, k_{d1}) is:

$$k = A \exp(-E_a/RT) \qquad (5\text{-}3.3)$$

$$Lnk = LnA - E_a/RT \qquad (5\text{-}3.4)$$

where A is the frequency factor, E_a is the energy of activation, and k represents the rate constant k_{s1} or k_{d1}. The plot of Lnk_{s1} or Lnk_{d1} against 1/T should result in a linear relationship giving a slope equal to $-E_a/R$ for the labile surface adsorption or the intraparticle diffusion, respectively.

The results for these thermodynamic parameters are shown in Table 5-3.5 and Figs. 5-3.7 to 5-3.9. As seen above, the fitted line for $\bar{K}_1$ gives a near zero value of ΔH^o (0.67 ± 3.2 kJ mol^{-1}), and the fitted data for activation energies from k_{s1} and k_{d1} are 22 ± 2.4 and 89 ± 7.3 kJ mol^{-1}, respectively.

A number of authors have studied sorption mechanisms by evaluating these thermodynamic parameters, and relatively small changes in enthalpy for the surface adsorption as compared to larger intraparticle diffusion activation energies have been reported in the literature (124,226). It is generally known that the energy of activation E_a is a measure of the energy barrier that must be overcome by reacting molecules (84). And, low E_a values (<42 kJ mol^{-1}) usually indicate diffusion-controlled processes (typically, 17-21 kJ mol^{-1} for film diffusion and 21-42 kJ mol^{-1} for particle diffusion),

Table 5-3.5, Temperature Dependence of $\bar{K}_1$, k_{s1}, and k_{d1} (van't Hoff and Arrhenius treatments)

Temp. (°K)	$\bar{K}_1$(Avg) (10^4 M^{-1})	$Ln(\bar{K}_1)_{exp}$	$Ln(\bar{K}_1)_{fit}$	k_{s1}(Avg) (d^{-1})	$Ln(k_{s1})_{exp}$	$Ln(k_{s1})_{fit}$	D(Avg) (10^{-11} cm^2s^{-1})	$Ln(D/l^2)_{exp}$	$Ln(D/l^2)_{fit}$
278.16	2.95	10.29	10.38	0.498	-0.697	-0.768	1.26	-15.79	-16.01
283.16	3.35	10.42	10.38	0.549	-0.600	-0.602	1.87	-15.40	-15.33
288.16	3.75	10.53	10.39	0.589	-0.529	-0.441	3.37	-14.81	-14.68
298.16	3.03	10.32	10.40	0.831	-0.185	-0.136	10.5	-13.67	-13.43
308.16	3.32	10.41	10.41	1.24	0.215	0.150	54.0	-12.04	-12.27

	Const.	Std.err.	Coeffi.	Std.err.	R^2
ΔH° by $\bar{K}_1$ (0.673 ± 3.21 kJ mol^{-1}):	10.67	0.11	-80.94	385.99	0.014
E_a by k_{s1} (21.8 ± 2.39 kJ mol^{-1}):	8.66	0.08	-2622.11	288.00	0.965
E_a by k_{d1} (89.0 ± 7.30 kJ mol^{-1}):	22.48	0.25	-10705.64	877.49	0.980

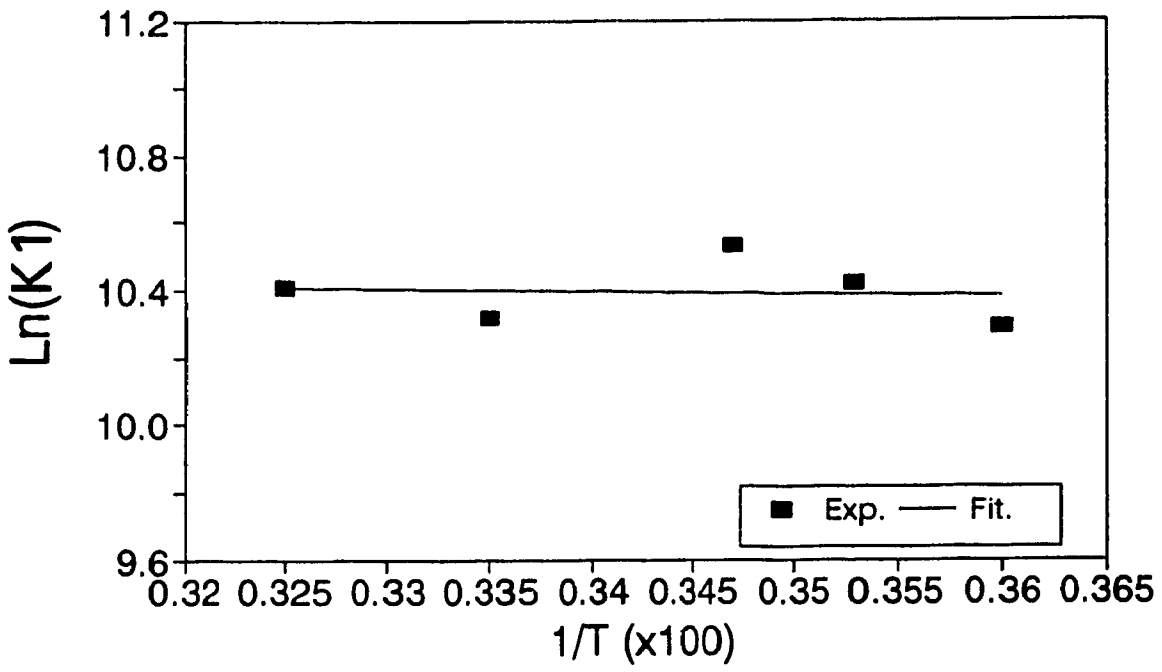

Fig. 5-3.7. $\bar{K}_1$ Temperature Dependence (van't Hoff plot)

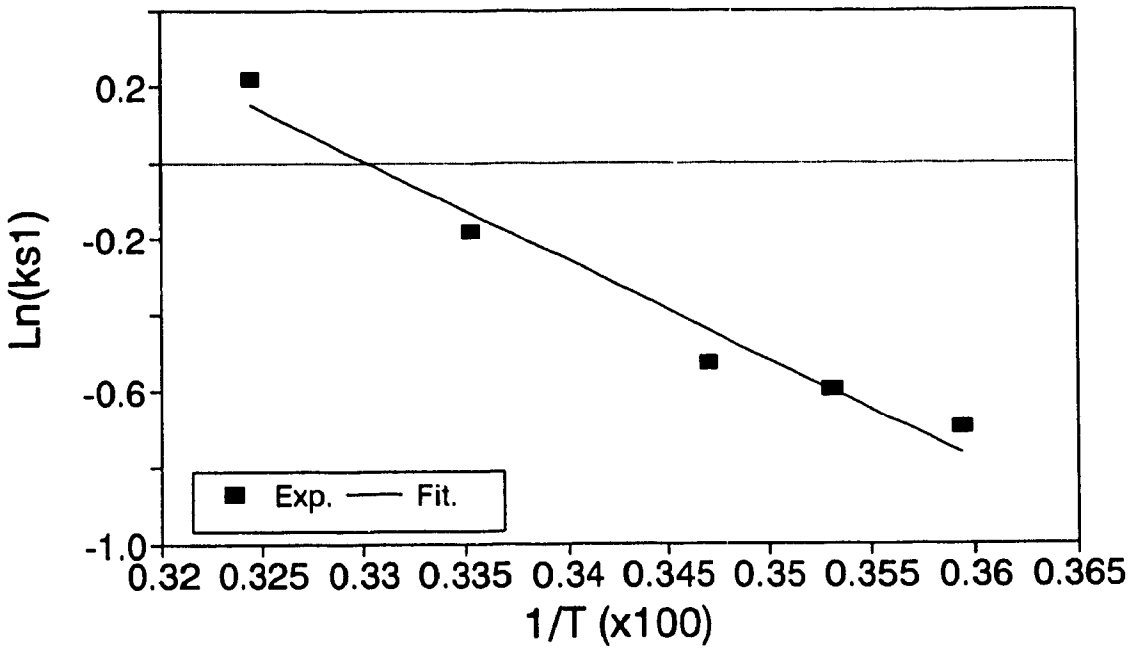

Fig. 5-3.8, k_{s1} Temperature Dependence (Arrhenius plot)

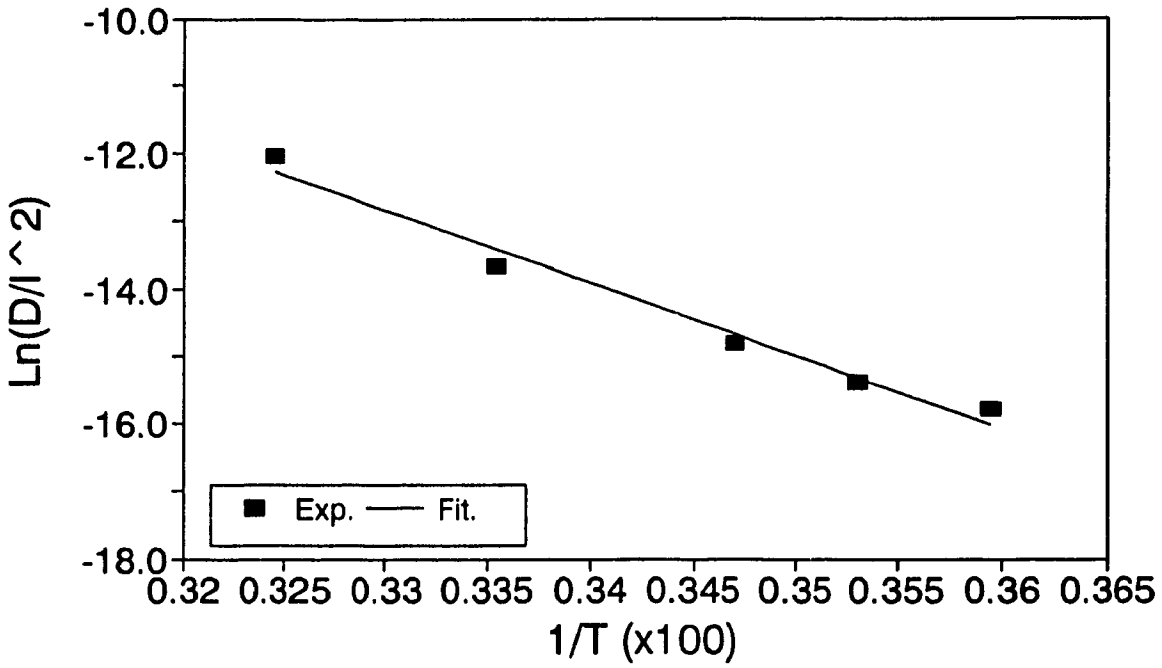

Fig. 5-3.9, k_{dl} Temperature Dependence (Arrhenius plot)

whereas higher E_a values suggest chemical reaction barriers (26,226,235,257,258,261). For example, in a kinetic study of the adsorption/desorption processes of three biologically active organic compounds, 2,4-D, isocil, and bromacil, from aqueous solution onto illite clay and silica gel surfaces, Lindstrom et al. (173) reported a low activation enthalpy ($\Delta H^{\ddagger}$), ranging from -2.3 to 31 kJ mol^{-1} for adsorption process and -2.3 to 61 kJ mol^{-1} for desorption process, and also an activation energy (ΔE_a) with similar magnitudes. They indicated that the low magnitude of $\Delta H^{\ddagger}$ or ΔE_a ruled out the possibility of chemisorption, and the most probable mechanism of the adsorption was of the physical type. In addition, Leenheer and Ahlrichs (167) calculated the differential heat of adsorption by using the van't Hoff equation for the adsorption of carbaryl and parathion upon soil organic matter surfaces conducted at 5, 25, and 40 °C. The low heats of adsorption (about 8.3 kJ mol^{-1}) are as one would have expected for physical adsorption rather than chemisorption (129). They further pointed out that the initial (within 10 min) pesticide adsorption rates appear to be controlled by solute transfer through the water film surrounding the soil particles to the surfaces, even in vigorously stirred suspensions. After about 10 min, however, labile intraparticle transport is the dominant rate-limiting process. Similar observations have been reported by Haque et al. (114), Khan (150), Bloom and Erich (21), and others (129). These studies do not deal with the nonlabile part.

Small exothermic and even endothermic enthalpies (ΔH°) have been also observed in the sorption of nonpolar organics (47,123). Hassett et al. (122) indicated that the small enthalpy changes can be explained as being due to the lack of strong bond formation

between the sorbing species and the sorbent. Nonpolar organics form weak van der Waals bonds with the solvent (water) as well as with the sorbent (humus) and, hence, the difference between the magnitude of these bonds (ΔH°) is small upon sorption. In analogy to this, some type of weak bond formation could be expected to interpret the low enthalpy change (ΔH°) and activation energy (E_a) in the labile adsorption stage for the case of polar atrazine uptake by soil GB 843.

5-4. SUMMARY

Most earlier studies of temperature effects on pesticide uptake dealt only with the effects on the total adsorbed amount or on the distribution coefficient (K_d). A few recent reports described the adsorption process with a two-domain model, including reversible and retarded processes. However, more detailed kinetic studies of the effect of temperature have been lacking.

The main points observed in this chapter for the correlation of atrazine uptake by soil GB 843 with temperature ranging from 5 °C to 35 °C are:

(1). The sorption equilibrium parameters, such as $\bar{K}_1$, K_d and X_1, as well as the total sorbed amount defined as a sum of the surface adsorbed and the intraparticle diffused atrazine reveal no statistically significant temperature dependence. In contrast, a trend has been noted for the time to approach the labile sorption maximum, decreasing with increasing temperature.

(2). As expected, temperature has a rather significant effect on the rate constants. The

k_{s1}, D and k_{d1} increased with temperature by factors of 2.5 up to 40, when comparing the values at 35 °C with those at 5 °C.

(3). The resulting thermodynamic parameters ΔH^{o} and E_a obtained by using van't Hoff and Arrhenius equations to treat the correlations of $\bar{K}_1$, k_{s1} and k_{d1} as a function of temperature suggest that the labile surface uptake of atrazine may only involve weak physisorption ($\Delta H^{o} \approx 0$ kJ mol^{-1}), and is dominated by film diffusion in the overlying solution and pore fluid, or similar process (E_a = 22 kJ mol^{-1}), while the nonlabile intraparticle diffusion of atrazine is mainly controlled by a chemisorption process (E_a = 89 kJ mol^{-1}).

Much attention to this topic is required for in-depth exploration of the impact of temperature on the physicochemical behavior of pesticide uptake in future research.

CHAPTER 6

APPLICATION OF THE TWO STAGE MECHANISM IN A HYDROLOGY MODEL: PESTFADE

6-1. INTRODUCTION

Nonpoint source groundwater pollution by pesticides is now recognised as a problem in many areas of North America. Significant ground water pollution is thought to be occurring on intensively farmed lands where pesticides are being used in increasing amounts.

The herbicide atrazine (2-chloro-4-ethylamino-6-isopropylamino-s-triazine) is of interest in Canada. It has been detected in 85% of the streams and rivers in southwestern Ontario (81). Junk et al. (140) found atrazine concentrations as high as 88 $\mu g\ L^{-1}$ in groundwater under a corn field. About 50% of the 351 wells in southwestern Ontario were found to contain atrazine residues. Herbicides have also been detected in tile drainage water. Gold and Loudon (107) measured concentrations of atrazine ranging from 80 to 170 $\mu g\ L^{-1}$ in drain outflows caused by a storm 4 days after planting and application.

Computer models can be used as a tool for predicting fate and behavior in the

environment on a site specific basis. One option which has the capability to evaluate the fate and complex behavior of chemicals in any geohydrological environment, and yet is less burdensome compared to actual field experiments, is the development of predictive mathematical models. They are being used to assess water quality impacts as well as to develop management strategies which can reduce environmental pollution from chemicals. Popular models include CREAMS (156), PRZM (39,40), GLEAMS (168), LEACHM (280), VULPEST (279), RUSTIC (72), ARM (75) and PESTFADE (59-62); to name a few.

PESTFADE (PESTicide Fate And Dynamics in the Environment) (59,60,62) is a one-dimensional transient mathematical model that can simulate simultaneous movement of water and pesticides in the unsaturated and saturated zones of soil, as affected by runoff, leaching, dispersion, diffusion, volatilization, plant uptake, chemical and microbial degradation, sorption/desorption, and macropore flow. The model incorporates our approaches to equilibria and kinetics for sorption/desorption of pesticides (90,93), along with the traditional soil-water partitioning concepts, such as one-site type equilibrium sorption and two-site type equilibrium/nonequilibrium sorption. The model is very versatile, and it can be used under both humid and arid or semi-arid conditions. Furthermore, the model can be used to evaluate the role of different water table management systems, such as subsurface drainage, controlled drainage, or subirrigation systems, on the fate and transport of agricultural pesticides. It can also be used to determine the best management practices (BMPs) for a farm by evaluating the effects of certain management practices, such as different types of tillage systems, cropping

practices, and surface residues, etc., on pesticide movement.

Although the model is physically based and the initial-boundary value problem overseeing pesticide fate and transport has been solved by well-known and proven mathematical methods, and also the various components of the model have been checked against published analytical solutions, the model has undergone only limited field testing (59-61). In addition, some exploratory work which has been done in the field tests on the introduction of our kinetic sorption mechanism into atrazine trasport modeling has indicated that this integration of chemistry, soil science, and hydrology shows promise (59-61). It was therefore decided that the objective of this work would be to validate the model under controlled laboratory conditions, testing the improvements following from introduction of the two stage analysis. A soil column study was consequently undertaken for this purpose. This chapter presents soil column experiments, the modified PESTFADE model, the two stage equilibrium/kinetic mechanism with parameters used as inputs, and model simulation results. As a comparison, a conventional adsorption approach has also been included.

6-2. EQUIPMENT AND SOIL COLUMN EXPERIMENTS

Spatial variability in field measurements on pesticide fate and transport usually precludes any detailed model verification. Therefore, to validate the modified PESTFADE model, a column study was undertaken in the laboratory. Three intact soil columns, 19.1 cm internal diameter and 21, 63 and 65 cm long, were extracted from a

clay loam soil at the Central Experimental Farm in Ottawa. The columns were instrumented for making soil moisture content and suction water measurements at six depths at 10 cm increments from the surface. At each depth, there was a set of two TDR (Time Domain Reflectometry) probes, tensionmeters, and suction samplers to obtain representative measurements for each depth. In addition, the leachate was collected at the bottom of each core. Tables 6-2.1 and 6-2.2 show the main operating conditions for the column studies and the basic properties of soil cores used in this work.

Three runs were made on each column, each with a different set of hydraulic conditions, while maintaining a steady flow of water through the columns. For example, one run was made by keeping the soil column at saturated hydraulic conductivity (108 cm d^{-1}), the other run at one-half the conductivity, and the third run at one-fiftieth of the conductivity. Each run lasted, on an average, about a week to three months. Radio-labelled atrazine (^{14}C) was initially applied (sprayed in methanol) at normal application rates along with KCl. The chloride was used as a conservative tracer to determine some of the physicochemical properties of the soil columns. After each run, the columns were flushed with water and were checked to make sure that there was no significant amount of residue left from the last run. The detailed procedure can be found in a previous work (256).

All the simulations have been conducted on an IBM PS/2 386 on the Computer Network of Macdonald Campus of McGill University, or a Digital VAX-2 at the Computer Centre of the Computer Science Department of Concordia University.

Table 6-2.1, Main Operating Conditions for the Soil Columns

Run	v_o^*	Atrazine(mg)	KCl(g)
C1R1	54	9.52	5.1
C1R2	108	9.52	7.65
C1R3	2.2	9.52	5.1
C2R1	2.2	9.56	5.1
C2R2	108	9.56	5.1
C2R3	54	9.56	7.65
C3R1	2.2	9.52	5.1

* v_o = Hydraulic conductivity or Darcy flux in cm d^{-1}.

6-3. MODIFIED PESTFADE MODEL

(1). *Mathematical model*

Most subsurface pesticides usually undergo multiple interactions, such as sorption/desorption, volatilization, biological and chemical degradations, in addition to the normal transport processes of advection and hydrodynamic dispersion (45,178,186,240,246,290). Obviously, an ideal prediction of solute distributions among the solution, solid and vapor phases of a soil environment requires an in-depth understanding of the operative physicochemical and biological processes and of the relationships among these processes. It has been proven that adsorption is a fundamental process and plays an important role in governing the fate and transport of pesticides. In recent years, a number of mathematical models have been proposed to simulate these processes in various systems (8,33,196,287,288,291).

Table 6-2.2, Basic Properties of the Soil Cores Used in This Study

Depth (cm)	O.C.* (%)	pH	Clay (%)	Silt (%)	Sand (%)	M.C.** (%)
Column 1						
10	1.62	5.43	16.51	39.69	43.81	32.24
20	1.20	5.33	19.80	42.41	37.78	37.60
30	0.48	5.58	23.10	53.73	23.18	37.46
40	0.75	5.67	27.70	53.30	19.00	42.11
50	0.44	5.78	31.72	54.42	13.87	42.30
60	0.59	5.85	34.78	53.80	11.42	43.41
Column 2						
10	1.42	5.00	19.86	39.99	40.15	31.91
20	0.87	5.05	21.00	40.96	38.05	37.38
30	0.21	5.45	18.88	41.03	40.09	36.77
40	0.08	5.65	29.33	45.66	25.02	40.55
50	0.10	5.75	25.82	55.39	18.81	39.92
60	0.08	5.74	31.26	45.79	22.94	39.45

* Organic carbon; ** Moisture content.

The PESTFADE model (59,60,62) was designed to overcome most of the limitations (60) of existing non-point source pollution models, such as PRZM and LEACHMP (39,40,280), and to provide an in-depth representation of the soil-pesticide processes and a comprehensive treatment of the transport mechanisms occurring in the vadose zone. The general governing partial differential equation (PDE) for simultaneous water and solute transport is:

$$\partial C/\partial t\ (\theta_w + \rho K_d + \epsilon k_h) = \partial/\partial x\ [(\theta_w D)\ \partial C/\partial x - qC] - \phi \qquad (6\text{-}3.1)$$

where C is the solute solution concentration, θ_w is the volumetric soil moisture, ρ is the dry soil bulk density, ϵ is the air-filled porosity, q is the water flux, D is the moisture- and flux-dependent dispersion coefficient, K_d is the distribution coefficient, k_h is the Henry's constant, x is the distance from the surface, and ϕ represents all the sink terms such as volatilization (ϕ_{VOL}), chemical degradation (ϕ_{CHM}), and microbial degradation (ϕ_{MIC}).

In fields where the contribution of macropores appears to be significant, the above can be modified to include preferential flow and non-equilibrium sorption in macropores, and the following final mathematical model is obtained:

$$(1 + \rho f K_d/\theta_w + \epsilon k_h)\ \partial C/\partial t + \rho/\theta_w\ \partial S_2/\partial t$$
$$= D\partial^2 C/\partial x^2 - v\partial C/\partial x - \phi_{VOL} - \phi_{CHM} - \phi_{MIC} \qquad (6\text{-}3.2)$$

where f is the fraction of micropores, S_2 is the mass of solute adsorbed in macropores (59,60), and v is the pore-water velocity.

As stated in Chapter 3, Gamble, Langford, and coworkers (93-95,97,103; Chapter 3) have assumed a two stage adsorption/diffusion mechanism to account for a relatively

fast labile adsorption between soil particle surfaces (on the outside and in larger pores) and nearby solution, followed by a highly retarded intraparticle diffusion between surfaces and interiors. These processes can be briefly described with following equations.

(i). For the labile surface adsorption:

$$\bar{K}_1 = \theta_L/\theta_o M_{AT} \qquad (4\text{-}4.3)$$

$$\theta_c = \theta_L + \theta_o \qquad (3\text{-}2.7)$$

$$X_1 = \theta_L/\theta_c \qquad (3\text{-}2.8)$$

$$K_d = \bar{K}_1\theta_c(1-X_1) \qquad (3\text{-}2.10)$$

$$-dM_{AT}/dt = k_{b1}M_{AT}(W/V)\theta_o - k_{s2}(W/V)\theta_L \qquad (3\text{-}2.2)$$

where $\bar{K}_1$ is the atrazine sorption equilibrium function (M^{-1} or L of soil solution mol^{-1}), θ_L is the sorption sites occupied by atrazine (moles g^{-1} of dry soil), θ_o is the unoccupied sites (moles g^{-1} of dry soil), M_{AT} is the atrazine molarity in soil solution (moles L^{-1} of soil solution), θ_c is the labile sorption capacity (moles g^{-1} of dry soil), X_1 is the mole fraction of occupied sites (dimensionless), K_d is the distribution coefficient (L of soil solution g^{1} of dry soil). Eq. 3-2.2 is a rate expression for the adsorption/desorption processes, in which k_{b1} and k_{s2} are the rate constants for adsorption (in L mol^{-1} d^{-1}) and desorption (d^{-1}), respectively; the term W/V is a unit converting factor (g L^{-1}).

The resulting K_d is very useful for calculating the mass transfer of atrazine by the adsorption process and the remaining concentration in soil solution in the modified PESTFADE model.

$$S_1(i) = K_d(i)*C(i) \qquad (6\text{-}3.3)$$

$$C(i) = lhs(i)/(\theta_w(i) + \rho*K_d(i) + \epsilon*k_h) \qquad (6\text{-}3.4)$$

where $S_1(i)$ has the same meaning as θ_L (but, in $\mu g\ g^{-1}$ of dry soil), and C(i) is the same as M_{AT} (but, in ppm or mg L^{-1} of soil solution). The other symbols in eqs. 6-3.3 and 6-3.4 refer to the left-hand side of the PDE, the moisture content, the soil bulk density, the gas-filled porosity, and the Henry's law constant, respectively. The symbol i denotes the nodal points.

(ii). For the intraparticle diffusion:

$$d\theta_D/dt = k_{dl}\theta_L \qquad (3\text{-}2.15)$$

$$k_{dl} = Q(D/l^2) \qquad (4\text{-}4.4)$$

where θ_D is the nonlabile uptake by intraparticle diffusion (moles g^{-1} of dry soil), k_{dl} is the first-order rate constant for intraparticle diffusion (d^{-1}), D is the diffusion coefficient ($cm^2\ s^{-1}$), l is the mean particle radius (cm), and Q is a factor for converting units of time (86,400 s d^{-1}).

The temperature dependence of k_{dl} is given by the following equations:

$$u = b_o + b_1/T \qquad (6\text{-}3.5)$$

$$k_{dl} = e^u \qquad (6\text{-}3.6)$$

where b_o and b_1 are empirical constants, and T is the absolute temperature (°K).

The resulting k_{dl} has been used to calculate the mass transfer by intraparticle diffusion process in the model:

$$\text{pintra}(i) = \text{pintra}(i) + k_{dl}*S_1(i)*\text{step} \qquad (6\text{-}3.7)$$

where pintra(i) has the same meaning as θ_D (but, in $\mu g\ g^{-1}$ of dry soil), and step means the time advance (days).

In addition, the modified PESTFADE model retains the sink terms such as microbial

degradation and volatilization. It can be seen that, in contrast to the PESTFADE model (59,60), the use of calculated K_d values (eq. 3-2.10) instead of a fixed value, and the consideration of mass transfer by intraparticle diffusion (eqs. 3-2.15 and 4-4.4) with a temperature dependence (eqs. 6-3.5 and 6-3.6) are the main features of the modified model.

(2). ***Model components/execution***

PESTFADE (59,60,62) consists of two major programs (SWACROP and CADD), three subprograms (MOISTE, RUNOFF and HEAT), and five subroutines (CONDUC, INTER, CHMDGD, MICDGD and VOLAT). A detailed description of the PESTFADE computer package with respect to its components/submodels, and model organization is given in the PESTFADE User's Guide (62).

To simulate the steady flow of soil columns, the main program for the modified PESTFADE model has been structured by the Numerical Method of Lines (NMOL) technique (INITAL, DERV, and PRINT), and organized in a more simplified, straightforward fashion, and specifically designed to run the two stage sorption equilibrium/kinetic formulas. Fig. 6-3.1 shows the information transfer among the model components, where the open boxes represent the modified PESTFADE model.

The modified PESTFADE model is executed as follows:

- Run the MOISTE submodel to obtain the moisture distribution on a nodal-point basis.

- Run the HEAT submodel to evaluate the soil temperature distribution and thermal

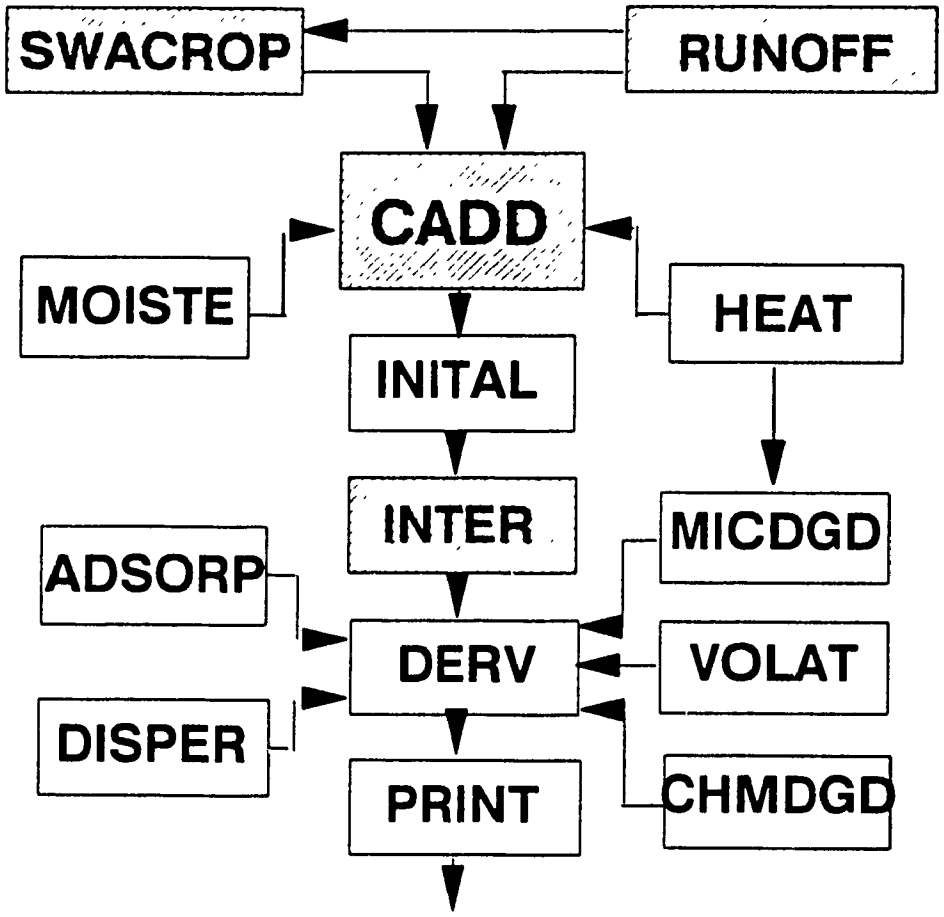

Fig. 6-3.1, Information Transfer Diagram for the Model Components

(MOISTE = moisture, ADSORP = adsorption, DISPER = dispersion, HEAT = temperature, MICDGD = microbialdegradation, CHMDGD = chemicaldegradation, VOLAT = volatilization, SWACROP, RUNOFF and CADD = program names, INITAL, DERV and PRINT = subroutine names (59,60,62))

conductivity.

- Execute the main program to perform the initialization, reading, interpolation, calculations and printing of results, handled by the internal subroutines such as INITAL, DERV and PRINT. In addition, the user-suppled subroutines for chemical degradation (CHMDGD), microbial degradation (MICDGD), and volatilization (VOLAT) are executed.

- Plot the simulation output in the form of concentration profiles with time or depth.

(3). *Input data and code specification*

Considering the experimental conditions of the soil columns, a steady-state water flow and transient atrazine movement scheme has been assumed. In order to simulate the nature of the soil cores, the modified model employed a calculated value as the initial condition for applied atrazine level at the soil surface (C_o = 13.88 ppm for Column 1 and 13.97 ppm for Column 2) instead of the RUNOFF subprogram. It must be noted that, unlike Column 2, Column 1 contained some levels of pre-loaded background atrazine which have to be reflected in the INITAL subroutine of the main program. When constant velocity (v_o = 2.2 cm d^{-1}) is assumed and constant moisture contents (θ_{wo} = 0.39 and 0.38 for Columns 1 and 2, respectively) are specified, then the moisture content file STEADY.DAT can be introduced without the use of the programs SWACROP and MOISTE.

Prior to running the main program (functioning as CADD), the input data files (PARAM1.DAT, GAMBL.DAT, STEADY.DAT, MICRO.DAT, VOLAT.DAT,

TFLOW.OUT, and standard DATA file) were prepared. These were generally based on the experimental conditions, soil properties, chemical constants, and the two stage equilibrium/kinetic results as presented in the previous chapters. The temperature profile over the nodes (TFLOW.OUT file) was obtained by running the HEAT and CONDUC subprograms. In addition, the various CODEs in PARAM1.DAT file that supervise the functions of the modified model components have been assigned as: CODE1 = 0 for the steady-state water and transient solute transport; CODE2 = 1 for the variable D (θ_w, v) value calculated by the program; CODE3 = 0 for the Dirichlet upper boundary condition; CODE4 = 1 for the solute flux dependent lower boundary; CODE5 = 0 for the conventional adsorption mechanism and 1 for the two stage mechanism (97). The main input data files for the modified PESTFADE can be found in Appendix A.

(4). ***Model verification***

To validate the modified PESTFADE model, a verification process has been carried out in which the numerical solutions from the modified model were compared with the analytical solutions under the same initial and boundary conditions and input parameters (277). One of the verifications was for the simple convection-dispersion problem (Fig. 6-3.2). The other was for the convection-dispersion and equilibrium sorption (one-site) problem (Fig. 6-3.3).

Results from both the numerical and analytical models are approximately the same, which suggests that the proposed model is valid as a predictive model as far as the simulation of similar problem domains is concerned. The main data files for the model

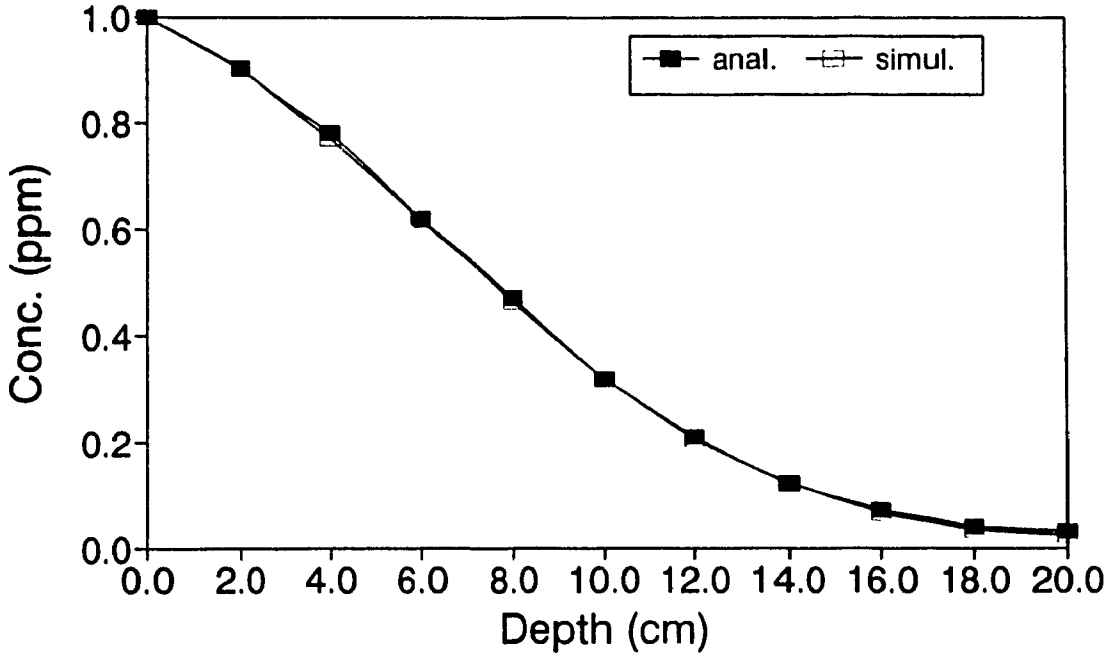

Fig. 6-3.2, Concentration Profile with Depth (For Advection only, t=5 h, K_d=0)

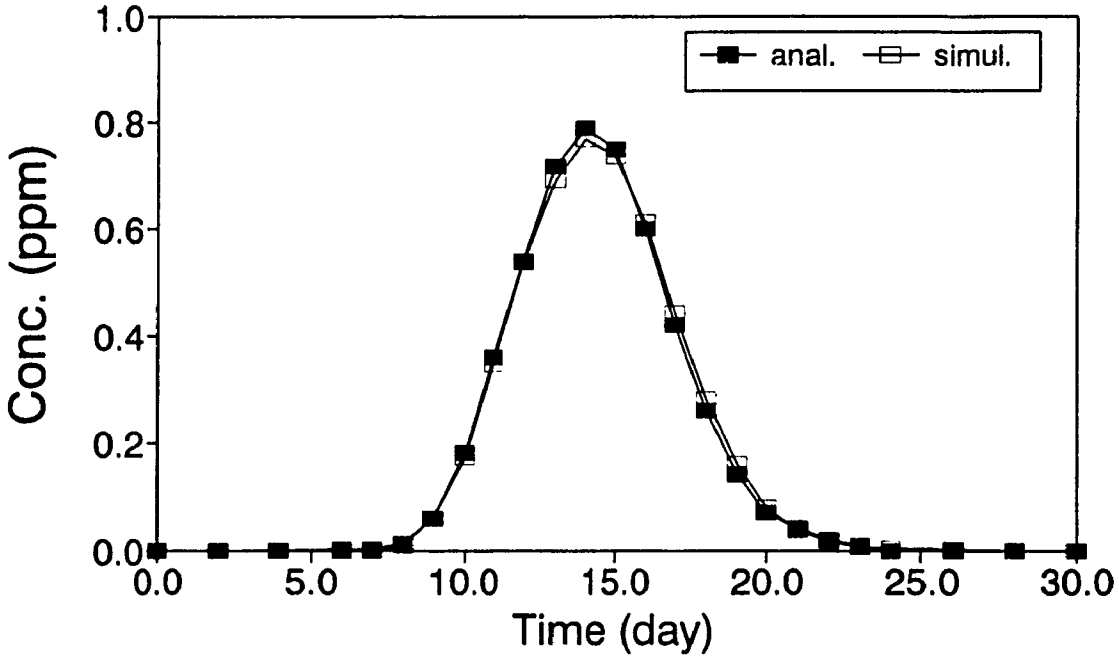

Fig. 6-3.3, Concentration Profile with Time (For 1-site, x = 100 cm, K_d = 0.62 $cm^3\ g^{-1}$)

verifications are listed in Appendix B.

6-4. RESULTS AND DISCUSSION

(1). *Output data*

The main output of the computer simulation consists of the solution concentrations of atrazine and the mass transfers by the labile adsorption, intraparticle diffusion, microbial degradation and volatilization with depth (cm) and time (day). The selected data at 10 cm intervals from the surface for both measured and simulated values are tabulated in Appendix C. Figs. 6-4.1 to 6-4.7 show the results plotted as atrazine concentration profile versus time or depth, respectively.

It can be seen that the measured atrazine concentration at 30 cm depth for Column 1 initially increases over the first 14 days after which it shows a gradual decrease (Fig. 6-4.1). The initial rise could be due to greater adsorption of the chemical onto the soil particles in the first 30 cm of the soil profile which is then leached down with the continuous incoming water which is being applied at a steady rate, resulting in a decrease in solution concentration over the remaining period. For example, at 30 cm depth, an increase from 0.006 to 0.035 mg L^{-1} or ppm was observed for the first 14 days after which the slope of the curve decreases gradually and becomes almost constant at 0.038 ppm. A similar trend has been seen for Column 2 (Fig. 6-4.4), but, over a slightly shorter time (12 days) and with a higher concentration (0.043 ppm). The atrazine concentration decreases with depth at any given time (Figs. 6-4.3 and 6-4.6), thus

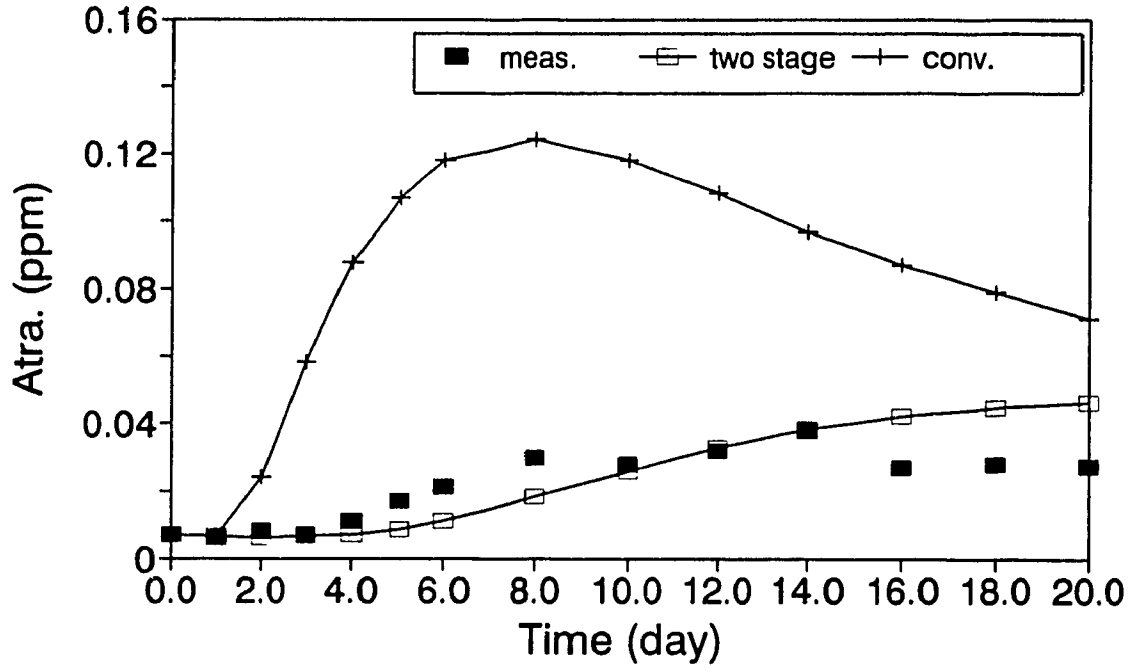

Fig. 6-4.1, Atrazine Conc. Profile with Time: 30 cm (Column 1)

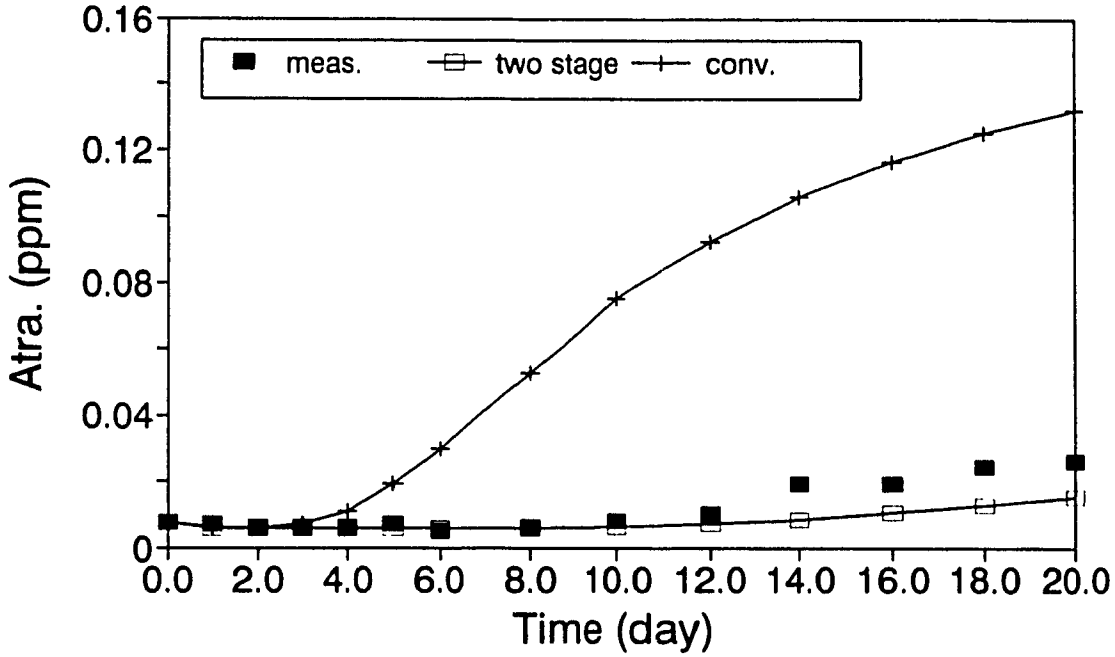

Fig. 6-4.2, Atrazine Conc. Profile with Time: 50 cm (Column 1)

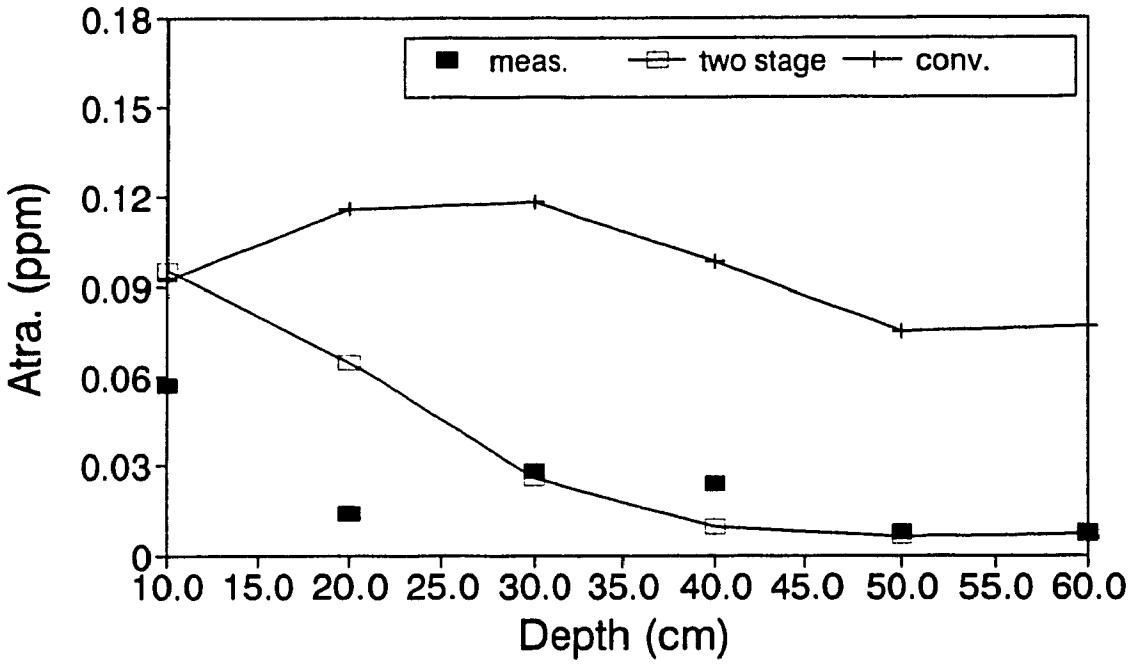

Fig. 6-4.3, Atrazine Conc. Profile with Depth: 10 days (Column 1)

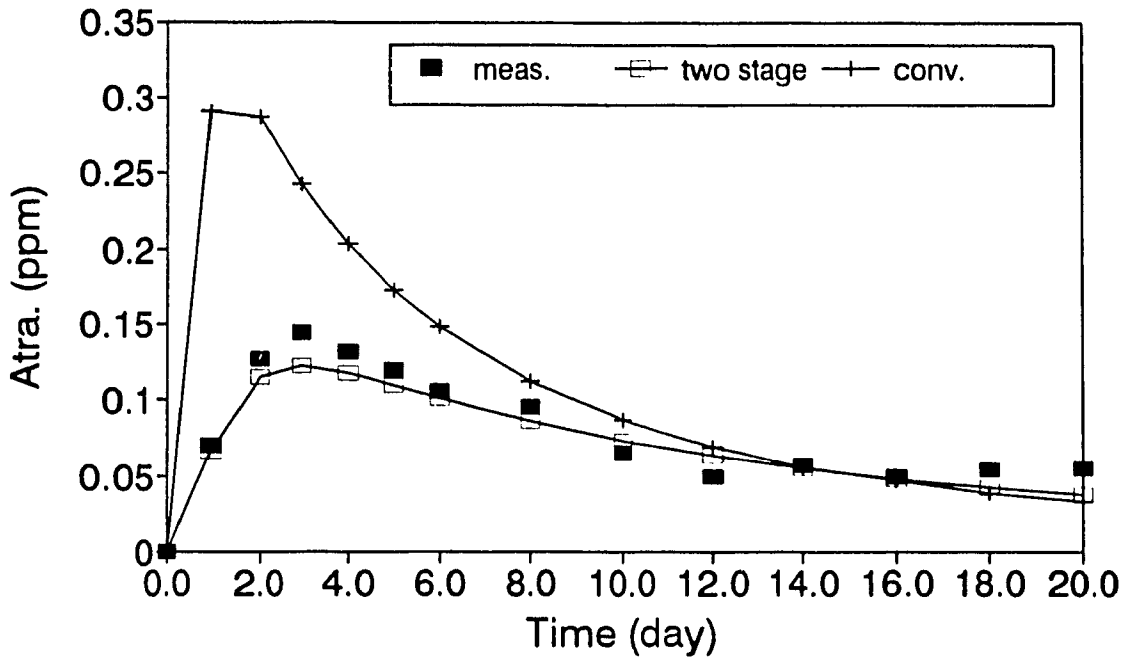

Fig. 6-4.4, Atrazine Conc. Profile with Time: 10 cm (Column 2)

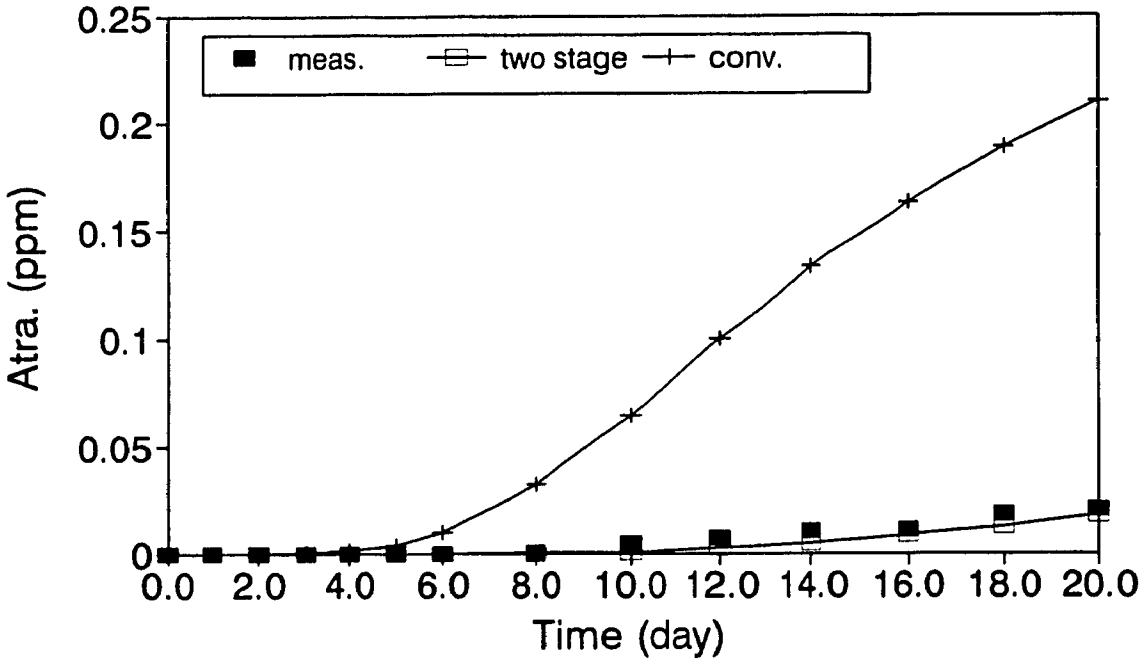

Fig. 6-4.5, Atrazine Conc. Profile with Time: 60 cm (Column 2)

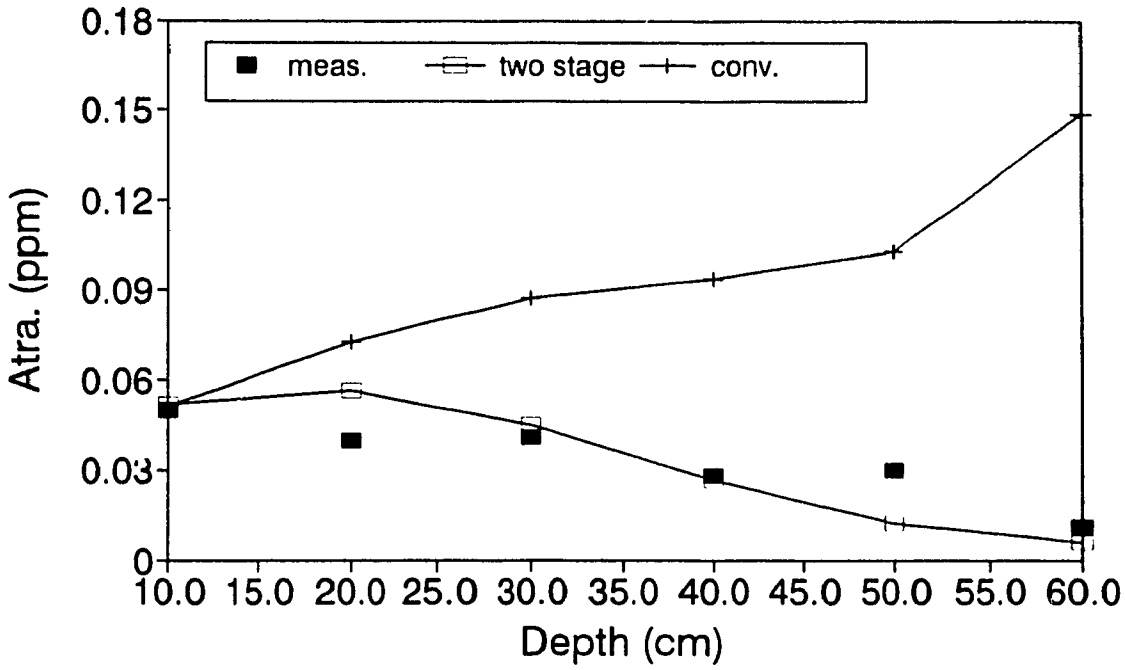

Fig. 6-4.6, Atrazine Conc. Profile with Depth: 15 days (Column 2)

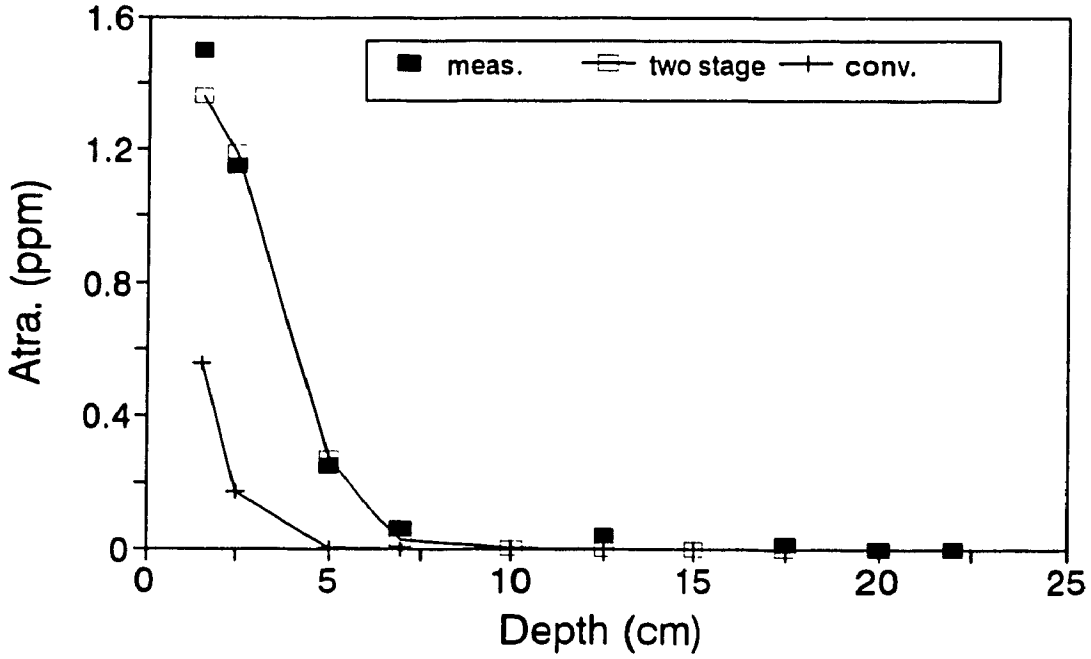

Fig. 6-4.7, Atrazine Conc. Profile with Depth: 0.6 days (Short column)

showing that most of the atrazine is retained near the surface of the column. A high rate of adsorption may retard solute transport down the soil profile. Table 6-2.2 shows lower values of pH at and near the surface than at lower depths, thus leading to stronger adsorption of the chemical onto the organic matter in the first few centimetres of the soil column (153,281-283). Also, high organic matter content will reduce the leaching of atrazine (153,281-283). The organic matter content decreases with the depth of the soil column (Table 6-2.2), e.g., for Column 1, it is 1.62% at 10 cm, and 0.44% at 50 cm, while for Column 2, it is 1.42% at 10 cm, and 0.10% at 50 cm. Therefore, the lower values of pH and higher values of organic matter content in both the soil columns can explain the greater adsorption and lower leaching of the chemical in the upper layers than the lower layers of the soil profile.

The simulated concentration values are also plotted in Figs. 6-4.1 to 6-4.7. The model was run with both the two stage model and the conventional single-valued K_d type kinetics. The values obtained with the two stage model show a much better agreement with the measured values than does the conventional approach. The latter overestimates concentrations most of the time. The improvement in the two stage model can be attributed to the appropriate evaluations of adsorption, diffusion, degradation and sorption capacity (θ_c) as a function of moisture content and soil tortuosity, and to the fact that the distribution coefficient (K_d) is not treated as a constant. These factors more properly represent the physicochemical properties of both atrazine and the soil cores (see the next section).

In addition, Table 6-4.1 shows the relative distribution of atrazine concentration over

Table 6-4.1, Atrazine Concentration Distribution (by two stage)

Time (day)	Node	Depth (cm)	Soln. (mg/L)	Ads. (ug/g)	Bnd. (ug/g)	Micdgd. (ug/g)	Vola. (mg/L.b.s.)
Column 1							
0	1	0.5	13.88	0	0	0	0
0	11	10	0.0170	0	0	0	0
0	31	30	0.0068	0	0	0	0
0	51	50	0.0074	0	0	0	0
5	1	0.5	0.1248	2609	1.3434	0.0401	4.017E-08
5	11	10	0.1222	163.7	0.2963	0.0084	0
5	31	30	0.0085	23.35	0.0224	6.378E-04	0
5	51	50	0.0056	21.56	0.0194	5.504E-04	0
10	1	0.5	0.0711	2638	1.6400	0.0485	4.629E-08
10	11	10	0.0954	197.3	0.6457	0.0184	0
10	31	30	0.0260	28.28	0.0774	0.0022	0
10	51	50	0.0062	23.35	0.0383	0.0011	0
15	1	0.5	0.0488	2652	1.8284	0.0538	5.015E-08
15	11	10	0.0729	216.7	0.9133	0.0261	0
15	31	30	0.0404	36.40	0.1885	0.0054	0
15	51	50	0.0094	25.16	0.0630	0.0018	0
Column 2							
0	1	0.5	13.97	0	0	0	0
0	11	10	0	0	0	0	0
0	31	30	0	0	0	0	0
0	51	50	0	0	0	0	0
5	1	0.5	0.0925	1236	0.6640	0.0213	3.299E-08
5	11	10	0.1098	3.710	0.1926	0.0057	0
5	31	30	0.0103	0.6341	0.0046	1.378E-04	0
5	51	50	3.356E-05	9.105E-04	6.673E-06	1.979E-07	0
10	1	0.5	0.0495	1248	0.7994	0.0253	3.738E-08
10	11	10	0.0734	98.74	0.3750	0.0112	0
10	31	30	0.0364	4.614	0.0561	1.669E-03	0
10	51	50	0.0032	0.1680	0.0023	6.676E-05	0
15	1	0.5	0.3219	1253	0.8804	0.0277	3.999E-08
15	11	10	0.0516	107.4	0.4999	0.0149	0
15	31	30	0.0450	10.58	0.1421	0.0042	0
15	51	50	0.0120	1.243	0.0177	5.239E-04	0

the different phases at selected depths and times for both columns. Similarly, the amount (or mass) distribution is shown in Table 6-4.2, also in Figs. 6-4.8 and 6-4.9. It can be seen that the labile adsorption phase accounts for the largest percentage of atrazine, being as much as 2 orders of magnitude higher than those of the intraparticle diffusion within the time steps. This more or less differs from the laboratory batch results (97). This is an important test of the physical chemical mechanism, as well as the model into which it has been incorporated. The reason is that the extrapolation beyond the conditions of the laboratory experiments that produced the equilibrium and kinetic parameters gives reasonably valid answers, while nonpredictive empirical parameters cannot do this properly. On this scale, both microbial degradation and volatilization can be ignored. The atrazine amounts, in terms of solution (sol), adsorption (ads), diffusion (bnd), microbial degradation (mic), and volatilization (vol) phases, have been calculated in the model as:

$$\text{sumsol} = \text{sumsol} + 1.0\text{d-}03*C(i)*\theta_w(i)*dx*A \qquad (6\text{-}4.1)$$

$$\text{sumads} = \text{sumads} + 1.0\text{d-}03*C(i)*K_d(i)*bd*dx*A \qquad (6\text{-}4.2)$$

$$\text{sumbnd} = \text{sumbnd} + 1.0\text{d-}03*k_{d1}*C(i)*K_d(i)*bd*dx*A*step \qquad (6\text{-}4.3)$$

$$\text{summic} = \text{summic} + 1.0\text{d-}03*\text{phimic}(i)*dx*A*step \qquad (6\text{-}4.4)$$

$$\text{sumvol} = \text{sumvol} + (-\text{phivol}(i))*dx/2.0d0*A*step \qquad (6\text{-}4.5)$$

where the sum terms represent the total atrazine at a certain time step (in mg), and the dx*A or dx/2.0d0*A denotes the volume of the soil core concerned (in cm^3).

For the purpose of comparison, Tables 6-4.3 and 6-4.4 show the distribution coefficient (K_d) and mole fraction (X_1) profiles with nodal points or depth for Column 2. Three observations can be made from these results. First, with the two stage kinetics,

Table 6-4.2, Atrazine Amount Distribution (in mg, by two stage)

Time (day)	Soln. (mg)	Ads. (mg)	Bnd. (mg)	Micdgd. (mg)	Volat. (mg)
Column 1					
0	0	0	0	0	0
1	0.2942	2.417	0.0003	9.101E-06	4.585E-10
3	0.2866	2.400	0.0016	4.525E-05	1.294E-09
5	0.2832	2.385	0.0035	9.906E-05	2.034E-09
7	0.2804	2.368	0.0060	1.703E-04	2.794E-09
10	0.2767	2.344	0.0097	2.763E-04	3.667E-09
15	0.2711	2.302	0.0182	5.196E-04	5.094E-09
20	0.2657	2.260	0.0302	8.613E-04	6.608E-09
Column 2					
0	0	0	0	0	0
1	0.2532	1.356	0.0002	5.331E-06	3.336E-10
3	0.2472	1.349	0.0016	4.772E-05	1.566E-09
5	0.2443	1.341	0.0037	1.108E-04	2.666E-09
7	0.2419	1.331	0.0065	1.944E-04	3.771E-09
10	0.2388	1.317	0.0107	3.186E-04	5.004E-09
15	0.2338	1.293	0.0328	6.037E-04	6.922E-09
20	0.2289	1.268	0.0463	1.004E-03	8.866E-09

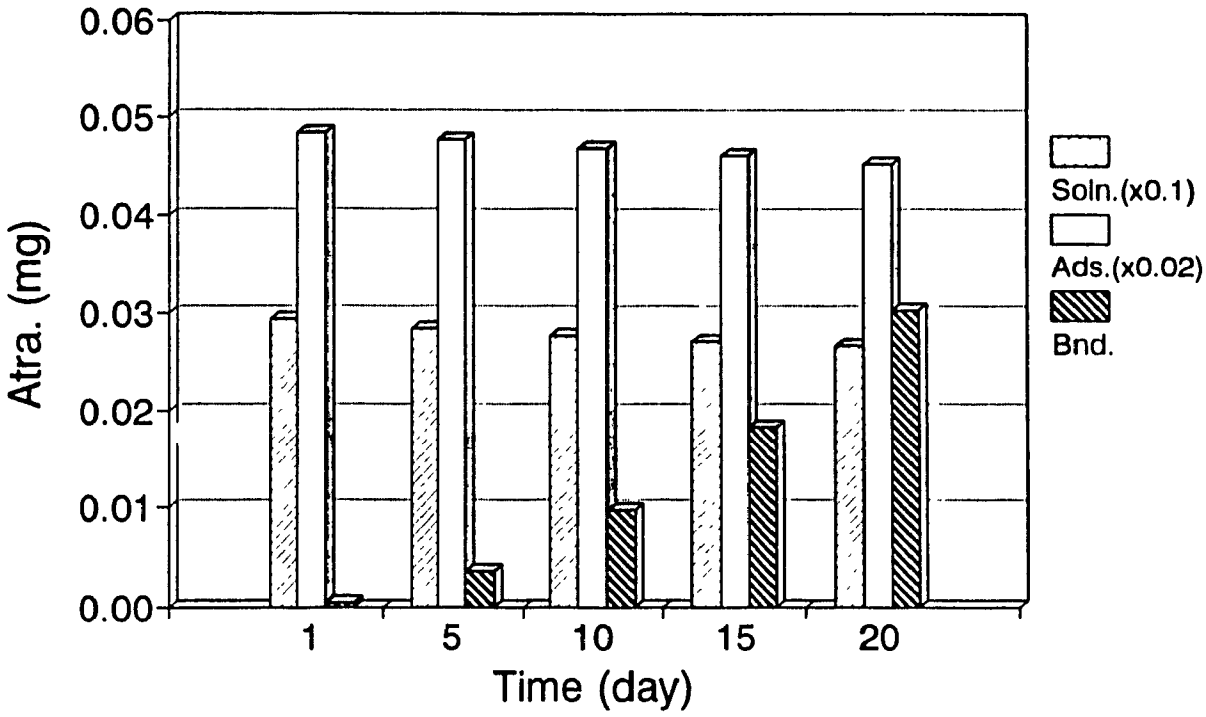

Fig. 6-4.8, Atrazine Amount Distribution (Column 1 by two stage)

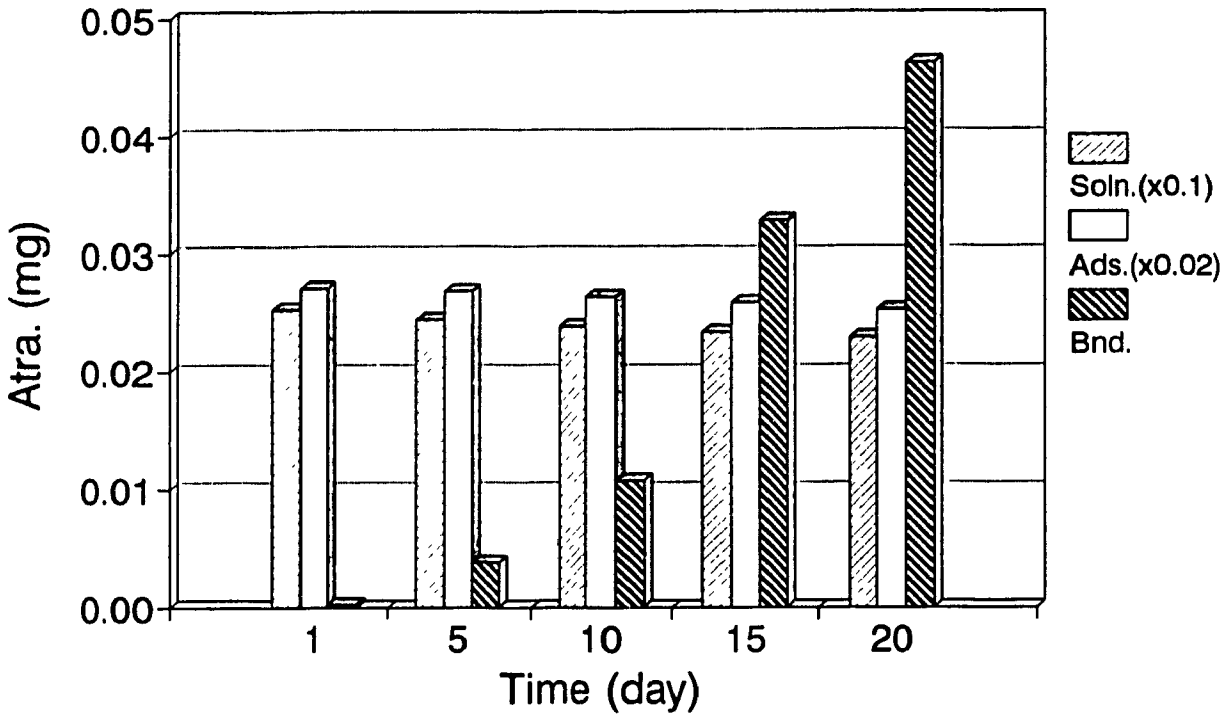

Fig. 6-4.9, Atrazine Amount Distribution (Column 2 by two stage)

Table 6-4.3, K_d Profile with Nodal Points for Column 2*

Depth	Time(day)					
(cm)	0	1	5	10	15	20
0	4.535E-4	1.448E-3	1.512E-3	1.523E-3	1.528E-3	1.530E-3
10	1.536E-3	1.519E-3	1.508E-3	1.517E-3	1.523E-3	1.526E-3
20	1.536E-3	1.536E-3	1.523E-3	1.519E-3	1.522E-3	1.524E-3
30	1.536E-3	1.536E-3	1.534E-3	1.527E-3	1.525E-3	1.525E-3
40	1.536E-3	1.536E-3	1.536E-3	1.533E-3	1.529E-3	1.528E-3
50	1.536E-3	1.536E-3	1.536E-3	1.535E-3	1.533E-3	1.531E-3
60	1.536E-3	1.536E-3	1.536E-3	1.536E-3	1.535E-3	1.532E-3

* K_d in L of soil solution g^{-1} of dry soil.

Table 6-4.4, X_1 Profile with Nodal Points for Column 2

Depth	Time(day)					
(cm)	0	1	5	10	15	20
0	7.254E-1	5.945E-2	1.601E-2	8.635E-3	5.631E-3	3.983E-3
10	0	1.151E-2	1.895E-2	1.276E-2	9.003E-3	6.639E-3
20	0	0	8.989E-3	1.127E-2	9.844E-3	8.107E-3
30	0	0	1.802E-3	6.357E-3	7.853E-3	7.709E-3
40	0	0	0	2.326E-3	4.663E-3	5.857E-3
50	0	0	0	0	2.109E-3	3.754E-3
60	0	0	0	0	1.063E-3	3.075E-3

K_d values vary slightly with nodal points or depth, although the differences are not larger than 2%. Second, by comparison with Chapter 4, K_d values are basically 10 times lower in the column experiments than those in the batch experiments. Finally, X_1 values vary with depth, and are also 10 times lower than they are in the batch experiments. In both cases the reason is that the column experiments had higher atrazine concentrations than the batch experiments because the water content of the soil cores is much lower than that in the slurry.

(2). ***Sensitivity analyses***

A series of sensitivity analyses have been performed in order to determine the factors to which the simulation is most sensitive.

(i). Initial concentration (C_o):

Using Column 2 as an example, the initial concentration was set to 8.65 and 7.27 ppm, in addition to C_o = 13.97 ppm. The results show similar trends which imply C_o is not an important factor. Other factors are therefore expected to dominate. Also, the dissolution of the herbicide atrazine was found to require an extended time period (days)(282). The present C_o (13.97 ppm) was based on an assumption of one-day completion of the dissolution which might be an under-estimate.

(ii). Sorption capacity (θ_c):

As discussed earlier, K_d is a key parameter in governing the overall simulation process. The working equation for calculating K_d is:

$$K_d = \bar{K}_1 * p\theta_c / (1 + \bar{K}_1 * M_{A1}) \qquad (6\text{-}4.6)$$

Except M_{AT} which was evaluated by C(i), both θ_c (here as $p\theta_c$) and $\bar{K}_1$ are all the sensitive factors determining K_d.

The value of θ_c provided in the GAMBL.DAT file was determined using properly designed laboratory batch experiments, in which the system was a uniform aqueous suspension, as described in Chapter 3. It has been recognized from the simulation that the real conditions in the soil cores, such as water-unsaturation, and tortuosity, etc., are much different from the batch system. In fact, it is the interface between the pore liquid and the solid particle surfaces that is responsible for the so-called soil-atrazine interactions (288). If $p\theta_c$ represents the sorption capacity of the bulk soil, a relationship of $p\theta_c << \theta_c$ can be reasonably established. In this work, the $p\theta_c$ was calculated by:

$$p\theta_c = \theta_c * (\theta_w / \theta_{ws}) * \tau^{-1} \qquad (6\text{-}4.7)$$

where θ_w is the volumetric moisture content (cm^3 of soil solution cm^{-3} of bulk soil), θ_{ws} is the saturated volumetric moisture content (0.48 in this case), (θ_w/θ_{ws}) is therefore an expression of the relative water content as a fraction of the saturation value, and τ is the tortuosity (≥ 1). For clay loam soils, τ^{-1} has the value of 0.1 to 0.2 under air content equal to ~ 0.10 (239).

Fig. 6-4.10 shows the results of Column 2 obtained using selected τ^{-1} values, and considerable shifts of the simulated curves are observed. This simulation employed τ^{-1} = 0.20 and 0.13 for Columns 1 and 2, respectively.

(iii). Sorption equilibrium function ($\bar{K}_1$):

As with the above, $\bar{K}_1$ is also a factor to which the simulation is sensitive. In this work $\bar{K}_1$ values of 3.76d+4, 2.50d+4, and 1.20d+4 were tested. $\bar{K}_1$ has been shown to

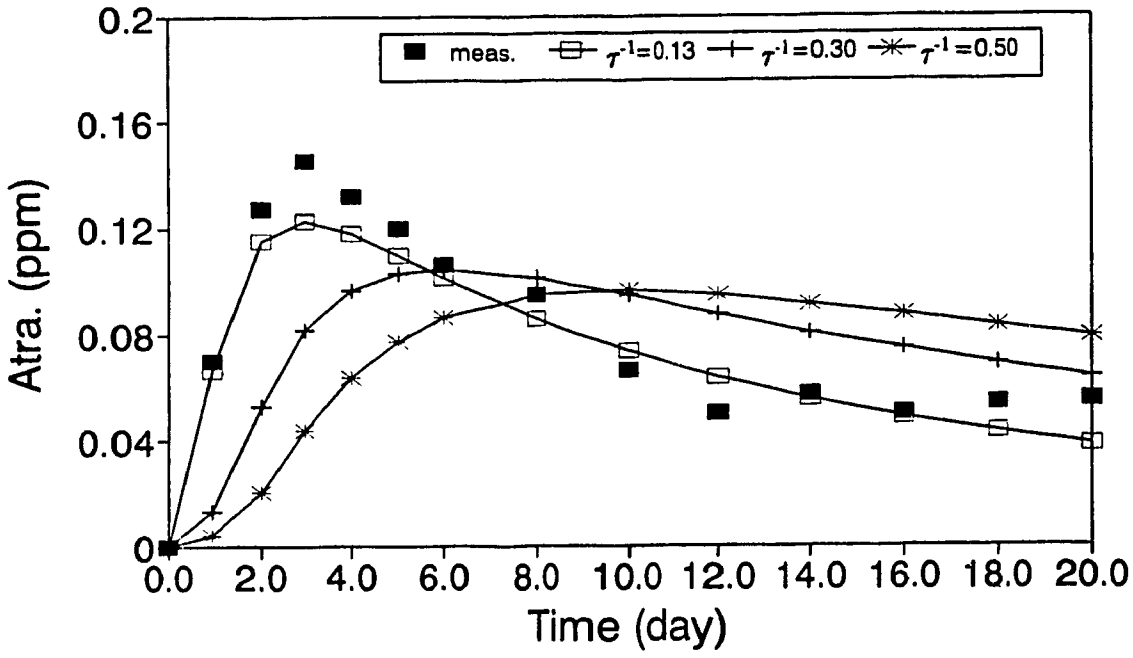

Fig. 6-4.10, Sensitivity Analysis: 10 cm (τ^{-1} for Column 2)

be a decreasing function of the site-loading (X_1) (103). Therefore, a theoretical treatment should take the site-loading into account for the $\bar{K}_1$ evaluation unless the site-loading remains small. For the conditions of natural fields and soil columns, the quantity of applied atrazine is usually quite low. As a result, this work used a fixed value of $\bar{K}_1$ (3.76d+4).

(iv). Dispersivity (λ):

This parameter is an empirical number which describes the dispersive behavior of atrazine in solution phase at the node points. Three values, 6, 10, and 14, have been tried for Column 2. Values of 10 and 14 revealed similar, better simulations. Larger λ values represent more facile movement of atrazine at a given hydrodynamic velocity (v_o = 2.2 cm d^{-1} in this case).

(3). *Comparison with conventional adsorption approach*

The output data of both columns obtained by conventional adsorption simulation have been tabulated in Appendix C and shown in the corresponding figures. Table 6-4.5 presents the results at selected depths and times for Column 1. Compared with the two stage sorption model (Table 6-4.1), a significant over-estimation of atrazine in the solution phase and an under-estimation in the adsorption phase have been observed. The reasons for these are not difficult to understand. The over-estimation is caused by the neglect of the intraparticle diffusion and the sink terms, and the use of a fixed partition coefficient K_d (0.522 cm^3 g^{-1}, which is lower than that used in the two stage kinetic model by a factor of $\sim$2) results in the under-estimation.

Table 6-4.5, Atrazine Concentration Distribution (for Column 1 by conventional approach)

Time (day)	Node	Depth (cm)	Soln. (mg/L)	Ads. (ug/g)	Bnd. (ug/g)	Micdgd. (ug/g)	Vola. (mg/L.b.s.)
0	1	0.5	13.88	7.245	0	0	0
0	11	10	0.0170	0.0089	0	0	0
0	31	30	0.0068	0.0036	0	0	0
0	51	50	0.0074	0.0039	0	0	0
5	1	0.5	0.1180	0.0616	0	0	3.283E-08
5	11	10	0.1792	0.0935	0	0	0
5	31	30	0.1074	0.0560	0	0	0
5	51	50	0.0191	0.1000	0	0	0
10	1	0.5	0.0540	0.0282	0	0	3.588E-08
10	11	10	0.0916	0.0478	0	0	0
10	31	30	0.1177	0.0614	0	0	0
10	51	50	0.0747	0.0390	0	0	0
15	1	0.5	0.0306	0.0160	0	0	3.745E-08
15	11	10	0.0540	0.0282	0	0	0
15	31	30	0.0921	0.0481	0	0	0
15	51	50	0.1116	0.0582	0	0	0

Statistical analyses. Statistical analyses have been conducted as shown in Figs. 6-4.11 and 6-4.12 (the relative error = the difference between simulated and measured values divided by the measured value), which clearly indicates improvements in the prediction by the two stage model over the conventional approach.

As indicated by Richie and Hoover (238), traditional numerical schemes normally produce oscillations and smearing which result in numerical dispersion. The oscillation causes deviations from the expected attenuation of concentration while the smearing phenomena may result in a larger spread of solute. The noticeable discrepancy between the theoretical and experimental results could also be attributed to some problems with soil sampling. The graphs for both columns show that the relative error in conventional adsorption mechanism was high, i.e., about 10% to 700%, as compared to the two stage kinetics in which the relative error varied between 5% to 65%. The deviation between the values predicted by the two stage kinetics and the measured values appears to be explicable owing to the oscillation, smearing and soil sampling problems.

6-5. SUMMARY

In this chapter the introduction of the two stage adsorption/diffusion mechanism into the PESTFADE model for simulating atrazine uptake processes actually occurring in the subsurface soil environment was proven to be a promising research strategy. It can be seen that:

(1). The modified PESTFADE model has been successfully validated by soil column

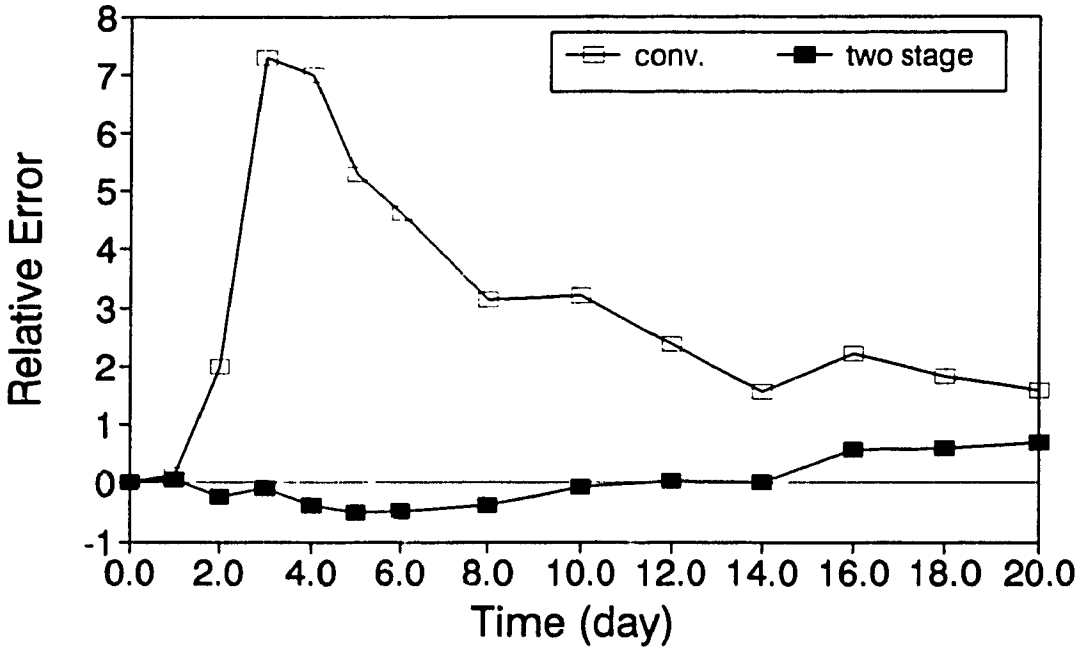

Fig. 6-4.11, Statistical Analysis: 30 cm (Column 1)

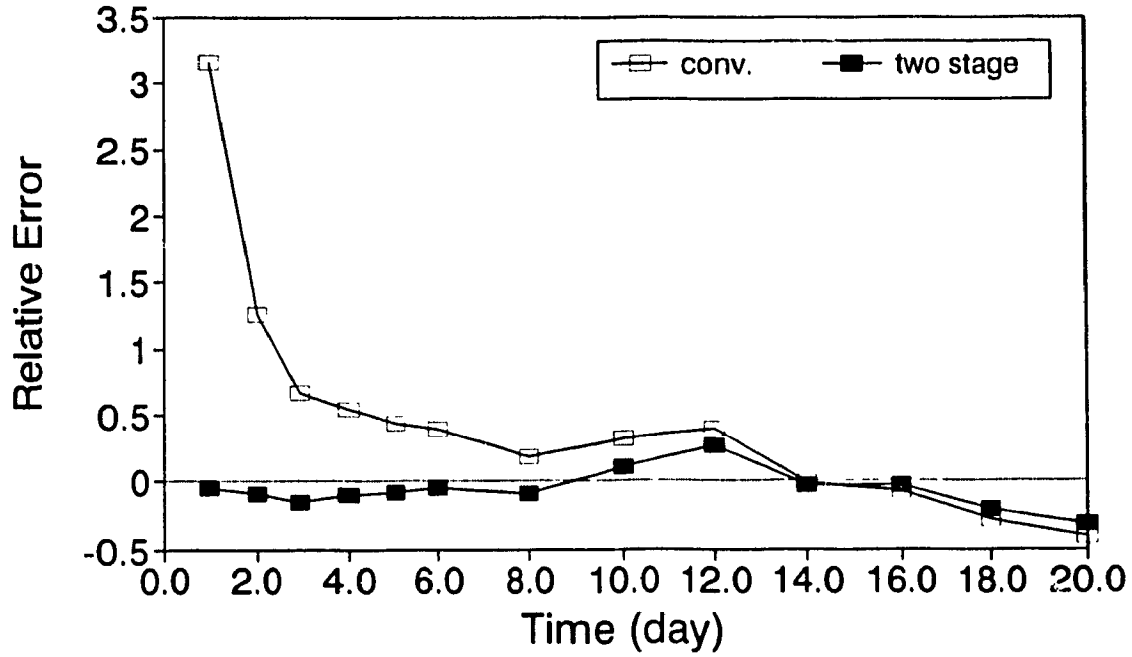

Fig. 6-4.12, Statistical Analysis: 10 cm (Column 2)

experiments under controlled laboratory conditions.

(2). The two stage sorption equilibrium/kinetic approach has shown a closer agreement with the measured values than does the conventional adsorption mechanism. This work, together with the previous application in field tests (59-61), indicates a significant progress in the development of efficient and cost-effective process models.

(3). The simulated concentration distribution of atrazine has been shown to be more sensitive to certain parameters in the input data files, such as distribution coefficient (K_d), sorption capacity (θ_c), labile sorption equilibrium function ($\bar{K}_1$), and dispersivity (λ). These are mainly subject to the actual soil conditions concerned. Accordingly, a careful evaluation of these parameters appeared to be quite crucial.

(4). It is important to recognize the differences shown in atrazine concentration or mass distribution between the simulated soil core results and laboratory batch results over the first 20 days. The two should not be comparable however, due to the different conditions (batch slurry and soil core). It is expected that over a prolonged period (150 days, for example) the simulated intraparticle diffusion portion will be becoming more dominant compared to other portions.

Nonetheless, some uncertainties existing in the mass balance evaluations, macropore flow impacts on the simulation, and larger Darcy fluxes (108 cm d^{-1}, for example) remain to be further investigated in future research.

CHAPTER 7

CONCLUSION AND SUGGESTION FOR FUTURE RESEARCH

7-1. CONCLUSION

As stated in Chapter 1, the research of this thesis follows the research strategy for pesticide-soil interactions which has been evolving in our research group during the course of the last several years. The work presented in Chapters 3 to 6 has systematically studied the uptake of the polar herbicide atrazine by mineral soil GB 843, including the development of mechanistic model, determination of equilibrium and kinetic parameters, examination of the effects of temperature and soil size fractions, interpretation of sorption mechanisms, and application of the mathematical model and laboratory results into a hydrology model. The stirred-batch setup combined with the on-line microfiltration-HPLC technique was introduced for both short-term and long-term equilibrium/kinetic studies. In addition, the work concerning the interaction between the slightly polar insecticide lindane and Laurentian fulvic acid presented in Chapter 2 provided a further confirmation of the site binding model using an ultrafiltration-GC method, which is fundamental to the model in the research strategy.

(1). For the uptake of atrazine by mineral soil GB 843, the following processes or

stages have been observed:

(i). A relatively fast reversible process and a subsequent slower reversible process.

(ii). The first of the two processes is assigned to physisorption onto the outer and intrapore surfaces from the bulk solution, while the second is retarded intraparticle diffusion from the surfaces into the particle interiors, with an activation energy suggesting chemisorption.

(2). Corresponding to the above, a two stage surface-adsorption/intraparticle-diffusion model has been derived from conventional kinetics, and a particular solution of Fick's diffusion law. That is:

(i). For the first stage:

$$d\theta_1/dt = -(V/W)dM_{AT}/dt$$

$$= k_{b1}(V/W)M_{AT}\theta_o - k_{s2}\theta_L \qquad (3\text{-}2.2)$$

(ii). For the second stage:

$$d\theta_D/dt = k_{d1}\theta_L - (V/W)R_{d2} \qquad (3\text{-}2.14)$$

(iii). The total rate law:

$$(d\theta_1/dt)_I = d\theta_1/dt - d\theta_D/dt$$

$$= k_{b1}(V/W)M_{AT}\theta_o - k_{s2}\theta_L - k_{d1}\theta_L + (V/W)R_{d2} \qquad (3\text{-}2.17)$$

(3). The labile surface sorption has been shown to have a definite sorption capacity (θ_c or C_c), with an experimentally measured value of 0.397 ± 0.036 μmoles g^{-1} of soil or 7.94 ± 0.72 μmoles L^{-1} of slurry for the bulk soil at 25 °C. This provided the basis for applying rigorous chemical stoichiometry in quantitative approaches to the equilibrium

and kinetics of the atrazine-soil GB 843 system.

(4). Both labile sorption and intraparticle diffusion exhibited rapid early uptakes within the first few minutes to hours. For bulk soil, the rate constant (k_{s1}) of labile sorption was about 8 times higher than that of intraparticle diffusion (k_{d1}). The two stage model described the labile sorption process of atrazine uptake generally by a second-order rate law. With the understanding that the pseudo first-order rate constant (k_{s1}) was an approximation for early uptake, instead, the first-order sorption (eq. 3-2.19) or diffusion (eq. 3-2.15) rate model has been demonstrated to be suitable for both processes. By using the initial rate approximation calculations, the resulting rate parameters (D, k_{d1}, and k_{s1}) compared well with those reported elsewhere.

(5). Over a certain reaction period ($\sim$2 to 11 days for labile sorption, after $\sim$70 days for intraparticle diffusion) both curves approached plateau regions, indicating the attainments of apparent equilibrium or steady state. With respect to the much longer equilibrating time scale, intraparticle diffusion can be considered the rate-limiting process in comparison with labile surface sorption.

(6). The experiments with soil size fractions have shown relatively small changes in atrazine uptake, showing a close mass-weighted feature. Both rate constant (k_{s1}) and sorption capacity (θ_c) varied inversely with particle size (e.g., k_{s1} for the finest fraction differing from the coarsest by a factor of $\sim$4), and were linearly correlated to specific surface area and organic carbon content. In contrast, intraparticle diffusion revealed a more complex behavior, considering the observed fact that both diffusion coefficient (D) and rate constant (k_{d1}) decreased with decreasing particle size, but in a nonlinear fashion.

(7). The experiments with varying temperature have shown the variation of atrazine uptake with temperature. The equilibrium parameters such as $\bar{K}_1$, K_d and X_1, as well as the total sorbed atrazine, defined as a sum of the surface adsorbed plus the intraparticle diffused, revealed no statistically significant temperature dependence. In contrast, the rate parameters, such as k_{s1}, k_{d1} and D, increased substantially with temperature by factors of 2.5 up to 40, comparing the values at 35 °C with those at 5 °C.

(8). The resulting ΔH° and E_a data by van't Hoff and Arrhenius treatments can provide an insight into the uptake mechanisms, and suggested that the main process for labile surface uptake was weak physisorption ($\Delta H^\circ \approx 0$ kJ mol^{-1} and $E_a = 22$ kJ mol^{-1}), while intraparticle diffusion was dominated by a chemisorption process ($E_a = 89$ kJ mol^{-1}).

(9). Introduction of the two stage model into a newly-developed solute transport model PESTFADE for simulating atrazine movement processes actually occurring in controlled soil columns proved to be a promising research strategy. The two stage model with the physicochemical parameters from this research has generally shown a much closer agreement with the observed values than the conventional approach. This work, together with its field application, indicated significant progress toward developing efficient and cost-effective process models.

(10). The experiments investigating the interaction between the slightly polar insecticide lindane and Laurentian fulvic acid gave further support to the binding site complexation model. A small (~ 1 μmole g^{-1} of FA) and limited binding capacity was observed for this system, and it varied as a function of solution pH, ionic strength, and

FA concentration. This result favored a definite binding site model which was related to the protonation of carboxylate groups, and suggested that these hydrophobic sites were created by conformational equilibria of the FA polyelectrolyte. This confirmed the choice of the complexation model for this work.

(11). The soil Green Belt (GB 843) has been characterized with respect to soil minerals, soil fractions, soil pH, modal analyses, element identification, cation exchange capacity (CEC), specific surface area, and organic carbon content, etc. The average values for particle size, soil pH, CEC, specific surface area, and organic carbon content of the bulk soil are: 1.91 ± 2.34 μm, 5.63 ± 0.02, 8.8 ± 0.2 meq/100 g soil, 38.9 ± 2.3 m^2 g^{-1} soil, and 0.83 ± 0.01%, respectively.

7-2. SUGGESTION FOR FUTURE RESEARCH

(1). This thesis and earlier work have demonstrated that the stirred-batch setup combined with the microfiltration-HPLC technique is a powerful tool for simultaneous speciation studies of the equilibria and kinetics occurring in heterogeneous systems. Clearly, more extensive uses could be profitable for clays, clays having hydrous metal oxide coatings, whole soils, microbiological cultures, and tissue cultures, etc. The requirement is that samples should have small particles that can be maintained in suspension by stirring. Because cation-exchange columns are available for HPLC use, it should also be possible to extend the method to metal ion interactions with some or all of the above types of samples.

(2). As an important achievement of the research strategy of our research group during the past years, the two stage adsorption/diffusion model has been shown to be suitable for describing the uptake behavior of atrazine by soil. The resulting physicochemical parameters agree well with those reported previously, and have undergone practical tests. However, this model needs further testing and modification, including the application to many systems, and refinement of the mathematical expressions. In particular, as shown earlier, collecting at least two categories of data, one is the data for rapid early uptake (within the first few minutes) of the first stage and one is the data for outward intraparticle diffusion (R_{d2}) of the second stage, is definitely needed for a thorough understanding.

(3). As indicated earlier, the two stage model described the intraparticle diffusion (θ_D) with first-order kinetics (eq. 3-2.15), by assuming the existence of a steady state labile surface coverage (θ_l) which served as the driving force. In light of this, some questions may arise: (i) How does this scheme relate to commonly discussed diffusion mechanisms such as the pore diffusion model and the surface diffusion model? (ii) How should one model the solute migration behavior through a particle interior restricted within an individual grain? It is evident that a further understanding of the uptake process mechanisms, and especially more detailed microscopic interpretation and expression, should be the subject of future research.

(4). The labile sorption capacity (θ_c) has been demonstrated to be a key parameter in applying chemical stoichiometry to naturally-mixed geochemical systems. On the basis of the site binding model, it should generally display explicit distributions as a function

of factors such as pH, organic matter content, specific surface area, temperature, particle size, soil water content, and soil tortuosity, etc. for a particular combination of pesticide-soil system. Therefore, more detailed investigations of this parameter with properly designed experimental methods and critical data analyses should be carried out in future research.

(5). Introducing the two stage mechanism with resulting equilibrium/kinetic parameters into a hydrology computer model has shown promise in both field tests and soil column studies. However, there are some uncertainties in mass balance calculations. Also, some discrepancies exist in the case of higher Darcy fluxes that might be attributed to the effect of macropore activities. These problems remain for future research in order to upgrade the related transport simulation.

REFERENCES

1. Adams, R.S.,Jr. and Li, P., *Soil Sci. Soc. Am. Proc.* **1971**, *35*, 78.

2. Adams, R.S., *Residue Rev.* **1973**, *47*, 1-54.

3. Adamson, A.W., *Physical Chemistry of Surfaces*. 3rd ed. John Wiley and Sons, New York. **1976**.

4. Albery, W.J., Bartlett, P.N., Wilde, C.P. and Darwent, J.R., *J. Am. Chem. Soc.* **1985**, 107, 1854-1859.

5. Alfheim, J.A. and Langford, C.H., *Anal. Chem.*, **1985**, *57*, 861.

6. Anderson, M.A. and Malotky, D.T., *J. Colloid interface Sci.*, **1979**, *72*, 413.

7. Anderson, M.P., *CRC Critical Reviews in Environmental Control*, pp.97-156, CRC Press, Boca Baton, Fla., **1979**.

8. Angley, J.T., Brusseau, M.L., Miller, W.L. and Delfino, J.J. *Environ. Sci. Technol.*, **1992**, *26*, 1404-1410.

9. Ball, W.P., Ph.D. Dissertation, Stanford University, Stanford, CA. October **1989.**

10. Ball, W.P. and Roberts, P.V., Rate-Limited Sorption of Halogenated Aliphatice onto Sandy Aquifer Material-Experimental Results and Implications for Solute Transport. *ES*, **1985**, *66*, 894.

11. Ball, W.P. and Roberts, P.V., *Environ. Sci. Technol.*, **1991**, *25*, 1223-1236.

12 Ball, W.P. and Roberts, P.V., *Environ. Sci. Technol.*, **1991**, *25*, 1237-1249.

13. Ball, W.P., Buehler, Ch., Harmon, T.C., Mackay, D.M. and Roberts, P.V., *J. Contam. Hydrol.*, **1990**, *5*, 253-295.

14. Baluja, G., Murado, M.A. and Tejedor, M.C., in P. Koivistoinen, ed., *Pesticides: IUPAC, Third International Congress of Pesticide Chemistry*, pp. 243-249, Georg. Thiem. publishers. Munich, **1975**.

15. Barrow, N.J. and Shaw, T.C., *J. Soil Sci.*, **1979**, *30*, 67-76.

16. Benjamin, M.M. and Leckie, J.O., *J. Colloid interface Sci.*, **1981**, *79*, 209-221.

17. Benjamin, M.M. and Leckie, J.O., In *Contaminants and Sediments*. R.A. Baker, ed. Vol. 2, Ch. 16, pp305-22, Ann Arber Sci., Ann Arber, MI. **1980**.

18. Berner, R.A., *Early Diagenesis*. Princeton Univer. Press. Princeton. N.J. **1980**.

19. Bisdom, E.B.A., Henstra, S., Hornsveld, E.M., Jongerius, A. and Letsch, A.C., *Neth. J. Agric. Sci.*, **1976**, *24*, 209-222.

20. Blatt, W.F., Robinson, S.M. and Bikler, H.J., *J. Anal. Biochem.*, **1968**, *26*, 151.

21. Bloom, P.R. and Erich, M.S., *Soil Sci. Soc. Am. J.*, **1987**, *51*, 1131-1136.

22. Borggaard, O.K. and Streibid, J.C., *Acta Agric. Scand.*, **1988**, *38*, 293-301.

23. Boucher, F.R. and *Diss. Abstr.*, **1968**, *28*, 5102b.

24. Boucher, F.R. and Lee, G.F., *Environ. Sci. Technol.* **1972**, *6*, 538.

25. Bowden, J.W., Posner, A.M. and Quirk, J.P., *Aust. J. Soil Res.*, **1977**, *15*, 121.

26. Boyd, G.E., Adamson, A.W. and Meyers, L.S., Jr. *J. Am. Chem. Soc.*, **1947**, *69*, 2836-2848.

27. Brusseau, M.L., Jessup, R.E. and Rao, P.S.C., *Water Resour. Res.*, **1989**, *25*, 1971.

28. Brusseau, M.L. and Rao, P.S.C., *Geoderma*. **1990**, *46*, 169.

29. Brusseau, M.L. and Rao, P.S.C., *Chemosphere*. **1989**, *18*, 1691.

30. Brusseau, M.L., Jessup, R.E. and Rao, P.S.C., *Environ. Sci. Technol.*, **1991**, *25*, 134-142.

31. Brusseau, M.L. and Rao, P.S.C., *Environ. Sci. Technol.*, **1991**, *25*, 1501-1506.

32. Brusseau, M.L., Jessup, R.E. and Rao, P.S.C., *Environ. Sci. Technol.*, **1990**, *24*,

727-735.

33. Brusseau, M.L. and Rao, P.S.C., *Critical Reviews in Environmental Control*, **1989**, *19*, 33-99.

34. Buffle, J., Deladoey, P. and Haerdi, W., *Anal. Chim. Acta*, **1978**, *101*, 339-357.

35. Burns, R.G., *Proc. Br. Weed Control Congr.*, 11th, Brighton, pp. 1203-1209, **1972.**

36. Calderbank, A., *Residue Reviews*, **1989**, *108*, 71-103.

37. Cameron, D.A. and Klute, A., *Water resour. Res.*, **1977**, *13* , 183-188.

38. Caron, G. and Suffet, I.H., in Suffet, I.H. and MacCarthy, P. (Eds.), *Aquatic Humic Substances (Advances in Chemistry Series)*, Vol.219, pp.117-130, ACS, Washington, D.C., **1989**.

39. Carsel, R.F., Smith, C.N., Mulkey, L.A., Dean, J.D. and Jowise, P. *User's Manual for the Pesticide Root Zone Model (PRZM)*: Release 1 EPA-600/3-84-109, U.S. EPA, Athens GA, **1984**.

40. Carsel, R.F., Mulkey, L.A., Lorber, M.N. and Baskin, L.B. *Ecological Modelling.* **1985**, *30*, 49-69.

41. Carski, T.H. and Sparks, D.L., *Soil Sci. Soc. Am. J.*, **1985**, *49*, 1114-1116.

42. Carter, C.W. and Suffet, I.H., *Environ. Sci. Tecnol.*, **1982**, *16*, 735-740.

43. Chang, R., *General Chemistry*. Random House, New York. 1st ed., p 384, **1986**.

44. Chantong, A. and Massoth, F.E., *AIChE J.*, **1983**, *29*, 725- 731.

45. Cheng, H.H. *Pesticides in the Soil Environment*; Soil Science Society of America, Inc.: Madison, WI, **1990**.

46. Chiba, M., *Residue Rev.* **1969**, *30*, 63-113.

47. Chiou, C.T., Peters, L.J. and Freed V.H., *Science.* **1979**, *206*, 831-832.

48. Chiou, C.T., In J. Saxena and F. Fisher (ed.) *Hazard assessment of Chemicals: Current Developments*. Academic Press, New York. p117-153, **1981.**

49. Chiou, C.T., In P. MacCarthy et al. (ed.) *Humic Substances in Soil and Crop Sciences. SSSA*, Madison, WI. **1989.**

50. Chiou, C.T., Peters, L.J. and Freed V.H., *Science*, **1981**, *213*, 684.

51. Chiou, C.T., Porter, P.E. and Schmedding, D.W., *Environ. Sci. Tecnol.*, **1983**, *17*, 227-231.

52. Chiou, C.T., Porter, P.E. and Shoup, T.D., *Environ. Sci. Tecnol.*, **1984**, *18*, 295-297.

53. Chiou, C.T., In B.L. Sawhney and K. Brown (ed.) *Reactions and Movement of Organic Chemicals in Soils*. SSSA, Madison, WI. p1-29, **1989.**

54. Chiou, C.T., Schmedding, D.W. and Manes, M., *Environ. Sci. Technol.*, **1982**, *16*, 4-10.

55. Chiou, C.T., Malcolm, R.L., Brinton, T.I. and Kile, D.E., *Environ. Sci. Technol.*, **1986**, *20*, 502-508.

56. Chou, L. and Wollast, R., *Geochim. Cosmochim. Acta*. **1984**, *48*, 2205-2217.

57. Choudhry, G.G., *Humic Substances*. Gordon and Bresch, New York. **1983.**

58. Clarter, D.L., Mortland, M.M. and Kemper, W.D., In *Methods of Soil Analysis, Part 1-Physical and Mineralogical Methods*. Klute, A., Ed., 2nd Ed., Chapter 16, p 413, Madison, Wisconish, USA, **1986**.

59. Clemente, R.S., *A Mathematical Model for Simulating Pesticide Fate and Dynamics in the Environment (PESTFADE)*. Ph.D. thesis, Macdonald Campus of Mcgill University, **1991**.

60. Clemente, R.S., Prasher, S.O. and Barrington, S.F., *Trasactions of the ASAE*. **1993**, *36*, 357-367.

61. Clemente, R.S. and Prasher, S.O., *Trasactions of the ASAE*. submitted. **1992**.

62. Clemente, R.S. and Prasher, S.O., *PESTFADE Model User's Guide and Documentation*. Macdonald Campus of McGill University, Ste-Anne de Bellevue, PQ, Canada. **1993**.

63. Coates, J.T. and Elzerman, A.W., *J. Contam. Hydrol.*, **1986**, *1*, 191.

64. Cooney, D.O., Adesanya, B.A. and Hines, A.L., *Chem. Eng. Sci.*, **1983**, *38*, 1535-1541.

65. Cotterill, E.G., *Pestic. Sci.* **1980**, *11*, 23-28.

66. Crank, C., *The mathematics of Diffusion*, Oxford University Press, 2nd edition, p 26, London, **1975**.

67. Curtis, G.P., Roberts, P.V. and Reinhard, M., *Water Resour. Res.* **1986**, *22*, 2059.

68. Curl, R.L. and Keolelan, G.A., *Environ. Sci. Tecnol.*, **1984**, *18*, 916-922.

69. Curtis, G.P., Reinhard, M. and Roberts, P.V., in Davis, J.A. and Hayes, K.F. (Eds.), *Geochem. Processes at Mineral Surfaces*, pp.191-216, ACS Symposium Series 323, Washington, D.C., **1986**.

70. Damanakis, M., Drennan, D.S.H., Fryer, J.D. and Holly, K., *Weed Res.* **1970**, *10*, 264-277.

71. Davis, J.A., James, R.O. and Leckie, J.O., *J. Colloid interface Sci.*, **1978**, *67*, 90.

72. Dean, J.D., P.S. Huyakorn, A.S.Jr. Donigian, K.A. Voos, R.W. Schanz, Y.J. Meeks, and R.F. Carsel. Risk of Unsaturated Transport and Transformation of Chemical Concentration (RUSTIC) Model. *U.S. Environmental Protection Agency*, Athens, Georgia. **1989**.

73. Degens, E.T. and Mopper, K., In *Chemical Oceanography*. 2nd ed. Riley, J.P., Chester, R., eds. Academic Press, New York. Vol. 6, Ch. 31, pp 59-112, **1976.**

74. Di Toro, D.M.and Horzempa, L.M., *Environ. Sci. Technol.*, **1982**, *16*, 594-602.

75. Donigian, A.S., Jr. and Crawford, N.H., *EPA-600/3-76-083*, EPA Technological Service, U.S. Environmental Protection Agency, Athens, GA. **1976**.

76. Duursma, E.K. and Bosch, C.J., *Neth. J. Sea Res.*, **1970**, *4*, 395-469.

77. Elrick, D.E., Erh, K.T. and Krupp, H.K., *Water Resour. Res.*, **1966**, *2*, 717.

78. Fara, A. and Eyring, H., *J. Phys. Chem.* **1956**, *60*, 890-898.

79. Fields, D.E., *CHNSED*, Natl. Sci. Found., Washington, D.C., ORNL/NSF/EATC Rep. no.19, Natl. Tech. Inf. Serv., U.S. Dep. of Commerce, Springfield, Va.

80. Fong, F.K. and Mulkey, L.A., *Water Resour. Res.*, **1990**, *26*, 843-853.

81. Frank, R., In *Proc. of the first conference on regenerative agriculture*, 1-13. Macdonald Campus of McGill University, Ste-Anne de Bellevue, Quebec, **1986**.

82. Fredeen, F.J.H., Arnason, A.P. and Berek, B., *Nature*, **1953**, *171*, 700-701.

83. Freeman, D.H. and Cheung, L.S., *Science*, **1981**, *214*, 790-792.

84. Frost, A.A. and Pearson, R.G., *Kinetics and Mechanism*. Wiley, New York. **1961.**

85. Gamble, D.S., *Can. J. of Chem.*, **1972**, *50*, 2680-2690.

86. Gamble, D.S., Langford, C.H. and Underdown, A.W. *Org. Geochem.*, **1985**, *8*, 35-39.

87. Gamble, D.S., Underdown, A.W. and Langford, C.H. *Anal. Chem.*, **1980**, *52*, 1901-1908.

88. Gamble, D.S., *Can. J. Soil Sci.* **1989**, *69*, 313-325.

89. Gamble, D.S. and Khan, S.U., *Can. J. Soil Sci.* **1985**, *65*, 435-443.

90. Gamble, D.S. and Khan, S.U., *Can. J. Chem.* **1988**, *66*, 2605-2617.

91. Gamble, D.S., Khan, S.U. and Tee, O.S., *Pestic. Sci.* **1983**, *14*, 537-545.

92. Gamble, D.S., Schnitzer, M., Kerndorff, H. and Langford, C.H. *Geochim. Cosmochim. Acta*, **1983**, *47*, 1311-1323.

93. Gamble, D.S. and Khan, S.U., *J. Agric. Food Chem.*, **1990**, *38*, 297-308.

94. Gamble, D.S. and Ismaily, L.A., *Can. J. Chem.*, **1992**, *70*, 1590-1596.

95. Gamble, D.S. and Khan, S.U., *Can. J. Chem.*, **1992**, *70*, 1597-1603.

96. Gamble, D.S. and Langford, C.H., *Environ. Sci. Technol.*, **1988**, *22*, 1325-1335.

97. Gamble, D.S., Li, J., Gilchrist, G.F.R. and Langford, C.H., *Environ. Sci. Technol.*, **1993**, in preparation.

98. Gamble, D.S., Haniff, M.I. and Zienius, R.H., *Anal. Chem.*, **1986**, *58*, 732-734.

99. Gamble, D.S., Haniff, M.I. and Zienius, R.H., *Anal. Chem.*, **1986**, *58*, 727-731.

100. Gee, G.W. and Bauder, J.W., In *Methods of Soil Analysis, Part 1-Physical and Mineralogical Methods*. Klute, A., Ed., 2nd Ed., Chapter 15, p 384, Madison, Wisconish, USA, **1986**.

101. Gee, G.W and Bauder, J.W., In *Methods of Soil Analysis, Part 1-Physical and Mineralogical Methods*. Klute, A., Ed., 2nd Ed., Chapter 15, p 393, Madison,

Wisconish, USA, **1986**.

102. Giddings, J.C. and Eyring, H., *J. Phys. Chem.*, **1955**, *59*, 416.

103. Gilchrist, G.F.R., Gamble, D.S., Kodama, H. and Khan, S.U., *Environ. Sci. Technol.* in press. **1993**.

104. Glass, R.L., *J. Agric. Food Chem.*, **1987**, *35*, 497-500.

105. Green, R.E., Rao, P.S.C. and Corey, J.C., In *Proc. 2nd Symp. Transport Phenomena Porous Media*. IAHR and ISSS, Guelph, Canada. **1972**, *2*, 733.

106. Greenland, D.J. and Hayes, M.H.B., In D.J. Greenland and M.H.B. Hayes (ed.) *The Chemistry of Soil Processes*. John Wiley and Sons, Chichester, England. p1-35, **1981**.

107. Gold, A.J. and T.L. Loudon. Nutrient, sediment and herbicide losses in tile drainage under conservation tillage. *ASAE Paper No. 82-254*. St.Joseph, MI. **1982**.

108. Griffith, S.M. and Schnitzer, M., *Soil Sci. Soc. Am. Proc.*, **1975**, *39*, 861-867.

109. Grover, R., *Can. J. Soil Sci.* **1975**, *55*, 127-135.

110. Gutzman, D.W. and Langford, C.H., *Water Pollut. Res. J. Can.*, **1988**, *23*, 379.

111. Hague, R., Ed., *Dynamics, Exposure, and Hazard Assessment of Toxic Chemicals*, Ann Arbor Science, Ann Arbor, MI, **1980**.

112. Hamaker, J.W., goring, C.A.L. and Youngson, C.R., *Organic Pesticides in the Environment*, ACS, Washington, DC, **1966**, p 23.

113. Hamaker, J.W. and Thompson, J.M., In C.A.I. Goring and J.W. Hamaker (ed.) *Organic Chemicals in the Environment*. Marcel Dekker, New York. p49-143, **1972**.

114. Hanque, R., Lindstrom, F.T., Freed, V.H. and Sexton, R., *Environ. Sci. Technol.*, **1968**, *2*, 207-211.

115. Haque, R. and Sexton, R., *J. Coll. Interface Sci.*, **1968**, *27*, 818-827.

116. Haque, R. and Coshow, R.W., *Environ. Sci. Technol.*, **1971**, *5*, 138-141.

117. Harmon, T.C., Ball, W.P. and Roberts, P.V., In *Reactions and Movements of Organic Chemicals in Soils*. Sawhney, B.L., Brown, K., eds., Soil Science Society of America, Inc. and American Society of Agronomy, Inc., Madison, WI, **1989**,

Chapter 16.

118. Harris, G.I. and Warren, G.F., *Weeds*, **1964**, *12*, 120-126.

119. Harter, R.D. and Lehmann, R.G. *Soil Sci. Soc. Am. J.*, **1983**, *47*, 666-669.

120. Hassett, J.J., Banwart, W.L., Wood, S.G. and Means, J.C., *Soil Sci. Soc. Am. J.*, **1981**, *45*, 38-42.

121. Hassett, J.P. and Anderson, M.A., *Environ. Sci. Technol.*, **1979**, *13*, 1526-1529.

122. Hassett, J.J., Banwart, W.L. and Griffin, R.A., In C.W. Francis and S.I. Auerbach (ed) *Environment and Solid wastes*. Butterworths, Boston. p161-178, **1983**.

123. Hassett, J.J., Means, J.C., Banwart, W.L. and Wood, S.G., *Sorption properties of Sediments and Energy-related Pollutants*. EPA-600/3-80-041. U.S. Environmental Protection Agency, Washington, DC. **1980**.

124. Hassett, J.J. and Banwart, W.L., In B.L. Sawhney and K. Brown (ed.) *Reactions and Movement of Organic Chemicals in Soils*. SSSA, Madison, WI. p31-44, **1989**.

125. Hayes, K.F. and Leckie, J.O., *J. Colloid Interface Sci.*, **1987**, *115*, 564-572.

126. Hayes, M.H.B., *Residue Rev.*, **1970**, *32*, 131-174.

127. Hayes, M.H.B. and Swift, R.S., In *the Chemistry of Soil Constituents*. Wiley, New York.Ch. 3, pp179-320, **1978**.

128. Hayes, M.H.B. and Himes, F.L., In P.M. Huang and M.Schnitzer (ed.) *Interaction of Soil Minerals with Natural Organics and Microbes*. SSSA, Madison, WI. p103-158, **1986**.

129. Hayward, D.O. and Trapnell, B.M.W., *Chemisorption*. Butterworths, London. **1964**.

130. Hohl, H. and Stumm, W., *J. Colloid interface Sci.*, **1976**, *55*, 281.

131. Holdern, G.R. and Speyer, P.M., *Am. J. Sci.*, **1985**, *285*, 994-1026.

132. Holdern, G.R. and Speyer, P.M., *Geochim. Cosmochim. Acta*. **1987**, *51*, 2311-2318.

133. Hornsby, A.G. and Davidson, J.M., *Soil Sci. Soc. Am. Proc.*, **1973**, *37*, 823-828.

134. Howard, P.H., *Handbook of Environmental Fate and Exposure Data for Organic Chemicals, Volume III, Pesticides*; Lewis Publishers: Chelsea, MI, **1991**.

135. Horzempa, L.M., and Di Toro, D.M., *Water Res.*, **1983**, *17*, 851-859.

136. Israelachvili, J.N., *Intermolecular and Surface Forces*. Academic Press, London. **1985**.

137. Issacson, P.J. and Frink, C.R., *Environ. Sci. Tecnol.*, **1984**, *18*, 43-48.

138. Jaffe, P.R. and Ferrara, R.A., *J. Environ. Eng. Div. ASCE*, **1983**, *109*, 859.

139. Johnson, R.C. and Crawford, N.H., Hydrocomp Inc., Palo Alto, calif. Prepared for USEPA, Athens, Ga.Inerim Rep. under Contract no. R803726-01, EPA, ORD Report,Conttract no. R803726-01, Hydrocomp Inc.,Palo Aito, Calif.

140. Junk, G.A., R.F. Spalding, and J.J. Richards. *J. Environ. Qual.* **1980**, *8*, 223-229.

141. Karickhoff, S.W., Brown, D.S. and Scott, T.A., *Water Res.*, **1979**, *13*, 241-248.

142. Karickhoff, S.W., *J. Hydaul. Engr.*, **1984**, *110*, 707-735.

143. Karickhoff, S.W., In *Contaminants and Sediments*, Baker, R.A. Ed., Ann Arbor Sci., Ann Arbor, MI. Vol. 2, Chapter 11, pp 193-205, **1980**.

144. Karickhoff, S.W. and Morris, K.R., *Environ. Toxic. Chem.*, **1985**, *4*, 469-479.

145. Karickhoff, S.W. and Brown, D.S., *J. Environ. Qual.*, **1978**, *7*, 246-252.

146. Kaufman, D.D., Still, G.G., Paulson, G.D. and Bandal S.K.(ed.) *Bound and Conjugated Pesticide Residues*. ACS Symp. Ser. 29, Am. Chem. Soc., Washington, DC. **1976**.

147. Kay, B.D. and Elrick, D.E., *Soil Sci.*, **1967**, *104*, 314.

148. Kearney, P.C., *ASC Symp. Ser.*, **1976**, *29*, 378-382.

149. Khan, A., Hassett, J.J., Banwart, W.L., Means, J.C. and Wood, S.G., *Soil Sci.*, **1979**, *128*, 297-302.

150. Khan, S.U., *Can. J. Soil Sci.*, **1973**, *53*, 429-434.

151. Khan, S.U., *Residue Reviews*, **1982**, *84*, 1-24.

152. Khan, S.U. and Schnitzer, M., *Can. J. Chem.*, **1971**, *13*, 2302-2309.

153. Khan, S.U. and Schnitzer, M., *Geochim. Cosmochim. Acta*, **1971**, *36*, 745-754.

154. Khan, S.U., *Pesticides in the Soil Environment*, Elsevier, Oxford. **1980**.

155. Kishk, F.M., Abu-Sharar, T.M., Bakry, N.M. and Abou- Donia, M.B., *Arch. Environm. Contam. Toxicol.*, **1979**, *8*, 637-645.

156. Knisel, W.G. CREAMS: A Field Scale Model for Chemicals, Runoff, and Erosion from Agricultural Management Systems. *U.S. Dep. of Agric., Sci. and Educ. Adm. Conserv. Res. Rep. No.26.* **1980**.

157. Koshinen, W.C. and O'Connor, G.A. and Cheng, H.H., *Soil Sci. Soc. Am. J.*, **1979**, *43*, 871-874.

158. Laird, D.A., Barriuso, E., Dowdy, R.H. and Koskinen, W.C., *Soil Sci. Soc. Am. J.*, **1992**, *56*, 62-67.

159. Langford, C.H. and Gutzman, D.W. *Anal. Chim. Acta*, **1992**, *256*, 183-201.

160. Langford, C.H., Kay, R., Quance, G.W. and Khan, T.R., *Anal. Lett.*, **1977**, *10*, 1249.

161. Langford, C.H. and Kham, T.R., *Can. J. Chem.*, **1975**, *53*, 2979.

162. Langford, C.H. and Mak, M.K.S., *Comments Inorg. Chem.*, **1983**, *2*, 127.

163. Langford, C.H., Wong, S.M. and Underdown, A.W., *Can. J. Chem.*, **1981**, *59*, 181.

164. Langford, C.H., in S. Petrucci (Ed.), *Ionic Interactions*, Vol. 2, Academic Press, New York, **1971**, p. 16.

165. Lavigne, J.A., Langford, C.H. and Mak, M.K.S., *Anal. Chem.*, **1987**, *59*, 2616.

166. Lee, L.S., Rao, P.S.C. and Brusseau, M.L., *Environ. Sci. Technol.*, **1991**, *25*, 722-729.

167. Leenheer, J.A. and Ahlrichs, J.L., *Soil Sci. Soc. Am. proc.*, **1971**, *35*, 700-705.

168. Leonard, R.A., Knisel, W.G. and Still, D.A., *Transactions of the ASAE.* **1987**, *30*, 1403-1418.

169. Li, J., Gamble, D.S., Pant, B.C. and Langford, C.H. *Environ. Technol.*, **1992**, *13*, 739-749.

170. Li, J., Gamble, D.S., Gilchrist, G.F.R. and Langford, C.H., *76th CSC Conference Proc.* EA-D1, 425, Sherbrooke, **1993**.

171. Li, J., Prasher, S.O., Gamble, D.S. and Langford, C.H., *76th CSC Conference Proc.* BM-G2P, 750, Sherbrooke, **1993**.

172. Lichtenstein, E.P., Schulz, K.R., Skrentny, R.F. and Tsukano, Y., *Arch. Environ. Health*, **1966**, *12*, 199-212.

173. Lindstrom, F.T., Haque, R. and Coshow, W.R., *J. phys. Chem.*, **1970**, *74*, 495-502.

174. Liu, L.G., Gibes-Viade, H. and Koo, F.K.S., *Weed Sci.*, **1970**, *18*, 470-474.

175. Lotse, E.G., Graetz, D.A., Chesters, G., Lee, G.B. and Newland, L.W., *Environ. Sci. Technol.*, **1968**, *2*, 353-357.

176. Macalady, D.L. and Wolfe, N.L., *ACS Symp. Ser.*, **1984**, *259*, 221-244.

177. MacIntyre, W.G. and Smith, C.L., *Environ. Sci. Tecnol.*, **1984**, *18*, 295-297.

178. Mackay, D.M., Roberts, P.V. and Cherry, J.A. *Environ. Sci. Technol.* **1985**, *19*, 384.

179. Mak, M.K.S. and Langford, C.H., *Can. J. Chem.*, **1982**, *60*, 2023.

180. Mak, M.K.S and Langford, C.H., *Inorg. Chim. Acta*, **1983**, *70*, 237.

181. Marking, L.L. and Kimberle, R.A., *Proc. Second Annual Symposium on Aquatic Toxicology*, ASTM STP 667, ASTM, Philadelphia, PA, **1979**.

182. Matolcsy, G., Nadasy, M. and Andriska, V., *Pesticide Chemistry (Studies in Environmental Science 32)*, p.64, Elsevier, **1988**.

183. Mayer, F.L. and Hamelink, J.L., *Proc. First Annual Symposium on Aquatic Toxicology*, ASTM STP 634, ASTM, Philadelphia, PA, **1977**.

184. McCall, P.J. Swan, R.L., Laskowski, D.A., Unger, S.M., Vrona, S.A. and Dishburger, H.J., *Bull. Environ. Contam. Toxicol.*, **1980**, *24*, 190-195.

185. McCall, P.J. and Agin, G.L., *Environ. Toxicol. Chem.* **1985**, *4*, 37-44.

186. McCarty, P.L., Reinhard, M. and Rittman, B.E. *Environ Sci. Technol.* **1981**, *15*, 40.

187. McGlamery, M.D. and Slife, F.W., *Weeds*, **1966**, *14*, 237-239.

188. McKeague, J.A., Sheldrick, B.H. and Desjardin, J.G., *Compilation of Data for CSSC Reference Soil Samples*, Land Resources Research Centre, Ottawa, **1978**.

189. McKeague, J.A. and Wang, C., *Can. J. Soil Sci.*, **1980**, *60*. 9-21.

190. McLean, E.O. In *Methods of Soil Analysis, Part 1-Physical and Mineralogical Methods*. Klute, A., Ed., 2nd Ed., Chapter 12, p 199, Madison, Wisconish, USA, **1986**.

191. Means, J.C., Wood, S.G., Hassette, J.J. and Banwart, W.L., *Environ. Sci. Technol.*, **1982**, *16*, 93-98.

192. Mebius, L.J., *Anal. Chim. Acta*, **1960**, *22*, 120-124.

193. Melcer, M.E., Zalewski, M.S., Brisk, M.A. and Hassett, J.P., *Chemosphere*, **1987**, *16*, 1115-1121.

194. Melcer, M.E., Zalewski, M.S. and Hassett, J.P., in I.H. Suffet and P. MacCarthy (Eds.), *Aquatic Humic Substances (Advances in Chemistry Series)*, Vol.219, pp.173-183, ACS, Washington, D.C., **1989**.

195. Mill, T., *Dynamics, Exposure and Hazard Assessment of Toxic Chemicals*, Hague, R. Ed., Ann Arbor Science, Ann Arbor, MI, **1980**, pp 297-322.

196. Miller, C.T. and Pedit, J.A., *Environ. Sci. Technol.*, **1992**, *26*, 1417-1427.

197. Miller, C.T., Rabideau, A.J. and Mayer, A.S., *Res. J. Water Pollut. Control Fed.* **1991**, *63*, 552.

198. Miller, C.T. and Weber, W.J.,Jr., *J. Contam. Hydrol.*, **1986**, *1*, 243-261.

199. Miller, C.T. and Weber, W.J.Jr., *Water Res.*, **1988**, *22*, 465.

200. Miller, C.T. and Weber, W.J.Jr., *Ground Water*. **1984**, *22*, 584.

201. Mills, A.G. and Biggar, J.W., *Soil Sci. Soc. Am. Proc.* **1969**, *33*, 210.

202. Mills, W.B., Porcella, D.B., Ungs, M.J., Gherini, S.A., Summers, K.V., Lingfung Mok, Rupp, G.L. and Bowie, G.L., *Water quality assessment: A screening*

procedure for toxic and conventional pollutants in surface and groundwater. EPA/600/6-85/002a, U.S. Environmental Protection Agency, Athens, Ga., **1985**.

203. Mingelgrin, U. and Gerstl, Z., *J. Environ. Qual.*, **1983**, *12*, 1-11.

204. Moore, J.W., *Physical Chemistry*. 3rd ed. Prentice Hall, Englewood Cliffs, NJ. p180, **1962**.

205. Moore, J.W., *Physical Chemistry*. 3rd ed. Prentice Hall, Englewood Cliffs, NJ. p273, **1962**.

206. Moore, J.W. and Pearson, R.G., *Kinetics and Mechanism*, John Wiley & Sons, New York, 3rd Ed., p 66, **1981**.

207. Morillo, E., Perez-Rodriguez, J.L. and Magueda, C., *Clay Minerals*, **1991**, *26*, 269-279.

208. Mortland, M.M., *Adv. Agron.*, **1970**, *22*, 75-117.

209. Mott, H.V. and Weber, J.W.Jr., *Environ. Sci. Technol.*, **1991**, *25*, 1708-1715.

210. Nelson, D.W. and Sommers, L.E., In *Methods of Soil Analysis: Part 2-Chemical and Microbiological Properties*. Page, A.Z., Miller, R.H. and Keeney, D.R., Eds., 2nd Ed., Madison, Wisconish, USA, Chapter 29, p 539, **1982**.

211. Oddson, J.K., Letey, J. and Weeks, L.V., *Soil Sci. Soc. Am. proc.*, **1970**, *34*, 412-417.

212. Ogwada, R.A. and Sparks, D.L., *Soil Sci. Soc. Am. J.*, **1986**, *50*, 300-305.

213. Ogwada, R.A. and Sparks, D.L., *Soil Sci. Soc. Am. J.*, **1986**, *50*, 1158-1162.

214. Ogwada, R.A. and Sparks, D.L., *Soil Sci. Soc. Am. J.*, **1986**, *50*, 1162-1164.

215. Oliver, B.G., *Chemosphere*, **1985**, *14*, 1087.

216. Olmstead, K.P. and Weber, J.W.Jr., *Environ. Sci. Technol.*, **1990**, *24*, 1693-1700.

217. Ortiz, de Serra M.I. and Schnitzer, M., *Soil Biol. Biochem.* **1973**, *5*, 281-286.

218. Parris, G.E., *Environ. Sci. Technol.* **1980**, *14*, 1099-1106.

219. Pavlostathis, S.G. and Mathavan, G.N., *Environ. Sci. Technol.*, **1992**, *26*, 532-538.

220. Peck, D.E., Corwin, D.L. and Farmer, W.J., *J. Environ. Qual.*, **1980**, *9*, 101-106.

221. Perdue, E.M. and Wolfe, N.L. *Environ. Sci. Technol.*, **1983**, *17*, 635-642.

222. Perdue, E.M. and Wolfe, N.L., *Environ. Sci. Technol.*, **1982**, *16*, 847-852.

223. Phelan, P.J. and Mattigod, S.V., *Soil Sci. Soc. Am. J.*, **1987**, *51*, 336-341.

224. Pierce, Jr., R.H., Olney, C.E. and Felbeck, Jr., G.T., *Environ. Letters*. **1971**, *1*, 157-172.

225. Pierce, R.H.,Jr., Olney, C.E. and Felbeck, G.T.,Jr., *Geochim. Cosmochim. Acta*, **1974**, *38*, 1061-1073.

226. Pignatello, J.J., In *Reaction and Movement of Organic Chemicals in Soils*, Sowhney, B.L. and Brown, K., Eds., SSSA Special Publication No.22, Soil Science Society of America, Madison, WI. p45-80, **1989**.

227. Pignatello, J.J., *Environ. Toxicol. Chem.*, **1990**, *9*, 1117.

228. Power, J.F. and Langford, C.H., *Anal. Chem.*, **1988**, *60*, 842.

229. Purkayastha, R. and Cochrane, W.P., *J. Agric. Food Chem.* **1973**, *21*, 93-98.

230. Rache, K.D. and Lichtenstein, E.P., *J. Agric. Food Chem.*, **1985**, *33*, 938-943.

231. Rao, P.S.C., Davidson, J.M., Jessup, R.E. and Selim, H.M., *Soil Sci. Soc. Am. J.*, **1979**, *43*, 22-28.

232. Rao, P.S.C. and Davidson, J.M., In M.R. Overcash and J.M. davidson (ed.) *Environmental Impact of Nonpoint Source Pollution*. Ann Arbor Sci. Publ., Ann Arbor, MI. pp 23-67, **1980**.

233. Rao, P.S.C. and Jessup, R.E., *Soil Sci.*, **1982**, *133*, 342-349.

234. Readman, J.W. and Mantoura, R.F.C., *Sci. Total Environ.*, **1987**, *66*, 73.

235. Reichenberg, D., Properties and behavior: kinetics, electrolyte penetration, and absorption of nonelectrolytes. In *Ion Exchangers in Organic and Biochemistry*. C. Calmon and L.R.E. Kressman, eds., pp. 66-85. Wiley, New York. **1957**.

236. Rhoades, J.D. In *Methods of Soil Analysis, Part 1-Physical and Mineralogical Methods*. Klute, A., Ed., 2nd Ed., Chapter 8, p 149, Madison, Wisconish, USA, **1986**.

237. Richardson, E.M. and Epstein, E., *Soil Sci. Soc. Am. Proc.*, **1971**, *35*, 884-887.

238. Richie, E.B. and J.R., Hoover. Numerical Simulation of the transport of a noninteractive pollutant through a porous media. *Paper presented at the 1982 Annual Meeting of the American Society of Agricultural Engineers*, North Atlantic Region, Burlington, VT. **1982**.

239. Richter, J. *The Soil as a Reactor: Modelling Processes in the Soil*; Destedt: CATENA VERLAG, D-3302 Cremlingen, WestGermany, **1987**, p52.

240. Roberts, P.V., Reinhard, M. and Valocchi, A.J. *J. Am. Water Works Assoc.* **1982**, *74*, 408.

241. Roberts, T.R., *Pure and Appl. Chem.* **1984**, *56*, 945-956.

242. Rounds, S.A. and Pankow, J.F., *Environ. Sci. Technol.*, **1990**, *24*, 1378-1386.

243. Rutherford, D.W., Chiou, C.T. and Kile, D.E., *Environ. Sci. Technol.*, **1992**, *26*, 336-340.

244. Ruthven, D.M. and Loughlin, K.F., *Chem. Eng. Sci.*, **1971**, *26*, 577-584.

245. Santana-Casiano, J.M. and Gonzalez-Davila, M., *Environ. Sci. Technol.*, **1992**, *26*, 90-95.

246. Sawhney, B.L. and Brown, K. *Reactions and Movement of Organic Chemicals in Soils*; Soil Science Society of American, Inc., and American Society of Agronomy, Inc.: Madison, WI, **1989**.

247. Schnitzer, M., The Chemistry of Humic Substances. In *Environmental Biochemistry*, Vol. 1 (Nriagu, J.O. ed.). Ann Arbor Science, Ann Arbor, MI. pp 89-107, **1976**.

248. Schnitzer, M., In *Soil Organic Matter*. Schnitzer, M. and Khan, S.U. eds. Elsevier, New York. Ch.1, pp 1-64, **1978**.

249. Selim, H.M., Davidson, J.M. and Mansell, R.S., In *Proc. Summer Computer Simulation Conf.*, 12-14 July. Washington, DC. p44-448, **1976**.

250. Sharma, D.K., Villamagna, F. and Langford, C.H., *Can. J. Spectrosc.*, **1983**, *28*, 181.

251. Sheldrick, B.H. ed., *Analytical Methods Manual*, Land Resource Research Institute, Ottawa, Ontario. LRRI Contribution No. 84-30. Chapter 4, pp 47/1-9, **1984**.

252. Shen, H.W., In *Stochastic approaches to Water Resources*, Shen, H.W. Ed., P.O. Box 606, Fort Collins, Colo., Chap. 26, pp 1-33, **1976**.

253. Singh, R., Gerritse, R.G. and Aylmore, L.A.G., *Aust. J. Soil Res.*, **1989**, *28*, 227-243.

254. Smith, A.E., *J. Agric. Food Chem.* **1981**, *29*, 111-115.

255. Smith, A.E. and Milward, L.J. *J. Agric. Food Chem.* **1983**, *31*, 633-637.

256. Smith, W.N., Prasher, S.O., Khan, S.U. and Barthakur, N.N., *Transactions of the ASAE.* **1992**, *35*, 1213-1220.

257. Sparks, D.L., *Adv. Agron.*, **1985**, *38*, 231-266.

258. Sparks, D.L., In *Soil Physical Chemistry* (D.L. Sparks, ed.). pp 83-178, CRC Press, Boca Raton, Florida. **1986**.

259. Sparks, D.L., *Kinetics of Soil Chemical Processes.* Academic Press, New York. Ch. 2, p 31, **1989**.

260. Sparks, D.L., *Kinetics of Soil Chemical Processes.* Academic Press, New York. Ch. 5, p 104, **1989**.

261. Sparks, D.L., *Kinetics of Soil Chemical Processes.* Academic Press, New York. Ch. 6, p 136, **1989**.

262. Sposito, G., *The Chemistry of Soils.* Oxiford University Press, New York. **1984**.

263. Stark, F.L., Cornell Univ. Agr. Exp. Sta., *Memoir 278*, **1948**.

264. Steinberg, S.M., Pignatello, J.J. and Sawhney, B.L., *Environ. Sci. Technol.*, **1987**, *21*, 1201-1208.

265. Stevenson, F.J., *Humus Chemistry, Genesis, Composition, Reactions.* Wiley, New York. p 443, **1982**.

266. Stevenson, F.J., Geochemistry of Soil Humic Substances. In *Humic Substances in Soil, Sediment, and Water: Geochemistry, Isolation, and Characterization.* (Aiken, G.R., McKnight, D.M., Werchaw, R.L. and MacCarthy, P. eds.). John Wiley & Sons, New York, pp 13-52, **1985**.

267. Stevenson, F.J., *ACS Symp. Ser.*, **1976**, *29*, 180-207.

268. Sullivan, Jr., J.D. and Felbeck, Jr., G.T., *Soil Sci.*, **1968**, *106*, 42-52.

269. Summ, W., Huang C.P. and Jenkins, S., *Croat. Chem. Acta.* **1970**, *43*, 223.

270. Swanson, C.L.W., Thorp, F.C. and Friend, R.B., *Soil Sci.* **1954**, *78*, 379.

271. Swanson, R.A. and Dutt, G.R., *Soil Sci. Soc. Am. proc.*, **1973**, *37*, 872-876.

272. Talbert, R.E. and Fletchall, O.H., *Weeds*, **1965**, *13*, 46-52.

273. Terce, M., *Argonomie*, **1983**, *3*, 883-890.

274. Tramonti, V., Zienius, R.H. and Gamble, D.S., *Intern. J. Environ. Anal. Chem.*, **1986**, *24*, 203-212.

275. Underdown, A.W., Langford, C.H. and Gamble, D.S. *Environ. Sci. Technol.*, **1985**, *19*, 132-136.

276. Van Genuchten, M.Th., Davidson, J.M. and Wierenga, P.J., *Soil Sci. Soc. Am. proc.*, **1974**, *38*, 29-35.

277. Van Genuchten, M.Th. *Journal of Hydrology*. **1981**, *49*, 213-233.

278. Van Genuchien, M.T., Wierenga, P.J. and O'Connor, G.A., *Soil Sci. Soc. Am. J.*, **1977**, *41*, 278-284.

279. Villenueve, J.P., O. Banton, P. Lafrance, and P.G.C. Cambell, A new model for the evaluation of groundwater vulnerability to non-point contamination by pesticides. *Proceedings and Information No. 38 of the International Conference on Vulnerability of Soil and Groundwater to Pollutants*. The Hague, The Netherlands. **1987**.

280. Wagenet, R.J. and Hutson, J.L. *LEACHM: Leaching Estimation and Chemistry Model*. Center for Environmental Research, Cornell University, Ithaca, NY, **1987**.

281. Wang, Z.D., Gamble, D.S. and Langford, C.H., *Anal. Chim. Acta*, **1990**, *232*, 181-188.

282. Wang, Z.D., Gamble, D.S. and Langford, C.H., *Anal. Chim. Acta*, **1991**, *244*, 135-143.

283. Wang, Z.D., Gamble, D.S. and Langford, C.H., *Environ. Sci. Technol.*, **1992**, *26*, 560-565.

284. Wang, Z.D., Pant, B.C. and Langford, C.H., *Anal. Chim. Acta*, **1990**, *232*, 43-49.

285. Weast, R.C. (ed.) *Handbook of Chemistry and Physics*. CRC Press, Boca Raton, FL. **1981**.

286. Weber, J.B., Perry, P.W. and Upchurch, R.P., *Proc. Soil Sci. Soc. Amer.*, **1965**, *29*, 678-688.

287. Weber Jr., W.J. and Smith E.H., *Environ. Sci. Technol.*, **1987**, *21*, 1040-1050.

288. Weber Jr., W.J., McGinley, P.M. and Katz, L.E., *Water Res.*, **1991**, *25*, 499-528.

289. Weber, W.J.Jr. and Miller, C.T., *Water Res.*, **1988**, *22*, 457.

290. Weber, J.B. and Miller, C.T. In *Reactions and Movement of Organic Chemicals in Soils*; Sawhney, B.L., Brown, K., Eds., Soil Science Society of American, Inc. and American Society of Agronomy, Inc.: Madison, WI, **1989**, pp 305-334.

291. Weber, W.J.Jr., McGinley, P.M. and Katz, L.E., *Environ. Sci. Technol.*, **1992**, *26*, 1955-1962.

292. Wershaw, R.L., *J. Contam. Hydrol.*, **1986**, *1*, 29.

293. Witkowski, P.J. Jaffe, P.R. and Ferrara, R.A., *J. Contam. Hydrol.* **1987**, *2*, 249-269.

294. Wollast, R. and Chou, L., In *the Chemistry of Weathering*, (J.I. Drever, ed.). pp 75-96, Reidel Publ., Dordrecht, The Netherlands. **1985**.

295. Woodwell, G.M., Craig, P.P. and Johnson, H.A., *Science*, **1971**, *174*, 1101-1107.

296. Wu, S. and Gschwend, P.M., *Environ. Sci. Technol.*, **1986**, *20*, 717-725.

297. Wu, S.C. and Gschwend, P.M., *Water Resour. Res.*, **1988**, *24*, 1373-1383.

298. Yaron, B. and Saltzman S., *Soil Sci. Soc. Amer. Proc.*, **1972**, *36*, 583-586.

299. Yonge, D.R., Keinath, T.M., Poznanska, K. and Jiang, Z.P., *Environ. Sci. Technol.*, **1985**, *19*, 690.

300. Zasoski, R.G. and Burau, R.G., *Soil Sci. Soc. Am. J.*, **1978**, *42*, 372-374.

APPENDICES

CHAPTER 3:

(1). Appendix A Spreadsheet Showing Raw Data Input (Exp. #14, part)

RAW DATA INPUT

Anl. no.	Solution Type	Peak Areas Atrazine	Peak Areas Hydroxy-atrazine	Month	Day	Hour	Min.
1	standard 1	52100					
	filtrate	38700		9	6	15	37.00
	standard 1	55400					
	standard 1	55400					
	slurry	43100		9	6	16	2.00
	standard 1	55300					
2	standard 1	55300					
	filtrate	40200		9	6	16	31.00
	standard 1	52600					
	standard 1	52600					
	slurry	41200		9	6	16	48.00
	standard 1	52600					
3	standard 1	52600					
	filtrate	41100		9	6	17	7.00
	standard 1	53600					
	standard 1	53600					
	slurry	40700		9	6	17	24.00
	standard 1	53600					
4	standard 1	56100					
	filtrate	41400		9	7	9	39.00
	standard 1	57600					
	standard 1	57600					
	slurry	42200		9	7	9	56.00
	standard 1	52200					

(2). Appendix B Spreadsheet Showing Interpolated Data for Filtrate and Slurry at Rounded Times by Curve Fitting (Exp. #14)

MOLARITIES INTERPOLATED FOR ROUNDED TIMES

Anl. no.	Filtrate		Unfiltered		Rounded Time (days)
	Atrazine (Moles/L of Slurry)	Hydroxyatrazine	Atrazine (Moles/L of Slurry)	Hydroxyatrazine	
1	7.3701E-06	0.0000E+00	7.5328E-06	0.0000E+00	0.180
2	7.3619E-06	0.0000E+00	7.5295E-06	0.0000E+00	0.215
3	7.3561E-06	0.0000E+00	7.5271E-06	0.0000E+00	0.240
4	7.2001E-06	0.0000E+00	7.4621E-06	0.0000E+00	0.929
5	7.1943E-06	0.0000E+00	7.4596E-06	0.0000E+00	0.955
6	7.1864E-06	0.0000E+00	7.4571E-06	0.0000E+00	0.982
7	6.9056E-06	0.0000E+00	7.3297E-06	0.0000E+00	2.332
8	6.9005E-06	0 0000E+00	7.3272E-06	0.0000E+00	2.358
9	6.8955E-06	0.0000E+00	7.3249E-06	0.0000E+00	2.383
10	6 7718E-06	0.0000E+00	7.2646E-06	0.0000E+00	3 022
11	6.7669E-06	0.0000E+00	7.2621E-06	0.0000E+00	3 048
12	6.7620E-06	0 0000E+00	7.2596E-06	0.0000E+00	3.074
13	6 6012E-06	0.0000E+00	7.1762E-06	0.0000E+00	3.958
14	6.5964E-06	0.0000E+00	7.1737E-06	0.0000E+00	3.985
15	6 5919E-06	0 0000E+00	7.1712E-06	0.0000E+00	4.011
16	6.5875E-06	0.0000E+00	7.1689E-06	0.0000E+00	4.036
17	6 4389E-06	0.0000E+00	7.0857E-06	0.0000E+00	4 917
18	6.4348E-06	0 0000E+00	7.0834E-06	0 0000E+00	4 942
19	6 4304E-06	0.0000E+00	7.0808E-06	0.0000E+00	4.969
20	6 2794E-06	0 0000E+00	6.9893E-06	0.0000E+00	5.938
21	6.2756E-06	0 0000E+00	6.9870E-06	0.0000E+00	5.963
22	6 2716E-06	0 0000E+00	6.9844E-06	0.0000E+00	5.990
23	6 1382E-06	0.0000E+00	6.8968E-06	0.0000E+00	6.919
24	6.1346E-06	0.0000E+00	6.8943E-06	0.0000E+00	6.945
25	6 1312E-06	0.0000E+00	6.8920E-06	0 0000E+00	6 970
26	6 0066E-06	0.0000E+00	6.8030E-06	0.0000E+00	7.913
27	6.0032E-06	0.0000E+00	6.8004E-06	0.0000E+00	7.940
28	5 9999E-06	0.0000E+00	6.7979E-06	0.0000E+00	7.966
29	5 8771E-06	0 0000E+00	6.7021E-06	0.0000E+00	8 982
30	5.8741E-06	0 0000E+00	6.6996E-06	0.0000E+00	9.008
31	5.8712E-06	0.0000E+00	6.6972E-06	0.0000E+00	9.033
32	5.6721E-06	0 0000E+00	6.5200E-06	0.0000E+00	10 911
33	5 6692E-06	0 0000E+00	6 5172E-06	0 0000E+00	10.941
34	5 6667E-06	0 0000E+00	6.5147E-06	0 0000E+00	10 967
35	5 4899E-06	0 0000E+00	6.3268E-06	0.0000E+00	12.958
36	5 4874E-06	0.0000E+00	6.3239E-06	0.0000E+00	12.989
37	5 4854E-06	0.0000E+00	6 3215E-06	0 0000E+00	13.014
38	5 3415E-06	0.0000E+00	6 1385E-06	0.0000E+00	14.953
39	5.3397E-06	0.0000E+00	6.1363E-06	0.0000E+00	14.979
40	5 3379E-06	0.0000E+00	6.1336E-06	0.0000E+00	15.005
41	5.2148E-06	0 0000E+00	5.9483E-06	0.0000E+00	16.969
42	5 2130E-06	0.0000E+00	5.9453E-06	0.0000E+00	17.000
43	5.2115E-06	0.0000E+00	5 9430E-06	0 0000E+00	17.025
44	5 0629E-06	0.0000E+00	5.6773E-06	0.0000E+00	19.840
45	5.0613E-06	0 0000E+00	5.6743E-06	0 0000E+00	19.872
46	5 0600E-06	0.0000E+00	5.6716E-06	0.0000E+00	19.900

Remarks: Rounded time = the mean value of t (Filtrate) and t (Slurry).

(3). Appendix C Spreadsheet Showing Data for Sorption/Desorption Kinetic Calculations (Exp. #14, part)

DATA FOR ATRAZINE SORPTION/DESORPTION KINETICS

No.	Ln(M2/M1)	F(t)	(Cat/Mat)	(t2-t1)	t
1	0.0000E+00	0.0000E+00	2.2080E-02	0.000	0.180
2	-1.1060E-03	7.6206E-04	2.2762E-02	0.035	0.215
3	-1.8951E-03	1.3217E-03	2.3249E-02	0.060	0.240
4	-2.3333E-02	2.1679E-02	3.6390E-02	0.749	0.929
5	-2.4130E-02	2.2630E-02	3.6876E-02	0.775	0.955
6	-2.4957E-02	2.3631E-02	3.7379E-02	0.802	0.982
7	-6.5088E-02	9.0905E-02	6.1407E-02	2.152	2.332
8	-6.5838E-02	9.2519E-02	6.1847E-02	2.178	2.358
9	-6.6557E-02	9.4081E-02	6.2269E-02	2.203	2.383
10	-8.4663E-02	1.3755E-01	7.2772E-02	2.842	3.022
11	-8.5388E-02	1.3946E-01	7.3187E-02	2.868	3.048
12	-8.6112E-02	1.4138E-01	7.3601E-02	2.894	3.074
13	-1.1018E-01	2.1287E-01	8.7116E-02	3.778	3.958
14	-1.1090E-01	2.1523E-01	8.7510E-02	3.805	3.985
15	-1.1159E-01	2.1752E-01	8.7889E-02	3.831	4.011
16	-1.1225E-01	2.1973E-01	8.8253E-02	3.856	4.036
17	-1.3507E-01	3.0317E-01	1.0046E-01	4.737	4.917
18	-1.3570E-01	3.0569E-01	1.0078E-01	4.762	4.942
19	-1.3638E-01	3.0842E-01	1.0114E-01	4.789	4.969
20	-1.6016E-01	4.1235E-01	1.1307E-01	5.758	5.938
21	-1.6075E-01	4.1518E-01	1.1335E-01	5.783	5.963
22	-1.6140E-01	4.1824E-01	1.1366E-01	5.810	5.990
23	-1.8289E-01	5.2837E-01	1.2358E-01	6.739	6.919
24	-1.8347E-01	5.3158E-01	1.2383E-01	6.765	6.945
25	-1.8403E-01	5.3467E-01	1.2408E-01	6.790	6.970
26	-2.0456E-01	6.5548E-01	1.3257E-01	7.733	7.913
27	-2.0513E-01	6.5906E-01	1.3279E-01	7.760	7.940
28	-2.0568E-01	6.6250E-01	1.3301E-01	7.786	7.966

Remarks: The formula for calculating Ln(M2/M1) is: @LN($B9/$BS9);
for (Cat/Mat) is: +($C9/$B9); and for (t2-t1) is: +($H9-$HS9).
The F(t) is integrated results of (Cat/Mat) vs. t.

(4). Appendix D Calculation of k_{bl} by Three Methods Outlined in 3-2.(4)

(i). *Chemical species (data from LIGL7.WK1)*

No.	Sol'n ($moles L^{-1}$)	Lab.sorbed ($moles L^{-1}$)	Nonlab.sorbed ($moles L^{-1}$)	Reaction time (days)
1	9.9581E-7	0.0000E+0	0.0000E+0	0.000
2	9.7778E-7	1.1895E-8	1.0321E-8	0.001
3	9.4509E-7	4.3776E-8	1.1138E-8	0.004
4	9.1009E-7	7.7755E-8	1.2158E-8	0.008
5	8.7091E-7	1.1550E-7	1.3586E-8	0.012
6	8.5310E-7	1.3250E-7	1.4402E-8	0.015

(ii). *Constants for iterative calculations*

Constant	Value	Unit
C_1	1.000E-6	moles L^{-1}
W/V	20.00	g L^{-1}
$\underline{\theta}_o$ (mean)	3.950E-7	moles g^{-1}
K_1	3.760E+4	L mol^{-1}
k_{dl}	0.135	d^{-1}
Q	8.640E+4	s d^{-1}
t_1	0.000	days

(iii). *Calculation results of k_{bl}*

Method	k_{bl}±Std.err. (L $mol^{-1}d^{-1}$)
(1). Initial rate approximation	(1.38±0.20) x 10^6
(2). Iterative calculation with labile sorption curve (θ_1) (eqs. 3-2.29 & 30)	(1.59±0.05) x 10^6
(3). Iterative calculation with solution phase curve (M_{AT}) (eqs. 3-2.33 & 34)	(1.08±0.16) x 10^6
Average	(1.35±0.20) x 10^6

(iv). *An example showing the iterative result of k_{b1} by method (iii)*

Iter. no.	k_{b1} value	Std. err.
0	5.568E+05	3.917E+04
1	8.051E+05	9.529E+04
2	9.357E+05	1.251E+05
3	1.004E+06	1.408E+05
4	1.041E+06	1.490E+05
5	1.059E+06	1.534E+05
6	1.069E+06	1.556E+05
7	1.075E+06	1.568E+05
8	1.077E+06	1.574E+05
9	1.079E+06	1.578E+05
	(1.08E+06)	(1.58E+05)

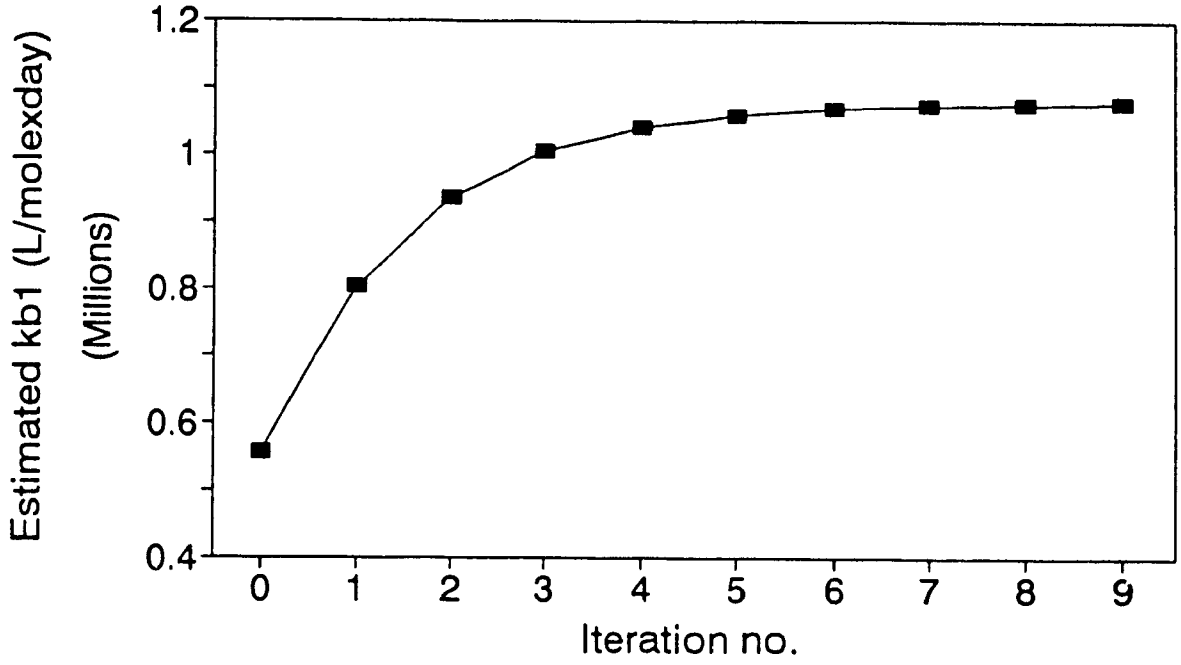

(v). *Assessment of the Calculation (correction term)*

Correction term = $I(t)/Y(t) \times 100$ (%)

$$Y(t) = k_{b1}C_o(t_2-t_1) - \int_{t1\text{-}t2} F(t)dt$$

$$I(t) = \int_{t1\text{-}t2} F(t)dt$$

$$F(t) = (k_{b1}/\bar{K}_1 - k_{d1})(C_t/M_{AT})$$

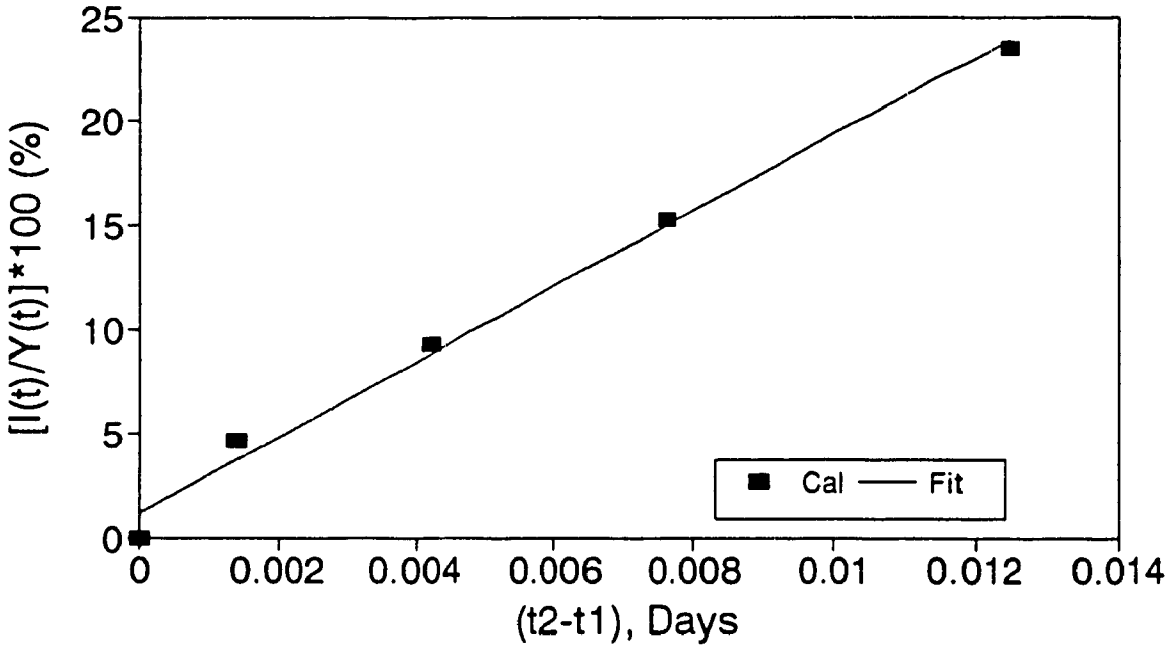

CHAPTER 6:

(1). Appendix A Main Input Data Files for the Modified PESTFADE (Column 1)

PARAM1.DAT

```
64  1  20  0.0  1.0  0  1  0  1  1
63.00  13.88  1.378  2.65  0.001  10.0  0.0012 14.0  0.43  7.73d-09  0.522
0.20  286.38
```

GAMBL.DAT

```
3.76d+04  0.397d-06  37.4058  -1.175d+04
```

STEADY.DAT

```
2.2    0.39
```

MICRO.DAT

```
126.0d0 0.499d0 12200.0d0 25.0d0
```

VOLAT.DAT

```
0.50d0 0.50d0
```

DATA

```
pesticide movement model - pestfade
10.0      30.0      1.00
  64 1000    1    1 rel    0.0001
END OF RUNS
```

(2). Appendix A Main Input Data Files for the Modified PESTFADE (Column 2)

PARAM1.DAT

```
66  1  20  0.0  1.0  0  1  0  1  1
65.00  13.97  1.378  2.65  0.001  10.0  0.0012 14.0  0.43  7.73d-09  0.522
0.13  286.38
```

GAMBL.DAT

```
3.76d+04  0.397d-06  37.4058  -1.175d+04
```

STEADY.DAT

```
2.2    0.38
```

MICRO.DAT

```
126.0d0 0.499d0 12200.0d0 25.0d0
```

VOLAT.DAT

```
0.50d0 0.50d0
```

DATA

```
pesticide movement model - pestfade
10.0      30.0      1.00
  64 1000    1    1  rel    0.0001
END OF RUNS
```

(3). Appendix B Main Data Files for Model Verification

Fig. 6-3.2:

PARAM1.DAT

```
21  1  26  25.0  4.0  0  0  0  0  0
20.0  1.0  1.50  2.65  0.001  10.0  0.0012  14.0  0.43  7.73d-09  0.0d0
```

STEADY.DAT

```
0.20    0.20
```

DATA

```
pesticide movement model - pestfade
10.0      35.0      1.00
  21 1000    1     1  rel    0.0001
END OF RUNS
```

Fig. 6-3.3:

PARAM1.DAT

```
101  1  31  5.0  37.5  0  0  0  0  0
100.0  1.0  1.30  2.65  0.001  10.0  0.0012  14.0  0.43  7.73d-09  0.62d0
```

STEADY.DAT

```
10.0    0.40
```

DATA

```
pesticide movement model - pestfade
10.0      40.0      1.00
  101 1000    1     1  rel    0.0001
END OF RUNS
```

(4). Appendix C Main Output Data for the Modified PESTFADE
(Column 1)

depth	time	meas.	twostage	conv.	depth	time	meas.	twostage	conv.
10 cm					40 cm				
	0	0.0170	0.0170	0.0170		0	0.0056	0.0056	0.0056
	1	0.0200	0.0437	0.2990		1	0.0060	0.0063	0.0062
	2	0.0190	0.0956	0.2960		2	0.0070	0.0063	0.0072
	3	0.0330	0.1178	0.2504		3	0.0080	0.0062	0.0150
	4	0.0340	0.1236	0.2110		4	0.0110	0.0061	0.0310
	5	0.0440	0.1222	0.1792		5	0.0080	0.0061	0.0490
	6	0.0510	0.1179	0.1540		6	0.0100	0.0063	0.0650
	8	0.0590	0.1066	0.1170		8	0.0170	0.0073	0.0880
	10	0.0570	0.0954	0.0920		10	0.0240	0.0096	0.0984
	12	0.0660	0.0855	0.0732		12	0.0420	0.0129	0.1020
	14	0.0650	0.0768	0.0596		14	0.0370	0.0167	0.1010
	16	0.0430	0.0693	0.0491		16	0.0420	0.0206	0.0980
	18	0.0570	0.0628	0.0410		18	0.0370	0.0243	0.0960
	20	0.0490	0.0572	0.0350		20	0.0390	0.0275	0.0930
20 cm					50 cm				
	0	0.0068	0.0068	0.0068		0	0.0074	0.0074	0.0074
	1	0.0050	0.0062	0.0350		1	0.0070	0.0058	0.0060
	2	0.0050	0.0081	0.1200		2	0.0060	0.0057	0.0058
	3	0.0060	0.0153	0.1610		3	0.0060	0.0056	0.0069
	4	0.0040	0.0258	0.1720		4	0.0060	0.0056	0.0111
	5	0.0060	0.0365	0.1690		5	0.0070	0.0056	0.0191
	6	0.0090	0.0457	0.1600		6	0.0050	0.0056	0.0297
	8	0.0120	0.0583	0.1380		8	0.0060	0.0058	0.0530
	10	0.0140	0.0646	0.1160		10	0.0080	0.0062	0.0750
	12	0.0230	0.0670	0.0980		12	0.0100	0.0071	0.0920
	14	0.0230	0.0670	0.0830		14	0.0190	0.0085	0.1060
	16	0.0150	0.0655	0.0710		16	0.0190	0.0104	0.1166
	18	0.0140	0.0632	0.0610		18	0.0240	0.0126	0.1250
	20	0.0140	0.0606	0.0520		20	0.0260	0.0151	0.1320
30 cm					60 cm				
	0	0.0068	0.0068	0.0068		0	0.0033	0.0033	0.0033
	1	0.0060	0.0063	0.0067		1	0.0040	0.0036	0.0049
	2	0.0080	0.0062	0.0240		2	0.0050	0.0041	0.0064
	3	0.0070	0.0063	0.0580		3	0.0050	0.0047	0.0080
	4	0.0110	0.0069	0.0880		4	0.0050	0.0052	0.0095
	5	0.0170	0.0085	0.1070		5	0.0050	0.0056	0.0131
	6	0.0210	0.0111	0.1180		6	0.0060	0.0061	0.0198
	8	0.0300	0.0183	0.1240		8	0.0070	0.0068	0.0440
	10	0.0280	0.0260	0.1180		10	0.0080	0.0075	0.0770
	12	0.0320	0.0329	0.1080		12	0.0090	0.0082	0.1140
	14	0.0380	0.0383	0.0970		14	0.0130	0.0090	0.1480
	16	0.0270	0.0422	0.0870		16	0.0120	0.0101	0.1790
	18	0.0280	0.0448	0.0790		18	0.0150	0.0116	0.2050
	20	0.0275	0.0464	0.0711		20	0.0170	0.0135	0.2270

(5). Appendix C Main Output Data for the Modified PESTFADE (Column 2)

depth	time	meas.	twostage	conv.	depth	time	meas.	twostage	conv.
10 cm					40 cm				
	0	0.0000	0.0000	0.0000		0	0.0000	0.0000	0.0000
	1	0.0700	0.0662	0.2905		1	0.0000	0.0000	0.0000
	2	0.1270	0.1154	0.2869		2	0.0000	0.0000	0.0011
	3	0.1450	0.1228	0.2424		3	0.0030	0.0000	0.0093
	4	0.1320	0.1179	0.2036		4	0.0070	0.0002	0.0251
	5	0.1200	0.1098	0.1727		5	0.0110	0.0009	0.0430
	6	0.1060	0.1013	0.1481		6	0.0130	0.0023	0.0592
	8	0.0950	0.0859	0.1122		8	0.0150	0.0071	0.0815
	10	0.0660	0.0734	0.0875		10	0.0250	0.0133	0.0920
	12	0.0500	0.0634	0.0698		12	0.0270	0.0193	0.0952
	14	0.0570	0.0552	0.0567		14	0.0300	0.0245	0.0947
	16	0.0500	0.0484	0.0466		16	0.0260	0.0285	0.0924
	18	0.0540	0.0428	0.0388		18	0.0250	0.0315	0.0896
	20	0.0550	0.0380	0.0327		20	0.0240	0.0335	0.0867
20 cm					50 cm				
	0	0.0000	0.0000	0.0000		0	0.0000	0.0000	0.0000
	1	0.0000	0.0004	0.0282		1	0.0000	0.0000	0.0000
	2	0.0020	0.0085	0.1135		2	0.0000	0.0000	0.0000
	3	0.0060	0.0251	0.1546		3	0.0005	0.0000	0.0009
	4	0.0060	0.0405	0.1652		4	0.0030	0.0000	0.0049
	5	0.0110	0.0516	0.1621		5	0.0050	0.0000	0.0127
	6	0.0230	0.0586	0.1535		6	0.0060	0.0002	0.0231
	8	0.0350	0.0646	0.1317		8	0.0080	0.0011	0.0460
	10	0.0390	0.0648	0.1110		10	0.0120	0.0032	0.0668
	12	0.0430	0.0622	0.0933		12	0.0220	0.0063	0.0837
	14	0.0410	0.0585	0.0787		14	0.0260	0.0101	0.0971
	16	0.0310	0.0544	0.0669		16	0.0300	0.0140	0.1075
	18	0.0290	0.0504	0.0572		18	0.0320	0.0178	0.1155
	20	0.0340	0.0465	0.0495		20	0.0280	0.0214	0.1218
30 cm					60 cm				
	0	0.0000	0.0000	0.0000		0	0.0000	0.0000	0.0000
	1	0.0000	0.0000	0.0005		1	0.0000	0.0000	0.0000
	2	0.0000	0.0001	0.0176		2	0.0000	0.0000	0.0000
	3	0.0000	0.0013	0.0518		3	0.0000	0.0000	0.0001
	4	0.0050	0.0048	0.0815		4	0.0000	0.0000	0.0007
	5	0.0080	0.0103	0.1012		5	0.0000	0.0000	0.0034
	6	0.0080	0.0165	0.1121		6	0.0000	0.0000	0.0094
	8	0.0120	0.0280	0.1174		8	0.0010	0.0001	0.0321
	10	0.0210	0.0364	0.1117		10	0.0040	0.0006	0.0643
	12	0.0280	0.0416	0.1021		12	0.0070	0.0020	0.0996
	14	0.0300	0.0443	0.0919		14	0.0100	0.0044	0.1332
	16	0.0360	0.0453	0.0824		16	0.0110	0.0079	0.1631
	18	0.0410	0.0451	0.0740		18	0.0180	0.0124	0.1884
	20	0.0430	0.0442	0.0668		20	0.0200	0.0175	0.2093